

**Universidade do Minho**  
Escola de Engenharia

Márcia Teresa da Silva Rodrigues

**DEVELOPMENT OF TISSUE ENGINEERED  
STRATEGIES COMBINING STEM CELLS  
AND SCAFFOLDS AIMED TO REGENERATE  
BONE AND OSTEOCHONDRAL INTERFACES**

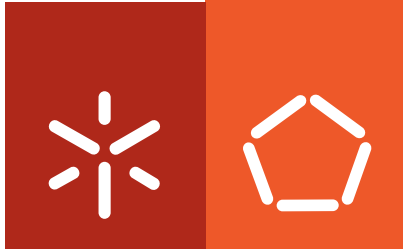
**DEVELOPMENT OF TISSUE ENGINEERED STRATEGIES COMBINING STEM CELLS  
AND SCAFFOLDS AIMED TO REGENERATE BONE AND OSTEOCHONDRAL INTERFACES**

Márcia Teresa da Silva Rodrigues

U Minho | 2011

Setembro de 2011





**Universidade do Minho**  
Escola de Engenharia

Márcia Teresa da Silva Rodrigues

**DEVELOPMENT OF TISSUE ENGINEERED  
STRATEGIES COMBINING STEM CELLS  
AND SCAFFOLDS AIMED TO REGENERATE  
BONE AND OSTEOCHONDRAL INTERFACES**

Tese de Doutoramento em Engenharia de Tecidos,  
Medicina Regenerativa e Células Estaminais

Trabalho efectuado sob a orientação do  
**Professor Rui L. Reis**  
e da  
**Doutora Manuela E. Gomes**

Setembro de 2011

É AUTORIZADA A REPRODUÇÃO PARCIAL DESTA TESE APENAS PARA EFEITOS DE INVESTIGAÇÃO, MEDIANTE DECLARAÇÃO ESCRITA DO INTERESSADO, QUE A TAL SE COMPROMETE

---

Márcia Teresa da Silva Rodrigues

## Acknowledgments

During my PhD, several people contributed to the accomplishment of this important step in my life, and to whom I wish to express my gratefulness.

First and foremost, I would like to thank Prof. Rui Reis for the opportunity of performing my PhD in 3B's Research Group. Prof. Rui has been an inspiration as a mentor and as a leader, from whom I learnt that high goals are accessible with the right dose of motivation, resilience, effort and determination. Thank you for believing in my abilities and for the chance to overcome many scientific challenges in the last 6 years. This journey has been a unique and enriching experience both personally and professionally, for all defying challenges and conquered achievements. I also appreciate the opportunity of participating in parallel projects and scientific meetings that sometimes seemed an overwhelming assignment. Prof. Rui pulled me out from the comfort zone, which made me question and test my limits. This exercise made me stronger and open-minded to forthcoming scientific challenges.

I also wish to express my gratitude to Prof. Manuela Gomes, or should I say Manela, my co-supervisor in this project. Thank you for everything... basically! For your guidance, support, and dedication to your students, and to research... Your amazing strength and determination in pursuing all of your goals is inspirational, and encouraged me moving forward every step of the way. Throughout this journey, I became a better and more confident scientist, mostly because you believed in me and you brought up in me abilities that I didn't think I have.

Thank you for sharing with me that cosy felling of companionship, when mentoring and friendship come together. Because of that I can only remember good things, even in the most stressful moments, as you were always there for me (even when you were overwhelmed in work or at home with your newborn children).

I really enjoy working with you and having you as a mentor and a very good friend...

I also would like to acknowledge Prof. James Yoo and Dr Sang Jin Lee for permitting me to do part of my PhD plan at WFIRM, and for all the support given in USA. Working at WFIRM gave me the opportunity to learn and grow scientifically. It was a positive experience I will always remember.

I gratefully acknowledge the funding institutions that materialized my PhD project. First of all my appreciation goes to the Portuguese Foundation for Science and Technology (FCT) for awarding me a PhD grant. I am also grateful to the projects: Hippocrates and Find&Bind as well as the network of excellence Expertissues for all the support in achieving my PhD plan. Finally, I also recall Calouste Gulbenkian Foundation in this acknowledgment for supporting my attendance to International Conferences.

To all researchers from the Biomaterials group, and technicians that participated in my project at WFIRM, with a special thanks to Dr Bu Kyu Lee for the guidance in the surgeries, and also for all scientific details in the bone project, and to Tom Shiner, who assisted me with my work.

A special thanks also to Pedro Baptista who helped me most with my integration process at Winston-Salem, and with many scientific questions and doubts.

To my dear friends Liliya and Olga, thank you for your friendship and for a closer feeling of home...

I could never forget, of course, my dear friends and colleagues at 3Bs Research Group that helped me to improve not only my scientific knowledge but also my social and human skills:

- Belinha, it has been great to work with you, I loved the brainstorming we had for our projects. I will never forget your daily support when I was homesick in the USA. The distance made our friendship grow stronger.

- To my colleagues that participated in the projects compiled to make this Thesis possible: Albino Martins, Vitor Araújo, Nathalie Gröen, and Sofia Caridade.

- To other colleagues and friends that did not actively participate in this Thesis but took also part in my scientific journey: Sílvia Gomes, Helena Lima, Simone Silva, Maria Susano, Alexandra Gonçalves, Ana Dias, and João Requicha. Thank you for your support and friendship...

I also wish to express my gratitude to Dra Isabel Dias and Dr Carlos Viegas, who performed the orthopaedic surgeries in the goat model, and for all assistance and dedication.

Thank you Fernando Muñoz and Monica, for assisting me with your expertise in the processing of calcified bone samples, and with the histological and histomorphometric analysis.

Very special thanks to my close friends: Elena Popa and Pedro Carvalho, who shared with me most of the cheerful moments as well as the most stressful situations of this voyage. Every

time I decided to test my working abilities (quite frequently I must say) and embrace one task after another combining a few projects simultaneously, you were there and assisted me with little things that made a huge difference; “Little drops of water make the mighty ocean!” Thank you so much! My PhD would not be the same without you, guys!

I cannot forget my dear cousin and friend Gi, who was invaluable in her help with the image formatting throughout this Thesis, as well as with all the formatting cues of the submitted papers.

I am deeply thankful to my family for all the support, love, dedication and comprehension, especially my dear parents and my grandmother. Thank you for listening and for understanding my choices and decisions, and encouraging me to pursue my goals.

Finally, I have to thank to my beloved husband, Jorge, for his endless support and patience, for his understanding and love all these years, and ever since we are together. Every time I complained about how difficult and stressful science was, you would listen and reply with a smile. Despite the distance in some periods of my PhD, you were always there for me. I learnt from you that the glass is never half empty rather than half full. This thought was present in many complex situations and helped me focus on what was really important to accomplish my goals.





## Abstract

Bone is a specialized tissue characterized by its rigidity and hardness, yet light weighed to fulfill diverse functions as mineral storage, organ protection or body support and locomotion. Despite its extraordinary healing ability, bone response may be unsuccessful to repair severe damage caused by injury or degenerative diseases. Furthermore, when bone is affected, other tissues and interfaces might be quite distressed as well. Cartilage and bone interface of the joints (osteochondral interfaces) is particularly affected by traumatic injuries and aging diseases. The challenge lies in balancing the structural, functional and biological needs of bone and cartilage in a stable milieu. As currently used therapies do not provide the ideal treatment, the development of biological substitutes through tissue engineering (TE) approaches may provide the ultimate solutions to restore, maintain, or improve bone and osteochondral tissue function.

Scaffolds play an imperative role in most TE strategies, where they are expected to guide cellular distribution and colonization, similarly to the natural occurring communications between cells and tissue, and to provide mechanical support during tissue regeneration. Nevertheless, in large damaged areas, scaffolding alone might be insufficient to promote a satisfactory healing response. Culturing stem cells onto the scaffolds has demonstrated to promote the regeneration of damaged tissues. Stem cells (SCs) can be found in almost every tissue, evidencing their role in repairing injuries. Bone marrow stem cells (BMSCs) are the most studied, and promising candidates for autologous TE approaches minimizing disease transmission risks but shown to be donor age-affected and had limited self-renewal capability. These limitations directed research into other stem cells sources, such as amniotic fluid (AF), that have shown to be an almost unlimited SCs source with high proliferative and osteogenic potential. Along with the almost endless ability to expand without telomere shortening, amniotic fluid stem cells (AFSCs) share with embryonic stem cells some markers and a high self renewal capacity.

In this Thesis several potential approaches were considered aiming at bone and osteochondral TE, focusing on distinct scaffold design and composition, previously or newly developed, and distinct stem cells sources. Different animal models were used to evaluate the proposed strategies with scaffolds and/or cell-scaffold constructs.

As a first approach, a multilayered scaffold was developed composed of tricalcium phosphate (TCP) granules entrapped in a polycaprolactone (PCL) nanofiber mesh, inspired from the natural organic-inorganic nanostructure of bone. A synergistic effect of PCL-TCP

scaffolds and mechanical stimulation was observed in the osteogenic differentiation of BMSCs cultured onto these scaffolds, resulting in the production of a mineralized ECM, even in basal medium. Composite multilayered scaffolds showed an interesting behavior under dynamic conditions using cell culturing media without osteogenic supplements.

Another approach consisted in the combination of wet-spinning technology and a calcium silicate solution to produce SPCL (starch and polycaprolactone blend) wet-spun fiber meshes with functionalized silanol groups (SPCL-Si). The purpose was to develop new bioactive materials linking the properties of classical bioactive ceramics, and the processability and degradability of an organic polymer. SPCL-Si scaffolds own intrinsic properties to sustain *in vitro* osteogenic features, and thus holding a great potential for bone engineering approaches. Additionally, this Thesis aimed at designing a new construct for the repair of osteochondral (OC) interfaces, proposing a novel bilayered scaffold, combining the well described agarose gels for cartilage and the promising SPCL scaffolds for bone, encapsulated/seeded with amniotic stem cells (AFSCs). An OC engineered system was successfully developed, where both osteo- or chondrogenic differentiated AFSCs maintained long term viability and phenotypic expression, even in basal medium after assembling of the bilayered construct.

Another major original objective of this Thesis was to explore the potential of amniotic fluid stem cells (AFSCs), as compared to bone marrow stem cells (BMSCs), for bone TE applications. Besides their source, the environmental conditions are known to influence cell response, and thus, both AFSCs and BMSCs were seeded/cultured in either 2D or 3D (using SPCL scaffolds) conditions. AFSCs and BMSCs expressed different bone-related markers at different time points. This study demonstrated that the selection of a particular stem cell type may not be a simple and direct process and relies on the target TE strategy.

Finally, non-critical sized defects were induced in goat femurs so as to understand the role of the scaffold material -SPCL- and the influence of culturing autologous mesenchymal cells with/without pre-culture in osteogenic medium. Neobone formation and cellular distribution was increased in cell seeded SPCL scaffolds (pre-differentiation condition), showing the relevance of implanted cells in the bone regeneration process, and suggesting the importance of the stage of osteogenic differentiation of seeded cells.

In a similar approach, femoral critical sized defects were induced in nude rats and SPCL scaffolds were implanted with or without AFSCs under different stages of osteogenic differentiation. The bridging effect between the bone segments was more prominent in scaffolds with osteogenic committed cells, and large blood vessels were observed, especially in SPCL scaffolds seeded with undifferentiated cells or osteogenic-like cells. Both *in vivo* studies

showed the potential of SPCL scaffolds as a tissue 3D support for the regeneration of bone and underlined the importance of stem cells and stem cells stage of differentiation for achieving enhanced bone tissue regeneration.

In summary, the described scaffold design and composition show a great potential to be tailored to specific applications in bone tissue regeneration strategies. Nevertheless, SPCL meshes obtained from melt spun fibers are clearly one step ahead as scaffold structures, showing to provide the necessary support for bone and osteochondral TE strategies using different sources of stem cells. Most importantly, the work described in this Thesis clearly demonstrated that bone tissue engineering requires the presence of stem cells, and that their pre-differentiation into the osteoblastic phenotype facilitates bone regeneration.



## Resumo

O osso é um tecido especializado, caracterizado pela sua rigidez e dureza embora a sua estrutura leve permita a realização de diversas funções, incluindo a reserva de minerais, protecção de órgãos ou suporte do organismo e locomoção. Apesar da sua capacidade regenerativa extraordinária, a resposta natural do osso revela-se, por vezes, limitada na reparação de danos severos resultantes de traumas graves ou doenças degenerativas. Além disso, quando o osso se deteora, outros tecidos e interfaces poderão estar igualmente comprometidos. A interface cartilagem-osso presente nas articulações (interfaces osteocondrais) é particularmente afectada por traumas e doenças associadas ao envelhecimento. Uma vez que as terapias convencionais não garantem o tratamento ideal destes tecidos, o desenvolvimento de substitutos biológicos através da engenharia de tecidos propõe-se como uma alternativa para restaurar, manter ou melhorar a funcionalidade do osso e do sistema osteocondral.

Na maioria das estratégias em engenharia de tecidos, as estruturas tridimensionais de suporte ou *scaffolds* desempenham um papel fundamental, conduzindo a distribuição e colonização celulares, de modo semelhante à comunicação que ocorre naturalmente entre as células e o tecido, proporcionando também um suporte mecânico durante o processo de regeneração. No entanto, em áreas danificadas de grandes dimensões, as estruturas tridimensionais de suporte poderão ser insuficientes para promover uma resposta terapêutica satisfatória. A cultura de células estaminais nestas estruturas tem demonstrado estimular a regeneração de tecidos lesados; células estas que podem ser encontradas em quase todos os tecidos, evidenciando o seu papel na reparação de lesões. Actualmente, as células estaminais da medula óssea (*bone marrow stem cells, BMSCs*) têm sido as mais estudadas, revelando-se candidatas promissoras para aplicações autólogas em engenharia de tecidos, reduzindo o risco de transmissão de doenças, embora o seu potencial possa ser comprometido pela idade do dador e pela limitada capacidade de auto-renovação. Estas limitações conduziram a investigação científica na procura de novas fontes de células estaminais, como o fluído amniótico que demonstrou ser uma fonte quase inesgotável de células estaminais com grande potencial de proliferação e de diferenciação osteogénica. Além disso, as células estaminais do fluído amniótico (*amniotic fluid stem cells, AFSCs*) partilham com as células estaminais embrionárias marcadores genéticos e uma elevada capacidade de auto-renovação.

Nesta Tese foram estudadas diferentes estratégias de engenharia de tecidos, considerando o seu potencial para aplicação em osso e em interfaces osteocondrais. Estas estratégias

baseiam-se na utilização de estruturas distintas de suporte tridimensionais (*scaffolds*), desenvolvidos prévia ou especificamente para este projecto, e em células estaminais de diferentes fontes. Também foram analisados vários modelos animais para avaliação *in vivo* das estratégias desenvolvidas, nomeadamente as estruturas de suporte tridimensionais na presença/ausência de células estaminais.

Numa primeira abordagem, desenvolveu-se uma estrutura de suporte tridimensional constituída por grânulos de fosfatos de tricálcio envolvidos numa matriz de nano fibras de policaprolactona (PCL). Esta estrutura foi inspirada na nanoestrutura orgânica-inorgânica do osso. Observou-se um efeito sinérgico das estruturas de suporte tridimensional de PCL-fosfatos e da estimulação mecânica no processo de diferenciação osteogénica das BMSCs cultivadas nestes suportes, resultando na produção de uma matriz extracelular mineralizada, mesmo em meio de cultura basal. As estruturas compósitas de suporte tridimensional de multi-camada demonstraram ser relevantes em condições dinâmicas utilizando meios de cultura celular sem suplementos osteogénicos.

Numa segunda estratégia, combinou-se a tecnologia de extrusão líquida (*wet-spinning*) e uma solução de silicato de cálcio para produzir uma matriz de suporte tridimensional de uma mistura polimérica de amido e policaprolactona (*starch-polycaprolactone blend, SPCL*) com grupos funcionais de silanol (SPCL-Si). O objectivo consistiu no desenvolvimento de novos materiais bioactivos, reunindo as propriedades dos materiais cerâmicos clássicos e a processabilidade e degradabilidade de um polímero orgânico. As matrizes desenvolvidas apresentam propriedades intrínsecas capazes de sustentar as propriedades osteogénicas das células *in vitro*, e, conseqüentemente, com potencial para engenharia de tecidos ósseos.

Nesta Tese foi também investigado o desenvolvimento de estruturas de suporte tridimensionais híbridas com células estaminais para a regeneração de interfaces osteocondrais, através da criação de uma estrutura de suporte tridimensional de bi-camada, combinando os géis de agarose, já estudados para a cartilagem, e as estruturas de suporte tridimensionais promissoras de SPCL para osso, cultivados ou encapsulados, respectivamente com AFSCs. Foi desenvolvido um sistema osteocondral, no qual as células estaminais do líquido amniótico se diferenciaram nas linhagens condro- e osteogénicas, mantendo a viabilidade e a expressão fenotípica ao longo do tempo, após a montagem do sistema de bicamada e em meio de cultura basal.

O potencial das células estaminais do líquido amniótico (AFSCs) foi também explorado e comparado com as células estaminais da medula óssea (BMSCs) para aplicações em engenharia de tecido ósseo. A origem e o meio envolvente são condicionantes da resposta

celular e, assim sendo, as AFSCs e as BMSCs foram cultivadas em ambientes de duas e três dimensões (utilizando as estruturas de suporte tridimensionais de SPCL). Os dois tipos celulares revelaram diferentes perfis de expressão de vários marcadores associados à diferenciação osteogénica, analisados ao longo do tempo em cultura, demonstrando que a selecção de um tipo de células estaminais não é uma escolha simples e directa, e que se encontra dependente da estratégia específica que se pretende.

Em seguida, estudos de defeitos ósseos não-críticos foram realizados em fémures de cabras com o propósito de analisar o papel das estruturas de suporte tridimensionais de SPCL e da influência do cultivo de células autólogas da medula óssea, com ou sem pré-cultura em meio de diferenciação osteogénico. A formação de novo tecido ósseo e a distribuição celular foram mais pronunciadas nos locais implantados com os suportes tridimensionais híbridos com células pré-diferenciadas, evidenciando a importância das células implantadas e sugerindo também a relevância do estadio de diferenciação celular no processo regenerativo ósseo.

Posteriormente, foram induzidos defeitos críticos em fémures de ratos atímicos, onde se implantaram também estruturas de suporte tridimensionais de SPCL, na presença ou ausência de AFSCs, em diversos estadios de diferenciação osteogénica. A aproximação dos dois segmentos ósseos no defeito criado foi mais pronunciado na presença das estruturas de suporte tridimensionais híbridas com AFSCs comprometidas com o fenótipo osteogénico, enquanto que os maiores vasos sanguíneos foram observados nos defeitos preenchidos com estruturas de suporte tridimensionais híbridadas com AFSCs no estadio indiferenciado ou com AFSCs no estadio considerado osteogénico. Ambos os estudos *in vivo* demonstraram o potencial das estruturas tridimensionais de SPCL para suporte e regeneração de tecido ósseo, salientando uma vez mais a importância das células estaminais e do estadio de diferenciação celular numa melhor regeneração tecidual.

Resumidamente, o *design* e composição das estruturas de suporte tridimensionais, descritos anteriormente, demonstraram potencial para aplicação em estratégias de regeneração óssea. No entanto, as matrizes de SPCL obtidas por *melt spun*, estão um passo à frente como estruturas de suporte uma vez que demonstraram garantir o suporte tridimensional de estratégias para osso e interface osteocondral, utilizando células estaminais de diferentes origens. Em conclusão, o trabalho descrito nesta Tese demonstra claramente que a engenharia de tecidos do osso requer a presença de células estaminais e que a sua pré-diferenciação no fenótipo osteogénico facilita a regeneração óssea.

---

*O resumo em português desta Tese não se encontra redigido segundo o novo acordo ortográfico.*





## Table of Contents

Acknowledgments .....	iii
Abstract .....	vii
Resumo.....	xi
Table of Contents.....	xv
Short Curriculum Vitae.....	xxiii
This Thesis is based on the following publications .....	xxv
List of Figures.....	xxvii
List of Tables .....	xxxiii
List of Abbreviations and Symbols.....	xxxv
SECTION I	
GENERAL INTRODUCTION .....	1
Chapter I	
CURRENT STRATEGIES FOR OSTEOCHONDRAL REGENERATION: FROM STEM CELLS TO PRE- CLINICAL APPROACHES .....	3
I.1.Abstract .....	5
I.2.Introduction .....	6
I.2.1.    Osteochondral defects (OCD) .....	7
I.2.2.    Weight bearing influence in biomechanics of the joint .....	8
I.2.3.    Current treatments in clinical field .....	8
I.2.4.    TE strategies to improve available treatments.....	9
I.2.4.1.    Cells to promote healing .....	9
I.2.4.2.    Biomaterials: human designs to mimic natural extracellular material .....	11
I.2.4.3.    Assisted Devices: bioreactor systems .....	13
I.2.5. <i>In vivo</i> models for osteochondral tissue engineering .....	14
I.3.Conclusions .....	15
I.4.References .....	15
SECTION II	
MATERIALS AND METHODS .....	21
Chapter II	
MATERIALS & METHODS .....	23

II.1. Abstract .....	25
II.2. Materials.....	25
II.2.1. Polycaprolactone .....	25
II.2.2. Starch-polycaprolactone blend.....	26
II.2.3. Tri-calcium phosphates .....	27
II.2.4. Agarose.....	27
II.3. Scaffold fabrication .....	28
II.3.1. Melt fiber extrusion - Fiber bonding.....	29
II.3.2. Electrospinning .....	29
II.3.3. Tricalcium Phosphates production by solid state reaction .....	30
II.3.4. Wet-spinning .....	30
II.3.4.1. Designing of an in situ functionalized surface .....	30
II.4. Scaffold characterization .....	31
II.4.1. In vitro bioactivity of SPCL-Si wet-spun fiber mesh scaffolds.....	31
II.4.2. Scanning electron microscopy .....	32
II.4.3. Dynamic Mechanical Analysis.....	32
II.4.4. Micro-computed tomography .....	32
II.4.5. Thin-film X-ray diffraction .....	33
II.4.6. <i>Fourier transform infrared spectroscopy with attenuated total reflectance</i> .....	34
II.4.7. Inductively coupled plasma optical emission spectrometer .....	34
II.5. Scaffold sterilization prior to cell culturing studies.....	35
II.6. Biological assays.....	35
II.6.1. Harvesting, isolation and culture of stem cells.....	35
II.6.1.1. Harvesting and isolation of goat bone marrow stromal cells.....	35
II.6.1.2. Harvesting and isolation of human amniotic fluid stem cells.....	37
II.6.2. Cell culturing and expansion .....	37
II.6.2.1. Goat bone marrow stromal cells.....	38
II.6.2.2. Human amniotic fluid stem cells.....	38
II.6.2.3. Human mesenchymal stem cells from bone marrow .....	38
II.6.3. Osteogenic differentiation .....	39
II.6.4. Osteochondral differentiation .....	39
II.6.5. Seeding on 2D cultures .....	40
II.6.6. Seeding cells onto 3D matrices.....	40

II.6.6.1.	gBMSCs, hAFSCs or hBMSCs onto SPCL scaffolds .....	40
II.6.6.2.	gBMSCs onto SPCL-Si scaffolds .....	41
II.6.6.3.	Encapsulating hAFSCs into agarose gels.....	41
II.6.7.	Characterization of cell-scaffold constructs .....	41
II.6.7.1.	Cell viability methods – MTS and Calcein AM.....	42
II.6.7.2.	Cellular proliferation assay (DNA quantification) .....	43
II.6.7.3.	Histology .....	44
II.6.7.4.	Osteogenic markers.....	44
II.6.7.4.1.	Alkaline Phosphatase Activity (ALP) .....	44
II.6.7.4.2.	Alizarin Red Staining.....	46
II.6.7.4.3.	Fourier Transformed Infrared Spectroscopy with Attenuated Total Reflectance .....	46
II.6.7.4.4.	Immunocytochemistry: Collagen I and Osteocalcin.....	47
II.6.7.4.5.	Immunofluorescence: Collagen I and RunX-2.....	47
II.6.7.5.	Chondrogenic markers .....	48
II.6.7.5.1.	Safranin O staining .....	48
II.6.7.5.2.	Immunofluorescence: aggrecan and collagen II .....	48
II.6.7.6.	Evaluation of cell morphology and distribution.....	49
II.6.7.6.1.	Confocal laser scanning microscopy (CLSM).....	49
II.6.7.6.2.	SEM.....	49
II.6.7.6.3.	Energy dispersive X-ray analysis or EDS analysis .....	50
II.7.	Animal models studies .....	50
II.7.1.	Goat model – non critical defects .....	50
II.7.1.1.	Implantation surgery .....	51
II.7.1.2.	Imprinting new bone with fluorescent dyes.....	52
II.7.1.3.	Explant retrieval and characterization .....	52
II.7.1.3.1.	Histological characterization.....	52
II.7.2.	Nude rat model - non-union defects.....	53
II.7.2.1.	Implantation .....	54
II.7.2.2.	Explant retrieval and characterization .....	55
II.7.2.2.1.	Micro-computed tomography (bone formation assessment) .....	55
II.7.2.2.2.	X-rays.....	55
II.7.2.2.3.	Histological Characterization .....	56
II.7.2.2.4.	Histomorphometric analysis.....	56

II.8. Statistical analysis.....	57
II.9. References .....	57
SECTION III	
SCAFFOLD DESIGN AND CHARACTERIZATION .....	63
Chapter III	
SYNERGISTIC EFFECT OF SCAFFOLD COMPOSITION AND DYNAMIC CULTURING ENVIRONMENT IN MULTI-LAYERED SYSTEMS FOR BONE TISSUE ENGINEERING .....	65
III.1. Abstract.....	67
III.2. Introduction .....	68
III.3. Materials and Methods .....	69
III.3.1. Development of the nanofibrous multilayered composite scaffolds .....	69
III.3.2. Characterization of the composite scaffolds.....	70
III.3.2.1. Thin-film X-ray diffraction (TF-XRD) .....	70
III.3.2.2. Fourier Transformed Infrared Spectroscopy with attenuated total reflectance (FTIR-ATR) .....	70
III.3.2.3. Scanning electron microscopy (SEM) .....	70
III.3.3. <i>In vitro</i> culture of bone marrow mesenchymal stromal cells onto nanofibrous scaffolds	70
III.3.3.1. Cell proliferation and osteogenic differentiation in multi-stacked nanofibrous scaffolds .....	71
III.3.3.1.1. DNA assay .....	71
III.3.3.1.2. ALP assay .....	72
III.3.3.1.3. Alizarin Red staining .....	72
III.3.3.1.4. Immunocytochemistry .....	72
III.3.4. Statistical Analysis.....	72
III.4. Results and Discussion.....	73
III.5. Conclusions .....	78
III.6. References .....	79
Chapter IV	
FUNCTIONAL BIODEGRADABLE SCAFFOLDS FOR BONE TISSUE ENGINEERING: BIOACTIVITY PROFILE AND OSTEOGENIC DIFFERENTIATION OF MARROW MESENCHYMAL STROMAL CELLS	83
IV.1. Abstract .....	85
IV.2. Introduction .....	86
IV.3. Materials and Methods .....	87
IV.3.1. Materials .....	87

IV.3.2.	Wet-spun fiber mesh scaffolds processing .....	88
IV.3.3.	Evaluation of the <i>in vitro</i> bioactivity of wet-spun fiber mesh scaffolds.....	88
IV.3.3.1.	Scanning electron microscopy (SEM) .....	88
IV.3.3.2.	Thin-film X-ray diffraction (TF-XRD) .....	89
IV.3.3.3.	Micro-computed tomography ( $\mu$ -CT) analysis: .....	89
IV.3.3.4.	Dynamic mechanical analysis (DMA):.....	89
IV.3.3.5.	Induced-coupled plasma emission spectroscopy (ICP) .....	90
IV.3.4.	Cell culture study .....	90
IV.3.4.1.	Harvesting and seeding gBMSCs onto wet-spun fiber mesh scaffolds .....	90
IV.3.4.2.	Cell viability assay.....	91
IV.3.4.3.	Cell proliferation assay .....	91
IV.3.4.4.	ALP assay .....	91
IV.3.4.5.	SEM.....	91
IV.3.5.	Statistical Analysis.....	92
IV.4.	Results and Discussion .....	92
IV.4.1.	Bioactivity assessment .....	92
IV.4.1.1.	DMA analysis.....	96
IV.4.2.	Biological assays.....	97
IV.5.	Conclusions.....	100
IV.6.	References .....	100

## Chapter V

BILAYERED CONSTRUCTS AIMED AT OSTEOCHONDRAL STRATEGIES: THE INFLUENCE OF MEDIA SUPPLEMENTS IN THE OSTEO- AND CHONDRO-GENIC DIFFERENTIATION OF AMNIOTIC FLUID-DERIVED STEM CELLS .....		105
V.1.	Abstract .....	105
V.2.	Introduction .....	108
V.3.	Materials and Methods .....	110
V.3.1.	Viability assay with Calcein AM .....	111
V.3.2.	SEM (scanning electronic microscopy).....	112
V.3.3.	Histological characterization .....	112
V.4.	Results and Discussion .....	113
V.4.1.	AFSCs-agarose system.....	113
V.4.2.	Agarose-SPCL bilayered system.....	116
V.4.2.1.	AFSCs-SPCL layer .....	116

V.5. Conclusions.....	123
V.6. References.....	124
SECTION IV	
DOES STEM CELL ORIGIN INFLUENCE STEM CELL RESPONSE ? .....	127
Chapter VI	
AMNIOTIC FLUID STEM CELLS VERSUS BONE MARROW MESENCHYMAL STEM CELLS AS A SOURCE FOR BONE TISSUE ENGINEERING .....	129
VI.1. Abstract .....	131
VI.2. Introduction .....	132
VI.3. Materials and Methods .....	134
VI.3.1. Cell culture.....	134
VI.3.2. Calcein AM assay .....	134
VI.3.3. Alkaline Phosphatase (ALP) staining .....	135
VI.3.4. Alizarin Red Staining (AR) .....	135
VI.3.5. Immunofluorescence .....	135
VI.3.6. Scanning electronic microscopy (SEM) .....	136
VI.4. Results and Discussion .....	136
VI.4.1. Osteogenic differentiation of AFSCs and BMSCs in a 2D culture environment.	136
VI.4.2. Osteogenic differentiation of hAFSCs and hBMSCs seeded on SPCL scaffolds (3D environment) .....	138
VI.5. Discussion .....	141
VI.6. Conclusions.....	143
VI.7. References.....	144
SECTION V	
<i>IN VIVO</i> STUDIES .....	147
Chapter VII	
TISSUE ENGINEERED CONSTRUCTS BASED ON SPCL SCAFFOLDS CULTURED WITH GOAT MARROW CELLS: FUNCTIONALITY IN FEMORAL DEFECTS .....	149
VII.1. Abstract .....	151
VII.2. Introduction .....	152
VII.3. Materials and Methods .....	154
VII.3.1. Production of SPCL scaffolds .....	154
VII.3.2. gBMSCs harvesting.....	154
VII.3.3. <i>In vitro</i> cell seeding and culture.....	155

VII.3.4. <i>In vitro</i> characterization of cells-scaffold constructs .....	155
VII.3.5. Animals Study .....	156
VII.3.5.1. Implantation procedures .....	157
VII.3.5.2. Harvesting samples after implantation .....	158
VII.3.6. Statistical Analysis.....	159
VII.4. Results and Discussion .....	159
VII.4.1. <i>In vitro</i> characterization of autologous gBMSCs-SPCL constructs .....	159
VII.4.2. <i>In vivo</i> studies .....	161
VII.4.2.1. Histologic and Fluorescence analysis .....	161
VII.5. Conclusions.....	164
VII.6. References .....	165

## Chapter VIII

THE EFFECT OF THE DIFFERENTIATION STAGE OF AMNIOTIC FLUID STEM CELLS SEEDED ONTO BIODEGRADABLE SCAFFOLDS IN THE REGENERATION OF NON-UNION DEFECTS .....	169
VIII.1. Abstract.....	171
VIII.2. Introduction .....	172
VIII.3. Materials and Methods .....	174
VIII.3.1. <i>In vitro</i> Study.....	174
VIII.3.1.1. Alizarin Red (AR) and Alkaline phosphatase (ALP) staining .....	174
VIII.3.1.2. SEM (scanning electronic microscopy) .....	175
VIII.3.1.3. FTIR-ATR (Fourier transform attenuated total reflectance infrared spectroscopy) .....	175
VIII.3.1.4. Immunofluorescence.....	176
VIII.3.2. <i>In vivo</i> Study.....	176
VIII.3.2.1. $\mu$ -CT scanning.....	177
VIII.3.2.2. Tissue processing .....	177
VIII.3.2.3. Histomorphometrical Analysis.....	178
VIII.3.3. Statistical Analysis.....	178
VIII.4. Results and Discussion.....	178
VIII.4.1. <i>In vitro</i> study .....	178
VIII.4.2. <i>In vivo</i> study .....	182
VIII.4.2.1. Neobone formation assessment.....	183
VIII.4.2.2. Histology characterization .....	185
VIII.4.2.2.1. Histomorphometric Analysis .....	186

VIII.5. Conclusions .....	190
VIII.6. References .....	191
SECTION VI	
GENERAL CONCLUSIONS .....	195
Chapter IX	
FINAL REMARKS AND FUTURE STUDIES .....	197
IX.1 .General Conclusions .....	199
IX.2. Final Remarks and Future Studies .....	204



## Short Curriculum Vitae

Márcia Teresa da Silva Rodrigues was born in Porto (Portugal) in 1981. She was graduated in Applied Biology at the School of Sciences in University of Minho (Portugal) in June 2004.

She started her PhD in 2005 at the 3Bs Research Group-University of Minho (under the supervision of Professor Manuela E. Gomes and Professor Rui L. Reis) in cooperation with the Department of Regenerative Medicine at the Wake Forrest Institute of Regenerative Medicine (Winston-Salem, NC, USA) under the local supervision of Dr Sang Jin Lee and Professor James Yoo.

She was also involved in the preparation of European (FP7) and National (Portuguese Foundation for Science and Technology) research projects proposals. She was co-responsible for the internal cell culture training at the 3B's Research Group and the Headquarters of the European Institute of Excellence on Tissue Engineering and Regenerative Medicine. She is also a Credited Technician on Animal Experimentation, accreditation Issued by Direcção Geral de Veterinária, Ministério da Agricultura, do Desenvolvimento Rural e das Pescas on February 8<sup>th</sup> 2007, after performing the *Laboratory Animal Science Course* by FELASA in 2006.

During the course of her PhD, she was part of the organization committee of the TERMIS-EU, held in Porto, Portugal (2008). She was invited to be a scientific abstract reviewer in the annual conference of Society for Biomaterials in 2008 (Atlanta, USA) and 2009 (San Antonio, USA), and a reviewer for the Journal of Tissue Engineering and Regenerative Medicine.

As a result from her research, she has participated in the most relevant conferences and workshops in the Biomaterials and Regenerative Medicine field, with a total of 13 oral communications and 15 poster presentations. She has been awarded a Fundação Calouste Gulbenkian Travel award for attendance at Society of Biomaterials Meeting 2006 (Chicago, USA) and the award for the "Best 50 abstracts awards" submitted to the Tissue Engineering and Regenerative Medicine International Society - European Chapter Conference (TERMIS-EU) in 2008.

Presently, Márcia Teresa da Silva Rodrigues is author of 9 published papers in international refereed journals, 1 paper in press, 5 papers submitted for publication, 1 invited review paper and 1 book chapter.



## This Thesis is based on the following publications

### Papers in international refereed journals:

**Rodrigues MT**, Gomes ME and Reis RL, Current strategies in osteochondral regeneration: from stem cells to pre-clinical approaches, *Current Opinion in Biotechnology, Tissue, Cell and Pathway Engineering* issue 22: 1-8 - invited review paper (2011).

**Rodrigues MT**, Martins A, Dias IR, Viegas CAA, Neves NM, Gomes ME and Reis RL, Synergistic effect of scaffold composition and dynamic culturing environment in multi-layered systems for bone tissue engineering, accepted for publication in *Journal of Tissue Engineering and Regenerative Medicine* (2011).

**Rodrigues MT**, Groen N, Leonor I, Carvalho PP, Dias, Caridade S, Mano JF, van Blitterswijk CA, Gomes ME and Reis RL, Functional biodegradable scaffolds for Bone Tissue Engineering - degradation behaviour, bioactivity prolife and osteogenic differentiation of marrow mesenchymal cells, *submitted*

**Rodrigues MT**, Lee SJ, Gomes ME, Reis RL, Atala A, Yoo J, Bilayered constructs aimed at osteochondral strategies: the influence of media supplements in the osteo and chondrogenic differentiation of amniotic fluid-derived stem cells, *submitted*

**Rodrigues MT**, Lee SJ, Gomes ME, Reis RL, Atala A, Yoo J, Amniotic fluid stem cells versus bone marrow mesenchymal stem cells for bone tissue engineering, *submitted*

**Rodrigues MT**, Gomes ME, Viegas CAA, Azevedo JT, Dias IR, Gúzon FM and Reis RL, Tissue Engineered Constructs based on SPCL Scaffolds Cultured with Goat Marrow Cells: Functionality in Femoral Defects, *Journal of Tissue Engineering and Regenerative Medicine* 2011; 5: 41-49.

**Rodrigues MT**, Lee BK, Shiner T, Lee SJ, Gomes ME, Reis RL, Atala A, Yoo J, The effect of the differentiation stage of amniotic fluid stem cells seeded onto biodegradable scaffolds in the regeneration of non-union defect, *submitted*

### Book Chapters:

Gomes ME, Oliveira JT , **Rodrigues MT**, Santos MI , Tuzlakoglu K, Viegas C A A, Dias IR and Reis RL, Sarch-polycaprolactone based scaffolds in bone and cartilage tissue engineering approaches, In *Natural-based polymers for biomedical applications*, eds. RL Reis, J Mano, N Neves, H Azevedo , AP Marques, ME Gomes, Woodhead Publishing, Cambridge, 337-356 (2008).



## List of Figures

### Chapter I

#### ***Current strategies for osteochondral regeneration: from stem cells to pre-clinical approaches***

Figure I.2.1 – Clinical and Tissue Engineering strategies to promote the regeneration of osteochondral defects. ....6

### Chapter II

#### ***Materials and Methods***

Figure II.2.1 – Ring opening polymerization of  $\epsilon$ -caprolactone to polycaprolactone. .... 25

Figure II.2.2 – Chemical structure of starch components: amylose (A) and amylopectin (B). .... 26

Figure II.2.3 – Structure of agarose molecule ..... 28

Figure II.6.1 - Harvesting marrow from the goat iliac crest. .... 36

Figure II.6.2 - 2D culture of gBMSCs after 10 days in basal medium. .... 38

Figure II.6.3 – Calcein AM cleavage by viable cells. .... 43

Figure II.7.1 - Non-critical size defects drilled in the posterior femur of a goat model. .... 52

### Chapter III

#### ***Synergistic effect of scaffold composition and dynamic culturing environment in multi-layered systems for bone tissue engineering***

Figure III.4.1 - FTIR-ATR analysis of multi-layered scaffolds. Membranes of PCL nanofiber mesh (PCL) were used as controls. .... 73

Figure III.4.2 - XRD analysis of multi-layered PCL-TCP scaffolds. Membranes of PCL nanofiber mesh (PCL) were used as controls. .... 74

Figure III.4.3 – SEM analysis of multilayer scaffolds; the upper SEM micrographs refer to the PCL-TCP multilayer scaffolds while the lower pictures correspond to the control of PCL nanofiber mesh (left to right: 100 x, 300 x and 1000 x magnifications). .... 74

Figure III.4.4 – gBMSCs proliferation given by DNA quantification was assessed onto PCL-TCP scaffolds and PCL membranes (control) after 7, 14 or 21 days in basal or osteogenic media in either static (st) or dynamic (dyn) conditions. Symbols \*, \*\*, and \*\*\* denote study groups with statistically significant differences ( $p < 0.05$ ), as using One Way ANOVA method. .... 75

Figure III.4.5 – gBMSCs osteogenic differentiation given by ALP/DNA ratio was assessed onto PCL-TCP scaffolds and PCL membranes (control) after 7, 14 or 21 days in basal or osteogenic media in either static (st) or dynamic (dyn) conditions. Symbols \*, and \*\* denote st groups with statistically significant differences ( $p < 0.05$ ), as using One Way ANOVA method. .... 76

Figure III.4.6 – Osteogenic phenotype characterization of gBMSCs seeded onto PCL-TCP scaffolds after 21 days in culture with basal or osteogenic media, either in static or dynamic conditions. Immunocytochemistry (ICC) was performed for Collagen I and Osteocalcin, as well as Alizarin Red staining. Insets represent PCL meshes (control) under the same conditions. .... 77

## Chapter IV

### ***Functional biodegradable scaffolds for bone tissue engineering: bioactivity profile and osteogenic differentiation of marrow mesenchymal stromal cells***

Figure IV.4.1 - TF-XRD patterns of SPCL fiber meshes produced by wet-spinning, where a calcium silicate solution was used as a coagulation bath (SPCL-Si), and subsequently soaked in SBF for 7 days. SPCL was used as control. .... 93

Figure IV.4.2 - 2D and 3D micro-CT and SEM images of SPCL-Si scaffolds before and after 1, 3 or 7 days in SBF. Control scaffolds of SPCL (without silanol groups) (CTR) after 7 days in SBF. Blue corresponds to the apatite deposition. .... 94

Figure IV.4.3 - Changes in calcium (Ca), phosphorus (P) and silicon (Si) concentration in the SBF solution after different immersion periods of the SPCL or SPCL-Si scaffolds. Symbols o and + denote study groups with statistically significant differences ( $o = p < 0.001$  and  $+ = p < 0.05$ , respectively), as using Two Way ANOVA method. .... 94

Figure IV.4.4 - Variation of the storage modulus as a function of frequency between 0.1 and 15 Hz after equilibration at 37 °C with the samples immersed in PBS solution. .... 96

Figure IV.4.5 - Results obtained from the MTS test performed on gBMSCs seeded onto SPCL-Si scaffolds (SPCL-Si) and SPCL-Si scaffolds pre-coated with an apatite layer (SPCL-Si-7SBF), and cultured in osteogenic medium for 7 or 14 days. Symbol \* denote study groups with statistically significant differences ( $p < 0.05$ ), as using Two Way ANOVA method. .... 97

Figure IV.4.6 - Results from ALP assays performed on seeded onto SPCL-Si scaffolds (SPCL-Si) and SPCL-Si pre-coated with an apatite layer layer (SPCL-Si-7SBF) and, after culture in osteogenic medium for 7 or 14 days. .... 98

Figure IV.4.7 - SEM pictures showing the gBMSCs morphology when seeded onto SPCL-Si (SPCL-Si) scaffolds and SPCL-Si scaffolds pre-coated with apatite (SPCL-Si-7SBF), followed by culture in osteogenic medium for 7 or 14 days. Inset micrographs refer to scaffolds, SPCL-Si (C2) and SPCL-Si pre-coated (C4) after 7 days in osteogenic medium. .... 98

Figure IV.4.8 - Assessment of calcified matrix production by gBMSCs seeded onto SPCL-Si scaffolds (SPCL-Si) after 14 days in osteogenic medium..... 99

**Chapter V**

***Bilayered constructs aimed at osteochondral strategies: the influence of media supplements in the osteo and chondrogenic differentiation of amniotic fluid-derived stem cells***

Figure V.4.1 – Calcein AM stained samples of AFSCs encapsulated in agarose gels after 7, 14, and 21 days in chondrogenic and basal medium (control). ..... 113

Figure V.4.2 – Immunofluorescent analysis of collagen type II expression in AFSCs encapsulated in agarose gels after 7, 14, and 21 days in chondrogenic and basal media (control). Magnification, 200X..... 114

Figure V.4.3 - Immunofluorescent analysis for aggrecan expression in AFSCs encapsulated in agarose gels after 7, 14 and 21 days in chondrogenic or basal media (control). Magnification, 200X..... 115

Figure V.4.4 - SEM micrographs of the osteogenic layer (AFSCs seeded onto SPCL scaffold) of the bilayered scaffolds after 7 or 14 days in OC culture media. IGF-1(+) indicates culture medium supplemented with IGF-1 while IGF-1(-) refers to the same culture medium without IGF-1. The basal culture medium consisted of the basic medium currently used for AFSC expansion and maintenance, and was used as the control medium in these studies. .... 116

Figure V.4.5 - Immunofluorescence for RunX-2 expression in the osteogenic layer (AFSCs seeded onto SPCL scaffolds) of the bilayered scaffolds after 14 days (14d) in the OC culture media. IGF-1(+) indicates culture medium supplemented with IGF-1 while IGF-1(-) refers to the same culture medium without IGF-1. “Basal” refers to the basic medium currently used for AFSC expansion and maintenance, and was used as a control in this assay..... 119

Figure V.4.6 - Viability of the chondrogenic layer (AFSCs in agarose gels) of the bilayered scaffold after 7 (7d) or 14 days (14d) in the OC culture media. IGF-1(+) indicates culture medium supplemented with IGF-1 while IGF-1 (-) refers to the same culture medium without IGF-1. “Basal” represents the basic medium currently used for AFSC expansion and maintenance, and was used as a control. .... 120

Figure V.4.7 - Collagen type II expression (200x magnification) in the chondrogenic layer (AFSCs in agarose gels) of the bilayered scaffold after 7 or 14 days in OC culture medium. IGF-1(+) indicates culture medium supplemented with IGF-1 while IGF-1 (-) refers to the same culture medium without IGF-1. Cultures maintained in basal medium were used as controls. .... 121

Figure V.4.8 - Aggrecan immunofluorescence (200 x magnification) in the chondrogenic layer (AFSCs in agarose gels) of the bilayered scaffold after 7 or 14 days in OC culture

medium. IGF-1(+) indicates culture medium supplemented with IGF-1 while IGF-1(-) refers to the same culture medium without IGF-1. Culture in basal medium was used as a control. .... 121

Figure V.4.9 - Safranin-O (cartilage-specific) staining of the chondrogenic layer (AFSCs in agarose gels) of the bilayered scaffold after 14 days in OC culture medium. IGF-1(+) indicates culture medium supplemented with IGF-1 while IGF-1 (-) refers to the same culture medium without IGF-1. "Basal" represents the basic medium currently used for AFSC expansion and maintenance, and was used as a control. Magnification, 200X. .... 122

## Chapter VI

### ***Amniotic fluid stem cells versus bone marrow mesenchymal stem cells as a source for bone tissue engineering***

Figure VI.4.1– Viability assay (green) and Alizarin Red (red) staining of hAFSCs and hMSCs cultured in 2D environment for 0, 7, 14 or 21 days in osteogenic medium. .... 136

Figure VI.4.2- ALP staining of hAFSCs and hMSCs cultured in 2D environment for 0, 7, 14 or 21 days in osteogenic medium. .... 137

Figure VI.4.3 – Calcium quantification ( $\mu\text{g/ml/well}$ ) of AFSCs and BMSCs in 2D cultures in osteogenic medium for 0, 7, 14 or 21 days. .... 138

Figure VI.4.4 – Viability assay of AFSCs and BMSCs seeded onto SPCL scaffolds and cultured in osteogenic medium for 0, 7, 14 or 21 days. .... 138

Figure VI.4.5 - Scanning electron microscopy of AFSCs and BMSCs seeded onto SPCL scaffolds in osteogenic culture for 0, 7, 14 or 21 days. .... 139

Figure VI.4.6 - Calcium quantification ( $\mu\text{g/ml/construct}$ ) of AFSCs- and BMSCs-SPCL constructs in osteogenic medium for 0, 7, 14 or 21 days. .... 139

Figure VI.4.7 – Immunofluorescence of RunX2 expression in AFSCs- and BMSCs-SPCL constructs in osteogenic medium for 0, 7, 14 or 21 days. .... 140

Figure VI.4.8 – Immunofluorescence of Collagen I expression in AFSCs- and BMSCs-SPCL constructs in osteogenic medium for 0, 7, 14 or 21 days. .... 141

## Chapter VII

### ***Tissue engineered constructs based on SPCL scaffolds cultured with goat marrow cells: functionality in femoral defects***

Figure VII.3.1 - Diagram of the implantation site: A) empty drill defects, B) defects filled with SPCL (no cells), defects filled with cell-SPCL constructs after C) 1 day of culture and D) 7 days of culture in osteogenic medium. Implants were placed in the same anatomical site relative to both posterior femurs in each animal. .... 157



Figure VII.4.1 - SEM micrographs of SPCL scaffolds seeded with gBMSCs and <i>in vitro</i> cultured in osteogenic culture for 1 day (A) or 7 days (B).....	159
Figure VII.4.2 - <i>In vitro</i> double strand DNA concentration in SPCL scaffolds seeded with gBMSCs cultured in osteogenic culture for 1 and 7 days.....	160
Figure VII.4.3 - <i>In vitro</i> ALP activity in SPCL scaffolds seeded with gBMSCs cultured in osteogenic culture for 1 or 7 days. ....	160
Figure VII.4.4 - Drill sections marked with Lévai-Laczkó staining. In A) Control 1 – empty drill defects, B) Control 2 – defects filled with SPCL (no cells), C) defects filled with cells-SPCL constructs after C1) 1 day of culture and C2) 7 days of culture in osteogenic medium. ....	162
Figure VII.4.5 - Drill sections marked with Xylenol Orange (red), Calcein Green (green) and Tetracycline (not observed) fluorescence stainings. In A) Control 1 – empty drill defects, B) Control 2 – defects filled with SPCL (no cells), C) defects filled with cell-SPCL. ....	162
Figure VII.4.6 – New bone formation percentage in the different induced drills: A) empty drill defects, B) defects filled with SPCL (no cells), defects filled with cell-SPCL constructs after C) 1 day of culture and D) 7 days of culture in osteogenic medium. ....	163
Figure VII.4.7 - New bone roundness measured for the different induced drills: A) empty drill defects, B) defects filled with SPCL (no cells), defects filled with cell-SPCL constructs after C) 1 day of culture and D) 7 days of culture in osteogenic medium. ....	164
 <b>Chapter VIII</b>	
<b><i>The effect of the differentiation stage of amniotic fluid stem cells seeded onto biodegradable scaffolds in the regeneration of non-union defects</i></b>	
Figure VIII.4.1 - SEM micrographs of hAFSCs-SPCL constructs after 0, 7, 14 or 21 days in osteogenic medium. ....	179
Figure VIII.4.2 – Characterization of AFSCs-SPCL constructs for ALP staining after 0, 7, 14 or 21 days in osteogenic culture.....	179
Figure VIII.4.3 - Characterization of AFSCs-SPCL constructs for collagen I by immunofluorescence, after 0, 7, 14 or 21 days in osteogenic culture. ....	179
Figure VIII.4.4 – Characterization of AFSCs-SPCL constructs by SEM and EDS analysis. SEM magnified images of calcium phosphate nodules at the surface and inside (inset) of these constructs after 21 days in osteogenic medium. The presence of calcium and phosphorus atoms was detected by EDS analysis after 0, 7, 14 and 21 days in osteogenic culture. SPCL spectrum represents a SPCL scaffolds without seeded cells.....	180
Figure VIII.4.5 - Calcium content measurement in AFSCs-SPCL constructs after 0, 7, 14 or 21 days in osteogenic culture. ....	181

Figure VIII.4.6 - Characterization of AFSCs-SPCL constructs by FT-IR analysis. The presence of calcium and phosphorus groups was detected after 0, 7, 14 or 21 days in osteogenic culture. SPCL spectrum represents a SPCL scaffolds without seeded cells. ....	182
Figure VIII.4.7 - Picture of dissected femurs after an end point. Femur on the left represents a femur post-implantation and on the right, the left rear femur, control. ....	182
Figure VIII.4.8 - m-CT images obtained from all defect conditions after 4 and 16 weeks of implantation. ....	183
Figure VIII.4.9 – Volumetric measurements of the defect section obtained from mCT analysis using Mimics software, representing the bone neoformation area.....	184
Figure VIII.4.10 – Detailed image of native bone and SCPL scaffold interface in vivo after 4 weeks showing the native bone remodeling process aiming at defect regeneration (both pictures are 200x magnified). ....	185
Figure VIII.4.11 – Histometric analysis for collagen I expression (%) in the studied conditions. Values are represented by mean $\pm$ standard error of mean. Symbol * denote study groups with statistically significant differences ( $p < 0.05$ ), as using Two Way ANOVA method.....	186
Figure VIII.4.12 – Histometric analysis for osteocalcin expression (%) in the studied conditions. Values are represented by mean $\pm$ standard error of mean. Symbol * denote study groups with statistically significant differences ( $p < 0.05$ ), as using Two Way ANOVA method.....	187
Figure VIII.4.13 – Histometric analysis for VEGF expression (%) in the studied conditions. Values are represented by mean $\pm$ standard error of mean.....	188
Figure VIII.4.14 – Detection of blood vessel formation in H&E stained sections for all conditions studied after 4 or 16 weeks of implantation. Pictures were 200x magnified. ....	189

## List of Tables

### Chapter I

#### ***Current strategies for osteochondral regeneration: from stem cells to pre-clinical approaches***

Table I.2.1 - Overview of the scaffold-cells constructs that have been studied for osteochondral tissue applications in pre-clinical models in the past 5 years. 13

### Chapter V

#### ***Bilayered constructs aimed at osteochondral strategies: the influence of media supplements in the osteo and chondrogenic differentiation of amniotic fluid-derived stem cells***

Table V.4.1 - Results obtained from EDS analysis concerning atomic percentage (At %) of several ions present in AFSCs-SPCL layer after 7 (7d) and 14 (14d) days in osteochondral culture medium (broader analysis). 116

Table V.4.2 - Results obtained from EDS analysis concerning atomic percentage (At %) of several ions present in AFSCs-SPCL layer after 7 (7d) and 14 (14d) days in osteochondral culture medium. EDS analysis was performed in mineralization aggregate areas of the constructs. 118



## List of Abbreviations and Symbols

### 2

2D: bidimensional

### 3

3D: tridimensional

### -A-

$\alpha$ -amylase: alpha-amylase  
 $\alpha$ -MEM: alpha-Modification Eagle Medium  
A/B: antibiotic/antimicrobial  
AFSCs: amniotic fluid stem cells  
ALP: alkaline phosphatase  
AR: alizarin red  
ARS: alizarin red staining

### -B-

$\beta$ -TCP: beta tricalcium phosphate  
BM: bone marrow

### -C-

cm<sup>2</sup>: square centimeter  
Ca or Ca<sup>2+</sup>: Calcium  
Calcein AM: Calcein acetoxymethyl ester  
CaP: calcium phosphates  
CD: cluster differentiation  
Cl<sup>-</sup>: chloride ion  
CaCl<sub>2</sub>: calcium chloride  
CPDA-1: citrate-phosphate-dextrose-adenine 1

### -D-

DAPI: 4',6-diamidino-2-phenylindole  
DMA: Dynamic Mechanical Analysis  
DMEM: Dulbecco Modified Eagle Medium  
DMSO: dimethyl sulfoxide  
DNA: deoxyribonucleic acid  
dsDNA: double-stranded DNA

### -E-

ECM: extracellular matrix  
EDS: energy dispersion spectroscopy  
EDTA: ethylenediaminetetraacetic acid  
ELISA: enzyme linked immunosorbent assay  
ES-FBS: embryonic stem cell screened FBS

Ex/Em: Excitation/Emission

### -F-

FBS: foetal bovine serum  
FDA: Food and Drug Administration  
FTIR-ATR: Fourier transformed infra-red spectroscopy with attenuated total reflectance

### -G-

g: gram  
gBMSCs: goat bone marrow cells  
GFP: green fluorescent protein

### -H-

h: hour  
hAFSCs: human amniotic fluid stem cells  
hBMSCs: human mesenchymal stem cells  
HA: hydroxyapatite  
HAc: hyaluronic acid  
HCl: hydrochloric acid  
HCO<sub>3</sub><sup>-</sup>: bicarbonate ion  
HPO<sub>4</sub><sup>2-</sup>: orthophosphate ion

### -I-

ICP: Induced-coupled plasma emission spectroscopy  
IGF-1: insuling growth factor 1  
IM: intramuscular  
ITS: insulin transferin selenium

### -K-

kPa: kilo pascal  
kV: kilo volt  
kVp: peak kilovoltage  
K<sup>+</sup>: potassium  
KCl: potassium *chloride*  
K<sub>2</sub>PO<sub>4</sub>·3H<sub>2</sub>O

### -M-

$\mu$ A: micro Ampere  
 $\mu$ g: microgram  
 $\mu$ m: micrometer  
mA: mili Ampere  
m-CT or  $\mu$ -CT: micro Computed Tomography

mL: milliliter  
mg: miligram  
mm: milimeter  
ms: milisecond  
mM: milimolar  
 $\mu\text{mol}/\text{ml}^{-1}$ : micro mol per mL  
M: molar  
Mg or  $\text{Mg}^{2+}$ : magnesium  
 $\text{MgCl}_2 \cdot 6\text{H}_2\text{O}$ : Magnesium Chloride Hexahydrate  
MSCs: mesenchymal stem cells  
MTS: (3-(4,5-dimethylthiazol-2-yl)-5-(3-carboxymethoxyphenyl)-2-(4-sulfophenyl)-2H-tetrazolium)

#### **-N-**

nm: nanometer  
 $\text{Na}^+$ : sodium  
NaOH: sodium hydroxide  
NaCl: sodium chloride  
 $\text{NaHCO}_3$ : sodium carbonate  
 $\text{NaSO}_4$ : sodium sulfate

#### **-O-**

OC: osteochondral  
OCa: osteocalcin  
OPF: oligo-polyethylene-glycol fumarate

#### **-P-**

P: phosphorus  
Pa: passage  
PBS: phosphate buffer saline  
PCL: polycaprolactone  
PGA: polyglycolic acid  
PLGA: polylactic-co-glycolic acid  
PLAGA: poly(lactic *acid*-co-glycolic *acid*)  
P/S: penicillin /streptomycin

#### **-R-**

RNA: ribonucleic acid  
rpm: rotation per minute

#### **-S-**

SEM: scanning electronic microscopy  
Si: silicium  
Si-OH: silanol groups  
SBF: simulated body fluid  
SPCL: blend of corn starch with polycaprolactone

SPCL-Si: blend of corn starch with polycaprolactone with functionalized silanol groups (with a silicate precipitation solution)  
 $\text{SO}_4^{2-}$ : sulphate

#### **-T-**

TCPs: tricalcium phosphates  
TE: tissue engineering  
TF-XRD: Thin-film X-ray diffraction  
TGF- $\beta$ 1: transforming growth factor beta 1  
 $(\text{CH}_2\text{OH})_3\text{CNH}_2$ : tris-hydroxymethyl-aminomethane

#### **-U-**

UI or U.I.: International Units  
UK: United Kingdom  
US: United States  
USA: United States of America

#### **-X-**

XRD: X-ray diffraction

#### **-W-**

WFIRM: Wake Forest Institute and Regenerative Medicine  
wt/v: weight/volume

**SECTION I**

**GENERAL INTRODUCTION**





## Chapter I

### **CURRENT STRATEGIES FOR OSTEOCHONDRAL REGENERATION: FROM STEM CELLS TO PRE-CLINICAL APPROACHES**

*This chapter is based on the following publication:*

Rodrigues MT, Gomes ME, Reis RL, Current strategies for osteochondral regeneration: from stem cells to pre-clinical approaches. *Current Opinion in Biotechnology* 22: 1-8 - *invited review paper* (2011).



**CURRENT STRATEGIES FOR OSTEOCHONDRAL REGENERATION:  
FROM STEM CELLS TO PRE-CLINICAL APPROACHES**

**I.1. Abstract**

Damaged cartilage tissue has no functional replacement alternatives and current therapies for bone injury treatment are far from being the ideal solutions emphasizing an urgent need for alternative therapeutic approaches for osteochondral regeneration.

The tissue engineering field provides new possibilities for therapeutics and regeneration in rheumatology and orthopaedics, holding the potential for improving the quality of life of millions of patients by exploring new strategies towards the development of biological substitutes to maintain, repair and improve osteochondral tissue function. Numerous studies have focused on the development of distinct tissue engineering strategies that could result in promising solutions for this delicate interface. In order to outperform currently used methods, novel tissue engineering approaches propose, for example, the design of multi-layered scaffolds, the use of stem cells, bioreactors or the combination of clinical techniques.

## I.2. Introduction

Osteochondral (OC) interfaces are part of the joint, being a specialized and integrated structure consisting of multiple connective tissue elements, including muscles, tendons, ligaments, synovium, cartilage, and bone, organized to permit stability and movement of the human skeleton.

OC injuries can lead to joint malfunction and ultimately to the development of degenerative diseases such as osteoarthritis. With an increasing aging population, OA represents a significant socio-economical burden worldwide. Although several procedures are available on the clinical market, an ideal solution has yet to be found in order to fulfill all necessary requirements for a long term successful regenerative approach.

This paper is aimed at reviewing distinct strategies aiming at a successful OC regeneration, involving cells, scaffolds, bioreactors or a combination of these elements. The rationale for currently used techniques as well as some promising studies in animal models will be also discussed in this review in order to highlight the state-of-the-art in OC over the past few years (Figure I.2.1).

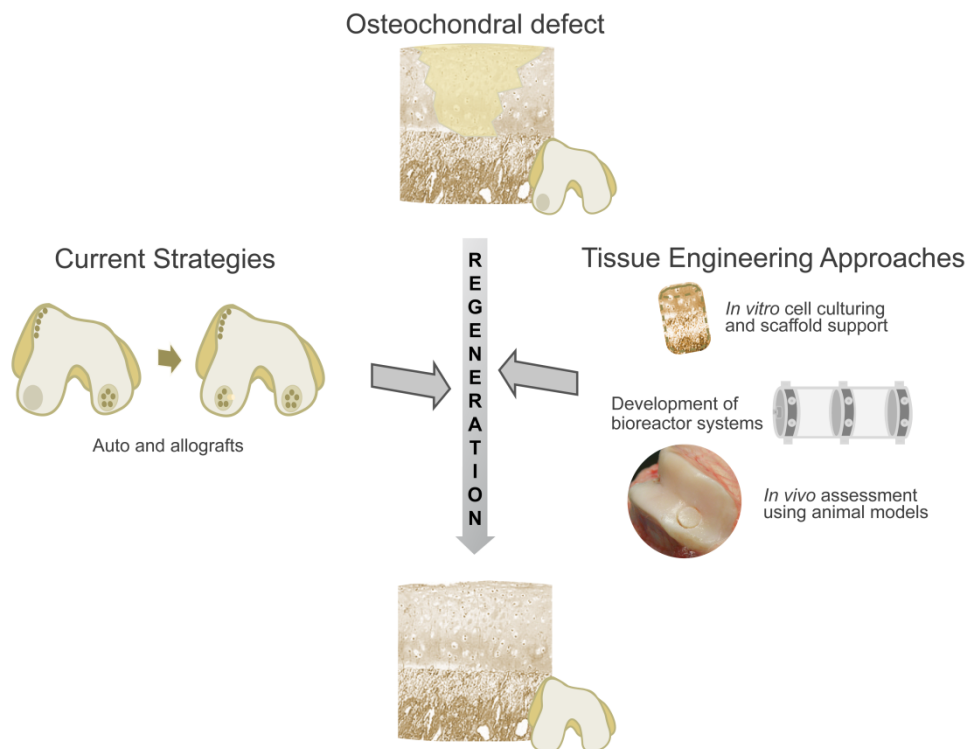


**Figure I.2.1** – Clinical and Tissue Engineering strategies to promote the regeneration of osteochondral defects.

One of the most challenging goals in bone and cartilage tissue engineering (TE) is the creation of an engineered OC interface to repair damaged areas. Similarly to the natural milieu, an engineered interface should distribute everyday mechanical stresses with low-friction load bearing, while interacting with different structural and biological needs in a stable environment. This is particularly more demanding and unique if one considers the distinctive requirements of bone and cartilage tissues as well as the several OC systems found in the human body, dependent on their location and functionality.

Several materials, shapes, stiffness and chemical compositions were described for bone[1-8] and cartilage scaffolds[8-21], considering the relevance of scaffold architecture to sustain the mechanical stresses of the joint as well as to guide the cells into the desired phenotype, and promoting a complete integration of the OC system in order to restore tissue functionality.

The selection of cells plays also an important element in this delicate interface headed for engineered grafts. Several potential cells sources were successfully described for bone[22-26], and cartilage[17, 22-27], which are likely to be useful for OC strategies[8].

The subsequent step towards the clinical application is the up-scale and custom made production of the OC implants to fit perfectly to the injured area and to provide the biological and structural needs required to restore tissue function. In order to automate and make the system cost-effective, several bioreactor models[28, 29] were designed and have been showing promising results.

### **1.2.1. Osteochondral defects (OCD)**

Most OC lesions or defects (OCD) and OC injury-associated diseases lead to loss of integrity or stability at the articular surface with resultant decrease range of motion of the involved joint, and, ultimately, premature osteoarthritis[30]. Although OCDs occur as a result of repetitive trauma within the joint, several factors, such as ischemia, genetics, abnormal vasculature, and metabolic disorders are associated to body processes leading to loss of cartilage[31] or to relevant changes in the architecture or composition of the bone[32]. Furthermore, joint healing is strongly dependent on age, as age is the strongest known risk factor for development of OA[33] and depth of injury is also age associated[34]. Aged cartilage also induces changes in chondrocyte function and material properties, and responds differently to cytokines and growth factors[33].

The location of a particular defect[35] does influence repair response of the cartilage as well as the mechanical alignment of the joint[36]. OC lesions are identified most frequently in

the femoral condyles[37], capitellum of the elbow[38], dome of the talus[30], and the dorsal surface of the patella[37].

### **I.2.2. Weight bearing influence in biomechanics of the joint**

Homeostasis of articular cartilage depends on mechanical loads generated during daily activity. Some joint areas are particularly more affected by weight pressure than others, which may progress to a more degenerative and diffuse joint involvement that translates to the patient by causing pain, swelling, clicking, and instability. Ultimately, inappropriate joint loads are associated to focal stress and result in focal degeneration of cartilage, as occurs in OA, and increase the stress on subchondral bone. Changes in pressure and shear stress induced by joint movement may induce changes in matrix protein expression and in the release of nitric oxide associated to joint pathogenesis[39].

The stress may also vary throughout the cartilage on a joint surface, because loading is not completely uniform, leading to gradients in stress and pressure[40]. This effect is evident in most patients, where the surface of the joints does not conform perfectly under loading and may result in an increased risk for OA progression[33].

### **I.2.3. Current treatments in clinical field**

Currently available treatments depend upon the size of the OC defect and the condition of the overlying cartilage. Using reparative surgery, cartilage treatments include arthroscopic debridement, abrasion arthroplasty and microfracture. These procedures stimulate the body to heal the injury, mainly resulting in the formation of fibrocartilage[41]. Fibrocartilage is a scar tissue presenting diminished resilience, reduced stiffness, and poor wear characteristics when compared to hyaline cartilage. Thus, fibrocartilage is unlikely to withstand physiological loading and cannot guarantee to function successfully in long term. Nevertheless, other options are available with restorative surgery, namely, autografts recurring to mosaicoplasty procedures, allografts[42, 43] and biologic replacement using cultured autologous chondrocytes[44, 45]. The biggest challenge with autografts is to achieve a final round shape that mimics the surface of the articular joints. Allografts procedure is similar to autografts[46] and mostly used after other surgeries have failed. It is not recommended for patients with OA, and the limited supply of donor tissue is a major problem of this practice.

Autologous chondrocyte transplantation/implantation[44] has also been described to help restoring the structural make up of the articular cartilage. The intermediate and long-term functional and clinical results are promising, especially regarding the durability of the repair in human patients follow up[45].

More recently[47], tissues from the covering of bone and cartilage are implanted into the lesion through periosteal and perichondral grafting to promote the repair and functionality of cartilage.

Despite the availability of procedures, all current treatment options inflict further tissue destruction before any therapeutic effect can be achieved.

#### **1.2.4. TE strategies to improve available treatments**

##### **1.2.4.1. Cells to promote healing**

Despite current knowledge in OC field, the selection of a cell source to promote efficient OC regeneration is a major issue that must to be considered. Ideally, a cell source should enable insignificant donor morbidity or tissue scarcity, resurface joints with cartilage, have no limitations in the amounts available and be easy to maintain/expand *in vitro*, be readily available, have no issues of immunogenicity or diseases transmission risks and be of low cost.

Tissue insufficient supply and morbidity, and host immune responses and disease transmission risks limit chondrocyte and osteoblast as ideal cells in OC strategies. Among adult stem cells, bone marrow mesenchymal stem cells (BMSCs)[15, 16, 19, 20, 22 ,48-51] and adipose-derived stem cells (ASCs)[9, 12, 26, 48, 50, 52] are the most investigated. Nevertheless, some studies described a higher chondro-[50] and osteogenic[48] potential of BMSCs when compared to ASCs. The effectiveness of autologous BMSCs transplantation for the repair of full-thickness articular cartilage defects was assessed in patellae lesions of two human patients[53]. A similar approach was also considered to repair full thickness femoral condyle defect in an athlete, who had reattained his previous activity level and experienced neither pain nor other complications[27].

Other cell sources, including synovial tissue and periosteum-derived stem cells have also showed potential for osteo- and chondro-genic differentiation[24, 54]. Cells from synovial membrane are harvested with minimal complications at the donor site due to a high self-regenerative capability[24] of synovial tissue. The periosteum is a specialized fibrous tissue composed of fibroblast, osteoblast, and progenitor cells that may also be a possible cell source

for OC TE based on its accessibility, rapid proliferation and differentiation potential[54]. Furthermore, after skeletal surgery procedures, periosteum is often used as a covering layer over tissue to stimulate local regeneration. Despite the potential, periosteum-derived cells should be more investigated for cellular therapies[55].

Umbilical cord stem cells (UCSCs) together with amniotic fluid derived stem cells (AFSCs) were also introduced to cartilage and bone TE [8, 23, 25] presenting interesting characteristics, since they are easier to obtain and represent an almost unlimited stem cell sources. Some risks were associated to human AFSCs harvesting but, as pregnant women are older than ever before, amniocentesis is likely to become a routine procedure in future years. More recently, cells from human fetal membranes and placenta, with similar features to human UCMSCs and AFSCs, have also been successfully differentiated into osteogenic and chondrogenic lineages[56]. Although embryonic stem cells (ES)[57] hoped for a promising future in regenerative medicine, its use is still ethically controversial and has major ethical considerations associated. Notwithstanding that human ES cells express molecules which could cause immune rejection[57] and present a high genomic instability[57], ES cells transplantation in a collagen gel have shown to induce the formation of cartilage tissue[17] under mechanical condition in rats aiming at OC regeneration.

More recently, iPS technology, where iPS cells are generated by reprogramming of somatic cells through the exogenous expression of transcription factors, holds great promise for regenerative medicine in autologous cell replacement therapies and in genetic defects by restoring cellular function[58]. Nevertheless and due to iPS recent development, cell characterization and *in vivo* functionality are to be addressed in bone and cartilage fields.

Stem cells obtained from different sources are likely to enable the most successful outcomes in OC regenerative approaches. Besides intrinsic characteristics of stem cells from a particular source, other factors should be monitored aiming at a successful strategy; such as final application, patient age, defect location and damage size. Cell culture media to induce chondrogenesis and osteogenesis of undifferentiated cells or maintain and proliferate primary chondrocytes and osteoblasts in an *ex vivo* atmosphere is commercially available. However, a common osteochondrocytic medium to co-culture or simultaneously differentiate bone and cartilage cells was not fully established yet, although some attempts have been described [8, 15, 59]. This approach can be advantageous to simplify cell culturing procedures and, simultaneously, reduce the time and production costs of an engineered graft towards a clinical scenario.



**1.2.4.2. Biomaterials: human designs to mimic natural extracellular material**

The implantation of cells in the afflicted area could be a direct approach in OC strategies, but the request for a support material to promote regeneration, especially in large sized defects, is to be critically considered. This idea is inspired in nature itself as, in the body, the majority of cells subsist in a 3D world, anchored onto a network of extracellular matrix (ECM), which scaffolding design proposes to recreate.

Scaffold characteristics will greatly influence cells and should mimic the complex and demanding environment to which cells are exposed to. Besides the tissue structural support and stimulation, either chemically or mechanically, the optimal scaffold should assist tissue functionality promoting the easy diffusion of nutrients, growth factors and cellular waste products[60]. Additionally, the ideal scaffold should be biocompatible and its biodegradability adjustable to the time required for tissue regeneration[60].

In the last few years, thousands of scaffolds have been proposed for reparative strategies made from different materials and production methodologies, with varying properties and composition. An OC scaffold should combine the better of the two worlds in a functional and integrated system. Lots of effort has been undertaken to achieve this goal and the most common approach is an independent cartilage or bone strategy, likely because chondrocytes and bone cells present different function-related characteristics including metabolic and structural features, yet communicating and interacting, in a unique culturing system.

Natural based polymers such as agarose[15, 61], starch[9], chitosan[9, 13, 14, 62], silk[14], gellan gum[12], hyaluronic acid[16], collagen[17, 63] or blends of these materials[9, 14, 18, 21], and synthetic materials such as polylactic acid (PLA)[8], polycaprolactone (PCL)[20] and oligo-polyethylene-glycol fumarate[49] have been proposed for cartilage applications. Most of these materials are processed into hydrogel and gel based matrices, which hold particular relevance for cartilage strategies because of their high water content, tissue-like elastic properties and the ability to encapsulate cells[64]. Also, gel structures partially tolerate shock absorption and deformation mimicking articular cartilage characteristics.

However, cartilage repair in OC interfaces should be accompanied by an adequate restoration of the underlying subchondral bone, enhancing the *in locus* integration of the OC system.

The minerals and the collagen fibers in the matrix are responsible for bone hardness and resistance. Nevertheless, the constant remodeling makes bone very plastic and capable of internal structural changes according to the stresses it is subjected to. Thus, bone regeneration

requires scaffolds with high mechanical and osteoconductive properties, and structurally strong enough to sustain weight bearing loads and avoid cartilage calcification, which leads to tissue malfunction and death. Scaffolds should also be biodegradable to keep up with the natural bone remodeling process. Despite the brittle behaviour and low tensile strength, inappropriate for significant torsion areas such as long bones, hydroxyapatite (HA) and tricalcium phosphate (TCP) are the most studied ceramics due to their osteoconductive and high mechanical properties, and are already used in some clinical applications[4,6]. Other materials, including silk[2, 7] , PCL and PCL blends[1, 3, 5], and PLA[8], have also been effectively tested as delivery systems[2] or artificial ECM[8], mimicking and recreating in some extent the structural organization of bone[1, 3, 7].

Some OC approaches successfully evaluated the *in vivo* application of scaffolds made of collagen fibrils with HA nanoparticles without implanted cells[65], which can be of particular importance if one considers the practical and commercial standpoint, as the engineered product could be a ready-to-use graft for surgery procedures. Furthermore, this approach would avoid tissue morbidity and scarcity of autologous cell sources or even immune reactions from allogenic sources and problems related to cell culturing methodologies (e.g., animal origin supplements).

Other strategies focus on the cellular interactions of implanted cells in the tissue surroundings, considering the reduced metabolism of cartilage. Chondrocytes in adult individuals do not divide or establish cell-to-cell contacts but are responsible to produce cartilage dense ECM[34], thus maintaining cartilage integrity.

Especially in elder patients, implanted cells could meliorate the native ECM properties, and improve the functionality of damaged tissue by stimulating fresh ECM production. In bony defects, the integration of cells in the implant may stimulate bone marrow cells and establish a metabolic balance favoring the neobone formation. Furthermore, in critical sized defects, cells are likely to participate in a molecular communication level bridging the native tissues to the implant towards a successful OC regeneration.

Different approaches to design an OC scaffold including hydrogels[49], combination of two distinct layers[21, 29, 62, 63] or a gradient scaffold[65], usually an association of a gel or a foam and a ceramic, have been developed as alternatives to this problem (Table I.2.1).

These complex scaffolds favor the integration into the native tissue after implantation and guide the cells, into the desired phenotype, according to the prearranged environment created from scaffold physical and chemical properties.

**Table I.2.1** - Overview of the scaffold-cells constructs that have been studied for osteochondral tissue applications in pre-clinical models in the past 5 years.

<i>Scaffolds</i>	<i>Cells</i>	<i>ref.</i>
OPF with gelatin microparticle hydrogel	Cell-free / marrow mesenchymal stem cells	[49]
PCL/TCP-PCL scaffold	Cell-free / marrow mesenchymal stromal cells	[20]
Hyaluronic acid gel sponges	Autologous mesenchymal stromal cells	[16]
Hyaluronate-type I collagen-fibrin scaffold	Cell-free /autologous chondrocytes	[18]
Hyaluronic acid-atelocollagen/ $\beta$ -TCP bilayered scaffold	Cell free / chondrocytes	[21]
Collagen/HA gradient scaffold	Cell free / autologous chondrocytes	[65,66]
Poly(lactide-co-glycolide)/nano-HA scaffold	Cell free / marrow mesenchymal stem cells	[51]
Poly(lactic acid (PLA)- coated polyglycolic acid (PGA) scaffold	Cell free / Autologous marrow mesenchymal stem cells	[19]
Collagen / $\beta$ -TCP bilayered scaffold	Cell free	[63]

More recently, emerging approaches include the incorporation of bone and/or cartilage growth factors in scaffolds[49, 63] to stimulate native tissue formation and differentiation *in vivo*. The inclusion of growth factors can ultimately recruit host cells into the damaged site, initiating a healing pathway, which could be promising for the treatment of OCDs.

#### **I.2.4.3. Assisted Devices: bioreactor systems**

The limited diffusion in static culture environments may constrain tissue ingrowth in engineered scaffolds. Bioreactors are usually designed to control the transport of nutrients and oxygen to cells in constructs promoting cellular expansion, and in some cases, enabling mechanical stimulation of cultured cells, thus enhancing cell differentiation and ECM formation.

The challenge is, once again, finding a compromise considering the different intrinsic properties of cartilage and bone tissues. In a bioreactor system, dynamic compression should be applied for cartilage ECM stimulation while, for bone, medium perfusion is required to control mass transport and provide shear-stress to stimulate neobone formation. To overcome this issue, studies have focused on the development of double chamber bioreactors with physical separation; described to fulfil the needs of tissue-specific mechanical forces for OC stimulation[28, 29].

The next step, barely explored, would be the automation of bioreactors controlled by computer software. The customization of engineered grafts through the development of anatomically moulded surfaces[61] have showed potential results headed to translational OC interfaces. As follows bioreactors would be a reliable system of automation and standardization of cell and scaffold methodologies reducing the time and production costs of functional custom-designed grafts.

### **1.2.5. *In vivo* models for osteochondral tissue engineering**

Animal studies still represent an essential tool to understand the biologic behavior of healing and tissue regeneration *in vivo*, though differences in the anatomy and metabolism of animal models must be considered in an experimental setup with human correlations.

Different animal models have been used in OC studies [16, 18-21, 49, 51, 63, 65]. Rats present distinctive characteristics, such as athymic nude or transgenic animals, not easily available in larger animal models. This model has been used to test the efficacy of a poly(lactide-co-glycolide)/nano-HA scaffold seeded with undifferentiated mesenchymal stem cells in OC defects[51]. After 12 weeks, defects treated with these constructs showed smooth and hyaline cartilage with abundant glycosaminoglycan and collagen type II deposition.

Rabbit also demonstrated to be a successful model for OC [16, 20, 21, 49], especially in femoral regions with the successful application of hyaluronate-atelocollagen/beta-TCP-hydroxyapatite scaffolds in the patellar groove[21], which promoted, in some extent, OC regeneration without the formation of fibrocartilage.

Sheep is also a popular animal model due to their weight-bearing limbs and with metabolic and bone remodelling rates similar to that of humans as well as the sequence of events in bone graft incorporation and healing capacities. An OC interface was evaluated in sheep by the implantation of a composite scaffold of collagen and HA with or without autologous chondrocytes into a condyle critical defect[65]. Both conditions showed to support neobone formation and hyaline-like cartilage regeneration. With a similar implant, collagen/TCP, OC regeneration was evaluated in the trochlear groove of minipigs[63]. Although cells were absence in this strategy, the incorporation *in situ* of growth factors in the construct leads to fibrocartilage formation and partial reconstruction of the subchondral bone integrity in a short term follow up.

A pilot clinical trial with 13 patients using the collagen/HA cell free tri-layer scaffold[66] mentioned above, indicated promising results with tissue recovery in some extent after a six-month follow up.

### **I.3. Conclusions**

The currently available treatments based on “damage to heal approaches”, have a limited success. With an increasing aging population, tissue engineering strategies provide important cues and hope for the treatment of OC degeneration. Ultimately, the tissue engineered implant should be able to stimulate and replace old tissue and native lethargic cells in order to accomplish both regeneration and restoring function for a successful clinical achievement.

The challenge stands for the replication of the natural functional architecture and the translation of promising strategies towards patients needs. Success lies on the delicate balance of cartilage and bone characteristics combined in an engineered graft, and its integration *in vivo*. The implant must participate in the regenerative process, considering the specific properties of each OC interface, which can only be achieved through the design of scaffold materials accommodating the specific characteristics of bone and cartilage tissues, and providing stem cells with the necessary cues to satisfy both tissue cellular needs. The application of cells in critical defects or elder patient injuries is likely to be beneficial in stimulating native cells into the regenerative process. The use of bioreactors can improve the functionality of such constructs, accelerate the production, create custom-made systems, and reduce time costs for obtaining implants for OC applications.

### **I.4. References**

1. Rodrigues MT, Gomes ME, Viegas CA, Azevedo JT, Dias IR, Guzón F, Reis RL: Tissue Engineered Constructs based on SPCL Scaffolds Cultured with Goat Marrow Cells: Functionality in Femoral Defects. *J Tissue Eng Regen Med* 2011, 5: 41-49.
2. Bessa PC, Balmayor ER, Hartinger J, Zanoni G, Dopler D, Meinel A, Banerjee A, Casal M, Redl H, Reis RL, et al.: Silk fibroin microparticles as carriers for delivery of human recombinant bone morphogenetic protein-2: in vitro and in vivo bioactivity. *Tissue Eng Part C Methods* 2010, 16: 937-945.

3. Gomes ME, Azevedo HS, Moreira AR, Ella V, Kellomaki M, Reis RL: Starch-poly(epsilon-caprolactone) and starch-poly(lactic acid) fibre-mesh scaffolds for bone tissue engineering applications: structure, mechanical properties and degradation behaviour. *J Tissue Eng Regen Med* 2008, 2: 243-252.
4. Ogoose A, Hotta T, Kawashima H, Kondo N, Gu W, Kamura T, Endo N: Comparison of hydroxyapatite and beta tricalcium phosphate as bone substitutes after excision of bone tumors. *J Biomed Mater Res B Appl Biomater* 2005, 72: 94-101.
5. Leonor I, Rodrigues MT, Gomes ME, Reis RL: In Situ Functionalization of Wet-Spun Fibre meshes for Bone Tissue Engineering: One Step Approach. *J Tissue Eng Regen Med* 2011, 5: 104-111.
6. Muehrcke DD, Shimp WM, Aponte-Lopez R: Calcium phosphate cements improve bone density when used in osteoporotic sternums. *Ann Thorac Surg* 2009, 88: 1658-1661.
7. Kim HJ, Kim UJ, Kim HS, Li C, Wada M, Leisk GG, Kaplan DL: Bone tissue engineering with premineralized silk scaffolds. *Bone* 2008, 42: 1226-1234.
8. Wang L, Zhao L, Detamore MS: Human umbilical cord mesenchymal stromal cells in a sandwich approach for osteochondral tissue engineering. *J Tissue Eng Regen Med* 2011. doi: 10.1002/term.370
9. Sa-Lima H, Caridade SG, Mano JF, Reis RL: Stimuli-responsive chitosan-starch injectable hydrogels combined with encapsulated adipose-derived stromal cells for articular cartilage regeneration. *Soft Matter* 2010, 6: 5184-5195.
10. Oliveira JT, Reis RL: Polysaccharide-based materials for cartilage tissue engineering applications. *J Tissue Eng Regen Med* 2011, 5(6): 421-236.
11. Maher SA, Mauck RL, Rackwitz L, Tuan RS: A nanofibrous cell-seeded hydrogel promotes integration in a cartilage gap model. *J Tissue Eng Regen Med* 2009, 4: 25-29.
12. Oliveira JT, Gardel LS, Rada T, Martins L, Gomes ME, Reis RL: Injectable gellan gum hydrogels with autologous cells for the treatment of rabbit articular cartilage defects. *J Orthop Res* 2010, 28: 1193-1199.
13. Malafaya PB, Oliveira JT, Reis RL: The effect of insulin-loaded chitosan particle-aggregated scaffolds in chondrogenic differentiation. *Tissue Eng Part A* 2010, 16: 735-747.
14. Silva SS, Motta A, Rodrigues MT, Pinheiro AF, Gomes ME, Mano JF, Reis RL, Migliaresi C: Novel genipin-cross-linked chitosan/silk fibroin sponges for cartilage engineering strategies. *Biomacromolecules* 2008, 9: 2764-2774.
15. Grayson WL, Bhumiratana S, Grace Chao PH, Hung CT, Vunjak-Novakovic G: Spatial regulation of human mesenchymal stem cell differentiation in engineered osteochondral constructs: effects of pre-differentiation, soluble factors and medium perfusion. *Osteoarthritis Cartilage* 2010, 18: 714-723.
16. Kayakabe M, Tsutsumi S, Watanabe H, Kato Y, Takagishi K: Transplantation of autologous rabbit BM-derived mesenchymal stromal cells embedded in hyaluronic acid gel sponge into osteochondral defects of the knee. *Cytherapy* 2006, 8: 343-353.

17. Nakajima M, Wakitani S, Harada Y, Tanigami A, Tomita N: In vivo mechanical condition plays an important role for appearance of cartilage tissue in ES cell transplanted joint. *J Orthop Res* 2008, 26: 10-17.
18. Filova E, Rampichova M, Handl M, Lytvynets A, Halouzka R, Usvald D, Hlucilova J, Prochazka R, Dezortova M, Rolencova E, et al.: Composite hyaluronate-type I collagen-fibrin scaffold in the therapy of osteochondral defects in miniature pigs. *Physiol Res* 2007, 56 Suppl 1: S5-S16.
19. Zhou G, Liu W, Cui L, Wang X, Liu T, Cao Y: Repair of porcine articular osteochondral defects in non-weightbearing areas with autologous bone marrow stromal cells. *Tissue Eng* 2006, 12: 3209-3221.
20. Shao X, Goh JC, Hutmacher DW, Lee EH, Zigang G: Repair of large articular osteochondral defects using hybrid scaffolds and bone marrow-derived mesenchymal stem cells in a rabbit model. *Tissue Eng* 2006, 12: 1539-1551.
21. Ahn JH, Lee TH, Oh JS, Kim SY, Kim HJ, Park IK, Choi BS, Im GI: Novel hyaluronate-atelocollagen/beta-TCP-hydroxyapatite biphasic scaffold for the repair of osteochondral defects in rabbits. *Tissue Eng Part A* 2009, 15: 2595-2604.
22. Caplan AI: Adult mesenchymal stem cells for tissue engineering versus regenerative medicine. *J Cell Physiol* 2007, 213: 341-347.
23. De Coppi P, Bartsch G, Jr., Siddiqui MM, Xu T, Santos CC, Perin L, Mostoslavsky G, Serre AC, Snyder EY, Yoo JJ, et al.: Isolation of amniotic stem cell lines with potential for therapy. *Nat Biotechnol* 2007, 25: 100-106.
24. Fan J, Varshney RR, Ren L, Cai D, Wang DA: Synovium-derived mesenchymal stem cells: a new cell source for musculoskeletal regeneration. *Tissue Eng Part B Rev* 2009, 15: 75-86.
25. Arien-Zakay H, Lazarovici P, Nagler A: Tissue regeneration potential in human umbilical cord blood. *Best Pract Res Clin Haematol* 2010, 23: 291-303.
26. Rada T, Reis RL, Gomes ME: Adipose tissue-derived stem cells and their application in bone and cartilage tissue engineering. *Tissue Eng Part B Rev* 2009, 15: 113-125.
27. Kuroda R, Ishida K, Matsumoto T, Akisue T, Fujioka H, Mizuno K, Ohgushi H, Wakitani S, Kurosaka M: Treatment of a full-thickness articular cartilage defect in the femoral condyle of an athlete with autologous bone-marrow stromal cells. *Osteoarthritis Cartilage* 2007, 15: 226-231.
28. Malafaya PB, Reis RL: Bilayered chitosan-based scaffolds for osteochondral tissue engineering: influence of hydroxyapatite on in vitro cytotoxicity and dynamic bioactivity studies in a specific double-chamber bioreactor. *Acta Biomater* 2009, 5: 644-660.
29. Chang CH, Lin FH, Lin CC, Chou CH, Liu HC: Cartilage tissue engineering on the surface of a novel gelatin-calcium-phosphate biphasic scaffold in a double-chamber bioreactor. *J Biomed Mater Res B Appl Biomater* 2004, 71: 313-321.
30. Naran KN, Zoga AC: Osteochondral lesions about the ankle. *Radiol Clin North Am* 2008, 46: 995-1002

31. Hunter DJ: Risk stratification for knee osteoarthritis progression: a narrative review. *Osteoarthritis Cartilage* 2009, 17: 1402-1407.
32. Li B, Aspden RM: Composition and mechanical properties of cancellous bone from the femoral head of patients with osteoporosis or osteoarthritis. *J Bone Miner Res* 1997, 12: 641-651.
33. Sharma L, Kapoor D, Issa S: Epidemiology of osteoarthritis: an update. *Curr Opin Rheumatol* 2006, 18: 147-156.
34. Bhosale AM, Richardson JB: Articular cartilage: structure, injuries and review of management. *Br Med Bull* 2008, 87: 77-95.
35. Kuettner KE, Cole AA: Cartilage degeneration in different human joints. *Osteoarthritis Cartilage* 2005, 13: 93-103.
36. Moyer RF, Birmingham TB, Chesworth BM, Kean CO, Giffin JR: Alignment, body mass and their interaction on dynamic knee joint load in patients with knee osteoarthritis. *Osteoarthritis and Cartilage* 2010, 18: 888-893.
37. Peters TA, McLean ID: Osteochondritis dissecans of the patellofemoral joint. *Am J Sports Med* 2000, 28: 63-67.
38. Baker CL, 3rd, Romeo AA, Baker CL, Jr.: Osteochondritis Dissecans of the Capitellum. *Am J Sports Med* 2010, 38(9): 1917-1928.
39. Smith RL, Carter DR, Schurman DJ: Pressure and shear differentially alter human articular chondrocyte metabolism: a review. *Clin Orthop Relat Res* 2004: S89-95.
40. Elder BD, Athanasiou KA: Hydrostatic pressure in articular cartilage tissue engineering: from chondrocytes to tissue regeneration. *Tissue Eng Part B Rev* 2009, 15: 43-53.
41. Beris AE, Lykissas MG, Papageorgiou CD, Georgoulis AD: Advances in articular cartilage repair. *Injury* 2005, 36 Suppl 4: S14-23.
42. Lattermann C, Romine SE: Osteochondral allografts: state of the art. *Clin Sports Med* 2009, 28: 285-301.
43. Gross AE, Shasha N, Aubin P: Long-term followup of the use of fresh osteochondral allografts for posttraumatic knee defects. *Clin Orthop Relat Res* 2005: 79-87.
44. Gikas PD, Bayliss L, Bentley G, Briggs TW: An overview of autologous chondrocyte implantation. *J Bone Joint Surg Br* 2009, 91: 997-1006.
45. Peterson L, Brittberg M, Kiviranta I, Akerlund EL, Lindahl A: Autologous chondrocyte transplantation. Biomechanics and long-term durability. *Am J Sports Med* 2002, 30: 2-12.
46. Hangody L, Vasarhelyi G, Hangody LR, Sukosd Z, Tibay G, Bartha L, Bodo G: Autologous osteochondral grafting--technique and long-term results. *Injury* 2008, 39 Suppl 1: S32-39.
47. Ulutas K, Menderes A, Karaca C, Ozkal S: Repair of cartilage defects with periosteal grafts. *Br J Plast Surg* 2005, 58: 65-72.



48. Niemeyer P, Fechner K, Milz S, Richter W, Suedkamp NP, Mehlhorn AT, Pearce S, Kasten P: Comparison of mesenchymal stem cells from bone marrow and adipose tissue for bone regeneration in a critical size defect of the sheep tibia and the influence of platelet-rich plasma. *Biomaterials* 2010, 31: 3572-3579.
49. Guo X, Park H, Young S, Kretlow JD, van den Beucken JJ, Baggett LS, Tabata Y, Kasper FK, Mikos AG, Jansen JA: Repair of osteochondral defects with biodegradable hydrogel composites encapsulating marrow mesenchymal stem cells in a rabbit model. *Acta Biomater* 2010, 6: 39-47.
50. Im GI, Shin YW, Lee KB: Do adipose tissue-derived mesenchymal stem cells have the same osteogenic and chondrogenic potential as bone marrow-derived cells? *Osteoarthritis Cartilage* 2005, 13: 845-853.
51. Xue D, Zheng Q, Zong C, Li Q, Li H, Qian S, Zhang B, Yu L, Pan Z: Osteochondral repair using porous poly(lactide-co-glycolide)/nano-hydroxyapatite hybrid scaffolds with undifferentiated mesenchymal stem cells in a rat model. *J Biomed Mater Res A* 2010, 94: 259-270.
52. Mizuno H: Adipose-derived stem cells for tissue repair and regeneration: ten years of research and a literature review. *J Nippon Med Sch* 2009, 76: 56-66.
53. Wakitani S, Mitsuoka T, Nakamura N, Toritsuka Y, Nakamura Y, Horibe S: Autologous bone marrow stromal cell transplantation for repair of full-thickness articular cartilage defects in human patellae: two case reports. *Cell Transplant* 2004, 13: 595-600.
54. Ringe J, Leinhase I, Stich S, Loch A, Neumann K, Haisch A, Haupl T, Manz R, Kaps C, Sittinger M: Human mastoid periosteum-derived stem cells: promising candidates for skeletal tissue engineering. *J Tissue Eng Regen Med* 2008, 2: 136-146.
55. Jansen EJ, Emans PJ, Guldemond NA, van Rhijn LW, Welting TJ, Bulstra SK, Kuijer R: Human periosteum-derived cells from elderly patients as a source for cartilage tissue engineering? *J Tissue Eng Regen Med* 2008, 2: 331-339.
56. Soncini M, Vertua E, Gibelli L, Zorzi F, Denegri M, Albertini A, Wengler GS, Parolini O: Isolation and characterization of mesenchymal cells from human fetal membranes. *J Tissue Eng Regen Med* 2007, 1: 296-305.
57. Stojkovic M, Lako M, Strachan T, Murdoch A: Derivation, growth and applications of human embryonic stem cells. *Reproduction* 2004, 128: 259-267.
58. Kiskinis E, Eggan K: Progress toward the clinical application of patient-specific pluripotent stem cells. *J Clin Invest* 2010, 120: 51-59.
59. Li J, Mareddy S, Tan DM, Crawford R, Long X, Miao X, Xiao Y: A minimal common osteochondrocytic differentiation medium for the osteogenic and chondrogenic differentiation of bone marrow stromal cells in the construction of osteochondral graft. *Tissue Eng Part A* 2009, 15: 2481-2490.
60. Hutmacher DW, Schantz JT, Lam CX, Tan KC, Lim TC: State of the art and future directions of scaffold-based bone engineering from a biomaterials perspective. *J Tissue Eng Regen Med* 2007, 1: 245-260.

61. Hung CT, Lima EG, Mauck RL, Takai E, LeRoux MA, Lu HH, Stark RG, Guo XE, Ateshian GA: Anatomically shaped osteochondral constructs for articular cartilage repair. *J Biomech* 2003, 36: 1853-1864.
62. Oliveira JM, Rodrigues MT, Silva SS, Malafaya PB, Gomes ME, Viegas CA, Dias IR, Azevedo JT, Mano JF, Reis RL: Novel hydroxyapatite/chitosan bilayered scaffold for osteochondral tissue-engineering applications: Scaffold design and its performance when seeded with goat bone marrow stromal cells. *Biomaterials* 2006, 27: 6123-6137.
63. Gotterbarm T, Richter W, Jung M, Berardi Vilei S, Mainil-Varlet P, Yamashita T, Breusch SJ: An in vivo study of a growth-factor enhanced, cell free, two-layered collagen-tricalcium phosphate in deep osteochondral defects. *Biomaterials* 2006, 27: 3387-3395.
64. Nicodemus GD, Bryant SJ: Cell encapsulation in biodegradable hydrogels for tissue engineering applications. *Tissue Eng Part B Rev* 2008, 14: 149-165.
65. Kon E, Delcogliano M, Filardo G, Fini M, Giavaresi G, Francioli S, Martin I, Pressato D, Arcangeli E, Quarto R, et al.: Orderly osteochondral regeneration in a sheep model using a novel nano-composite multilayered biomaterial. *J Orthop Res* 2010, 28: 116-124.
66. Kon E, Delcogliano M, Filardo G, Pressato D, Busacca M, Grigolo B, Desando G, Marcacci M: A novel nano-composite multi-layered biomaterial for treatment of osteochondral lesions: technique note and an early stability pilot clinical trial. *Injury* 2010, 41: 693-701.

## **SECTION II**

### **MATERIALS AND METHODS**



## **Chapter II**

### **MATERIALS & METHODS**





fully biodegradable, with a slow degradation rate[1]. PCL also forms compatible blends and copolymers with a wide range of polymers producing materials with unique elastomer properties[4]. For all of these reasons, PCL is used to produce Food and Drug Administration (FDA) approved medical devices, and widely studied for several tissue engineering (TE) approaches and for other biomedical applications[6-10] including long term implantable devices.

The PCL used in this Thesis is commercially available as TONE™ polymer purchased from Union Chemicals and Plastics Divisions (Bound Brook, New Jersey, USA).

### II.2.2. Starch-polycaprolactone blend

Natural polymers have been presented as an interesting option to the currently used metal and synthetic materials, due to a higher biodegradability rate, non-cytotoxicity, and good mechanical properties. These polymers are synthesized involving enzyme-catalyzed, chain growth polymerization reactions of activated monomers, which are typically formed within cells by complex metabolic processes.

Starch is a biopolymer produced by green plants as an energy store. It is quite abundant in nature, and an almost unlimited source and low cost associated raw material. Starch consists of multiple glucose units linked by glycosidic bonds, resulting in a combination of two polymeric carbohydrates (polysaccharides) amylose (A), a linear and helical structure, and the branched amylopectin (B) (Figure II.2.2).

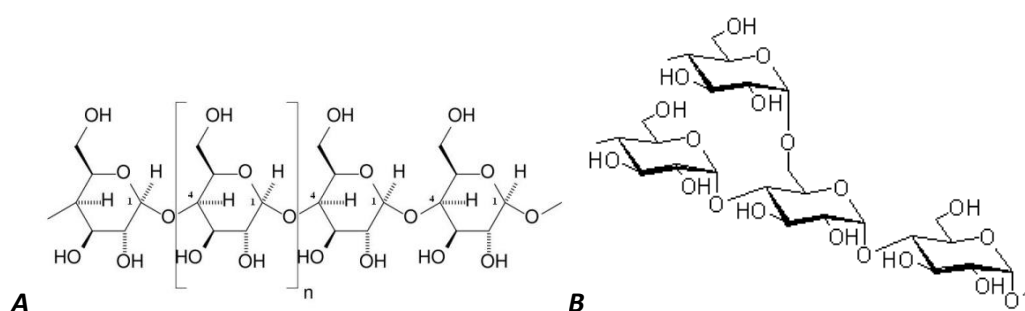


**Figure II.2.2** – Chemical structure of starch components: amylose (A) and amylopectin (B).

Scaffolds, based on blends of starch polymer with several different synthetic polymers, have been developed by our group using several methodologies[11-14], including by melt-based[15-17] and wet-spun[17-19] routes. Some of these scaffolds have previously shown



great potential for TE strategies aiming at bone[11, 14-16, 18, 20, 21] and cartilage[22, 23] applications.

Specifically, scaffolds based on blends of starch and polycaprolactone (SPCL) have been successfully used in a great number of studies showing to support the adhesion and proliferation of endothelial cells[21], chondrocytes[22] or osteoblasts, as well as the proliferation and differentiation of mesenchymal stem cells[16, 20, 23] obtained from different sources into osteoblasts[12] or chondrocytes[23]. Furthermore, *in vivo* studies not only indicate a good integration of the starch based materials in the host[17] but also that these biomaterials have a weak potential to stimulate an inflammatory reaction[24].

The 30:70 (wt %) SPCL blend used for the experimental studies described in the following chapters was obtained from Novamont (Novara, Italy).

### **II.2.3. Tri-calcium phosphates**

Ceramic materials have shown important scaffolding properties aiming at bone TE strategies[22, 25, 26]. These achievements are supported by fact that hydroxyapatite (HA) is the essential crystalline part of the calcified components of the skeleton, and is the principal mineral in bone, enamel, dentin, and cementum[26].

Ceramic materials evidence a high modulus yet brittle behavior[27] and their processability is limited. However, these materials offer advantages over most polymers regarding their stimulating biological properties, such as osteoconductivity, and cell bioactivity[28]. Among ceramics, HA and tri-calcium phosphates (TCPs) are the most commonly used in biomedical research, being HA the preferred ceramic for bone strategies[9, 29, 30]. However, the osteoconductive and bioreabsorbable nature of beta-TCPs are associated to an earlier incorporation into surrounding bone *in vivo* may be advantageous to HA, which remains unremodelled despite long periods upon implantation[31].

### **II.2.4. Agarose**

Agarose is a natural based polysaccharide obtained from agar (Figure II.2.3) used for a variety of life science applications, including immune-isolation purposes.

Agarose is heated to 90 °C to form a polymeric solution by solving agarose powder with water or phosphate saline buffer. When the temperature is lowered to close to room temperature (fluctuations may take place considering the several commercially available

agarose products) gelation occurs. Notwithstanding the wide application of agarose, gels produced from agarose have been used as cell encapsulation systems for cartilage TE. Despite the slow degradation profile, the soft and flexible structure provided by these gels recreates a better 3D environment, suitable for chondrocyte maintenance[32] and mesenchymal stem cell differentiation into the chondrogenic lineage[32].

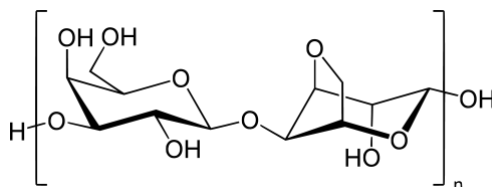


**Figure II.2.3 – Structure of agarose molecule**

In this Thesis, agarose gels (2 %, Invitrogen) were used as encapsulating systems for hAFSCs, as described in chapter V, by dissolving a 2 % agarose solution in ultra-pure water and cooling it down in a flat plastic surface before cutting the hydrogel discs.

### **II.3. Scaffold fabrication**

The design of a scaffold ultimately determines the functionality of the grown tissue. Scaffold design comprehends the combination of the selected materials and methods, considering a set of structure-properties specification for a target application. Several techniques were considered in the experimental chapters of this Thesis, namely fiber bonding of melt spun fibers, electro-spinning, and wet-spinning. The purpose of using these different methodologies was to try to develop a range of scaffold designs/properties and determine the ones that are likely to direct cell behavior in the most appropriate manner, considering the aimed application.

Scaffolds produced by fiber bonding of melt spun fibers presented a microporous structure with high porosity and interconnectivity so that cells can colonize the entire scaffold while communicating with each other; these scaffolds were studied in chapter V, VI, VII, and VIII. Conversely, electrospun scaffolds, studied under chapter III, resulted in a nanofiber mesh, resembling the biological scale of extracellular matrix (ECM), where calcium phosphates were included to improve the osteogenic potential of the mesh. Wet-spinning is another interesting

methodology to develop scaffolds with high porosity and interconnectivity allowing to, simultaneously, introduce chemical modifications, such as functionalizing scaffold surface for stimulating the communication between scaffold and cells. Scaffolds obtained by wet spinning were studied in chapter IV.

### **II.3.1. Melt fiber extrusion - Fiber bonding**

SPCL (a blend of starch with polycaprolactone, 30/70 % wt) fiber mesh scaffolds were produced by a fiber bonding process consisting of cutting and sintering the fibers, which were previously obtained by an extrusion/melt spinning process. Briefly, a selected amount of fibers was placed in a glass mould and heated in an oven at 150 °C. Immediately after removing the moulds from the oven, the fibers are slightly compressed by a Teflon cylinder (which runs within the mould) and then cooled at -20 °C. Then, samples were cut into cylinder discs, according to the experimental needs following sterilization by ethylene oxide. Scaffolds previously produced by this method showed interesting results for bone and cartilage TE applications[16, 20, 21, 23], and their mechanical and degradation profiles have also been described elsewhere[15].

### **II.3.2. Electrospinning**

The use of nanotechnology to tailor orthopaedic scaffolds arises from the need to mimic the ECM structure and complexity at a biological scale, since bone matrix is mainly composed of an intricate nanofiber structure of nonstoichiometric HA integrated in collagen fibers.

Electrospinning is an interesting approach for biomaterial processing enabling to control morphology, porosity and composition of the polymer with nanoscale properties[8, 33].

Composite scaffolds were developed in chapter III, combining electrospinning with  $\beta$ -TCP powder as indicated in the following section. PCL fiber meshes were produced using a polymeric solution of 17 % (wt/v) of PCL in a mixture of chloroform (Aldrich) and N,N-Dimethylformamide (Aldrich) at a 7:3 ratio. This solution was electrospun at 9-10 kV, with a flow rate of 1.0 mL/h collecting a random fiber mesh (20 cm away from the collector) on a flat aluminum foil.

The electrospinning experiments were conducted at room temperature, as well as the drying of the electrospun nanofiber meshes. PCL single layered membranes were used as negative controls of the multi-layered PCL- $\beta$ -TCP study.

### **II.3.3. Tricalcium Phosphates production by solid state reaction**

$\beta$ -TCP can be produced through a solid state reaction[34], an interesting synthesis route given its simplicity and yield. In our studies, the ceramic material,  $\beta$ -TCP, was obtained from a solid state reaction between stoichiometric amounts of calcium phosphate dibasic anhydrous (Fluka) and calcium carbonate (Sigma) followed by a 24 h sinterization at 800 °C. The powders were hand-sieved with stainless steel sieves (mesh 225-106  $\mu\text{m}$ ).

After obtaining  $\beta$ -TCP powder, a polymeric solution of 17 % (wt/v) PCL was electrospun to produce the polymeric nanofiber mesh layer and the TCPs were subsequently spattered over. Composite scaffolds were developed by assembling a total of three stacked layers of electrospun PCL- $\beta$ -TCPs at a ratio of 0.5 g  $\beta$ -TCP/130  $\text{cm}^2$  PCL meshes.

### **II.3.4. Wet-spinning**

Wet-spinning technology requires polymer dissolution prior to scaffold formation and, consequently, depends on polymer solubility and on solvent volatility. The development of SPCL wet spun scaffolds was described previously[18]. Briefly, to obtain a polymer solution with proper viscosity, SPCL was dissolved in chloroform (Sigma-Aldrich) at a concentration of 30 % (wt/v) followed by injection (internal diameter of 0.8 mm) to induce the formation of fiber structures by precipitation in a methanol (Sigma-Aldrich) coagulation bath. A programmable syringe pump (KD Scientific, World Precision Instruments) with a controlled pumping rate of 2.5 ml/hour was used to run fibres formation. The fiber mesh structure was formed by random movements of the syringe in the coagulation bath.

Scaffolds were air-dried at room temperature overnight to remove remaining solvent residues.

#### **II.3.4.1. Designing of an in situ functionalized surface**

Silicon ion plays a significant role in bone and cartilage development of higher organisms[35]. Furthermore, the release of silicon and calcium was reported to up-regulate and activate genes in osteoprogenitor cells[36]. Thus, in chapter IV, we propose to evaluate the relevance of the incorporation of silanol groups (Si-OH) in wet spun fiber mesh scaffolds of SPCL.

SPCL scaffolds with functionalized Si-OH groups were produced in a similar way to SPCL scaffolds described in the previous section. The main difference is the coagulation bath; instead of methanol, a calcium silicate solution was used with a molar ratio of  $\text{Si}(\text{OC}_2\text{H}_5)_4:\text{H}_2\text{O}:\text{C}_2\text{H}_5\text{OH}:\text{HCl}:\text{CaCl}_2$ , of 1.0 : 4.0 : 4.0 : 0.014 : 0.20 [18, 37] to assure the osteoconductivity of the polymeric scaffolds. Afterwards, fiber meshes were air-dried at 60 °C for 24 h, and designated as SPCL-Si.

#### II.4. Scaffold characterization

Scaffold characterization is part of the process of designing a strategy for biomedical applications. Physic-chemical properties provide important information about the biomaterial and the manufacture of a 3D matrix while predicting some biological outcomes.

In the following sections, technical information is provided concerning analytic procedures selected for scaffold evaluation, either chemical or physical techniques, under the scope of this Thesis.

##### II.4.1. In vitro bioactivity of SPCL-Si wet-spun fiber mesh scaffolds

The concept of bioactivity is defined as one of the characteristics of an implant material which allows it to form a bond with living tissues[38, 39]. The assessment of apatite formation on the surface of a material in simulated body fluid (SBF) is useful for predicting the *in vivo* bioactivity of the material not only qualitatively but also quantitatively. SBF solution presents ion concentration of  $\text{Na}^+$  142.0,  $\text{K}^+$  5.0,  $\text{Ca}^{2+}$  2.5,  $\text{Mg}^{2+}$  1.5,  $\text{Cl}^-$  147.8,  $\text{HCO}_3^-$  4.2,  $\text{HPO}_4^{2-}$  1.0,  $\text{SO}_4^{2-}$  0.5 mM, similar to blood plasma's.

Bioactivity of SPCL-Si wet-spun fiber meshes was determined by soaking the scaffolds in 10 mL of SBF at 36.5 °C for up to 7 days. The SBF solution was prepared by dissolving reagent-grade chemicals of NaCl,  $\text{NaHCO}_3$ , KCl,  $\text{K}_2\text{PO}_4 \cdot 3\text{H}_2\text{O}$ ,  $\text{MgCl}_2 \cdot 6\text{H}_2\text{O}$ ,  $\text{CaCl}_2$  and  $\text{NaSO}_4$  into distilled water, at pH 7.40 buffered with tris-hydroxymethyl-aminomethane ( $(\text{CH}_2\text{OH})_3\text{CNH}_3$ ) and 1 M hydrochloric acid at 36.5 °C. After soaking, the substrates were removed from SBF, rinsed in distilled water and air-dried.

The bioactivity assay was conducted in order to assess *in vitro* the bioactive potential of wet-spun fiber meshes functionalized with silanol groups for bone TE applications.

#### **II.4.2. Scanning electron microscopy**

The scanning electron microscopy (SEM) was used as complementary method to evaluate the morphology of the scaffolds, including pore shape, size and distribution as well as the interconnectivity between these pores. The morphology of multilayered scaffolds of PCL-TCP from chapter III was evaluated by SEM to determine the distribution and integration of TCP granules in the PCL fiber meshes. Additionally, in chapter IV, film morphology as well as the presence of different elements was analyzed before and after immersing the scaffolds in simulated body fluid.

Prior to SEM analysis, the scaffolds were sputter coated with gold (Fisons Instruments, model SC502, England) for 2 minutes at 15 mA. Samples were assessed in a SEM (Leica Cambridge, model S360) equipment and micrographs recorded at 15 kV ranging from 100 to 1000x magnification.

#### **II.4.3. Dynamic Mechanical Analysis**

Cells and tissues exhibit a viscoelastic behavior[40], which an implantable scaffold or construct should match at physiological conditions[41] in order to participate in biophysical and biological responses.

Dynamic mechanical analysis (DMA) measures the viscoelastic properties of materials as a response to stress, temperature and frequency, and determines their time-dependent mechanical performance.

Dynamic mechanical analysis of SPCL-Si scaffolds from chapter IV was performed using a TRITEC8000B DMA from Triton Technology, equipped with a tensile mode. Before the analysis, scaffolds were immersed in PBS until equilibrium was reached. After equilibration at 37 °C, DMA spectra were obtained with a frequency scan between 0.1 and 25 Hz. The experiments were performed under constant strain amplitude (30 µm) and a static pre-load of 0.7 N was applied to keep the sample tight. During DMA analysis, scaffolds were immersed in a liquid bath in a Teflon® reservoir. Triplicates were used for each condition.

#### **II.4.4. Micro-computed tomography**

Micro-computed tomography (m-CT, µ-CT or micro-CT) has been successfully used in different branches of science for the study of porous or cavity-containing structures. Micro-CT

is a non-destructive model that uses x-rays to create multiple micrometer cross-sections of a 3D sample that later can be used to recreate a virtual 3D model. This technique is extremely useful for scaffold characterization in view of the fact that besides the morphological aspect of the scaffold, other properties such as porosity, pore interconnectivity or thickness can be quantitatively determined.

Micro-CT is also an interesting tool for those studies where a calcified layer is an expected result, either produced by the cells or as a precipitation coating as for bioactivity assays.

Calcified areas are easily detected in polymeric matrices by micro-CT due to the significant differences found in the density of polymer scaffolds and calcium phosphates present in the matrix[18]. Additionally, in small dimensioned scaffolds the distribution of the ECM over the scaffold can be observed and measured with appropriate software.

Micro-CT, using a Skyscan 1072 scanner (Skyscan, Kontich, Belgium), was performed to characterize SPCL-Si scaffolds after the bioactivity studies from chapter IV so as to observe the distribution of the apatite layer on the scaffolds after simulated body fluid immersion. X-ray scans were performed in triplicate using a resolution of 5.86  $\mu\text{m}$  and integration time of 1.9 sec. The X-ray source was set at 40 keV / 248  $\mu\text{A}$ . Approximately 400 projections were acquired over a rotation range of 180  $^\circ$  with a rotation step of 0.45  $^\circ$ . Data sets were reconstructed using standardized cone-beam reconstruction software (NRecon v1.4.3, SkyScan). Data sets of 200 slices were segmented into binary images with a dynamic threshold of 50 to 255 (grey values) to identify the organic and inorganic phase. This data was used for morphometric analysis (CTAnalyser, v 1.5.1.5, SkyScan) and to build 3D models (ANT 3D creator, v2.4, SkyScan).

#### **II.4.5. Thin-film X-ray diffraction**

X-Ray Diffraction Analysis (XRD) is a versatile, non destructive tool for investigating the crystallographic structure and sub-nanometric morphology of natural and synthetic materials.

Thin-film X-ray diffraction (TF-XRD, Philips X'Pert MPD, The Netherlands) was used to identify any crystalline phase present on the scaffolds from chapter III and IV.

In the case of PCL-TCP nanofiber meshes, XRD provides information about the type of calcium phosphate obtained by solid state reaction, whose granules were integrated in the multilayered structure. Results were compared to membranes of PCL, the negative control of this experiment.

In chapter IV, XRD was performed to characterize the crystalline/amorphous nature of the apatite films formed on the polymeric wet-spun fiber mesh after soaking in the calcium silicate solution or after immersion in simulated body fluid (results were compared to non immersed controls).

The data collection was performed by  $2\theta$  scan method with  $1^\circ$  as incident beam angle using  $\text{CuK}\alpha$  X-ray line and a scan speed of  $0.05^\circ/\text{min}$  in  $2\theta$ .

#### **II.4.6. Fourier transform infrared spectroscopy with attenuated total reflectance**

Fourier transform infrared spectroscopy with attenuated total reflectance (FTIR-ATR) is a non-destructive, fast and highly sensitive tool for material analysis, providing an infrared spectrum of absorption, emission, photoconductivity or Raman of a solid, liquid or gas. Data obtained from the infrared spectrum represents the molecular absorption and transmission of a specimen, creating a unique molecular fingerprint of the sample, thus permitting its identification, quality and the amount of components in a mixture.

FTIR-ATR was performed using an IRPrestige-21 (Shimadzu, Japan) with an attenuated total reflectance in PCL-TCP fiber mesh samples from chapter III, to determine if calcium phosphate granules were integrated in the PCL-TCP fiber mesh.

All spectra were recorded using at least 64 scans and  $2\text{ cm}^{-1}$  resolution, in the spectral range  $4000\text{--}600\text{ cm}^{-1}$ .

#### **II.4.7. Inductively coupled plasma optical emission spectrometer**

Inductively coupled plasma optical emission spectrometer (ICP-OES) uses the inductively coupled plasma to produce excited atoms and ions that emit electromagnetic radiation at wavelengths characteristic of a particular element. The intensity of this emission is indicative of the concentration of the element within the sample.

Elemental concentrations of calcium, phosphorus and silicium were measured by inductively coupled plasma atomic emission spectrometry (JY2000-2, Jobin Yvon, Horiba, Japan). Samples were firstly collected and  $0.22\ \mu\text{m}$  filtered and kept at  $-80^\circ\text{C}$  until usage. This technique was used to analyse the simulated body fluid solution before and after immersing the wet-spun fiber meshes with or without the silanol groups (bioactivity tests), in chapter IV. Triplicate samples were considered for ICP analysis.



## **II.5. Scaffold sterilization prior to cell culturing studies**

Prior to cell culture experiments, samples were cut into discs, whose dimensions were defined accordingly to the experiments to be performed, and ethylene oxide sterilized at Pronefro (Maia, Portugal) or at the WFIRM (Winston-Salem, North Carolina, USA). Typical conditions included a cycle temperature of 37 °C, a moisture level of 50 %, a cycle time of 14 hours, and a chamber pressure of 50 kPa.

The multi-layered PCL- $\beta$ -TCP scaffolds (developed on chapter III) were cut into 5 mm discs followed by two 30 minute-cycle of UV radiation, instead of ethylene oxide sterilization.

## **II.6. Biological assays**

### **II.6.1. Harvesting, isolation and culture of stem cells**

The interest in the potential of adult stem cells has been increasing due to the limited availability of tissue specific progenitor cells.

Bone marrow represents a source of mesenchymal adult stem cells[42-44] due to the availability of established culture techniques to isolate and expand cell populations from human donors. Additionally, expansion of bone marrow stem cells overcomes the tissue morbidity and donor tissue scarcity, minimizing the problems associated with other types of primary cells. In autologous strategies, the implantation of cells from the individual also reduces disease transmission risks.

Conversely, amniotic fluid is arising as an interesting source of stem cells. Amniotic fluid cells (AFSCs) are used for prenatal diagnosis of fetal abnormalities caused by genetic mutations. Along with the almost endless ability to expand without telomere shortening, AFSCs share with embryonic stem cells some markers and a high self renewal capacity without associated ethical concerns[45].

#### **II.6.1.1. Harvesting and isolation of goat bone marrow stromal cells**

Goat bone marrow stromal cells (gBMSCs) were used in the studies described in chapter III, IV, and VII. This animal model was selected for these studies, firstly due to their analogy to human bone marrow stem cells (hBMSCs), and also because goats are a high level vertebrate

with metabolic and bone remodelling rates similar to that of humans. The sequence of events in bone graft incorporation and healing capacities[46] are also comparable to humans, which explain how goats became increasingly popular as an animal model in the orthopaedic field. Goats have been widely used in studies of biocompatibility, and bone formation and regeneration[47-49]. Furthermore, the use of gBMSCs allows performing autologous experiments, as goat bone marrow aspirates can be obtained by a biopsy procedure, and the isolated cells can be cultured using serum from the same animal where ultimately, the same cells or cell-scaffold constructs will be implanted.

The methodology optimized for harvesting goat bone marrow (BM) was based on the techniques used to perform human BM biopsies from the iliac bone. Thus, through percutaneous puncture, bone marrow was aspirated from the iliac wings of goats using a biopsy needle, without erythrocyte contamination (Figure II.6.1).



**Figure II.6.1** - Harvesting marrow from the goat iliac crest.

The experimental protocol for BM aspirate was performed according to the national guidelines and after approval of the National Ethical Committee for Laboratory Animals from Direcção Geral da Agricultura. Prior to general anesthesia, goat iliac regions were shaved and disinfected. Animals were submitted to a pre-anesthetic medication with acepromazine maleate (5 mg EV, Calmivet®, Vetóquinol) and placed under general anesthesia by induction with thiopental sodium (20-25 mg/Kg EV, Pentothal® sodium, Abbott Labs), maintained by inhalation of a mixture of 1.5 % isoflurane (IsoFlo®, Abbott Labs, USA) and oxygen for a maximum of 30 minutes.

A bone marrow aspiration needle (Inter.V, Medical Device Technologies, Inc., Denmark) and a 10 mL syringe, already containing 1 mL heparin (5.000 U.I., Heparin sodium, B. Braun

Medical, Inc.) to avoid marrow coagulation, was used to collect 10 mL of bone marrow from the iliac crest of adult goats (Figure II.6.1), transferred into a sterile tube and resuspended in 30 mL of RPMI-1640 culture medium (Sigma-Aldrich), containing 1 % penicillin/streptomycin (Gibco) plus 1 mL of heparin (5.000 U.I.).

Afterwards, goat marrow stromal cells (gBMSCs) were centrifuged for 10 minutes at 1200 rpm and a dense cellular pellet was collected and cultured in a basic culture medium – DMEM (Dulbecco's Modified Eagle's Medium) (Sigma-Aldrich) supplemented with 10 % FBS (Gibco) and 1 % A/B (Invitrogen). Four days after the harvesting procedure, cells were rinsed in sterile PBS (Sigma) and medium was exchanged. Following gBMSCs expansion up to 90 % of confluence, cells were cryopreserved at 1 passage (Pa) in a solution of FBS with 10 % DMSO until needed for experimental purposes.

The advantage of this methodology is based on the acquisition of a higher quality of bone marrow samples with a simple technique that, after optimization, can be systematically used in subsequent experiments. The achieved optimization of this technique constitutes the first report in the scientific literature of harvesting bone marrow aspirate from percutaneous puncture in the goat model.

#### **II.6.1.2. Harvesting and isolation of human amniotic fluid stem cells**

Human amniotic stem cells (hAFSCs) were used in the studies described in chapters V, VI, and VIII. AFSCs were obtained from human amniotic fluid specimens collected from amniocentesis procedures, using backup cells that would otherwise be discarded. AFSCs were immunoselected with magnetic microspheres isolating the c-Kit-positive population[45], as C-kit or CD 117 has been described to be the receptor for stem cell factor. The protocol has been described in detail elsewhere[45]. AFS cells were grown in  $\alpha$ -MEM medium (Gibco, Invitrogen) containing 15 % embryonic stem cell screened FBS (ES-FBS, HyClone, USA), 1 % glutamine and 1 % penicillin/streptomycin (Gibco), supplemented with 18 % Chang B (Irvine Scientific), and 2 % Chang C (Irvine Scientific) at 37 °C with 5 % CO<sub>2</sub> atmosphere.

#### **II.6.2. Cell culturing and expansion**

Samples obtained from body tissues such as bone marrow or amniotic fluid usually have a cell number that is not sufficient for TE applications. Thus, stem cells should be isolated,

selected, and expanded towards the achievement of cell numbers enough to perform *in vitro* studies, and eventually a cell number relevant for clinical applications.

#### **II.6.2.1. Goat bone marrow stromal cells**

Cryopreserved cells to be used in experimental studies were thawed by placing the frozen cell vial in a 37 °C water bath. When the vial was almost defrosted, gBMSCs were removed from the bath and pipetted into cell culture flasks, and let to attach for 24 hours prior medium exchange. In general, cells were expanded up to 90 % confluence and sub-cultured to 2 Pa (Figure II.6.2) in basic medium (DMEM, 10 % FBS and 1 % A/B) before seeding/encapsulation procedures.



**Figure II.6.2** - 2D culture of gBMSCs after 10 days in basal medium.

In autologous approaches (chapter VII), gBMSCs were expanded in 10 % autologous serum instead of FBS. Autologous serum was isolated from goat peripheral blood every 3 weeks and centrifuged at 3,000 rpm for 10 minutes. Serum was stored at -20 °C until usage.

#### **II.6.2.2. Human amniotic fluid stem cells**

Human AFSCs were isolated as previously described[45] and cultured in basic amniotic fluid cell (BAFC) medium composed of  $\alpha$ -MEM (HyClone) with 18 % Chang B (Irvine Scientific) and 1 % Chang C (Irvine Scientific) media as well as 2 % L-glutamine (HyClone) and 15 % ES-FBS.

#### **II.6.2.3. Human mesenchymal stem cells from bone marrow**

Human mesenchymal stem cells from bone marrow (hBMSCs) were purchased from Lonza® and expanded as indicated in manufacturer datasheet. Basal culture medium was composed of

$\alpha$ -MEM (HyClone) supplemented with 10 % ES-FBS (HyClone) and 1 % penicillin/streptavidin solution.

### **II.6.3. Osteogenic differentiation**

The osteogenic differentiation of mesenchymal stem cells is dependent on mechanical and biochemical stimuli from their micro-environment. Dexamethasone, ascorbic acid and  $\beta$ -glycerol phosphate are known to induce osteogenic differentiation, and thus commonly used as osteogenic supplements provided in cell culture medium. Dexamethasone is a synthetic glucocorticoid shown to induce osteogenic differentiation of osteoprogenitors cells from fetal calvaria-derived cells[50] and adult bone marrow stromal-derived cells[51, 52]. In human body, ascorbic acid is an essential nutrient required for collagen synthesis, thus playing an essential role in the structure and function of skeletal tissues. When  $\beta$ -glycerol phosphate, a potential source of phosphate ions[52], is also present, a zone of hydroxyapatite-containing mineral is formed within collagen fibrils[53].

Thus, in order to induce the osteogenic phenotype, gBMSCs were cultured in minimal essential medium Eagle's  $\alpha$ -modification ( $\alpha$ -MEM; Sigma-Aldrich), A/B (1 %), FBS (10%) and supplemented with osteogenic factors, namely dexamethasone ( $10^{-8}$  M; Sigma-Aldrich), ascorbic acid (50  $\mu$ g/ml; Sigma) and  $\beta$ -glycerophosphate (10 mM; Sigma) for up to 3 weeks.

Minor variations in medium composition are indicated in experimental studies performed at WFIRM, USA (chapter V, VI and VIII). In this case, osteogenic medium prepared for hBMSCs and hAFSCs was composed of DMEM (HyClone) supplemented with 10 % FBS (HyClone), L-ascorbic acid (50  $\mu$ M; Sigma), dexamethasone (100 nM; Sigma), and glycerol 2-phosphate disodium salt hydrate (10 mM; Sigma).

### **II.6.4. Osteochondral differentiation**

The composition of the co-culture media used to maintain the osteogenic and chondrogenic phenotype of differentiated AFSCs (as described in chapter V) was prepared considering the inclusion of both osteo- and chondrogenic factors usually used in osteo- or chondrogenic culture media.

Several media from the literature were analyzed, and the most frequent supplements combined to obtain a co-culture medium composed of DMEM-LG (HyClone), 2 % FBS (HyClone), sodium pyruvate (1x, Sigma), ITS (1x, Sigma), 5 mM glycerol 2-phosphate (Sigma),

50 µg/ml ascorbic acid (Sigma), 10 mM dexamethasone (Sigma), 40 µg/ml L-proline (Sigma), either in the presence or absence of 100 ng/ml IGF-1 (Invitrogen).

Since TGF-β was removed from the media, another factor was added and its presence tested in the medium: IGF-1. IGF-1 or insulin growth factor-1 has been described to participate in both bone and cartilage development, which could maintain the induced phenotype of AFSCs. After 7 or 14 days in the co-culture media, constructs were removed and characterized for osteo- and chondrogenic specific markers. BAFC medium[45] was used as control of this experiment.

#### **II.6.5. Seeding on 2D cultures**

In order to compare the potential of hBMSCs and hAFSCs for bone tissue engineering applications (chapter VI), both cells were seeded onto culture treated 6-well plates (Costar) at passage 5 and passage 24, respectively, at a concentration of 30,000 cells/well. Both type of cells were cultured for 3 days with basal medium, and then, exchanged to osteogenic medium, composed of DMEM (HyClone Laboratories Inc.) supplemented with 10 % FBS (HyClone), 100 nM dexamethasone (Sigma), 50 µM L-ascorbic acid (Sigma) and 10 mM glycerol 2-phosphate disodium salt hydrate (Sigma), for up to 3 weeks (0, 7, 14 or 21 days). Before the osteogenic characterization, cells were briefly rinsed in PBS (HyClone Laboratories Inc.), and fixed in 10% neutral buffered formalin (Surgipath Medical Ind.).

#### **II.6.6. Seeding cells onto 3D matrices**

##### **II.6.6.1. gBMSCs, hAFSCs or hBMSCs onto SPCL scaffolds**

In chapter VII, a gBMSCs suspension of 2,500,000 cells/mL was prepared and seeded onto the SPCL porous scaffolds in a drop-wise manner, at a cellular density of 500,000 cells per SPCL scaffold (6 mm diameter x 2 mm height discs). Seeding chambers were used to improve cell seeding efficiency by avoiding cellular dispersion. Afterwards, constructs were cultured in non-treated 12-well plates (Costar, Becton Dickinson), to reduce cellular adhesion to the plates. Osteogenic medium described in previous sections was selected for 1 or 7 days of cell culturing prior to implantation. In chapter VII, autologous sera (10 %) were used. Autologous culture medium was changed twice a week.

In a similar way to gBMSCs, hBMSCs (only in chapter VI) and hAFSCs were seeded onto SPCL scaffolds (5 mm x 4 mm, 7 mm x 4 mm, and 6 mm x 3.8 mm cylinders in chapter V, VI and VIII, respectively) at a concentration of  $8.6 \times 10^5$ ,  $1.2 \times 10^6$ , and  $1.2 \times 10^6$  cells/scaffold, respectively, and cultured in basal medium for 3 days before adding osteogenic media for up to 3 weeks.

In chapter VI, hBMSCs and hAFSCs were seeded on culture treated 6-well plates (Costar) at a concentration of 30,000 cells per well in order to compare their behaviour with cells cultured in 3D SPCL scaffolds. Cells seeded on the 6-well plates were cultured for 3 days in basal medium, and then, exchanged to osteogenic medium, for up to 3 weeks (0, 7, 14 or 21 days).

#### **II.6.6.2. gBMSCs onto SPCL-Si scaffolds**

In chapter IV, gBMSCs were seeded onto SPCL-Si scaffolds (5 mm diameter discs) before and 7 days after scaffold immersion in a SBF solution, at a concentration of 100,000 cells per scaffold. After the seeding, constructs were cultured in osteogenic medium for 7 or 14 days.

#### **II.6.6.3. Encapsulating hAFSCs into agarose gels**

In chapter V, a 2 % agarose solution was used as encapsulating gel. Firstly, the agarose solution was prepared and kept at 37 °C while hAFSCs were trypsinized and counted. Then, hAFSCs were resuspended at a concentration of  $2 \times 10^6$  cells/mL of agarose. Cell-agarose system was left to gelify for a couple of minutes at room temperature inside a biological hood. Afterwards, 4 mm diameter discs were cut off from the cell encapsulated gel and placed in non treated 24 multi-well plates (Costar) with basal medium.

After 2 days, chondrogenic medium was prepared with DMEM (HyClone) supplemented with antibiotic/antimicotic solution, 50 µg/ml ascorbic acid (Sigma), 1 mM dexamethasone (Sigma), 40 µg/ml L-proline (Sigma), 100 µg/ml sodium pyruvate (Sigma), 1 % ITS (100x, Sigma) and 10 ng/ml TGF-β1 (Sigma), and added to the encapsulated system. Medium was exchanged once a week for up to 4 weeks in chondrogenic culture.

#### **II.6.7. Characterization of cell-scaffold constructs**

Cell seeded matrices were characterized in terms of cellular viability and proliferation as well as of osteo- or chondro-genic differentiation markers to assess cellular phenotypes, after

several pre-determined periods of culture. Cell viability was assessed by MTS or Calcein AM methodologies while proliferation was determined by a double strand DNA quantification kit.

Osteogenic differentiation was evaluated based on the activity of alkaline phosphatase (ALP) and the expression of RunX-2, a transcription factor involved in bone development. Furthermore, morphological features and the production of a mineralized matrix in bone strategies were also considered by SEM and EDS analysis, Alizarin Red staining as well as the expression of collagen I, the major organic component of bone ECM, and osteocalcin, and FTIR-ATR to assess chemical groups that may be present in the bony calcified matrix.

Chondrogenic differentiation was assessed through histological stains as Safranin O as well as immunochemistry for collagen II, and aggrecan, major molecules present on the cartilage ECM.

Techniques selected for cell-scaffold characterization are described in detail within the following sections of this chapter.

#### **II.6.7.1. Cell viability methods – MTS and Calcein AM**

The MTS (3-(4,5-dimethylthiazol-2-yl)-5-(3-carboxymethoxyphenyl)-2-(4-sulfophenyl)-2H-tetrazolium) assay is a colorimetric method for determining the number of viable cells in proliferation or cytotoxicity assays, and was used in chapter IV. The MTS compound is bio-reduced by cells, when reductase enzymes are active, into a colored formazan product that is soluble in culture medium. The quantity of formazan product measured at 490 nm absorbance, is directly proportional to the number of living viable cells in culture.

Calcein AM (Calcein acetoxymethyl ester) (Figure II.6.3) is a cell-permeant and non-fluorescent compound widely used for determining cell viability. In live cells the non-fluorescent calcein, AM is hydrolyzed by intracellular esterases into the strongly green fluorescent anion calcein. The fluorescent calcein is well-retained in the cytoplasm in live cells, and the fluorescence intensity is proportional to the amount of live cells. Calcein is a photostable reagent not influenced by intracellular pH. Its bright green fluorescence can be monitored at Ex/Em = 494 nm /520 nm.

This method was used in chapters V, VI, and VIII. After cell culturing according to predefined end points, hAFSC- and hBMSC-SPCL constructs were rinsed in PBS (HyClone) and incubated in culture medium with 3  $\mu$ M Calcein AM (Molecular Probes, Invitrogen) for 30 minutes at 37 °C in a 5 % CO<sub>2</sub> environment. Afterwards, constructs were rinsed again in PBS and fixed in 10 % buffered formalin (Surgipath Medical Industries, Inc.) overnight at 4 °C,



before observed under a confocal microscope. DAPI (Molecular Probes, Invitrogen), a fluorescent marker that binds to nucleic acids, DNA and RNA, and can enter live or dead cells, was used in chapter VI.

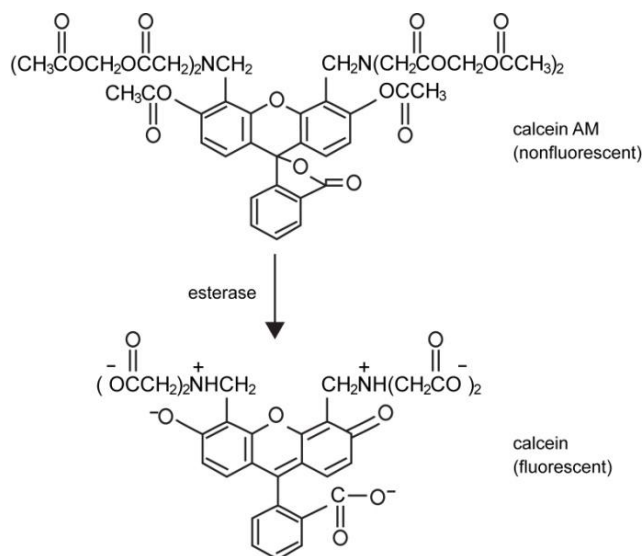


**Figure II.6.3** – Calcein AM cleavage by viable cells.

The main difference in these methods is that MTS is a quantitative method, while Calcein AM is qualitative. Small absorbance variations can be detected among samples with MTS assay. Although counting cells with Calcein AM method is possible, it is very time consuming, and with an intense fluorescence signal, counting individual cells can be a difficult task to perform. Nevertheless, Calcein AM procedure presents additional advantages as it enables, for instance observing the distribution and colonization of viable cells population on a scaffold or plate.

#### **II.6.7.2. Cellular proliferation assay (DNA quantification)**

The cell proliferation assay described in this Thesis (chapter III, IV and VII) is an ultra-sensitive fluorescent nucleic acid stain for quantitating double-stranded DNA (dsDNA) by measuring the fluorescence produced when PicoGreen dye (Molecular Probes, P-7589) is excited by UV light and binds to double-stranded DNA (dsDNA) present in the tested sample.

In this assay, the constructs were harvested from the culture medium, rinsed in PBS, followed by cell lysis in ultra pure water. Samples were kept at -80 °C until testing. Afterwards, samples were thawed and briefly sonicated for 15 minutes to rupture any remaining cell

membrane. Cell lysate is incubated with a dye that fluoresces when binds to DNA. The intensity of the fluorescence from the DNA–dye complex is then measured with a standard fluorometer. The number of cells in the sample is determined by comparing the fluorescence intensity of the sample to a previously generated standard curve (concentrations ranging from 0.0 to 1.5 µg/mL). The standard curve relates the number of cells in a sample to the intensity of the fluorescence from the DNA–dye complex. The fluorescence is read using a microplate ELISA reader (Synergie HT, BioTek) at an excitation of 485/20 nm and an emission of 528/20 nm.

### **II.6.7.3. Histology**

Histological analysis was performed in *in vitro* cultured AFSC-agarose systems from chapter V to assess the chondrogenic differentiation through staining and immunostaining procedures.

Samples for histological analysis were firstly rinsed in PBS and fixed in a 4 % buffered formalin solution overnight. Afterwards, samples were included in histological cassettes and dehydrated in a series of ethanol concentration followed by xylene solution to remove water from tissues in tissue processor equipment (Microm STP120, MICROM International GmbH, Germany). AFSC-agarose constructs were wrapped in foam before placed inside the cassettes. The foam encloses delicate and very small samples that could be lost or damaged during the procedure.

Samples were then embedded in paraffin wax (Microm EC 350-2, ThermoScientific, Spain), and included in blocks, and stored at room temperature. Blocks were then cut into 10 µm thick sections using a microtome, and then deparaffined. Since most stains and antibodies are aqueous solutions, deparaffinization (removing paraffin wax and re-hydration of samples) is a common step prior staining or immune-detection described below. After the histological protocol is completed, sections must be mounted before observed under a microscope.

### **II.6.7.4. Osteogenic markers**

#### **II.6.7.4.1. Alkaline Phosphatase Activity (ALP)**

Alkaline Phosphatases (ALP) are a group of enzymes found in several organs but the isoenzyme ALP-2 is primarily found in the bone, with a particular influence in bone

metabolism. As the name implies, this enzyme works best at an alkaline pH (a pH of 10), acting by splitting off phosphorus (an acidic mineral) creating an alkaline pH.

Bone ALP is present in vesicles secreted by osteoblasts to induce bone mineralization, and has been associated to the *in vitro* ECM development and maturation[54]. Consequently, ALP activity has been considered a marker of the osteogenic differentiation process of stem cells.

ALP can be detected by different methods based on enzymatic reaction followed by colorimetric analysis or by fast red violet dye. In this Thesis, ALP was evaluated according to the procedures mentioned above; fast red violet dye in constructs with BMSCs- and AFSCs seeded onto SPCL scaffolds from chapter VI and VIII, and a colorimetric assay using an ELISA microplate reader in samples with gBMSCs- seeded onto TCP-PCL nanofibers or seeded onto SPCL- and SPCL-Si- scaffolds from chapter III, VII, and IV, respectively.

The principle of the ALP staining, considered in chapter VI and VIII, relies on immersing the samples in a Naphthol AS-MX phosphate alkaline solution; a histochemical substrate used for the detection of ALP activity, commonly used in conjunction with Fast Violet B salt (Sigma). After each end point, cells were fixed in 10 % buffered formalin solution overnight at 4 °C, and then rinsed and kept in PBS until incubating the cells in a staining solution of 0.25 % Naphthol AS-MX phosphate alkaline solution (Sigma-Aldrich) and Fast Violet B salt (Sigma) for 30 minutes. To remove the excess of non-specific staining, samples were rinsed in PBS and observed under an inverted microscope (Leica, DMI4000B). Sample images were acquired using a camera Q-Imaging (Retiga-2000RV) or, in the case of full sized constructs, observed directly and images acquired using an Olympus SP-570UZ digital camera.

Beside the staining approach, ALP activity can be quantitatively evaluated using a colorimetric development assay, which was used in chapter III, IV, and VII. Despite the fact that this method is more sensitive to small ALP activity variations, it is an indirect evaluation method as only ALP molecules released into the sample solution can be measured. Thus, constructs were harvested from the culture medium, rinsed in PBS and placed in a microtube containing 1 mL of ultra-pure water and kept frozen at -80 °C until testing. Afterwards, samples were thawed and briefly sonicated for 15 minutes in order to rupture any cell that might have kept the membrane integrity after the osmotic treatment followed by a freezing/thawer cycle. Then, a substrate solution consisting of 0.2 % (wt/v) p-nitrophenyl phosphate (Sigma) in a substrate buffer with 1 M diethanolamine HCl (Merck), at pH 9.8 was added to each sample, at a proportion of 60 µl of solution to 20 µl of sample.

The plate containing the samples was incubated in the dark for 45 minutes at 37 °C, followed by the addition of a stop solution (2 M NaOH (Panreac) plus 0.2 mM EDTA (Sigma)) to

end the color development reaction. Standards were prepared with p-nitrophenol ( $10 \mu\text{mol}\cdot\text{ml}^{-1}$ ) (Sigma) in order to achieve final concentrations ranging between 0.0 -  $0.3 \mu\text{mol}\cdot\text{ml}^{-1}$ . Samples and standards were analyzed in triplicates. The colorimetric assay measures the conversion of the colorless substrate p-nitrophenol phosphate into the yellow soluble product p-Nitrophenol by the enzyme ALP. P-nitrophenyl phosphate absorbs at 405 nm, and is the preferred substrate for high sensitivity detection of ALP in ELISA assays. The absorbance was read in a microplate ELISA reader (Synergie HT, BioTek) at 405 nm and concentration values determined by intrapolation using a standard curve established by the standards.

#### II.6.7.4.2. *Alizarin Red Staining*

Alizarin red or 1,2-dihydroxyanthraquinone is an organic compound used for decades to identify calcium-rich deposits[55] in tissue sections or cells in culture. The reaction is not strictly specific for calcium, since magnesium, manganese, barium, strontium, and iron may interfere, but these elements usually do not occur in sufficient concentration to interfere with the staining. Calcium forms an Alizarin Red S-calcium complex in a chelation process, and the end product is birefringent. Alizarin red staining is particularly versatile since the method can be both qualitative and semi-quantitative as the dye can be extracted, dragging with it the calcium ions, and readily assayed. Then, using a calibration curve and appropriate standards, calcium concentration values can be achieved.

Alizarin Red was directly evaluated as a staining in constructs from chapter III and VI; gBMSCs seeded onto PCL-TCP nanofibers and hAFSCs- and hBMSCs- seeded onto 6-well plates, respectively. An alizarin red solution (0.2 % to 2 %, depending on specimens, Sigma-Aldrich) was prepared, pH adjusted to 4.1-4.3 and samples stained by immersion for 2 minutes.

The alizarin red stain found in BMSC- and AFSC- samples from chapter VI, and in the BMSC- and AFSC-SPCL constructs from chapter VI and VIII, was solubilized in cetylpyridinium chloride (Sigma) at pH 7.0 for 15 minutes under mild agitation and calcium-bounded to alizarin red quantified at 562 nm, using a plate reader (SpectraMax MS, Molecular Devices).

#### II.6.7.4.3. *Fourier Transformed Infrared Spectroscopy with Attenuated Total Reflectance*

FTIR spectroscopy has been successfully used to analyze the changes in minerals and components of bone tissue since vibrational spectroscopy in the mid-infrared region can provide molecular structure information about mineralized tissue[56].

The composition of the human AFSC-SPCL constructs considered in chapter VIII was analyzed by FTIR-ATR in order to detect molecular groups associated to ECM mineralization.

Before the analysis, samples were dehydrated in a series of ethanol concentrations and air-dried at room temperature. FTIR-ATR was performed in the spectral range of 1800-600  $\text{cm}^{-1}$  using the Spectrum 400 FT-IR/FT-NIR spectrometer (Perkin Elmer). Results were compared to cell-free scaffolds in order to exclude the contributions from the scaffold composition.

#### *II.6.7.4.4. Immunocytochemistry: Collagen I and Osteocalcin*

Immunocytochemistry for Collagen I and Osteocalcin was performed on gBMSCs- PCL-TCP samples from chapter III. Collagen I is the most abundant collagen of the human body and the major protein present in bone ECM, responsible for strengthen and support of bone tissue. On the other hand, osteocalcin (OCa) is a non-collagenous protein, produced by osteoblasts, that participates in the matrix mineralization of bone[57] as OCa binds to hydroxyapatite in a calcium-dependent manner[58].

Immunocytochemistry was performed according to R.T.U. Vectastain Universal Elite ABC kit (PK 7200) from VectorLabs, using R.T.U Normal Horse Serum to avoid unspecific reactions, a biotinilated secondary antibody (R.T.U. Biotinylated Universal Antibody, one-hour incubation), and a Peroxidase Substrat Kit (Vector SK-4100). 3,3'-Diaminobenzidine (DAB) was the colorimetric substrate used in the assays.

Primary antibodies used included Collagen I (MAB339, Chemicon) and Osteocalcin (Ab13418, Abcam), which were prepared using a 1/100 dilution. With the exception of primary antibodies, which were incubated overnight at 4°C, all the other steps of this procedure were performed at room temperature.

#### *II.6.7.4.5. Immunofluorescence: Collagen I and RunX-2*

Immunofluorescence for Collagen I was performed on BMSC- and AFSC-SPCL constructs from chapter VI and VIII, while RunX-2 expression was assessed in BMSC- and AFSC-SPCL constructs from chapter V and VI. Cbfa1/RunX-2 is a key transcription factor associated with osteoblast differentiation, essential for osteoblastic differentiation and skeletal morphogenesis[59].

Collagen I from Southern Biotech (1310-01) and RunX-2 (ab23981) purchased to Abcam were diluted to 1:100 and 1:20 ratio, respectively, and incubated overnight at 4 °C.

AlexaFluor 488 and 594 (Molecular Probes, Invitrogen; 1:200 dilution, one-hour incubation) were used as fluorescent secondary antibodies.

Instead of animal serum, blocking step was performed using protein block serum free (Dako). After the procedure, constructs were then observed under a confocal microscope (Axiovert 100 M, Zeiss) equipped with argon/He-Ne laser sources.

#### ***II.6.7.5. Chondrogenic markers***

##### *II.6.7.5.1. Safranin O staining*

Safranin, Safranin O or basic red 2 is a cationic dye frequently used as a counterstain, and for the detection of mucin, cartilage[60] and mast cells.

Following deparaffinization of AFSC-agarose sections from chapter V, slides were stained with Weigert's iron hematoxylin working solution (Merck) for 7 minutes. Samples were rinsed in tap water for 10 minutes, and subsequently rinsed quickly in 1 % acetic acid solution for about 10 to 15 second and stained in 0.1 % safranin O solution (Fluka) for 5 minutes.

##### *II.6.7.5.2. Immunofluorescence: aggrecan and collagen II*

Immunofluorescence for aggrecan and collagen II was performed on AFSCs encapsulated in agarose hydrogels from chapter V.

Aggrecan and collagen II, two of the main cartilaginous proteins, were evaluated to assess the chondrogenic differentiation under the scope of this Thesis. Aggrecan is a chondroitin sulfate proteoglycan that along with collagen II forms a major structural component of cartilage. About 90 % of articular cartilage is made of Collagen II, a protein responsible to entrap proteoglycan aggregates and provide the characteristic tensile strength to the tissue.

Samples were prepared as described previously in section II.6.7.6. Primary antibodies Collagen II (MAB1330, Chemicon) and Aggrecan (MCA1452 Serotec) were prepared with a 1/100 dilution. AlexaFluor 488 (Invitrogen; 1:200 dilution, one-hour incubation) was used as the fluorescent secondary antibody.

#### **II.6.7.6. Evaluation of cell morphology and distribution**

Cell morphology and distribution throughout a 3D matrix was evaluated in cell-scaffold constructs with confocal microscopy and scanning electron microscopy.

##### *II.6.7.6.1. Confocal laser scanning microscopy (CLSM)*

Confocal laser scanning microscopy (CLSM) is an optical imaging technique used to increase contrast and optical resolution, overcoming the limitations of conventional widefield microscopy. Simultaneously, CLSM facilitates the generation of high resolution 3D images from a relatively thick sample[61]. In some cases, the 3D reconstruction allows a better understanding of the distribution, organization or morphology of cells, or molecules of interest.

Confocal microscopy was a very useful technique to assess cellular viability by Calcein AM in human AFSCs and BMSCs seeded onto SPCL scaffolds and AFSCs encapsulated in agarose gels, described in chapter V and VI. CLSM was also used for the detection of specific bone markers, such as RunX-2 or collagen I in SPCL constructs seeded with AFSCs or BMSCs (chapter V, VI and VIII).

Samples were prepared accordingly to Calcein AM and immunofluorescence protocols above mentioned, before analyzed under a confocal microscope (Axiovert 100 M, Zeiss) equipped with argon/He-Ne laser sources.

##### *II.6.7.6.2. SEM*

Cell seeded constructs[18,62] were also examined by SEM to assess cellular morphology, distribution and relative proliferation between samples from different end points. In some cases, it is also possible to assess ECM mineralization by energy dispersion spectroscopy (EDS) coupled to SEM equipment.

All cell-scaffold constructs described in experimental chapters (chapters III, IV, V, VI, VII and VIII), namely gBMSC-PCL-TCP, gBMSC-SPCL and gBMSC-SPCL-Si samples, as well as hBMSC- and AFSC- seeded onto SPCL scaffolds, were observed by scanning electron microscopy (Leica Cambridge, model S360 or Hitachi S-2600N, Hitachi Science Systems, Ltd).

Constructs were fixed in formalin, and the samples from chapter III, IV and VII were dehydrated in a series of ethanol concentrations followed by air-dried. Conversely, constructs

from chapter V, VI and VIII were critical point dried (EMS850X, Electron Microscopy Sciences) after fixed in a formalin solution and dehydrated to 100 % ethanol.

All samples were gold sputtered (Fisons Instruments, model SC502 or Hummer 6.2 sputtering system, Anatech Ltd) for 2 minutes at 15 mA. Samples were further assessed by SEM and micrographs recorded at 15 kV ranging from 100x to 5000 x magnification.

#### *II.6.7.6.3. Energy dispersive X-ray analysis or EDS analysis*

Energy dispersive X-ray analysis or EDS is a technique used to identify the elemental composition of a sample, including bone tissue[63]. In terms of biological samples in this Thesis, EDS analysis proved to be very useful for the detection of a calcified/mineralized ECM (with calcium and phosphorus elements) produced by osteoblastic cells, when seeded in non-ceramic scaffolds.

Since samples for SEM can be used for EDS analysis, constructs preparation is the same as mentioned in the previous section. EDS and EDAX (Pegasus X4M) were used to determine the presence/absence of calcium and phosphorus in the ECM matrix produced by hAFSCs and hBMSCs cultured onto SPCL scaffolds (chapter V and VIII, respectively).

## **II.7. Animal models studies**

### **II.7.1. Goat model – non critical defects**

The selection of goat as an animal model was justified in a previous section (*II.6.1.1.*). The primary goal of this study was to analyse the role of the scaffold material and of BMSCs in a TE strategy aimed at bone regeneration. Thus, SPCL scaffolds, seeded or not seeded with gBMSCs under different stages of osteogenic differentiation were implanted in non-critical sized femoral defects.

Although many studies are conducted ectopically, orthotopic implants provide more relevant data since implants are located in the tissue/area of their target application and thus, any eventual site specific reaction such as cell recruitment or growth factor release either associated to the tissue healing or to an inflammatory process is expected to be similar to the ones that are likely to occur in a real clinical situation.



Four skeletally adult female goats weighing 30-45 kg were used in the study described in chapter VII. The housing care and experimental protocol were performed according to the national guidelines, after approval by the National Ethical Committee for Laboratory Animals (2007-07-27, document number 018939) and conducted in accordance with international standards on animal welfare as defined by the European Communities Council Directive of 2 November 1986.

#### **II.7.1.1. Implantation surgery**

After general anaesthesia, each goat was positioned in lateral recumbency, prepared and draped in a sterile manner to perform a surgical access to the lateral diaphysis of femur.

A skin incision was then performed from the greater trochanter and continued distally to the lateral femoral condyle. The subcutaneous tissue, tensor fascia lata and lateral fascia of the vastus muscle were incised. Biceps femoris muscles were retracted posteriorly, and the vastus muscle was retracted anteriorly, after being detached from the linea aspera and femora shaft, like the periosteum.

Non-critical size defects ( $\phi$  6 mm and 3 mm depth) were drilled in the lateral diaphysis of both posterior femurs of the 4 adult goats with a bone drill (Synthes®, Switzerland). The drill-hole technique selected was based on the one described by Hallfeldt *et al.*[64].

Eight drills were created bilaterally in the posterior femurs, with a separation distance between drills of 3 cm, in two non parallel sections to avoid fracture tension or neobone formation among drills. Two drills were left empty and 2 filled with scaffolds without cells, the control for this experiment. The remaining drills were filled in with constructs osteogenically cultured for 1 day (2 defects) or 7 days (2 defects).

Implants were gently pressed fit (Figure II.7.1). The muscle was replaced over the bone, and the fascia lata and skin were closed with resorbable and non-resorbable sutures, respectively.

During the first post-operative week, animals were medicated with flunixin meglumin (1 mg/kg IM, Finadyne® P.A., Schering-Plough II) for 2 days and amoxicillin (15 mg/kg IM, Clamoxyl® L.A., Pfizer) for 7 days. After implantation, animals were kept in a room, where goats could move freely and full weight-bear on the posterior limbs during the complete post-operative period.

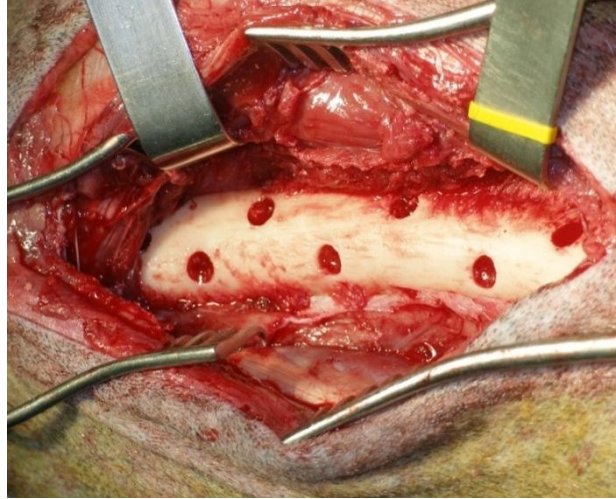


**Figure II.7.1** - Non-critical size defects drilled in the posterior femur of a goat model.

### **II.7.1.2. *Imprinting new bone with fluorescent dyes***

Fluorochrome sequential labelling of mineralizing tissues is commonly used in different fields of clinical and basic research[65]. Fluorochrome use in animal models makes it possible to determine the onset time and location of osteogenesis, which are the fundamental parameters in bone tissue engineering studies.

Intravital fluorescence markers, namely, xylenol orange (90 mg/kg, Aldrich), calcein green (10 mg/kg, Sigma) and tetracycline (25 mg/kg, Sigma) were injected subcutaneously after 2, 4 and 6 weeks of follow up, respectively, for monitoring bone formation and mineralization along with the implantation period.

### **II.7.1.3. *Explant retrieval and characterization***

Six weeks after surgery, and 24 h after tetracycline injection, animal euthanasia was performed using an overdose of pentobarbital sodium (Eutasil®, Sanofi). The femurs were explanted and cut into single-defect segments, which were fixed in a 4 % formaldehyde solution (pH 7.2) (Sigma) until further usage.

#### ***II.7.1.3.1. Histological characterization***

Single-defect segments were processed and embedded in glycol methacrylate solution (Technovit 7200® VLC–Heraus Kulzer GmbH) for histologic assessment of calcified bone.

Sections of 30 µm were prepared according to *Donath et al.* technique[66] using an Exakt-Cutting® System (Aparatebau GMBH, Germany).

Only the mid section of each bone segment was observed at the fluorescence microscope (Olympus BX51) for fluorochrome detection, and then selected for histomorphometric analysis.

Additional sections were stained with Lévai-Laczkó[67] to differentiate between native bone and the new bone formation using a stereo microscope (Olympus SZX9).

Quantitative measurement for bone neoformation was carried out after selecting relevant drill surrounding areas and quantified using Microimage 4.0 software.

### **II.7.2. Nude rat model - non-union defects**

Non-unions or critical sized defects were induced in a nude rat model using human AFSCs. The purpose of selecting the rat instead of the goat, one step backwards in the phylogenetic scale, relies on the fact that the rat is another popular subject in the TE field, and in particular in orthopaedics research. Regardless of the size, rat's popularity is mainly due to its low cost, easy handling, housing, operating, and follow up than goats. The rat plays an important role in studies of biocompatibility, including subcutaneous or intramuscular implantation of biomaterials[17,24] to bone defect repair[68,69]. The availability of rats with distinctive characteristics, such as athymic nude[69] or transgenic animals not easily available in larger animal models, amplifies the study possibilities in xenograft research and, consequently the implantation of human cells in a non-human host.

Despite the fact that AFS cells are unlikely to cause any minimal immune reaction, due to their described non-immunogenic features, AFSCs were used in critical-sized defects in nude rats. Several main reasons can justify this selection since in the human fetus, precursor cells, which will later evolve into immune cells, can be found as early as 4-8 weeks of gestation, and we wanted to prevent any possible interference with a human cell source. Furthermore, AFSCs present exciting properties that can be used as an alternative source to autologous approaches, as a highly proliferative and universally available source of stem cells.

Geriatric animals were used to better mimic the regenerative process in bone, which is particularly affected in elder patients. Thus, male athymic nude rats (36-40 week old) weighing 420-560 g (n=60) were purchased from Charles River and used in the study described in chapter VIII. Since this study was performed in collaboration with WIRM, all procedures were

performed in accordance with Wake Forest University Animal Care and Use Committee (ACUC) approved protocols (protocol number; A07-063/A10-032).

During the entire study, adequate measures were taken to minimize any pain or discomfort to the animals.

### **II.7.2.1. Implantation**

Animals were randomly assigned into 5 groups (n=6 / group) as follows: 1) no-repair group (empty defects, no implant), 2) scaffold-only group, and 3) scaffold with undifferentiated hAFSC cell group, 4) scaffold with hAFSC osteogenically committed group, and 5) scaffold with hAFSCs differentiated into osteoblast-like cells group.

Anesthesia was induced with 3 % isoflurane (USP, Novaplus) prior to surgical procedures. The dorsolateral side of the right leg was shaved and sterilized with routine aseptic agent. Under aseptic conditions, a 20 mm long incision was made on the skin over the femur of the right hind limb. The skin and the gluteus muscle were dissected to approach the femur. A periosteal incision was made on the periosteum of the femur, and the periosteum and the attached muscles were elevated to expose the femur. Retracting adjacent tissues, a 3.0 mm thick and 2.2 cm long custom-made bone plate was placed along the intact femur and was fixed with 4 stainless steel screws using a micro drill system (BS72-4950, Harvard apparatus, USA) to stabilize the femur after scaffold implantation.

A 5 mm bone segment in between screwed areas at both ends was removed from the femur using a bone cutting bur. The created defects were thoroughly irrigated with sterile saline to avoid residual bone particles at the site. Subsequently, the scaffolds and cell-scaffold constructs from the different study groups, according to our experimental design, were implanted to the bony defects and fixed in a press-fit manner. After inserting the scaffolds/constructs, the muscle and the skin were closed layer by layer using 5-0 *Vicryl* sutures (Ethicon, USA). The animals were maintained postoperatively according to the guideline of the ACUC.

Radiographic 2D images of the femoral defects were obtained from each animal every 4 weeks, using C-arm equipment (Siremobil Compact L, Siemens) to monitor plate stability and select animals for micro-CT analysis. Animals were kept under general anaesthesia during both (x-rays and micro-CT) procedures in order to minimize stress and assure animal welfare.

### **II.7.2.2. Explant retrieval and characterization**

Rats were euthanized 4 or 16 weeks after implantation accordingly to ACUC guidelines. Right femurs were retrieved, rinsed in PBS, placed in 10 % buffered formalin for 96 h and then kept in 60 % ethanol until histological processing.

#### *II.7.2.2.1. Micro-computed tomography (bone formation assessment)*

Bone ingrowth studies have been investigated involving micro-CT analysis for assessment of structural characteristics and mineralization of a tissue in continuous regeneration[70], creating new possibilities for biomedical applications.

Rats were anaesthetized during the real time live imaging of the femoral defects, obtained using a  $\mu$ -CT equipment, Siemens MicroCAT II (Siemens Preclinical Solutions, Knoxville, TN), where a MicroCAT II version 1.9d software was used to acquire raw data.

Scans were performed with an x-ray voltage of 70 kVp / 500  $\mu$ A, and an exposure time of 1600 ms (BIN Factor of 2, 360° rotation, 360 steps, 36 micron isotropic voxel dimension).

RVA version 4.2.9 and COBRA EXXIM version 4.9.52 were used to reconstruct the raw data into raw slice images, and then Amira version 3.1 was used for conversion to DICOM images. Analysis was done after transfer of images to TeraRecon AquariusNET Server (TeraRecon, Inc., San Mateo, CA) using TeraRecon software AquariusNET version 1.8.1.6. Another software packages used for image analysis and volumetric measurements included Mimics version 13 (Materialise, Leuven, Belgium).

#### *II.7.2.2.2. X-rays*

X-ray is a form of electromagnetic radiation that can penetrate solid objects, which has proved useful for medical purposes, including the detection of pathological conditions of the skeletal system as well as some disease process in soft tissues.

In this Thesis (chapter VIII), radiographic 2D images of the femoral defects were obtained from each animal every 4 weeks up to a maximum of 16 weeks, using C-arm equipment (Siremobil Compact L, Siemens) to monitor plate stability and select animals for micro-CT analysis.

#### II.7.2.2.3. *Histological Characterization*

Explants were decalcified using an acid solution of Immunocal® (Decal Chemical Corp), and tissue processed in a graded series of ethanol, xylene and embedded in paraffin blocks. Sections of 10 µm were obtained using a microtome, and stained with H&E. For this purpose, slides were stained with Mayer's hematoxylin for 4 minutes, followed by a rinse in water to remove excess of stain and 3 immersions in ammonia water. Then, samples were washed in tap water for 3 minutes and stained with eosin for another 3 minutes.

Hematoxylin, a base dye, stains nuclei blue due to an affinity to nucleic acids in the cell nucleus; eosin, an acidic dye, stains the cytoplasm pink.

After staining, samples were rinsed again in water and dehydrated before mounting the slides with non-aqueous medium, and observed under a microscope (Imager Z1m, Zeiss) equipped with an AxioCam MRc5 camera (Zeiss).

Immunocytochemistry was performed for bone related markers: collagen I and osteocalcin, as well as an angiogenic marker, VEGF, in explant sections from chapter VIII.

Primary antibodies anti- collagen I (1310-01, Southern Biotech; 1:20 dilution), osteocalcin (V-19, Santa Cruz Biotechnology, 1:100) and VEGF (147, Santa Cruz Biotechnology, 1:100) were diluted in antibody diluent with background reducing components from Dako (Denmark). Biotinylated secondary antibodies were obtained from Vector Lab (Burlingame, CA, USA) as well as R.T.U. HRP/Straptavidin (SA-5704). Immunocytochemistry visualization was assessed by NovaRED substrate kit (SK-4800, Vector Lab).

Specimen slides were observed under a microscope (Imager Z1m, Zeiss, Germany) equipped with a digital camera (AxioCam MRc5).

#### II.7.2.2.4. *Histomorphometric analysis*

Histomorphometrical analysis was carried out to quantify stained areas in samples retrieved from *in vivo* experiments of chapter VIII, after immunostaining for bone related markers, namely osteocalcin and collagen I as well as vascular markers by VEGF expression. For this purpose, an interest area was selected, and kept constant for all slides, where protein expression was detected and analyzed using the *Cell D* software (analysis image processing) and *MicroImage* software from Olympus Optical Co.

## II.8. Statistical analysis

Several statistical methods were used in this Thesis, accordingly to the experimental assay requirements.

In chapter III, the statistical analysis was carried out using One Way ANOVA test and Tukey's Multiple Comparison Test ( $p < 0.05$ ), and results presented as mean  $\pm$  standard deviation.

In chapter IV, results are also presented as means  $\pm$  standard deviation. Statistical differences between sample groups ( $p < 0.001$  or  $p < 0.05$ ) were assessed by two Way ANOVA.

Statistical analysis was also carried out in chapter VII by mean  $\pm$  standard error of mean using T-Test and 2-way ANOVA for *in vitro* and for *in vivo* measurements, respectively. At least 4 samples were considered in the *in vitro* assays (DNA, ALP, SEM) while 16 samples were considered *in vivo* for each condition; A) empty drill, B) drill with SPCL scaffold, drills with SPCL seeded with gBMSCs for either C) 1 or D) 7 days in osteogenic medium).

Results from chapter VIII, are presented as means  $\pm$  standard deviation in *in vitro* assays, while results from histomorphometric analysis are presented as means  $\pm$  standard error of mean. Two Way ANOVA test was applied to assess statistical significant differences between sample groups followed by Bonferroni's Multiple Comparison test ( $*=p < 0.05$ ).

## References

1. Middleton JC, Tipton AJ: Synthetic biodegradable polymers as orthopedic devices. *Biomaterials* 2000, 21(23): 2335-46.
2. Pitt CG, Gratzl MM, Kimmel GL, Surles J, Schindler A: Aliphatic polyesters II. The degradation of poly (DL-lactide), poly (epsilon-caprolactone), and their copolymers in vivo. *Biomaterials* 1981, 2(4): 215-20.
3. Tsuji H, Ikada Y: Blends of Aliphatic Polyesters. II. Hydrolysis of Solution-Cast Blends from Poly(L-lactide) and Poly (epsilon-caprolactone) in Phosphate-Buffered Solution. *Journal of Applied Polymer Science* 1998, 67: 495-415.
4. Tsuji H, Ikada Y: Blends of Aliphatic Polyesters. I. Physical Properties and Morphologies of Solution-Cast Blends from Poly(DL-lactide) and Poly(epsilon-caprolactone). *Journal of Applied Polymer Science* 1996, 60: 2367-2375.
5. Bezwada RS, Jamiolkowski DD, Lee IY, Agarwal V, Persivale J, Trenkenthin S, Ernetta M, Suryadevara J, Yang A, Liu S: Monocryl(R) Suture, a New Ultra-Pliable Absorbable Monofilament Suture. *Biomaterials* 1995, 16(15): 1141-1148.

6. Shin M, Yoshimoto H, Vacanti JP: In vivo bone tissue engineering using mesenchymal stem cells on a novel electrospun nanofibrous scaffold. *Tissue Eng* 2004, 10(1-2): 33-41.
7. Srouji S, Kizhner T, Suss-Tobi E, Livne E, Zussman E: 3-D Nanofibrous electrospun multilayered construct is an alternative ECM mimicking scaffold. *J Mater Sci Mater Med* 2008, 19(3): 1249-55.
8. Martins A, Araujo JV, Reis RL, Neves NM: Electrospun nanostructured scaffolds for tissue engineering applications. *Nanomedicine (Lond)* 2007, 2(6): 929-42.
9. Gupta D, Venugopal J, Mitra S, Giri Dev VR, Ramakrishna S: Nanostructured biocomposite substrates by electrospinning and electro spraying for the mineralization of osteoblasts. *Biomaterials* 2009, 30(11): 2085-94.
10. Li WJ, Tuli R, Huang X, Laquerriere P, Tuan RS: Multilineage differentiation of human mesenchymal stem cells in a three-dimensional nanofibrous scaffold. *Biomaterials* 2005, 26(25): 5158-66.
11. Salgado AJ, Coutinho OP, Reis RL: Novel starch-based scaffolds for bone tissue engineering: cytotoxicity, cell culture, and protein expression. *Tissue Eng* 2004, 10(3-4): 465-74.
12. Salgado AJ, Coutinho OP, Reis RL, Davies JE: In vivo response to starch-based scaffolds designed for bone tissue engineering applications. *J Biomed Mater Res A* 2007, 80(4): 983-9.
13. Elvira C, Mano JF, San Roman J, Reis RL: Starch-based biodegradable hydrogels with potential biomedical applications as drug delivery systems. *Biomaterials* 2002, 23(9): 1955-66.
14. Balmayor ER, Tuzlakoglu K, Marques AP, Azevedo HS, Reis RL: A novel enzymatically-mediated drug delivery carrier for bone tissue engineering applications: combining biodegradable starch-based microparticles and differentiation agents. *J Mater Sci Mater Med* 2008, 19(4): 1617-23.
15. Gomes ME, Azevedo HS, Moreira AR, Ella V, Kellomaki M, Reis RL: Starch-poly(epsilon-caprolactone) and starch-poly(lactic acid) fibre-mesh scaffolds for bone tissue engineering applications: structure, mechanical properties and degradation behaviour. *J Tissue Eng Regen Med* 2008, 2(5): 243-52.
16. Gomes ME, Bossano CM, Johnston CM, Reis RL, Mikos AG: In vitro localization of bone growth factors in constructs of biodegradable scaffolds seeded with marrow stromal cells and cultured in a flow perfusion bioreactor. *Tissue Eng* 2006, 12(1): 177-88.
17. Santos TC, Marques AP, Horing B, Martins AR, Tuzlakoglu K, Castro AG, van Griensven M, Reis RL: In vivo short-term and long-term host reaction to starch-based scaffolds. *Acta Biomater* 2010, 6(11): 4314-26.
18. Leonor I, Rodrigues MT, Gomes ME, Reis RL: In Situ Functionalization of Wet-Spun Fibre meshes for Bone Tissue Engineering: One Step Approach. *J Tissue Eng Regen Med* 2011, 5: 104-111.
19. Tuzlakoglu K, Pashkuleva I, Rodrigues MT, Gomes ME, van Lenthe GH, Muller R, Reis RL: A new route to produce starch-based fiber mesh scaffolds by wet spinning and subsequent



surface modification as a way to improve cell attachment and proliferation. *J Biomed Mater Res A* 2010, 92(1): 369-77.

20. Gomes ME, Holtorf HL, Reis RL, Mikos AG: Influence of the porosity of starch-based fiber mesh scaffolds on the proliferation and osteogenic differentiation of bone marrow stromal cells cultured in a flow perfusion bioreactor. *Tissue Eng* 2006, 12(4): 801-9.

21. Santos MI, Fuchs S, Gomes ME, Unger RE, Reis RL, Kirkpatrick CJ: Response of micro- and macrovascular endothelial cells to starch-based fiber meshes for bone tissue engineering. *Biomaterials* 2007, 28(2): 240-8.

22. Oliveira JT, Crawford A, Mundy JM, Moreira AR, Gomes ME, Hatton PV, Reis RL: A cartilage tissue engineering approach combining starch-polycaprolactone fibre mesh scaffolds with bovine articular chondrocytes. *J Mater Sci Mater Med* 2007, 18(2): 295-302.

23. Gonçalves A, Costa P, Rodrigues MT, Dias IR, Reis RL, Gomes ME: Effect of flow perfusion conditions in the chondrogenic differentiation of bone marrow stromal cells cultured onto starch based biodegradable scaffolds *Acta Biomaterialia* 2011, 7: 1644-1652

24. Marques AP, Reis RL, Hunt JA: An in vivo study of the host response to starch-based polymers and composites subcutaneously implanted in rats. *Macromol Biosci* 2005, 5(8): 775-785.

25. Tisdell CL, Goldberg VM, Parr JA, Bensusan JS, Staikoff LS, Stevenson S: The influence of a hydroxyapatite and tricalcium-phosphate coating on bone growth into titanium fiber-metal implants. *J Bone Joint Surg Am* 1994, 76(2): 159-171.

26. Schmitz JP, Hollinger JO, Milam SB: Reconstruction of bone using calcium phosphate bone cements: a critical review. *J Oral Maxillofac Surg* 1999, 57(9): 1122-1126.

27. Collins AM, Skaer NJV, Gheysens T, Knight D, Bertram C, Roach HI, Oreffo ROC, Von-Aulock S, Baris T, Skinner J, Mann S: Bone-like resorbable silk-based scaffolds for load-bearing osteoregenerative applications. *Advanced Materials* 2009, 21: 75-78.

28. Rezwan K, Chen QZ, Blaker JJ, Boccaccini AR: Biodegradable and bioactive porous polymer/inorganic composite scaffolds for bone tissue engineering. *Biomaterials* 2006, 27(18): 3413-3431.

29. Ngiam M, Liao S, Patil AJ, Cheng Z, Yang F, Gubler MJ, Ramakrishna S, Chan CK: Fabrication of mineralized polymeric nanofibrous composites for bone graft materials. *Tissue Eng Part A* 2009, 15(3): 535-546.

30. Li C, Vepari C, Jin HJ, Kim HJ, Kaplan DL: Electrospun silk-BMP-2 scaffolds for bone tissue engineering. *Biomaterials* 2006, 27(16): 3115-3124.

31. Ogose A, Hotta T, Kawashima H, Kondo N, Gu W, Kamura T, Endo N: Comparison of hydroxyapatite and beta tricalcium phosphate as bone substitutes after excision of bone tumors. *J Biomed Mater Res B Appl Biomater* 2005, 72(1): 94-101.

32. Mauck RL, Yuan X, Tuan RS: Chondrogenic differentiation and functional maturation of bovine mesenchymal stem cells in long-term agarose culture. *Osteoarthritis Cartilage* 2006, 14(2): 179-189.

33. Pham QP, Sharma U, Mikos AG: Electrospinning of polymeric nanofibers for tissue engineering applications: a review. *Tissue Eng* 2006, 12(5): 1197-1211.
34. Fernandez E, Gil FJ, Ginebra MP, Driessens FC, Planell JA, Best SM: Calcium phosphate bone cements for clinical applications. Part II: precipitate formation during setting reactions. *J Mater Sci Mater Med* 1999, 10(3): 177-183.
35. Pietak AM, Reid JW, Stott MJ, Sayer M: Silicon substitution in the calcium phosphate bioceramics. *Biomaterials* 2007, 28(28): 4023-4032.
36. Hench LL: Genetic design of bioactive glass. *Journal of the European Ceramic Society* 2009, 29(7): 1257-1265.
37. Oyane A, Kawashita M, Nakanishi K, Kokubo T, Minoda M, Miyamoto T, Nakamura T: Bonelike apatite formation on ethylene-vinyl alcohol copolymer modified with silane coupling agent and calcium silicate solutions. *Biomaterials* 2003, 24(10): 1729-1735.
38. Kokubo T, Takadama H: How useful is SBF in predicting in vivo bone bioactivity? *Biomaterials* 2006, 27(15): 2907-2915.
39. Kokubo T, Kushitani H, Sakka S, Kitsugi T, Yamamuro T: Solutions able to reproduce in vivo surface-structure changes in bioactive glass-ceramic A-W. *J Biomed Mater Res* 1990, 24(6): 721-34.
40. Darling EM, Topel M, Zauscher S, Vail TP, Guilak F: Viscoelastic properties of human mesenchymally-derived stem cells and primary osteoblasts, chondrocytes, and adipocytes. *J Biomech* 2008, 41(2): 454-464.
41. Mano JF, Reis RL, Cunha AM. Dynamic mechanical analysis in polymers for biomedical applications. In: Reis RL, Cohn D, eds. *Polymer based systems on tissue engineering, replacement and Regeneration*. Dordrecht, The Netherlands: Kluwer Academic Publishers, 2002: 139.
42. Mauney JR, Volloch V, Kaplan DL: Role of adult mesenchymal stem cells in bone tissue engineering applications: current status and future prospects. *Tissue Eng* 2005, 11(5-6): 787-802.
43. Pittenger MF, Mackay AM, Beck SC, Jaiswal RK, Douglas R, Mosca JD, Moorman MA, Simonetti DW, Craig S, Marshak DR: Multilineage potential of adult human mesenchymal stem cells. *Science* 1999, 284(5411): 143-7.
44. Tuan RS, Boland G, Tuli R: Adult mesenchymal stem cells and cell-based tissue engineering. *Arthritis Res Ther* 2003, 5(1): 32-45.
45. De Coppi P, Bartsch G, Jr., Siddiqui MM, Xu T, Santos CC, Perin L, Mostoslavsky G, Serre AC, Snyder EY, Yoo JJ, Furth ME, Soker S, Atala A: Isolation of amniotic stem cell lines with potential for therapy. *Nat Biotechnol* 2007, 25(1): 100-106.
46. Pearce AI, Richards RG, Milz S, Schneider E, Pearce SG: Animal models for implant biomaterial research in bone: a review. *Eur Cell Mater* 2007, 13: 1-10.

47. Kruyt MC, Dhert WJ, Yuan H, Wilson CE, van Blitterswijk CA, Verbout AJ, de Bruijn JD: Bone tissue engineering in a critical size defect compared to ectopic implantations in the goat. *J Orthop Res* 2004, 22(3): 544-51.
48. Li X, Feng Q, Liu X, Dong W, Cui F: Collagen-based implants reinforced by chitin fibres in a goat shank bone defect model. *Biomaterials* 2006, 27(9): 1917-1923.
49. Zhu L, Liu W, Cui L, Cao Y: Tissue-engineered bone repair of goat-femur defects with osteogenically induced bone marrow stromal cells. *Tissue Eng* 2006, 12(3): 423-433.
50. Bellows CG, Heersche JN, Aubin JE: Determination of the capacity for proliferation and differentiation of osteoprogenitor cells in the presence and absence of dexamethasone. *Dev Biol* 1990, 140(1): 132-138.
51. Aubin JE: Osteoprogenitor cell frequency in rat bone marrow stromal populations: role for heterotypic cell-cell interactions in osteoblast differentiation. *J Cell Biochem* 1999, 72(3): 396-410.
52. Maniatopoulos C, Sodek J, Melcher AH: Bone formation in vitro by stromal cells obtained from bone marrow of young adult rats. *Cell Tissue Res* 1988, 254(2): 317-330.
53. Franceschi RT, Iyer BS, Cui YQ: Effects of Ascorbic-Acid on Collagen Matrix Formation and Osteoblast Differentiation in Murine Mc3T3-E1 Cells. *Journal of Bone and Mineral Research* 1994, 9(6): 843-854.
54. Lian JB, Stein GS: Concepts of osteoblast growth and differentiation: basis for modulation of bone cell development and tissue formation. *Crit Rev Oral Biol Med* 1992, 3(3): 269-305.
55. Puchtler H, Meloan SN, Terry MS: On the history and mechanism of alizarin and alizarin red S stains for calcium. *J Histochem Cytochem* 1969, 17(2): 110-124.
56. Boskey A, Pleshko Camacho N: FT-IR imaging of native and tissue-engineered bone and cartilage. *Biomaterials* 2007, 28(15): 2465-2478.
57. Lian J, Stewart C, Puchacz E, Mackowiak S, Shalhoub V, Collart D, Zambetti G, Stein G: Structure of the rat osteocalcin gene and regulation of vitamin D-dependent expression. *Proc Natl Acad Sci U S A* 1989, 86(4): 1143-1147.
58. Lian JB, Stein GS, Stewart C, Puchacz E, Mackowiak S, Aronow M, Vondeck M, Shalhoub V: Osteocalcin - Characterization and Regulated Expression of the Rat Gene. *Connective Tissue Research* 1989, 21(1-4): 391-399.
59. Byers BA, Garcia AJ: Exogenous Runx2 expression enhances in vitro osteoblastic differentiation and mineralization in primary bone marrow stromal cells. *Tissue Eng* 2004, 10(11-12): 1623-1632.
60. Rosenberg L: Chemical basis for the histological use of safranin O in the study of articular cartilage. *J Bone Joint Surg Am* 1971, 53(1): 69-82.
61. Jones CW, Smolinski D, Keogh A, Kirk TB, Zheng MH: Confocal laser scanning microscopy in orthopaedic research. *Prog Histochem Cytochem* 2005, 40(1): 1-71.

62. Oliveira JM, Rodrigues MT, Silva SS, Malafaya PB, Gomes ME, Viegas CA, Dias IR, Azevedo JT, Mano JF, Reis RL: Novel hydroxyapatite/chitosan bilayered scaffold for osteochondral tissue-engineering applications: Scaffold design and its performance when seeded with goat bone marrow stromal cells. *Biomaterials* 2006, 27(36): 6123-37.
63. Mehta R, Chowdhury P, Ali N: Scanning electron microscope studies of bone samples: influence of simulated microgravity. *Nuclear instruments and methods in physics research B* 2007, 261: 908-912.
64. Hallfeldt KK, Stutzle H, Puhmann M, Kessler S, Schweiberer L: Sterilization of partially demineralized bone matrix: the effects of different sterilization techniques on osteogenetic properties. *J Surg Res* 1995, 59(5): 614-620.
65. van Gaalen SM, Kruyt MC, Geuze RE, de Bruijn JD, Alblas J, Dhert WJ: Use of fluorochrome labels in in vivo bone tissue engineering research. *Tissue Eng Part B Rev* 2010, 16(2): 209-217.
66. Donath K. Preparation of histologic sections by the cutting-grinding technique for hard tissue and other material not suitable to be sectioned by routine methods. In: *Exakt-Kulzer-Publication*, ed. Equipment and methodical performance, 1995.
67. Jenó L, Geza L: A simple differential staining method for semi-thin sections of ossifying cartilage and bone tissues embedded in epoxy resin. *Mikroskopie* 1975, 31(1-2): 1-4.
68. Vogelin E, Jones NF, Huang JI, Brekke JH, Lieberman JR: Healing of a critical-sized defect in the rat femur with use of a vascularized periosteal flap, a biodegradable matrix, and bone morphogenetic protein. *J Bone Joint Surg Am* 2005, 87(6): 1323-1331.
69. Jager M, Degistirici O, Knipper A, Fischer J, Sager M, Krauspe R: Bone healing and migration of cord blood-derived stem cells into a critical size femoral defect after xenotransplantation. *J Bone Miner Res* 2007, 22(8): 1224-1233.
70. Jones AC, Arns CH, Sheppard AP, Hutmacher DW, Milthorpe BK, Knackstedt MA: Assessment of bone ingrowth into porous biomaterials using MICRO-CT. *Biomaterials* 2007, 28(15): 2491-2504.

## **SECTION III**

### **SCAFFOLD DESIGN AND CHARACTERIZATION**



## Chapter III

# SYNERGISTIC EFFECT OF SCAFFOLD COMPOSITION AND DYNAMIC CULTURING ENVIRONMENT IN MULTI-LAYERED SYSTEMS FOR BONE TISSUE ENGINEERING

*This chapter is based on the following publication:*

Rodrigues MT, Martins A, Dias IR, Viegas CAA, Neves NM, Gomes ME, and Reis RL, Synergistic effect of scaffold composition and dynamic culturing environment in multi-layered systems for bone tissue engineering, *accepted for publication in Journal of Tissue Engineering and Regenerative Medicine*





### SYNERGISTIC EFFECT OF SCAFFOLD COMPOSITION AND DYNAMIC CULTURING ENVIRONMENT IN MULTI-LAYERED SYSTEMS FOR BONE TISSUE ENGINEERING

#### III.1. Abstract

Bone extracellular matrix (ECM) is composed of mineralized collagen fibrils which support biological apatite nucleation that participates in bone outstanding properties. Understanding and mimicking morphological and physiological parameters of bone at a biological scale is a major challenge in tissue engineering scaffolding. Emergent new (nano)technologies offer the possibility to improve scaffold design that may be critical to obtain highly functional tissue substitutes for bone applications.

This study aims to develop novel biodegradable composite scaffolds made of tricalcium phosphate (TCPs) and electrospun nanofibers of poly( $\epsilon$ -caprolactone) (PCL), in order to combine the osteoconductivity of TCPs with the biocompatibility and elasticity of PCL, thereby mimicking bone structure and composition. We hypothesized that scaffolds with such structure/composition would stimulate the proliferation and differentiation of bone marrow mesenchymal stromal cells (BMSCs) towards the osteogenic phenotype.

Composite scaffolds were developed by electrospinning using consecutive stacked layers of PCL and TCPs, and then characterized by Fourier Transform Infrared spectroscopy, X-Ray diffraction and scanning electronic microscopy. To assess cellular behavior, goat bone marrow mesenchymal stromal cells (gBMSCs) were seeded onto composite scaffolds and cultured in either static or dynamic conditions, using both basal and osteogenic differentiation medium during 7, 14 or 21 days. Cellular proliferation was quantified and osteogenic differentiation was confirmed by alkaline phosphatase activity, alizarin red staining and immunocytochemistry for osteocalcin and type I collagen. The results suggest that these PCL-TCP scaffolds provide a 3D support for gBMSCs proliferation and osteogenic differentiation, including the production of ECM matrix. In fact, the presence of TCPs is shown to positively stimulate the osteogenic process, especially under dynamic conditions, where the environment induced by PCL-TCP scaffolds is sufficient to promote osteogenic differentiation even in basal medium conditions. The enhancement of the osteogenic potential in dynamic conditions evidences the synergistic effect of scaffolds composition and dynamic stimulation in gBMSCs osteogenic differentiation.

### III.2. Introduction

Bone fracture defects, bone loss, infection or bone tumoral resections are serious problems requiring for bone surgery, and the implantation of auto- or allo-grafts has long been used as a standard procedure for bone reconstruction. Nevertheless, graft strategies are associated with significant disadvantages, namely tissue morbidity at the harvesting site, donor scarcity and immune response and disease transmission risks. To overcome these limitations, the challenge stands for designing novel tissue engineered products.

The selection of a biomaterial plays a key role in the development of an engineered product aimed at tissue regeneration and repair, as materials can tailor the biophysical and biochemical milieu at a molecular level, directing cellular behavior and function.

Synthetic polymers, such as poly  $\epsilon$ -caprolactone (PCL) are typically more versatile in tailoring a wide range of properties and structure features. Also, they represent a reliable source of raw materials, with adequate mechanical properties, and avoid immunogenicity problems[1, 2]. Nevertheless, polymers lack properties to stimulate biological functions, such as osteoconductivity, and cell bioactivity[3]. Concerning these properties, ceramic materials offer advantages over polymers, but their high modulus yet brittle behavior[4] limit their processability into 3D scaffolds[5, 6].

Designing scaffolds using nanotechnology tools aims at mimicking the extracellular matrix (ECM) structure and complexity at a biological scale, as bone natural matrix is mainly composed of an intricate nanofiber structure of nonstoichiometric hydroxyapatite integrated in collagen fibers. At a submicron level, this organic-inorganic combination confers the intrinsic, unique biomechanical and functional properties of bone 3D architecture.

The products of electrospinning technology are micro- and nano-structured scaffolds made of an ultra-fine and continuous fiber network with variable pore-size distribution, high microporosity and high surface-to-volume ratio, morphologically similar to natural ECM[7]. Several materials, including synthetic- and natural-origin polymers[8-16] and proteins[9, 10, 12, 17, 18], have been successfully electrospun into nanofiber scaffolds, which interacted positively with intercellular communications by sustaining cell adhesion, proliferation and differentiation towards the osteogenic phenotype both *in vitro*[9, 11, 14, 16, 18] and *in vivo*[9, 11, 15].

Considering the properties and flexibility of electrospun nanofiber meshes, the incorporation of biologically active factors, like matrix proteins[19] or minerals as calcium phosphates[8, 11-13], either in the spun fibers or as coatings, makes them attractive to improve scaffold designs for bony functional substitutes. Moreover an integrated composite

scaffold of a polymer with a ceramic material offers a chemical environment that would resemble the organic and inorganic components of bone native matrix[20].

In this study, we formulated a novel multilayer composite structure combining the osteoinductive properties of beta-tricalcium phosphate powder with a degradable polymer. PCL was selected due to its degradability and cellular compatibility, and because this material has been widely studied for biomedical applications[8, 9, 13-15]. Several studies suggested hydroxyapatite as the ceramic material preferred for bone strategies[8, 12, 19]. Nevertheless, the osteoconductive and bioreabsorbable nature of beta-tricalcium phosphate together with an earlier incorporation into surrounding bone *in vivo* may be advantageous to hydroxyapatite, which remains unremodeled despite long periods upon implantation[21].

The design of these 3D fibrous scaffolds is expected to enhance the synergistic effects of ceramic (osteoconductivity and bioactivity) and biopolymer features (elasticity and shape control). The possibility to combine and stack layers in such simple and thin structures can improve their tridimensionality, which has been described to be critical in structure, function and morphology of body tissues.

The limited diffusion in standard static culture environments is another important issue to considering when designing bone regeneration strategies, since this may constrain cell proliferation and uniform distribution in tissue engineered constructs[10, 22]. Therefore, we also propose to evaluate the effect of dynamic culturing in the osteogenic differentiation process of goat bone marrow mesenchymal stromal cells (gBMSCs), cultured in the multi-layer scaffolds, either in the presence of basic or osteogenic differentiation media.

### **III.3. Materials and Methods**

#### **III.3.1. Development of the nanofibrous multilayered composite scaffolds**

The ceramic material, beta-tricalcium phosphate ( $\beta$ -TCP), was obtained from a solid state reaction between stoichiometric amounts of calcium phosphate dibasic anhydrous (Fluka) and calcium carbonate (Sigma) followed by a 24 h sinterization at 800 °C. The powders were hand-sieved with stainless steel sieves (mesh 225 - 106  $\mu$ m). A polymeric solution of 17 % (w/v) polycaprolactone (PCL) in a mixture of chloroform (Aldrich) and N,N-dymethylformamide (Aldrich) at a 7:3 ratio was processed by electrospinning technique. This solution was electrospun at 9-10 kV, with a flow rate of 1.0 mL/h collecting a random fiber mesh (20 cm

away from the collector) on a flat aluminium foil. Composite scaffolds were then developed by assembling three stacked layers of electrospun PCL fibers and TCPs at a ratio of 0.5 g TCP per PCL mesh. 0.25 g of TCP powder was dispersed between each two consecutive PCL layers. The resulting PCL-TCP scaffolds, as well as TCPs powder and PCL meshes alone, were characterized by FTIR, XRD and SEM, as described below.

### **III.3.2. Characterization of the composite scaffolds**

#### **III.3.2.1. Thin-film X-ray diffraction (TF-XRD)**

TF-XRD patterns were recorded on a Philips X'Pert MPD (Philips, The Netherlands) diffractometer using  $\text{CuK}\alpha$  radiation to analyze the surface composition of the specimens.

#### **III.3.2.2. Fourier Transformed Infrared Spectroscopy with attenuated total reflectance (FTIR-ATR)**

FTIR-ATR was performed using IRPrestige-21 (Shimadzu, Japan) equipment. Spectra were taken with a resolution of  $2\text{ cm}^{-1}$  and averaged over 64 scans, covering the wave number range of  $4400\text{-}400\text{ cm}^{-1}$ .

#### **III.3.2.3. Scanning electron microscopy (SEM)**

SEM analysis was performed to characterize the morphology of the developed structures using Hitachi S-2600N (Hitachi Science Systems, Ltd) equipment. Prior to any SEM observations, sample surfaces were gold sputtered.

### **III.3.3. *In vitro* culture of bone marrow mesenchymal stromal cells onto nanofibrous scaffolds**

To assess cellular behavior, scaffolds were cut into 5 mm diameter discs, and then sterilized by means of two 30 minute-cycle of UV irradiation.

PCL nanofiber meshes without TCPs were considered as controls of the experiment.

Goat bone marrow mesenchymal stromal cells (gBMSCs) were harvested from iliac crests of adult goats and expanded in basal medium composed of DMEM (Dulbecco Modified Eagle Medium, Sigma-Aldrich), supplemented with 10 % FBS (Invitrogen) and 1 % antibiotic-antimicotic solution (A/A) (Gibco), and then seeded onto the PCL-TCP composites at a concentration of  $5.0 \times 10^4$  cells/mesh or scaffold. After the seeding, cell-scaffold constructs were maintained in non treated 48 multi-well plates (Costar) in basal medium for 24 h and then cultured under static or dynamic conditions in either basal or osteogenic differentiation medium during 7, 14 or 21 days.

Dynamic conditions were provided by an orbital shaker (Digisystem) under constant mild agitation (60 rpm), working permanently until the end of the experiment and kept in the same CO<sub>2</sub> incubator where constructs under static conditions were also cultured.

Osteogenic medium was prepared with  $\alpha$ -MEM (Minimal Essential Medium Eagle alpha modification, Sigma-Aldrich), 10 % FBS and 1 % A/A and osteogenic supplements namely ascorbic acid (50  $\mu$ g/ml) (Sigma-Aldrich), dexamethasone ( $10^{-8}$  M) (Sigma-Aldrich) and  $\beta$ -glycerophosphate (10 mM) (Sigma-Aldrich). In all conditions, cell culture medium was changed twice a week.

### **III.3.3.1. Cell proliferation and osteogenic differentiation in multi-stacked nanofibrous scaffolds**

Cell proliferation was assessed by a DNA quantification assay while the osteogenic differentiation was assessed by ALP quantification, alizarin red staining and immunocytochemistry (ICC) for osteocalcin (OCa) and type I collagen.

#### ***III.3.3.1.1. DNA assay***

Proliferation potential of gBMSCs seeded onto the developed scaffolds was considered by double strand DNA quantification (dsDNA). For this purpose, a fluorimetric dsDNA quantification kit (PicoGreen, Molecular Probes) was used.

The fluorescence was read using a microplate ELISA reader (BioTek) at an excitation of 485/20 nm and an emission of 528/20 nm.

#### *III.3.3.1.2. ALP assay*

ALP activity was measured in this study, as an osteogenic cell marker. A substrate solution consisting of 0.2 % (wt/v) p-nitrophenyl phosphate (Sigma) in a substrate buffer with 1 M diethanolamine HCl (Merck), at pH 9.8 was added to each sample. The plate was incubated in the dark for 45 minutes at 37 °C, followed by the addition of a stop solution (2 M NaOH (Panreac) plus 0.2 mM EDTA (Sigma)). Samples and standards (the latter prepared with p-nitrophenol (10  $\mu\text{mol}\cdot\text{ml}^{-1}$ ) (Sigma)) were analyzed in triplicates. The absorbance was read using a microplate ELISA reader (BioTek) at 405 nm.

#### *III.3.3.1.3. Alizarin Red staining*

Cell-scaffold constructs were removed from culture and fixed in 4 % formalin (Sigma) solution overnight at 4 °C. A 2 % Alizarin Red solution (Sigma) was prepared (pH adjusted to 4.1-4.3) to stain calcium ions that might be present resultant from mineral ECM produced by cells. Constructs were stained with alizarin red solution for about 2 minutes, washed with PBS until removal of excess of stain and let dry.

#### *III.3.3.1.4. Immunocytochemistry*

After overnight fixation with 4 % formalin, samples were kept in PBS until immunocytochemistry (ICC) analysis. ICC was performed according to R.T.U. Vectastain Universal Elite ABC kit (PK 7200) kit from VectorLabs, using R.T.U Normal Horse Serum to avoid unspecific reactions, a biotinylated secondary antibody (R.T.U. Biotinylated Universal Antibody) and a Peroxidase Substrate Kit (Vector SK-4100). Primary antibodies Collagen I (MAB339, Chemicon) and Osteocalcin (Ab13418, Abcam) were prepared using a 1/100 dilution.

### **III.3.4. Statistical Analysis**

Statistical analysis was carried out using One Way ANOVA test and Tukey's Multiple Comparison Test ( $p < 0.05$ ). All results are presented as mean  $\pm$  standard deviation.

In the present study controls of the experiment were considered using PCL nanofiber meshes without TCPs.

### III.4. Results and Discussion

Goat model is a popular animal model for orthopedics, whose stem cells can be applied to autologous approaches in bone TE. Previous studies have demonstrated the potential of gBMSCs to differentiate into the osteogenic lineage[23-25]. Furthermore, PCL nanofiber meshes, used in this study as positive controls for determining the applicability and improvement of multi-layered PCL-TCP scaffolds in bone-related strategies, have shown to promote cellular adhesion, proliferation and osteogenic differentiation of mesenchymal stem cells[26].

Multi-layered composite scaffolds were achieved through the dispersion of TCP onto electrospun PCL fibers. The calcium phosphate obtained from the chemical reaction presented a rhombohedral structure, typical of  $\beta$ -TCP, and the vibrational bands associated to the phosphate groups, as demonstrated by FTIR (Figure III.4.1) and XRD (Figure III.4.2) data.

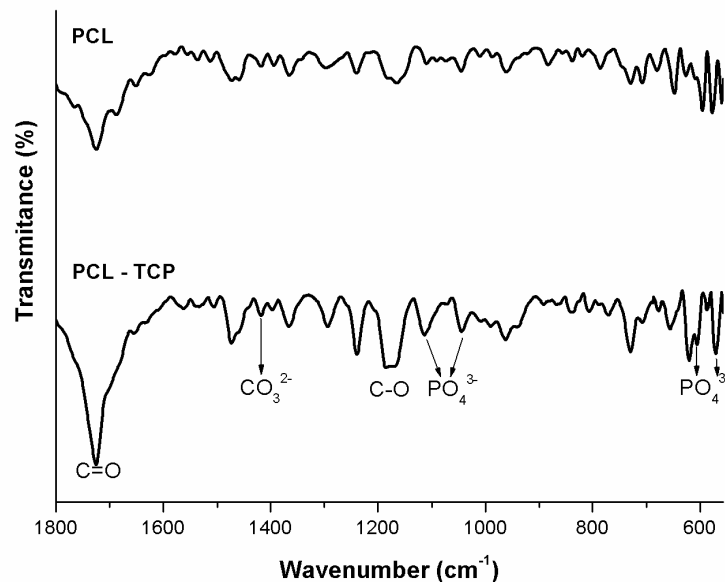


**Figure III.4.1** - FTIR-ATR analysis of multi-layered scaffolds. Membranes of PCL nanofiber mesh (PCL) were used as controls.

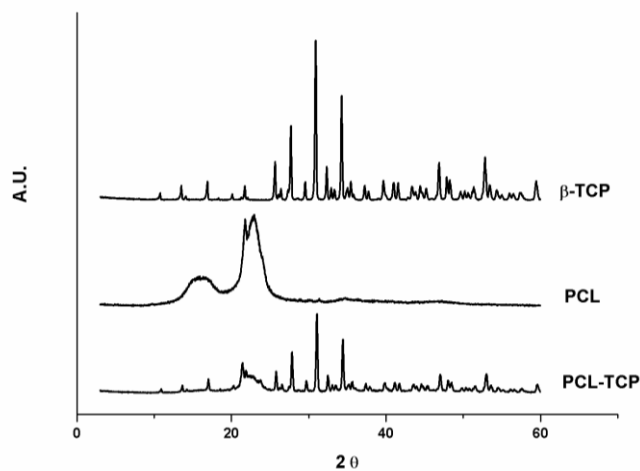


**Figure III.4.2** - XRD analysis of multi-layered PCL-TCP scaffolds. Membranes of PCL nanofiber mesh (PCL) were used as controls.

SEM observation indicated a dispersion of TCPs granules within the electrospun PCL nanofibers structure, in the produced composite scaffolds (Figure III.4.3).

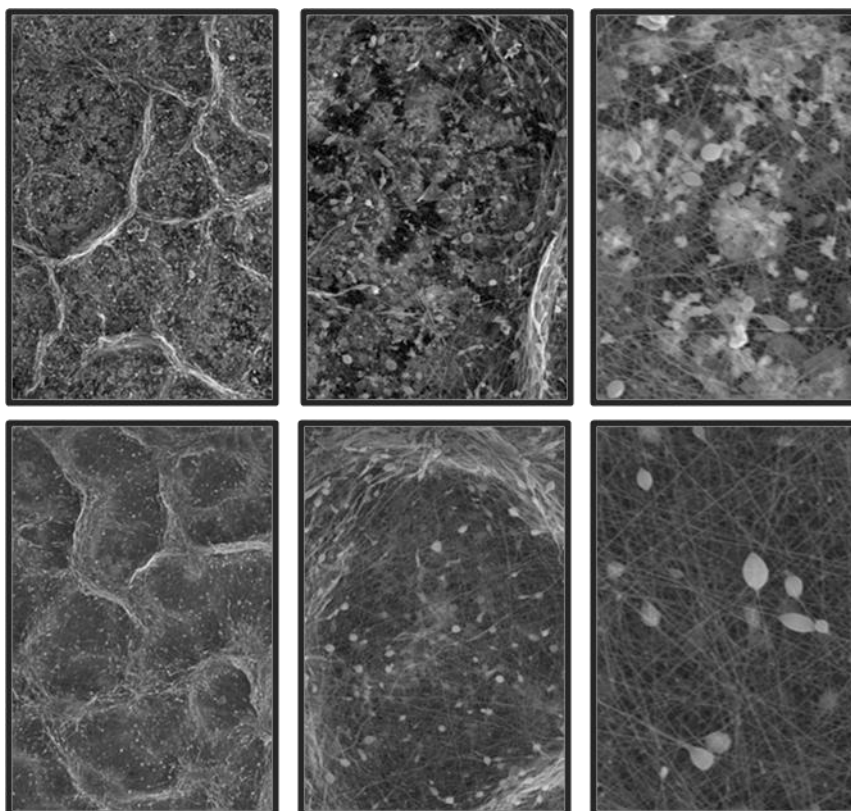


**Figure III.4.3** – SEM analysis of multilayer scaffolds; the upper SEM micrographs refer to the PCL-TCP multilayer scaffolds while the lower pictures correspond to the control of PCL nanofiber mesh (left to right: 100 x, 300 x and 1000 x magnifications).



A random distribution was observed not only with TCPs granules but also in nanofibers of the mesh-like stratified structure. Additionally, TCPs mineral particles were integrated within the structure of multi-layered nanofiber scaffolds.

In our study, gBMSCs attached, and proliferated into the PCL-TCP scaffolds, both in static and dynamic conditions, as well as in basal and osteogenic culture conditions. Similar results were achieved in control PCL meshes.

In terms of proliferation, gBMSCs showed two different behaviors ( $p > 0.05$ ); cell proliferation in PCL meshes increased with time in culture, while in PCL-TCP constructs, cells increased up to 14 days in basal or osteogenic culture conditions and then, the cell number decreased at week 3 (Figure III.4.4). This decreasing tendency of proliferation in PCL-TCP scaffolds may be a result of the osteogenic differentiation process, undertaken by the gBMSCs. Some studies indicate an inverse relationship between proliferation and differentiation of osteoprogenitor cells during bone formation[27].

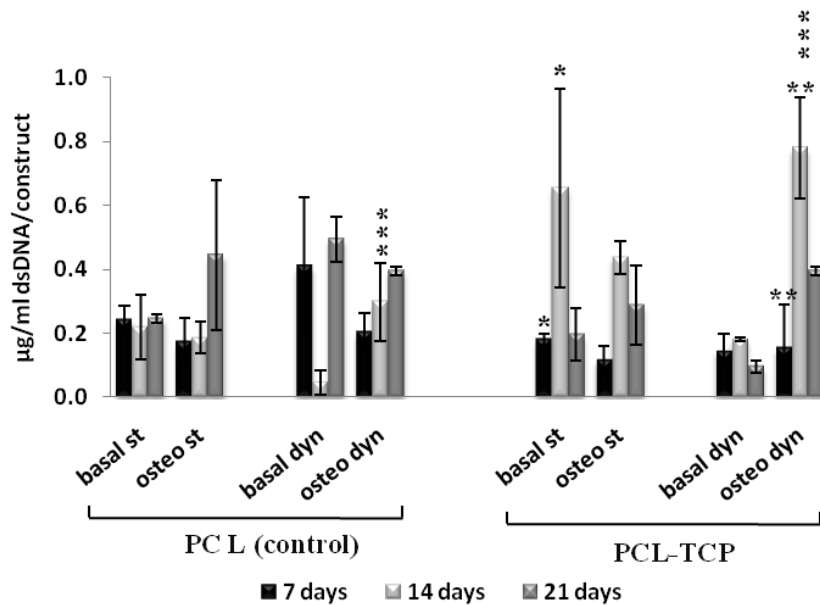


**Figure III.4.4** – gBMSCs proliferation given by DNA quantification was assessed onto PCL-TCP scaffolds and PCL membranes (control) after 7, 14 or 21 days in basal or osteogenic media in either static (st) or dynamic (dyn) conditions. Symbols \*, \*\*, and \*\*\* denote study groups with statistically significant differences ( $p < 0.05$ ), as using One Way ANOVA method.

ALP activity levels (Figure III.4.5) were not detected for samples cultured for 7 or 14 days, probably due to low basal concentrations of ALP enzyme in the samples.

The ALP/DNA ratio in PCL meshes cultured under dynamic conditions using osteogenic media is very similar to that found for PCL-TCP constructs cultured under static conditions in

the same medium, after 3 weeks in culture. Nevertheless, ALP is highly expressed in PCL-TCP constructs cultured under dynamic culture conditions in osteogenic medium as compared to all the remaining study groups ( $p < 0.05$ ). ALP activity data indicated a positive and synergistic effect of TCPs and mechanical stimulation on the formation of ECM by osteogenically differentiated gBMSCs.

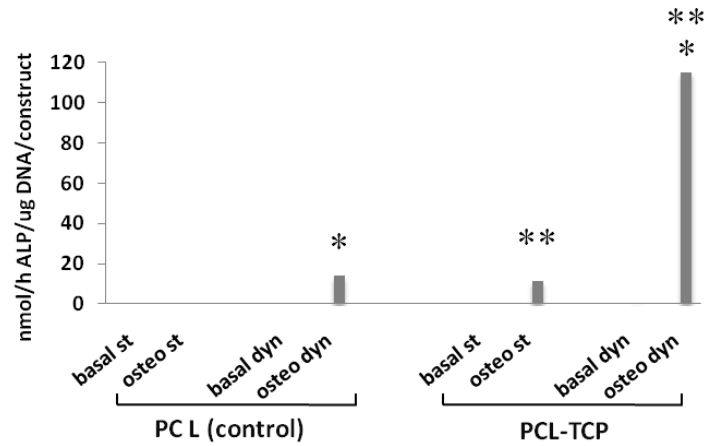


**Figure III.4.5** – gBMSCs osteogenic differentiation given by ALP/DNA ratio was assessed onto PCL-TCP scaffolds and PCL membranes (control) after 7, 14 or 21 days in basal or osteogenic media in either static (st) or dynamic (dyn) conditions. Symbols \*, and \*\* denote st groups with statistically significant differences ( $p < 0.05$ ), as using One Way ANOVA method.

Furthermore, to confirm gBMSCs differentiation onto PCL-TCP scaffolds, osteogenic phenotype characterization was assessed by immunocytochemistry analysis for type I collagen and osteocalcin (OCa), and alizarin red staining for calcium detection, after 21 days in culture (Figure III.4.6).

Collagen I is the major protein present in bone ECM. All PCL-TCP scaffolds seeded with gBMSCs were positively stained for Collagen I, although a more intense immunostain was observed in constructs cultured under dynamic conditions (Figure III.4.6). In gBMSC-PCL meshes (control), collagen I was more intense in basal medium culture. These results showed that a collagen I-rich ECM is being produced by gBMSCs either in PCL-TCP scaffolds or PCL meshes.

In addition to a collagen matrix, a calcified milieu is an important part of the native bone tissue. Osteocalcin (OCa) is a non-collagenous protein, produced by osteoblasts that participates in the matrix mineralization of bone[28]. OCa was found to be present in gBMSC-PCL-TCP constructs under dynamic environment, while in static cultures, OCa was only detected in the presence of constructs cultured in osteogenic medium. Furthermore, in

gBMSC-PCL meshes (control), OCa was only detected under static conditions in osteogenic differentiation medium (Figure III.4.6).

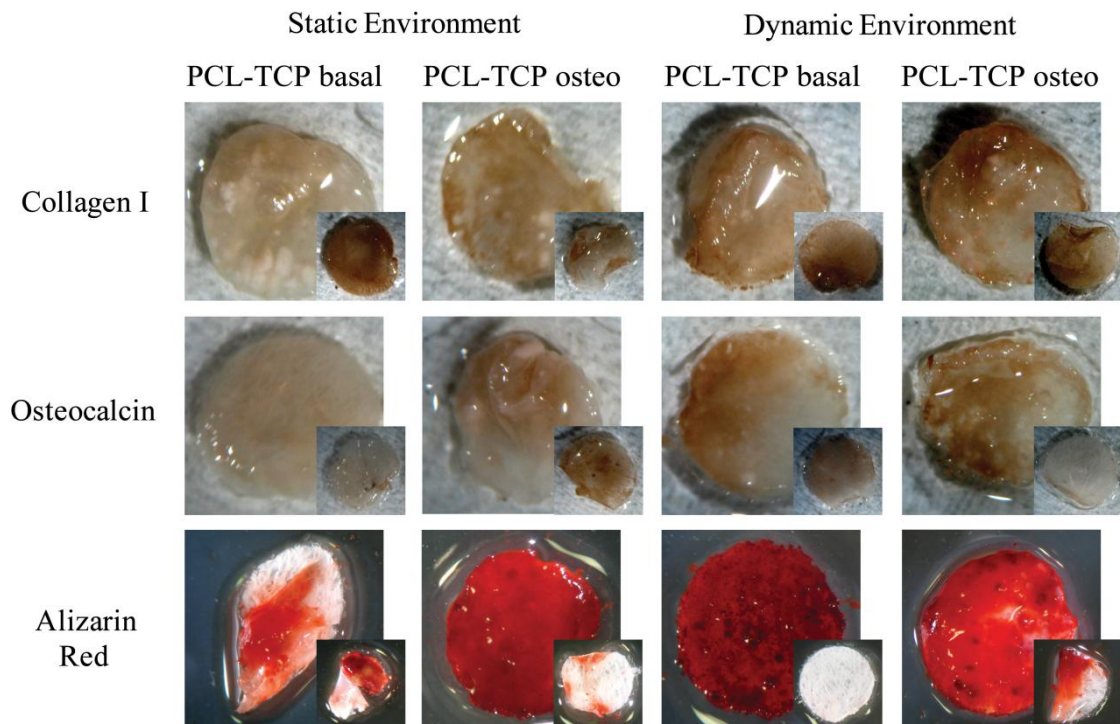


**Figure III.4.6** – Osteogenic phenotype characterization of gBMSCs seeded onto PCL-TCP scaffolds after 21 days in culture with basal or osteogenic media, either in static or dynamic conditions. Immunocytochemistry (ICC) was performed for Collagen I and Osteocalcin, as well as Alizarin Red staining. Insets represent PCL meshes (control) under the same conditions.

Alizarin red staining was assessed to detect calcium ions, essential for the ECM mineralization. After 21 days in culture, gBMSC-PCL-TCP constructs exhibited a stronger stain when compared to gBMSC-PCL membrane controls (Figure III.4.6). The stain was more intense under dynamic conditions, both in basal or osteogenic media, as well as in constructs cultured in osteogenic differentiation medium in a static environment, indicating the production of calcified ECM.

Oca and alizarin red staining followed a similar pattern in gBMSC-PCL-TCP constructs, which confirms the formation of a mineralized ECM, as OC is thought to bind to hydroxyapatite in a calcium-dependent manner[29], during the natural development of bone.

Even if in all culture conditions, gBMSC-PCL-TCP constructs expressed osteogenic markers to some extent, the combination of these markers was stronger in dynamic conditions, especially for Alizarin Red staining. It is important to highlight that mineralization nodules

(observed as darker red spots) are visible only in the dynamic culture conditions and in the multilayer composite scaffolds, corroborating the previous results of ALP activity. The fact that ALP, an enzyme associated to ECM development and maturation[27], is not expressed by cells seeded onto PCL-TCP constructs in basal/dynamic environment is quite interesting, since these cells are able to produce calcified ECM (Figure III.4.6). Salasznyk *et al.* reported the bone isoform of ALP is found only in osteogenic supplemented mesenchymal stem cells[30], which justifies the basal ALP activity levels in basal/dynamic environment, despite the mineralization of ECM. In their study, cells in basal medium did not differentiate when ALP was not expressed; but the presence of PCL-TCP constructs could stimulate gBMSCs to select a different pathway in the absence of osteogenic medium that could be also encouraged by the dynamic environment, as calcified ECM is reduced in basal/static conditions. Furthermore, in the presence of PCL-TCP scaffolds, gBMSCs achieved osteogenic differentiation and ECM mineralization even in the absence of osteogenic supplements after 3 weeks in culture.

Mechanical stimuli are required to maintain a healthy bone, and described to induce the up-regulation of osteogenic marker genes and increase matrix mineralization of the ECM in the presence of substrates coated with ECM proteins[31]. Furthermore, cyclic mechanical stretching was also described to participate in an increased ALP activity and mineralized matrix deposition[31].

In our study, the particular structure of PCL-TCP scaffolds mimicking bone natural ECM, both in structure and composition, stimulated gBMSCs to produce ECM matrix (collagen I and OCa). Under dynamic conditions, the environment induced by PCL-TCP scaffolds is sufficient to promote osteogenic differentiation even in basal medium conditions.

In summary, PCL-TCP scaffolds participate in the osteogenic process of gBMSCs, even in basal medium and static conditions. Nevertheless, the osteogenic potential is enhanced in dynamic environments, evidencing the synergistic effect of TCPs and mild mechanical stimulation in gBMSCs osteogenic phenotype.

### III.5. Conclusions

The production of multi-layered PCL-TCP scaffolds was successfully achieved as well as the *in vitro* assessment of their application aiming at bone tissue strategies. Moreover, considering that bone ECM is essentially an organic-inorganic composite and nano-scaled organized, the

developed multi-layered composite can be a promising system in the regenerative medicine field.

The results obtained suggest that the combination of PCL with calcium phosphates generated scaffolds with improved capacity to promote gBMSCs adhesion, proliferation, and expression of osteogenic phenotype, when compared to the synthetic polymer alone. Furthermore, the dynamic environment positively affected the gBMSCs behavior, and enhanced gBMSCs phenotypic expression and mineralized matrix synthesis. Interestingly, the synergistic effect of mild agitation and PCL-TCP scaffolds stimulated gBMSCs differentiation and production of a calcified ECM, even in the absence of osteogenic supplements from the culture medium.

The development of PCL nanofibers with ceramic materials, in a multi-layered structure, is an innovative methodology with great potential for the development of more adequate scaffolds for bone tissue engineering approaches.

### **III.6. References**

1. Tsuji H, Ikada Y: Blends of aliphatic polyesters .1. Physical properties and morphologies of solution-cast blends from poly(DL-lactide) and poly(epsilon-caprolactone). *Journal of Applied Polymer Science* 1996, 60: 2367-2375.
2. Bezwada RS, Jamiolkowski DD, Lee IY, Agarwal V, Persivale J, Trenkabethin S, Ermeta M, Suryadevara J, Yang A, Liu S: Monocryl(R) Suture, a New Ultra-Pliable Absorbable Monofilament Suture. *Biomaterials* 1995, 16: 1141-1148.
3. Rezwani K, Chen QZ, Blaker JJ, Boccaccini AR: Biodegradable and bioactive porous polymer/inorganic composite scaffolds for bone tissue engineering. *Biomaterials* 2006, 27: 3413-3431.
4. Collins AM, Skaer NJV, Gheysens T, Knight D, Bertram C, Roach HI, Oreffo ROC, Von-Aulock S, Baris T, Skinner J, et al.: Bone-like resorbable silk-based scaffolds for load-bearing osteoregenerative applications. *Advanced Materials* 2009, 21: 75-78.
5. Yang S, Leong KF, Du Z, Chua CK: The design of scaffolds for use in tissue engineering. Part I. Traditional factors. *Tissue Eng* 2001, 7: 679-689.
6. Chen GP, Ushida T, Tateishi T: Scaffold design for tissue engineering. *Macromolecular Bioscience* 2002, 2: 67-77.
7. Martins A, Reis RL, Neves NM: Electrospinning: processing technique for tissue engineering scaffolding. *International Materials Reviews* 2008, 53: 257-274.

8. Gupta D, Venugopal J, Mitra S, Giri Dev VR, Ramakrishna S: Nanostructured biocomposite substrates by electrospinning and electro spraying for the mineralization of osteoblasts. *Biomaterials* 2009, 30: 2085-2094.
9. Srouji S, Kizhner T, Suss-Tobi E, Livne E, Zussman E: 3-D Nanofibrous electrospun multilayered construct is an alternative ECM mimicking scaffold. *J Mater Sci Mater Med* 2008, 19: 1249-1255.
10. Hosseinkhani H, Hosseinkhani M, Tian F, Kobayashi H, Tabata Y: Ectopic bone formation in collagen sponge self-assembled peptide-amphiphile nanofibers hybrid scaffold in a perfusion culture bioreactor. *Biomaterials* 2006, 27: 5089-5098.
11. Ko EK, Jeong SI, Rim NG, Lee YM, Shin H, Lee BK: In vitro osteogenic differentiation of human mesenchymal stem cells and in vivo bone formation in composite nanofiber meshes. *Tissue Eng Part A* 2008, 14: 2105-2119.
12. Ngiam M, Liao S, Patil AJ, Cheng Z, Yang F, Gubler MJ, Ramakrishna S, Chan CK: Fabrication of mineralized polymeric nanofibrous composites for bone graft materials. *Tissue Eng Part A* 2009, 15: 535-546.
13. Araujo JV, Martins A, Leonor IB, Pinho ED, Reis RL, Neves NM: Surface controlled biomimetic coating of polycaprolactone nanofiber meshes to be used as bone extracellular matrix analogues. *J Biomater Sci Polym Ed* 2008, 19: 1261-1278.
14. Li WJ, Tuli R, Huang X, Laquerriere P, Tuan RS: Multilineage differentiation of human mesenchymal stem cells in a three-dimensional nanofibrous scaffold. *Biomaterials* 2005, 26: 5158-5166.
15. Shin M, Yoshimoto H, Vacanti JP: In vivo bone tissue engineering using mesenchymal stem cells on a novel electrospun nanofibrous scaffold. *Tissue Eng* 2004, 10: 33-41.
16. Xin X, Hussain M, Mao JJ: Continuing differentiation of human mesenchymal stem cells and induced chondrogenic and osteogenic lineages in electrospun PLGA nanofiber scaffold. *Biomaterials* 2007, 28: 316-325.
17. Li M, Mondrinos MJ, Gandhi MR, Ko FK, Weiss AS, Lelkes PI: Electrospun protein fibers as matrices for tissue engineering. *Biomaterials* 2005, 26: 5999-6008.
18. Sefcik LS, Neal RA, Kaszuba SN, Parker AM, Katz AJ, Ogle RC, Botchwey EA: Collagen nanofibres are a biomimetic substrate for the serum-free osteogenic differentiation of human adipose stem cells. *J Tissue Eng Regen Med* 2008, 2: 210-220.
19. Li C, Vepari C, Jin HJ, Kim HJ, Kaplan DL: Electrospun silk-BMP-2 scaffolds for bone tissue engineering. *Biomaterials* 2006, 27: 3115-3124.
20. Zhang YZ, Su B, Venugopal J, Ramakrishna S, Lim CT: Biomimetic and bioactive nanofibrous scaffolds from electrospun composite nanofibers. *Int J Nanomedicine* 2007, 2: 623-638.
21. Ogose A, Hotta T, Kawashima H, Kondo N, Gu W, Kamura T, Endo N: Comparison of hydroxyapatite and beta tricalcium phosphate as bone substitutes after excision of bone tumors. *J Biomed Mater Res B Appl Biomater* 2005, 72: 94-101.

22. Yu X, Botchwey EA, Levine EM, Pollack SR, Laurencin CT: Bioreactor-based bone tissue engineering: the influence of dynamic flow on osteoblast phenotypic expression and matrix mineralization. *Proc Natl Acad Sci U S A* 2004, 101: 11203-11208.
23. Oliveira JM, Rodrigues MT, Silva SS, Malafaya PB, Gomes ME, Viegas CA, Dias IR, Azevedo JT, Mano JF, Reis RL: Novel hydroxyapatite/chitosan bilayered scaffold for osteochondral tissue-engineering applications: Scaffold design and its performance when seeded with goat bone marrow stromal cells. *Biomaterials* 2006, 27: 6123-6137.
24. Rodrigues MT, Gomes ME, Viegas CA, Azevedo JT, Dias IR, Guzón F, Reis RL: Tissue Engineered Constructs based on SPCL Scaffolds Cultured with Goat Marrow Cells: Functionality in Femoral Defects. *J Tissue Eng Regen Med* 2011, 5: 41-49.
25. Leonor I, Rodrigues MT, Gomes ME, Reis RL: In Situ Functionalization of Wet-Spun Fibre meshes for Bone Tissue Engineering: One Step Approach. *J Tissue Eng Regen Med* 2011, 5: 104-111.
26. Binulal NS, Deepthy M, Selvamurugan N, Shalumon KT, Suja S, Mony U, Jayakumar R, Nair SV: Role of Nanofibrous Poly(Caprolactone) Scaffolds in Human Mesenchymal Stem Cell Attachment and Spreading for In Vitro Bone Tissue Engineering-Response to Osteogenic Regulators. *Tissue Eng Part A* 2010, 16: 393-404.
27. Lian JB, Stein GS: Concepts of osteoblast growth and differentiation: basis for modulation of bone cell development and tissue formation. *Crit Rev Oral Biol Med* 1992, 3: 269-305.
28. Lian JB, Stein GS, Stewart C, Puchacz E, Mackowiak S, Aronow M, Vondeck M, Shalhoub V: Osteocalcin - Characterization and Regulated Expression of the Rat Gene. *Connective Tissue Research* 1989, 21: 391-399.
29. Lian J, Stewart C, Puchacz E, Mackowiak S, Shalhoub V, Collart D, Zambetti G, Stein G: Structure of the Rat Osteocalcin Gene and Regulation of Vitamin-D-Dependent Expression. *Proceedings of the National Academy of Sciences of the United States of America* 1989, 86: 1143-1147.
30. Salaszyk RM, Klees RF, Westcott AM, Vandenberg S, Bennett K, Plopper GE: Focusing of gene expression as the basis of stem cell differentiation. *Stem Cells Dev* 2005, 14: 608-620.
31. Huang CH, Chen MH, Young TH, Jeng JH, Chen YJ: Interactive effects of mechanical stretching and extracellular matrix proteins on initiating osteogenic differentiation of human mesenchymal stem cells. *J Cell Biochem* 2009, 108: 1263-1273.





## Chapter IV

### **FUNCTIONAL BIODEGRADABLE SCAFFOLDS FOR BONE TISSUE ENGINEERING: BIOACTIVITY PROFILE AND OSTEOGENIC DIFFERENTIATION OF MARROW MESENCHYMAL STROMAL CELLS**

*This chapter is based on the following publication:*

Rodrigues MT, Gröen N, Leonor I, Carvalho PP, Caridade S, Mano JF, Dias IR, van Blitterswijk CA, Gomes ME, and Reis RL, Functional biodegradable scaffolds for Bone Tissue Engineering: bioactivity profile and osteogenic differentiation of marrow mesenchymal stromal cells, *submitted*



FUNCTIONAL BIODEGRADABLE SCAFFOLDS FOR BONE TISSUE ENGINEERING:  
BIOACTIVITY PROFILE AND OSTEOGENIC DIFFERENTIATION OF MARROW MESENCHYMAL  
STROMAL CELLS

#### IV.1. Abstract

Bone is a complex tissue, whose functionality can be restricted by trauma or degenerative diseases. Tissue engineering plays a key role in developing alternative strategies for bone regeneration, where scaffolds are expected to guide cellular distribution and colonization, similarly to the natural occurring communications between cells and tissue, and provide for needed support during tissue regeneration.

Cell behavior has been suggested to be mostly based on the response to the surface composition and topography of the support material. Surface design of biodegradable polymers has gained much attention and specifically the coating of an apatite layer is considered to be a promising approach in bone strategies, in order to stimulate the direct bonding to living bony tissue. Incorporation of functional groups into the surface of polymeric scaffolds has been also described to be capable of inducing an apatite layer formation, critical for cellular and molecular communications to most of implanted scaffolds aiming functional tissue regeneration. Therefore, the present study focuses on a fiber mesh scaffold produced from a blend of starch with polycaprolactone (SPCL) using wet-spinning technology by a method that enables the *in situ* incorporation of silanol groups (Si-OH).

These scaffolds (SPCL-Si) were designed into a well-defined 3D porous-architecture, highly interconnected, whose bioactive behaviour was analyzed considering its possible role *in vivo* during the regeneration/repair of bone tissue.

Results indicated that apatite nucleation is induced by SiOH groups incorporated on SPCL scaffolds after incubation in simulated body fluid (SBF), confirming its bioactive properties.

Cell culture assays indicated that goat marrow mesenchymal stromal cells not only proliferate and differentiate into the osteogenic phenotype onto SPCL-Si scaffolds, but seem to prefer SPCL-Si scaffolds alone rather than SPCL-Si scaffolds coated with an apatite layer formed by immersion in SBF. Therefore, SPCL-Si scaffolds present intrinsic properties to sustain *in vitro* osteogenic features, with great potential aiming at bone engineered approaches.

## IV.2. Introduction

Bone is one of the major tissues affected by trauma, age- and metabolic-related diseases which translate to a decline in the quality of life of thousands of patients worldwide, thus representing a major medical and a socio-economical problem. The challenge stands for developing multifunctional biomaterials[1] to keep up with the process of tissue repair, and restoring functionality by promoting polymer interactions with *in vivo* biological materials, and substitute currently used autografts, the gold standard for bone replacement.

The degree of success of bone tissue engineering (TE) approaches is greatly dependent on the intrinsic properties of materials used to obtain a biocompatible and biodegradable scaffold with osteoinductive, osteoconductive and osteogenic properties in order to assist the attachment, proliferation and differentiation of seeded cells toward the desired bone tissue[2, 3].

The use of starch blended with polycaprolactone to develop new scaffolds has been earlier investigated for TE, including bone regenerative approaches, demonstrating promising results[4-10]. However, all biodegradable polymers used within the TE field present a drawback for bone applications as they do not disclose osteoinductive properties, i.e., they are not able to induce bone formation by themselves[11].

It is well known that the direct bonding between an implant and bone may occur if a layer of bone-like mineral forms on the surface of the implant. Therefore, the focus on the surface design of biodegradable polymers has gained much attention as bioactivity can be induced on non-bioactive surfaces. Functional groups, as for example, silanol (Si-OH), can be incorporated on the surface of polymeric scaffolds, inducing apatite nucleation in a simulated body fluid (SBF) solution, resulting in the formation of an apatite layer[12-15]. Although calcium and phosphorus are the main elements of inorganic bone, other ions, whose role has not been fully studied yet, are key elements in the functionality of the bone metabolic system. Among them, the silicium (Si), a trace element found in animals and human nutrition, has been associated with calcium in the mineralization process, and is extremely important in active calcification sites in young bones[16], as a regulatory factor in bone formation. Furthermore, silicon compounds stimulate the DNA synthesis in osteoblast-like cells[17], the osteogenic differentiation of mesenchymal stem cells[15, 18, 19], and the collagen I synthesis at a physiological level[19].

A previous work[15] by our group, described the development of bioactive fiber meshes, in a new reliable and economical methodology that enables the control of pore size, shape and

orientation, based on a simple wet-spinning technique, using a calcium silicate solution as coagulation bath. Si-OH groups were successfully incorporated on the surface of the fibers, thus allowing for obtaining a bioactive scaffold without the need for further coating or chemical modifications.

The present study analyzed the effect of Si-OH groups on the structure and properties of wet spun SPCL fiber mesh scaffolds, in terms of bioactivity profile and biological response of bone marrow stromal cells (BMSCs), aiming at bone regeneration strategies. For this purpose, the bioactivity of wet spun SPCL fiber mesh scaffolds was assessed *in vitro* by means of soaking the samples in simulated body fluid (SBF), whose ion concentration is similar to those of human plasma. Dynamical-mechanical analysis was performed in order to assess the mechanical properties of SPCL and SPCL with silanol groups scaffolds under simulated physiological conditions. Bone marrow stromal cells have been described to have a great potential for bone regeneration strategies[20-23] as these cells can be easily guided into the osteogenic lineage, with applicability for autologous approaches[8, 24, 25]. The presence of seeded cells onto scaffolds should assist bridging the gap between structural support and *in locus* cellular and molecular communication towards functional tissue regeneration. Since apatite is naturally present in bone tissue, the apatite coating of the scaffold is expected to play an important role in the integration of the implant with the native tissue[19]. Thus, in this study it was also assessed the response of goat BMSCs towards the influence of the apatite coating on the surface of the scaffolds as compared with the bioactive uncoated wet spun starch-PCL fiber mesh scaffolds with functionalized silanol groups, in terms of osteogenic differentiation and extracellular matrix maturation.

### **IV.3. Materials and Methods**

#### **IV.3.1. Materials**

A biodegradable thermoplastic blend of corn starch with polycaprolactone (30/70 wt %), SPCL, previously described in other works by our group[4, 5, 8-10] has been selected for this study. Chloroform (CHCl<sub>3</sub>) and methanol (CH<sub>3</sub>OH) were obtained from Sigma-Aldrich.

Tetraethoxysilane (TEOS: Si(OC<sub>2</sub>H<sub>5</sub>)<sub>4</sub>) and calcium chloride (CaCl<sub>2</sub>) were obtained from Sigma-Aldrich. Ethyl alcohol (C<sub>2</sub>H<sub>5</sub>OH) was obtained from Panreac.

### IV.3.2. Wet-spun fiber mesh scaffolds processing

The polymer, a blend of corn starch with polycaprolactone (SPCL) was dissolved in chloroform at a concentration of 30 % (w/v). Then, the polymer solution was loaded into a disposable syringe, with a 0.8 mm internal diameter needle. A programmable syringe pump (KD Scientific, World Precision Instruments, UK) controlled the injection rate of the polymer solution in order to form the fiber mesh in the coagulation bath.

Two different coagulation baths were used: (i) methanol, the control, and (ii) a calcium silicate solution with a molar ratio  $\text{Si}(\text{OC}_2\text{H}_5)_4 / \text{H}_2\text{O} / \text{C}_2\text{H}_5\text{OH} / \text{HCl} / \text{CaCl}_2$  of 1.0 / 4.0 / 4.0 / 0.014 / 0.20 [15, 26], where the HCl was used as a catalyst. Control scaffolds in the methanol bath (SPCL scaffolds), were dried overnight at room temperature while fiber mesh scaffolds produced calcium silicate solution (SPCL-Si scaffold) were air dried at 60 °C for 24 h.

All scaffolds were cut into 5 mm diameter discs and sterilized by ethylene oxide.

### IV.3.3. Evaluation of the *in vitro* bioactivity of wet-spun fiber mesh scaffolds

The *in vitro* bioactivity tests of the SPCL and SPCL-Si wet-spun fiber meshes were carried out by soaking samples in 10 mL of acellular simulated body fluid (SBF) at 36.5 °C for up to 7 days. The SBF presents ions concentration similar to the one found in the human blood plasma[13, 27].

After each period of immersion the test samples were removed from SBF, washed with distilled water and dried at room temperature. The wet-spun fiber mesh scaffolds before and after bioactivity tests were analyzed by several techniques, as described in the sub-sections below.

#### IV.3.3.1. Scanning electron microscopy (SEM)

SEM with an attached energy dispersive electron probe X-ray analyser (EDS) (Leica Cambridge S360, UK) was used to observe the morphology of the wet-spun mesh scaffolds (SPCL and SPCL-Si) after the assays.

Previously to EDS and SEM analysis, sample surfaces were carbon coated (Fisons Instruments, Evaporation PSU CA508, UK) and gold sputtered (Fisons Instruments, Sputter Coater SC502, UK), respectively.

#### **IV.3.3.2. Thin-film X-ray diffraction (TF-XRD)**

TF-XRD was performed using a RINT2500 equipment (Rigaku Co., Japan) aiming to identify crystalline phases present on the polymeric wet-spun fiber mesh, with or without silanol groups, after immersion in SBF (results were compared to non immersed controls), and to characterize the crystalline/amorphous nature of the calcium phosphate films.

The data was collected by  $2\theta$  scan method with  $1^\circ$  as incident beam angle using  $\text{CuK}\alpha$  X-ray line and a scan speed of  $0.05^\circ/\text{min}$  in  $2\theta$ .

#### **IV.3.3.3. Micro-computed tomography ( $\mu$ -CT) analysis:**

Micro-CT analysis was conducted to evaluate morphology, porosity, pore interconnectivity as well as mean pore size, and mean fiber thickness after bioactivity assays, using a high-resolution  $\mu$ -CT, Skyscan 1072 scanner (Skyscan, Kontich, Belgium).

X-ray scans were performed in triplicate using a resolution of pixel size of  $5.86\ \mu\text{m}$  and integration time of 1.9 sec. The X-ray source was set at 40 keV of energy and 248  $\mu\text{A}$  of current. Approximately 400 projections were acquired over a rotation range of  $180^\circ$  with a rotation step of  $0.45^\circ$ . Data sets were reconstructed using standardized cone-beam reconstruction software (NRecon v1.4.3, SkyScan).

Representative data sets of 200 slices were segmented into binary images with a dynamic threshold of 50 to 255 (grey values) in order to identify the organic and inorganic phase. This data was used for morphometric analysis (CTAnalyser, v 1.5.1.5, SkyScan) and to build 3D models (ANT 3D creator, v2.4, SkyScan).

#### **IV.3.3.4. Dynamic mechanical analysis (DMA):**

Viscoelastic measurements were performed using a TRITEC8000B DMA from Triton Technology (Belgium)[14], equipped with a tensile mode. SPCL and SPCL-Si scaffolds were cut in 5 mm diameter discs to meet the distance between the clamps. The geometry of the samples was measured, samples clamped in the DMA apparatus and then immersed in a PBS solution. DMA spectra were obtained during a frequency scan between 0.1 and 25 Hz. The experiments were performed under constant strain amplitude ( $30\ \mu\text{m}$ ). A static pre-load of 0.7 N was applied during the test to keep the sample tight. During the DMA analysis, scaffolds were immersed in a liquid bath in a Teflon<sup>®</sup> reservoir. Three samples were used per condition.

#### **IV.3.3.5. Induced-coupled plasma emission spectroscopy (ICP)**

Elemental concentrations were measured in SBF, before and after immersing wet-spun fiber meshes (with or without Si groups), using inductively coupled plasma atomic emission spectrometry (ICP: JY2000-2, Jobin Yvon, Horiba, Japan).

Samples were collected at the end of each test period, filtered with a 0.22 µm filter and kept at -80°C until usage; for each condition and immersion time triplicate samples were analyzed.

#### **IV.3.4. Cell culture study**

In a previous study[15], SPCL (control) and SPCL-Si scaffolds produced by wet spinning were seeded with goat bone marrow stromal cells (gBMSCs) in osteogenic medium for up to 14 days. Preliminary data indicated that gBMSCs preferred SPCL-Si for cellular proliferation and osteogenic differentiation, evidencing the importance of silanol groups in SPCL-Si scaffolds for bone strategies. Thus, the present study focused on assessing the response of gBMSCs to SPCL scaffolds functionalized with silanol groups as compared to SPCL-Si pre-coated with an apatite layer, obtained by 7 days of immersion in SBF.

##### **IV.3.4.1. Harvesting and seeding gBMSCs onto wet-spun fiber mesh scaffolds**

Goat bone marrow mesenchymal stromal cells (gBMSCs) were harvested from the iliac crests of adult goats and cultured in DMEM (Dulbecco Modified Eagle Medium, Sigma) supplemented with 10 % foetal bovine serum (Gibco) and 1% antibiotic/antimycotic solution (Gibco) and cryopreserved. Cells were thawed, expanded and sub-cultured twice (2 Pa) before being seeded onto SPCL-Si scaffolds or SPCL-Si scaffolds after a 7 day incubation in SBF (SPCL-Si-7SBF) at a concentration of 100,000 cells/scaffold. After seeding, cells were cultured in alpha-MEM (Sigma) and in the presence of osteogenic supplements, namely 10<sup>-8</sup> M dexamethasone (Sigma), 50 µg/ml ascorbic acid (Sigma), 10 mM β-glycerophosphate (Sigma) for 7 and 14 days.



#### **IV.3.4.2. Cell viability assay**

The MTS test (Promega, USA) was used to assess cell viability in SPCL-Si or SPCL-Si-7SBF scaffolds seeded with gBMSCs, after 7 and 14 days of culture.

After each culturing end point, cells were rinsed in PBS and then incubated in a MTS solution (1 fraction of MTS reagent + 5 fraction of basal culture medium without phenol red (Sigma)) for 3 hours at 37 °C in a 5% CO<sub>2</sub> environment. Afterwards, absorbance was read at 490nm in a microplate ELISA reader equipment (BioTek).

#### **IV.3.4.3. Cell proliferation assay**

Proliferation of gBMSCs seeded onto constructs was also analyzed by double strand DNA quantification (dsDNA). For this purpose, a fluorimetric dsDNA quantification kit (PicoGreen, Molecular Probes) was used. The fluorescence was read using a microplate ELISA reader (BioTek) at an excitation of 485/20 nm and an emission of 528/20 nm.

#### **IV.3.4.4. ALP assay**

ALP activity has been considered an early osteogenic marker to assess osteogenic differentiation of gBMSCs seeded onto scaffolds under study. A substrate solution was added to each sample consisting of 0.2 % (wt/v) p-nitrophenyl phosphate (Sigma, USA) in a substrate buffer with 1 M diethanolamine HCl (Merck, Germany), at pH 9.8. Samples were then incubated in the dark for 45 minutes at 37 °C. After the incubation period, a stop solution (2 M NaOH (Panreac, Spain) plus 0.2 mM EDTA (Sigma, USA)), was added to each well containing the sample.

Standards were prepared with p-nitrophenol (10 μmol.ml<sup>-1</sup>) (Sigma, USA). Samples and standards were prepared in triplicates. The absorbance was read using a microplate ELISA reader (BioTek) at 405nm.

#### **IV.3.4.5. SEM**

gBMSCs morphology after culturing onto SPCL-Si and SPCL-Si-7SBF fiber meshes was observed by SEM. Before sputter coat with gold, cell-scaffold constructs were rinsed in PBS,

fixed in a 2.5% solution of gluteraldehyde (Sigma) overnight, dehydrated in a series of ethanol concentrations and air dried.

#### IV.3.5. Statistical Analysis

Results from ICP and DMA tests as well as biology assays are presented as means  $\pm$  standard deviation.

Statistical analysis was carried out using two Way ANOVA test was also applied to check the existence of statistical differences between sample groups ( $p < 0.001$ , or  $p < 0.05$ ).

### IV.4. Results and Discussion

#### IV.4.1. Bioactivity assessment

To understand the mechanism of apatite formation on bioactive materials, Kokubo *et al.* [13, 28] proposed a protein-free and acellular simulated body fluid (SBF) with pH 7.40 and ionic composition ( $\text{Na}^+$  142.0,  $\text{K}^+$  5.0,  $\text{Ca}^{2+}$  2.5,  $\text{Mg}^{2+}$  1.5,  $\text{Cl}^-$  147.8,  $\text{HCO}_3^-$  4.2,  $\text{HPO}_4^{2-}$  1.0,  $\text{SO}_4^{2-}$  0.5 mM) similar to the ones found in the human blood plasma. The bioactivity of artificial materials is commonly evaluated by examining the formation of apatite on the surface of the scaffold after immersion in SBF.

The figure IV.4.1 exhibits the TF-XRD patterns obtained for the SPCL fiber meshes produced by wet-spinning, and SPCL fiber mesh functionalized with silanol groups (SPCL-Si), after soaking in SBF for 7 days.

The TF-XRD patterns of the surface of the SPCL-Si sample, after a 7 day immersion in SBF, exhibit several broad diffraction peaks, whose position and intensities can be assigned to an apatite-like phase (ASTM JCPDS 9-432) (Figure IV.4.1). The peaks in  $2\theta$  and their correspondence to the diffraction planes of apatite are:  $10.82^\circ$  (1 0 0),  $25.87^\circ$  (0 0 2), and  $31.75^\circ$  (2 2 1). The apatite film formed presents low crystallinity, as the apatite peaks were comparatively broader than the crystalline apatite.

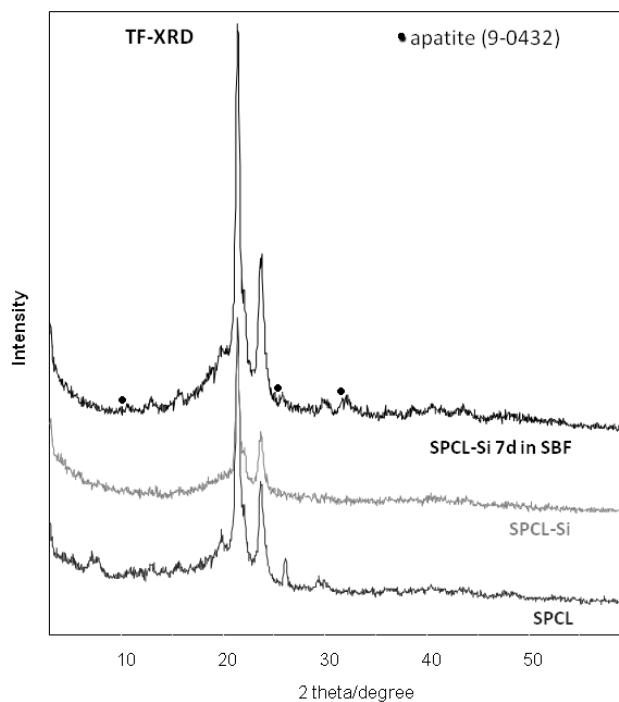


**Figure IV.4.1** - TF-XRD patterns of SPCL fiber meshes produced by wet-spinning, where a calcium silicate solution was used as a coagulation bath (SPCL-Si), and after 7 days of immersion in SBF (SPCL-Si 7d in SBF). SPCL was used as control. Apatite characteristic peaks are represented in the spectrum with black dots (●).

SPCL scaffolds, obtained by precipitation in methanol, could not induce the formation of an apatite layer even after 7 days in SBF. Conversely, in SPCL-Si scaffolds, obtained by precipitation in a calcium silicate bath, the formation of an apatite layer can be observed after only 1 day of immersion in a SBF solution, despite the fact that, after that time, the scaffold was not completely covered with the apatite layer, as observed by SEM (Figure IV.4.2).

Micro-CT analysis was used to follow up the formation and growth of an apatite layer (blue color) as function of time (Figure IV.4.2). Scaffold porosity, around 49.77 %, is similar to the values found before soaking the scaffolds in SBF, 56.84 %. As the immersion time in SBF increases, the apatite layer becomes more dense and compact but still homogeneously distributed, and thus without compromising the overall morphology and interconnectivity of the 3D-fiber mesh scaffolds.

These results clearly indicate that the presence of functional silanol groups is responsible for apatite formation in SPCL scaffolds after immersion in SBF solution (Figure IV.4.2).

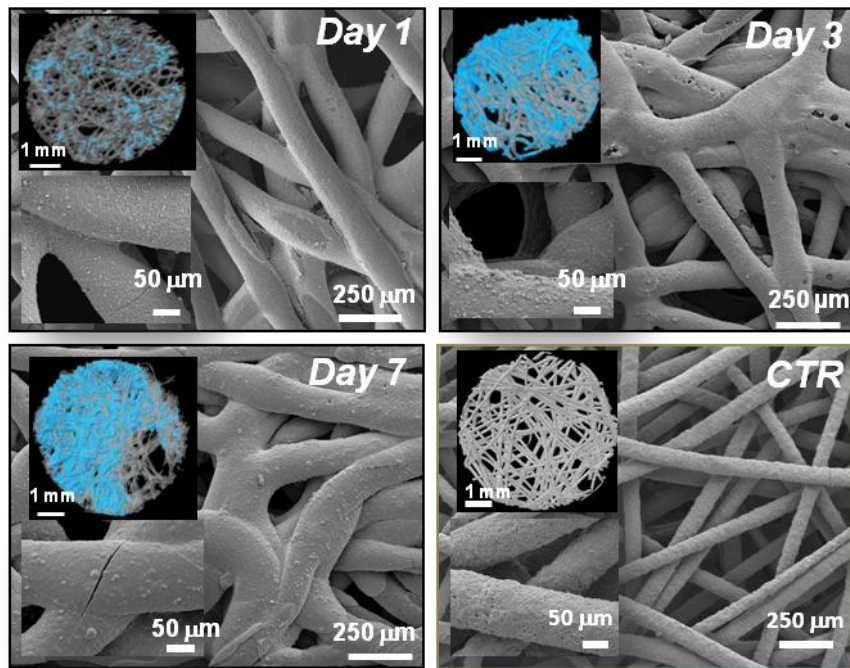


**Figure IV.4.2** - Morphological characterization by means of micro-CT and SEM micrographs of SPCL-Si scaffolds before and after 1, 3 or 7 days of immersion in SBF. Control (CTR) scaffolds of SPCL (without silanol groups) after 7 days in SBF. The blue color regions in micro-CT images correspond to the apatite deposition.

The concentrations of calcium, phosphorus and silicon in the SBF solution, after immersion of SPCL with and without Si-OH groups, measured by ICP analysis, are shown in Figure IV.4.3.

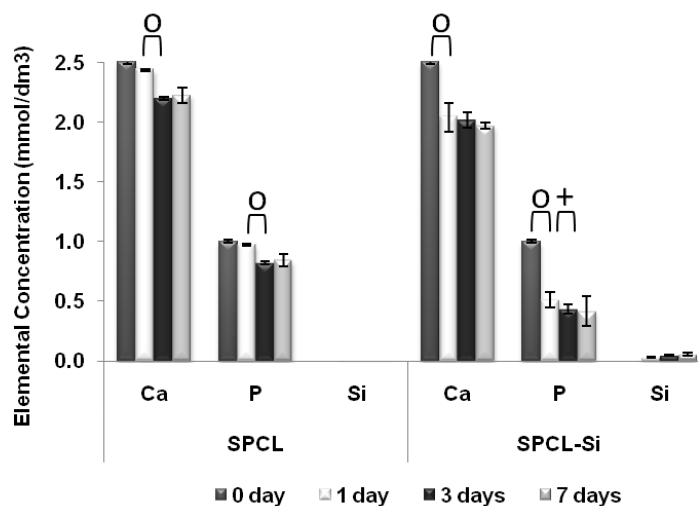


**Figure IV.4.3** - Changes in calcium (Ca), phosphorus (P) and silicon (Si) concentration in the SBF solution after different immersion periods of the SPCL or SPCL-Si scaffolds. Symbols o and + denote study groups with statistically significant differences (o=p<0.001 and +=p<0.05, respectively), as using Two Way ANOVA method.

For up to 7 days, an increment in silicon concentration was observed for SPCL-Si scaffolds. This increment is related to the release of silicon ions from the SPCL-Si fiber mesh scaffold, leading to the formation of Si-OH groups, responsible for the apatite nucleation. These results indicate that an organized arrangement of functional groups, Si-OH groups, on SPCL-Si fiber mesh scaffold is the key point to render a bioactive behavior, as the classic ceramic materials, such as Bioglass<sup>®</sup> [29]. For example, when this bioactive ceramic is soaked in SBF, the first reaction of this type of bioactive glass surface is ion exchange, in which  $\text{Ca}^{2+}$  and  $\text{Na}^+$  in the glass exchange for  $\text{H}_3\text{O}^+$  in the solution, resulting in an increase in pH of the solution as well as in the formation of a hydrated silica gel layer [29]. The formation of hydrated silica gel layer on the surface of Bioglass<sup>®</sup>, which is abundant in Si – OH groups, provides favourable sites for the calcium phosphate nucleation [30, 31]. Furthermore, the water molecules in the SBF react with the Si-O-Si bond to form additional Si-OH groups [32]. Then, these functional groups induce apatite nucleation, and the released  $\text{Ca}^{2+}$  and  $\text{Na}^+$  ions accelerate apatite nucleation by increasing of the ionic activity product (IAP) of apatite in the fluid. Also, Tanashi *et al.* [33] reported that Si-OH groups were effective in apatite nucleation. Therefore, the mineralization induced by the bioactive ceramics is due to the formation of specific surface functional groups such as Si-OH, which serve as effective sites for heterogeneous nucleation of calcium phosphate [34]. Additionally, an increase of IAP in the surrounding fluid could thereby promote the calcium phosphate nucleation and growth on the surface of bioactive ceramics [34].

In the case of SPCL scaffolds, no traces of Si element were detected in the control. For SPCL-Si, the differences in Si concentration are not statistically significant ( $p > 0.05$ ) along consecutive soaking periods, since the amount of Si released is just enough to promote the formation of the apatite layer, detected by TF-XRD and  $\mu$ -CT.

A slightly decrease in the calcium concentration is observed for the first 24 hours, which can be explained by the release of calcium ions available in the silica phase bond to the SPCL (Figure IV.4.3). This release into the SBF can lead to an increase of the ionic activity product of the surrounding fluid with respect to apatite. The Si-OH groups induced the apatite nucleation, and the increased ionic activity product accelerates the nucleation rate of apatite. Once apatite nuclei are formed, they can spontaneously grow into a uniform layer by consuming the calcium and phosphate ions from the SBF, since SBF is already highly supersaturated with respect to apatite [35].

As the soaking time in SBF increases, the calcium and phosphorus concentrations decreased gradually, as the apatite layer is forming on the fiber mesh scaffolds while consuming the

calcium and phosphate ions in SBF solution. The decrease in Ca and P concentrations is more evident in SPCL-Si scaffolds ( $p < 0.001$ ) after 3 and 7 days in the SBF solution.

In summary, the results obtained from the *in vitro* bioactivity tests clearly indicated that the presence of Si-OH functional groups in wet spun SPCL fiber meshes is a prerequisite for the apatite formation in simulated body fluid.

#### IV.4.1.1. DMA analysis

Figure IV.4.4 presents the dynamical mechanical behavior of the SPCL and SPCL-Si scaffolds with the variation of the frequency, assessed under simulated physiological condition, i.e., in a hydrated environment and at 37 °C [36-38]. The storage modulus ( $E'$ ) of all samples tends to increase with increasing frequency as observed in Figure IV.4.4.

However, for the SPCL samples  $E'$  increases from 5.54 MPa to 7.04 MPa while for the SPCL-Si samples,  $E'$  increases ( $p < 0.001$ ) from 11.38 MPa to 14.81 MPa indicating that the SPCL-Si possess a higher stiffness than SPCL's. This is possibly explained by the fact that the *in situ* functionalization improves the mechanical properties of the scaffold.

Thus, these results demonstrate that the described methodology allows obtaining bioactive polymeric scaffolds without prejudice to its mechanical properties.

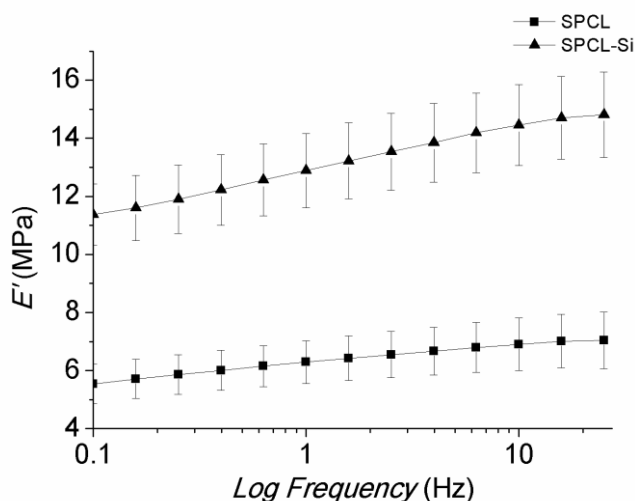


**Figure IV.4.4** - Variation of the storage modulus as a function of frequency between 0.1 and 15 Hz after equilibration at 37 °C with the samples immersed in PBS solution.

#### IV.4.2. Biological assays

Results obtained from previous experiments showed that the presence of silanol groups in SPCL scaffolds enhanced the proliferation and osteogenic differentiation of gBMSCs[15], evidencing the importance of these groups for bone TE strategies. Since studies on SPCL vs SPCL-Si wet spun scaffold were already conducted, in our study we did not include SPCL as experimental control, and focus the evaluation on the effect of pre-coating SPCL-Si scaffolds with an apatite layer.

In general, gBMSCs kept a good cell viability and proliferation rate when seeded onto both types of scaffolds. Nevertheless, viability levels are higher in the presence of SPCL-Si scaffolds alone, without the apatite coating, which tends to increase with the culturing time ( $p < 0.01$ ) (Figure IV.4.5).

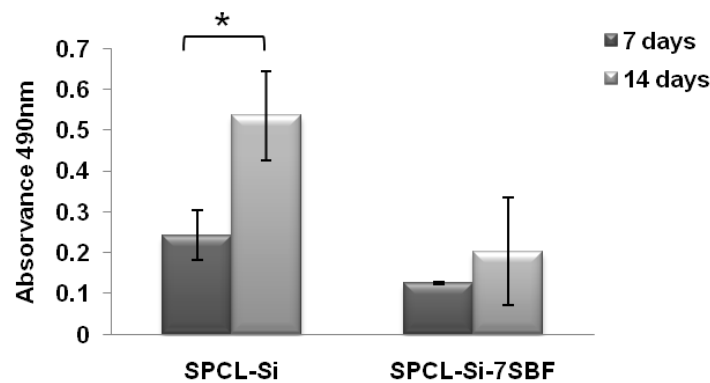


**Figure IV.4.5** - Results obtained from the MTS test performed on gBMSCs seeded onto SPCL-Si scaffolds (SPCL-Si) and SPCL-Si scaffolds pre-coated with an apatite layer (SPCL-Si-7SBF), and cultured in osteogenic medium for 7 or 14 days. Symbol \* denote study groups with statistically significant differences ( $p < 0.05$ ), as using Two Way ANOVA method.

The ALP/dsDNA ratio represents the amount of activity of ALP produced by the cells seeded on the scaffolds. In SPCL-Si previously coated with an apatite layer and seeded/cultured with gBMSCs, the ALP/dsDNA values are lower and decreased from day 7 to day 14, while in SPCL-Si constructs, ALP/DNA ratio seems to be stabilized and maintained through the culturing time (Figure IV.4.6).

Since ALP is a glycoprotein associated with the formation and maturation of the extracellular matrix[39], lower ALP levels indicate that the presence of an apatite layer on the

surface of SPCL-Si scaffolds may interfere with the development and maturation of the ECM produced by gBMSCs in SPCL-Si scaffolds. Also, and considering the expression of this osteogenic marker, cells seeded onto SPCL-Si and SPCL-Si pre-coated scaffolds are likely to be at different stages of the osteogenic process.

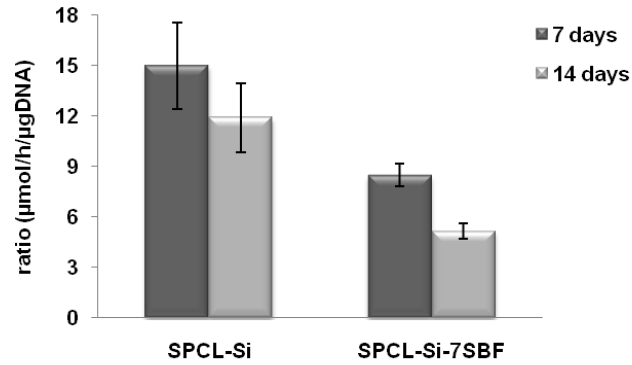


**Figure IV.4.6** - Results from ALP assays performed on seeded onto SPCL-Si scaffolds (SPCL-Si) and SPCL-Si pre-coated with an apatite layer layer (SPCL-Si-7SBF) and, after culture in osteogenic medium for 7 or 14 days.

In SEM micrographs (Figure IV.4.7), cells are shown to be more proliferative and homogeneously distributed onto SPCL-Si scaffolds both after 7 and 14 days in osteogenic culture. Furthermore, cells tend to proliferate by bridging between fibres, yet without closing the pores.

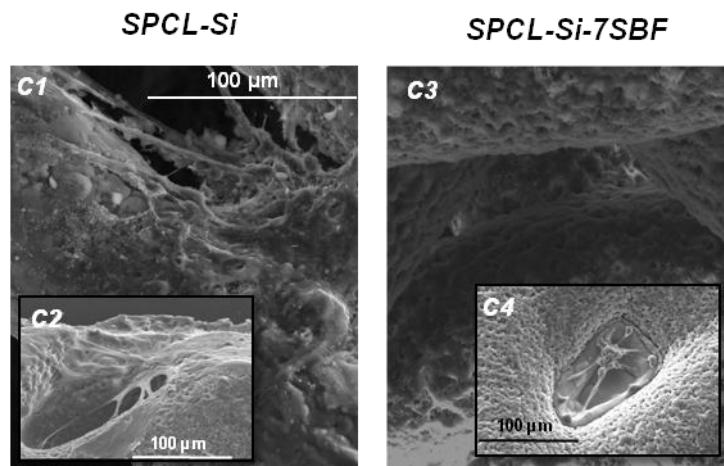


**Figure IV.4.7** - SEM pictures showing the gBMSCs morphology when seeded onto SPCL-Si (SPCL-Si) scaffolds and SPCL-Si scaffolds pre-coated with apatite (SPCL-Si-7SBF), followed by culture in osteogenic medium for 7 or 14 days. Inset micrographs refer to scaffolds, SPCL-Si (C2) and SPCL-Si pre-coated (C4) after 7 days in osteogenic medium.



Although calcium phosphate coating is considered to be excellent in promoting cell adhesion and stimulating cells into the osteogenic phenotype, the viability, colonization of the scaffolds, and osteogenic related markers indicate that the presence of silanol groups has a stronger positive impact in cells response. This was confirmed by the results obtained from all assays performed on samples for both for 7 and 14 days in culture.

Images obtained from the micro-CT analysis performed on constructs cultured for 14 days in osteogenic medium, showed the formation of a mineralized matrix in SPCL-Si scaffolds indicating that the presence of silicium improved the deposition of a calcified matrix produced by gBMSCs (Figure IV.4.8).

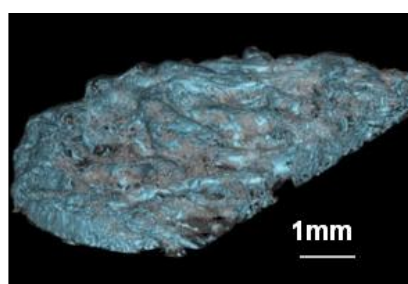


**Figure IV.4.8** - Assessment of calcified matrix production by gBMSCs seeded onto SPCL-Si scaffolds (SPCL-Si) after 14 days in osteogenic medium by  $\mu$ CT analysis.

Cells seeded onto SPCL-Si scaffolds seem to prefer the superficial silicium molecules to proliferate and to support the biomimetic growth of natural apatite for ECM synthesis. The favorable results of SPCL-Si alone may indicate that the mechanism involving silicium is likely to be more similar to the *in vivo* natural process than the SBF coating. Although silicium exists in minimal amounts in bone, has an important role in bone metabolism and osteoblast behaviour in terms of proliferation and differentiation[15-19].

These results also explain the ALP activity levels of gBMSCs seeded on SPCL-Si scaffolds as osteogenesis in guided bone regeneration has been described to be preceded by a localized, marked expression of ALP in an organized connective tissue environment[40].

The development of an apatite layer in SPCL-Si scaffold is atypical for biodegradable polymeric scaffolds, which has been commonly associated to ceramic materials[41]. Moreover the results suggest that SPCL-Si scaffolds interact more actively with cells without the presence of a calcium phosphate coating, confirming the osteoconductive properties associated to scaffolds containing silicium[15, 42] aiming at bone tissue strategies.

#### **IV.5. Conclusions**

In this study, the potential of functionalized wet-spun fibers for bone TE was assessed by physical, chemical and biological characterization.

The precipitation of SPCL in the calcium silicate solution leads to an incorporation of Si-OH groups in the structure of SPCL-Si scaffold and SPCL-Si scaffolds were shown to induce apatite nucleation (but not SPCL scaffolds) when incubated with SBF, confirming its bioactive properties. Dynamic mechanical analysis showed that SPCL-Si scaffold present higher stiffness than SPCLs, thus improved mechanical properties which are likely to be beneficial for bone related applications. Thus, the developed wet spun fiber meshes with incorporated Si-OH functional groups combine the properties of classical bioactive ceramics, and the degradability of an organic polymer.

The current work also confirms that not only Si-OH groups improve cellular functionality towards the osteoblastic phenotype, evidencing osteogenic and osteoconductive properties, but gBMSCs seems to prefer SPCL-Si scaffolds instead of SPCL-Si scaffolds coated with an apatite layer. The results obtained in SPCL-Si-gBMSC constructs may be related to the biological importance of silicium in bone metabolic processes, underlying the potential of SPCL-Si scaffolds for bone regeneration strategies.

#### **IV.6. References**

1. Place ES, George JH, Williams CK, and Stevens MM: Synthetic polymer scaffolds for tissue engineering. *Chem Soc Rev* 2009, 38(4): 1139-1151.
2. Shin H, Zygourakis K, Farach-Carson MC, Yaszemski MJ, and Mikos AG: Modulation of differentiation and mineralization of marrow stromal cells cultured on biomimetic hydrogels modified with Arg-Gly-Asp containing peptides. *J Biomed Mater Res A* 2004, 69(3): 535-543.
3. Liu C, Xia Z, and Czernuszka JT: Design and development of three-dimensional scaffolds for tissue engineering. *Chemical Engineering Research & Design* 2007, 85(A7): 1051-1064.
4. Gomes ME, Azevedo HS, Moreira AR, Ella V, Kellomaki M, and Reis RL: Starch-poly(epsilon-caprolactone) and starch-poly(lactic acid) fibre-mesh scaffolds for bone tissue engineering applications: structure, mechanical properties and degradation behaviour. *J Tissue Eng Regen Med* 2008, 2(5): 243-252.

5. Santos MI, Tuzlakoglu K, Fuchs S, Gomes ME, Peters K, Unger RE, Piskin E, Reis RL, and Kirkpatrick CJ: Endothelial cell colonization and angiogenic potential of combined nano- and micro-fibrous scaffolds for bone tissue engineering. *Biomaterials* 2008, 29(32): 4306-4313.
6. Tuzlakoglu K, Bolgen N, Salgado AJ, Gomes ME, Piskin E, and Reis RL: Nano- and micro-fiber combined scaffolds: a new architecture for bone tissue engineering. *J Mater Sci Mater Med* 2005, 16(12): 1099-1104.
7. Tuzlakoglu K, Pashkuleva I, Rodrigues MT, Gomes ME, van Lenthe GH, Muller R, and Reis RL: A new route to produce starch-based fiber mesh scaffolds by wet spinning and subsequent surface modification as a way to improve cell attachment and proliferation. *J Biomed Mater Res A* 92(1): 369-377.
8. Rodrigues MT, Gomes ME, Viegas CA, Azevedo JT, Dias IR, Guzón F, and Reis RL: Tissue Engineered Constructs based on SPCL Scaffolds Cultured with Goat Marrow Cells: Functionality in Femoral Defects. *J Tissue Eng Regen Med* 2011, 5: 41-49
9. Gomes ME, Bossano CM, Johnston CM, Reis RL, and Mikos AG: In vitro localization of bone growth factors in constructs of biodegradable scaffolds seeded with marrow stromal cells and cultured in a flow perfusion bioreactor. *Tissue Eng* 2006, 12(1): 177-188.
10. Gomes ME, Holtorf HL, Reis RL, and Mikos AG: Influence of the porosity of starch-based fiber mesh scaffolds on the proliferation and osteogenic differentiation of bone marrow stromal cells cultured in a flow perfusion bioreactor. *Tissue Eng* 2006, 12(4): 801-809.
11. Laurencin CT, Ambrosio AM, Borden MD, and Cooper JA, Jr.: Tissue engineering: orthopedic applications. *Annu Rev Biomed Eng* 1999, 1: 19-46.
12. Rhee SH: Bone-like apatite-forming ability and mechanical properties of poly(epsilon-caprolactone)/silica hybrid as a function of poly(epsilon-caprolactone) content. *Biomaterials* 2004, 25(7-8): 1167-1175.
13. Kokubo T, Takadama H: How useful is SBF in predicting in vivo bone bioactivity? *Biomaterials* 2006, 27(15): 2907-2915.
14. Ohtsuki C, Kamitakahara M, and Miyazaki T: Coating bone-like apatite onto organic substrates using solutions mimicking body fluid. *J Tissue Eng Regen Med* 2007, 1(1): 33-38.
15. Leonor I, Rodrigues MT, Gomes ME, and Reis RL: In Situ Functionalization of Wet-Spun Fibre meshes for Bone Tissue Engineering: One Step Approach. *J Tissue Eng Regen Med* 2011, 5: 104-111.
16. Carlisle EM: Silicon: a possible factor in bone calcification. *Science* 1970, 167(916): 279-280.
17. Keeting PE, Oursler MJ, Wiegand KE, Bonde SK, Spelsberg TC, and Riggs BL: Zeolite A increases proliferation, differentiation, and transforming growth factor beta production in normal adult human osteoblast-like cells in vitro. *J Bone Miner Res* 1992, 7(11): 1281-1289.
18. Obata AKasuga T: Stimulation of human mesenchymal stem cells and osteoblasts activities in vitro on silicon-releasable scaffolds. *J Biomed Mater Res A* 2009, 91(1): 11-17.

19. Reffitt DM, Ogston N, Jugdaohsingh R, Cheung HF, Evans BA, Thompson RP, Powell JJ, and Hampson GN: Orthosilicic acid stimulates collagen type 1 synthesis and osteoblastic differentiation in human osteoblast-like cells in vitro. *Bone* 2003, 32(2): 127-135.
20. Krampera M, Pizzolo G, Aprili G, and Franchini M: Mesenchymal stem cells for bone, cartilage, tendon and skeletal muscle repair. *Bone* 2006, 39(4): 678-83.
21. Mauney JR, Volloch V, and Kaplan DL: Role of adult mesenchymal stem cells in bone tissue engineering applications: current status and future prospects. *Tissue Eng* 2005, 11(5-6): 787-802.
22. Tuan RS, Boland G, and Tuli R: Adult mesenchymal stem cells and cell-based tissue engineering. *Arthritis Res Ther* 2003, 5(1): 32-45.
23. Pittenger MF, Mackay AM, Beck SC, Jaiswal RK, Douglas R, Mosca JD, Moorman MA, Simonetti DW, Craig S, and Marshak DR: Multilineage potential of adult human mesenchymal stem cells. *Science* 1999, 284(5411): 143-147.
24. Zhu L, Liu W, Cui L, and Cao Y: Tissue-engineered bone repair of goat-femur defects with osteogenically induced bone marrow stromal cells. *Tissue Eng* 2006, 12(3): 423-433.
25. Kruyt MC, Dhert WJ, Yuan H, Wilson CE, van Blitterswijk CA, Verbout AJ, and de Bruijn JD: Bone tissue engineering in a critical size defect compared to ectopic implantations in the goat. *J Orthop Res* 2004, 22(3): 544-551.
26. Oyane A, Kawashita M, Nakanishi K, Kokubo T, Minoda M, Miyamoto T, and Nakamura T: Bonelike apatite formation on ethylene-vinyl alcohol copolymer modified with silane coupling agent and calcium silicate solutions. *Biomaterials* 2003, 24(10): 1729-1735.
27. Kokubo T: Design of bioactive bone substitutes based on biomineralization process. *Materials Science & Engineering C-Biomimetic and Supramolecular Systems* 2005, 25(2): 97-104.
28. Kokubo T, Kushitani H, Sakka S, Kitsugi T, and Yamamuro T: Solutions able to reproduce in vivo surface-structure changes in bioactive glass-ceramic A-W. *J Biomed Mater Res* 1990, 24(6): 721-734.
29. Filgueiras MR, La Torre G, and Hench LL: Solution effects on the surface reactions of a bioactive glass. *J Biomed Mater Res* 1993, 27(4): 445-453.
30. Li P, Ohtsuki C, Kokubo T, Nakanishi K, Soga N, Nakamura T, and Yamamuro T: Effects of ions in aqueous media on hydroxyapatite induction by silica gel and its relevance to bioactivity of bioactive glasses and glass-ceramics. *J Appl Biomater* 1993, 4(3): 221-229.
31. Wen HB, Moradian-Oldak J, Zhong JP, Greenspan DC, and Fincham AG: Effects of amelogenin on the transforming surface microstructures of Bioglass in a calcifying solution. *J Biomed Mater Res* 2000, 52(4): 762-773.
32. Kokubo T, Kim HM, and Kawashita M: Novel bioactive materials with different mechanical properties. *Biomaterials* 2003, 24(13): 2161-2175.

33. Tanahashi M, Yao T, Kokubo T, Minoda M, Miyamoto T, Nakamura T, and Yamamuro T: Apatite coated on organic polymers by biomimetic process: improvement in its adhesion to substrate by NaOH treatment. *J Appl Biomater* 1994, 5(4): 339-347.
34. Kim HM: Ceramic bioactivity and related biomimetic strategy. *Current Opinion in Solid State & Materials Science* 2003, 7(4-5): 289-99.
35. Kim HM: Bioactive ceramics: challenges and perspectives. *Journal Ceramic Society of Japan* 2001, 109: S49-S57.
36. Mano JF, Neves NM, Reis RL, Mechanical Characterization of Biomaterials. *In Biodegradable Systems in Tissue Engineering and Regenerative Medicine*, Reis RL, Roman JS, Editor. 2005, CRC Press.
37. Mano JF: Viscoelastic properties of chitosan with different hydration degrees as studied by dynamic mechanical analysis. *Macromol Biosci* 2008, 8(1): 69-76.
38. Mano JF R, Reis RL, Cunha AM, Dynamic Mechanical Analysis in Polymers for Medical Applications in Mechanical Characterization of Biomaterials. *In Biodegradable Systems in Tissue Engineering and Regenerative Medicine*, Reis RL CD, Editor. 2002, Kluwer Academic Publishers. p. 139-164.
39. Lian JB, Stein GS: Concepts of osteoblast growth and differentiation: basis for modulation of bone cell development and tissue formation. *Crit Rev Oral Biol Med* 1992, 3(3): 269-305.
40. Stucki U, Schmid J, Hammerle CF, and Lang NP: Temporal and local appearance of alkaline phosphatase activity in early stages of guided bone regeneration. A descriptive histochemical study in humans. *Clin Oral Implants Res* 2001, 12(2): 121-127.
41. Vallet-Regi M: Ceramics for medical applications. *Journal of the Chemical Society-Dalton Transactions* 2001, (2): 97-108.
42. Huang Y, Jin X, Zhang X, Sun H, Tu J, Tang T, Chang J, and Dai K: In vitro and in vivo evaluation of akermanite bioceramics for bone regeneration. *Biomaterials* 2009, 30(28): 5041-5048.



## Chapter V

# **BILAYERED CONSTRUCTS AIMED AT OSTEOCHONDRAL STRATEGIES: THE INFLUENCE OF MEDIA SUPPLEMENTS IN THE OSTEO- AND CHONDRO-GENIC DIFFERENTIATION OF AMNIOTIC FLUID-DERIVED STEM CELLS**

*This chapter is based on the following publication:*

Rodrigues MT, Lee SJ, Gomes ME, Reis RL, Atala A, and Yoo J, Bilayered constructs aimed at osteochondral strategies: the influence of media supplements in the osteo and chondrogenic differentiation of amniotic fluid-derived stem cells, *submitted*





## Chapter V

### BILAYERED CONSTRUCTS AIMED AT OSTEOCHONDRAL STRATEGIES: THE INFLUENCE OF MEDIA SUPPLEMENTS IN THE OSTEO- AND CHONDROGENIC DIFFERENTIATION OF AMNIOTIC FLUID-DERIVED STEM CELLS

#### V.1. Abstract

The development of osteochondral (OC) tissue engineered interfaces would be a novel treatment for traumatic injuries and aging associated diseases that affect body joints. This study reports the development of a bilayered osteochondral construct based on biodegradable and natural based polymers. Amniotic fluid-derived stem cells (AFSCs) were either differentiated into cells of the osteogenic lineage after seeding onto starch-polycaprolactone (SPCL) scaffolds or into cells of the chondrogenic lineage after encapsulation in agarose gels. After these two constructs were assembled into a single construct, this bilayered system was cultured for 1 or 2 weeks in OC-defined culture media containing bone and cartilage growth factors (glycerol-2-phosphate, L-ascorbic acid, dexamethasone, and sodium pyruvate, ITS, L-proline, respectively). Additionally, the effect of the presence or absence of insulin-like growth factor-1 (IGF-1) in the culture medium was assessed. Cell viability and expression of bone- and cartilage-specific markers were analyzed in order to determine the influence of the culture media on cell phenotype. The results indicated that, after osteogenic differentiation, AFSCs that had been seeded onto SPCL scaffolds did not require OC medium to maintain their phenotype. In fact, they produced a protein-rich, mineralized extracellular matrix (ECM) for up to 2 weeks. However, AFSCs differentiated into chondrocyte-like cells appeared to require OC medium, but not IGF-1, to synthesize an ECM and maintain the chondrogenic phenotype. Thus, the results obtained show that IGF-1 was not essential for creating osteochondral constructs with AFSCs, and the OC supplements used appear to be quite important to generate cartilage in long-term tissue engineering approaches for osteochondral interfaces. In summary, this study suggests that constructs generated from agarose-SPCL bilayered scaffolds containing pre-differentiated AFSCs may be useful for potential applications in regeneration strategies for damaged or diseased joints.

## V.2. Introduction

Osteochondral (OC) interfaces are one of the most susceptible areas in the human body to traumatic injuries and aging associated diseases, such as, for instance, osteoarthritis[1-3]. Understanding and mimicking the complexity of the OC system is critical for designing a successful tissue engineering approach that can restore the functionality of a joint. However, bone and cartilage, which are the tissues that make up the OC interface, have different molecular compositions and cellular organizations, and consequently, differences in structural and mechanical properties between these tissues. Thus, current tissue engineering strategies are hampered by the difficulties inherent in designing a seamless interface between these two distinct tissues.

First, the ideal cell source for OC engineering strategies has not yet been found. The cell source should be proliferative, yet it should possess the phenotypic plasticity to differentiate into the various cell types that make up the OC interface. In addition, the cells should be able to maintain the differentiated phenotype in the presence of other cell types and after removal of the selective differentiation medium used in culture. The amniotic fluid has been recently appointed as a source of stem cells[4, 5, 6]. Amniotic fluid-derived stem cells (AFSCs) have the capacity to differentiate along both the chondrogenic[4, 5] and osteogenic[4] lineages. Importantly, they also share certain phenotypic characteristics with both adult and embryonic stem cells[6], and they have shown to be multipotential cells with no expansion limitations[4]. Also, the use of AFSCs does not raise the ethical concerns that are associated with the use of embryonic stem cells for research and therapy[6, 7].

OC interfaces are exposed to a number of different *in vivo* stresses and strains that result from the patient's daily activities and movements. Therefore, any cells used for OC tissue engineering must be supported by a scaffold that can withstand these stresses while regeneration takes place. In addition to providing mechanical support, a scaffold for OC regeneration should generate an efficient and integrated interface which enables different cell types to communicate and interact while keeping these various cells and their functions in the proper structural compartment.

Agarose gels have previously been used for cell culture and cartilage tissue engineering strategies[8-10]. The soft, flexible structure of this natural based gel recreates a 3D environment suitable for chondrocyte maintenance[11] as well as the differentiation of mesenchymal stem cells (MSCs) into the chondrogenic lineage[11]. In contrast, SPCL scaffolds, which are a blend of starch and polycaprolactone, have been previously used in tissue

engineering strategies designed for bone regeneration and replacement[12-15], as well as for cartilage applications[16, 17]. SPCL scaffolds are biodegradable and biocompatible, and they are based on naturally occurring materials. These scaffolds support the adhesion and proliferation of several cell types, including endothelial[12] and stem cells[13]. Furthermore, these scaffolds assist bone neoformation *in vivo*, especially when seeded previously with cells[13].

In addition to physical support (scaffold) and a biological interface (cells), the biochemical factors involved in stimulating cell communication, differentiation, and maintenance of phenotype should also be considered when designing a tissue engineering approach. Transforming growth factor-beta (TGF- $\beta$ ) is frequently used as a standard factor in media designed to induce chondrogenic differentiation. TGF- $\beta$  is part of the bone morphogenic protein (BMP) superfamily, and is involved in chondrogenesis, including differentiation of progenitor cells into chondrocytes[18]. Additionally, TGF- $\beta$  also induces proliferation and ECM production in articular chondrocytes[19, 20].

In bone differentiation, dexamethasone, ascorbic acid and  $\beta$ -glycerophosphate are commonly used supplements for culture media designed to induce osteogenic differentiation of various cell types. Dexamethasone, a synthetic glucocorticoid, has been shown to induce osteogenic differentiation of osteoprogenitor cells from adult bone marrow stromal-derived cells[21, 22]. Ascorbic acid plays an essential role in the structure and function of skeletal tissues as it is required for human collagen synthesis. Moreover, when a potential source of phosphate ions, such as  $\beta$ -glycerophosphate[22], is also present, a zone of hydroxyapatite-containing mineralized ECM is formed within the collagen fibrils[23], and this mineralization of the matrix is essential for formation of bone tissue. However, although osteo- and chondrogenic media are frequently described in the literature and are used to induce the differentiation of cells into these lineages, an efficient osteochondrogenic medium, which would be able to support both osteo- and chondrogenesis and the co-culture of both bone and cartilage cells, has not been completely established, although some attempts have been described[24].

In this study, we aimed to develop a novel approach for designing functional scaffolds that would support an OC interface. A novel OC medium, designed to support differentiation and maintenance of both bone and cartilage cell phenotypes, was also developed by combining some of the growth factors and nutrients associated with osteo- and chondrogenic media. Furthermore, insulin-like growth factor (IGF) was also evaluated as a potential factor for supporting OC constructs *in vitro*, since it is involved in several developmental and

physiological functions[25] of bone and cartilage, including cartilage and bone development; chondrocyte proliferation and ECM synthesis[26, 27], and osteoblast proliferation and bone formation[28].

In order to test the OC media and our novel scaffold design, human AFSCs were either cultured on SPCL scaffolds and differentiated into osteogenic cells or encapsulated in agarose gel and differentiated into chondrogenic cells. These two cell seeded scaffolds were then brought together in order to form a combination of scaffolds that would provide a highly supportive scaffold for bone formation as well as a soft matrix for cartilage growth. The resulting single constructs were cultured for 1 or 2 weeks in our novel OC media, either with or without IGF-1. At each time point, the constructs were characterized regarding the expression of bone and cartilage specific markers to evaluate the influence of the culture media on the osteogenic or chondrogenic phenotype of the differentiated cells.

### **V.3. Materials and Methods**

Human AFSCs were cultured in basic amniotic fluid cell (BAFC) medium. The BAFC medium (500 mL) contained liquid  $\alpha$ -MEM (HyClone Laboratories Inc., USA) with 18 % Chang B (Irvine Scientific, USA) and 1 % Chang C (Irvine Scientific) media as well as 2 % L-glutamine (HyClone Laboratories Inc.) and 15 % embryonic screened fetal bovine serum (ES-FBS, HyClone Laboratories Inc.) as previously described[4]. Briefly, back-up human amniocentesis cultures were harvested by trypsinization, and immunoselected with c-kit. AFS cells were then subcultured at a dilution of 1:8 and not permitted to expand beyond 60 % of confluence. The AFS cells passaged 2–3 times (passage 18-20) in BAFC medium. Then AFSCs were either encapsulated in agarose discs (2 %, Invitrogen, USA) at a concentration of  $2 \times 10^6$  cells/mL for the chondrogenic layer of the bilayered scaffold or seeded onto SPCL scaffolds at a concentration of  $8.6 \times 10^5$  cells/scaffold for the osteogenic layer. SPCL fibers were obtained by a fiber melt extrusion/fiber bonding process. Fiber-mesh scaffolds were prepared by cutting and sintering SPCL fibers by a melt-spinning process as previously described[14]. SPCL scaffolds were selected as 3D environment as these scaffolds have been extensively studied and characterized for bone TE strategies[12-16]. Prior to the cell culture assays, all scaffolds were cut into cylinders of 4 mm diameter and 5 mm length, and sterilized using ethylene oxide.

SPCL scaffolds seeded with hAFSCs and agarose gels with encapsulated hAFSCs were cultured for 2 days in BAFC culture medium, and then the medium was exchanged for either osteogenic or chondrogenic media, respectively. The chondrogenic medium consisted of DMEM (HyClone Laboratories Inc.) supplemented with 1 % antibiotic/antimycotic solution, 50 µg/mL L-ascorbic acid (Sigma, St Louis, MO, USA), 1 mM dexamethasone (Sigma), 40 µg/mL L-proline (Sigma), 100 µg/mL sodium pyruvate (Sigma), 1 % ITS (100x, Sigma) and 10 ng/mL TGF-β1 (Sigma). The osteogenic medium was composed of DMEM (HyClone Laboratories Inc.) supplemented with 10 % FBS (HyClone Laboratories Inc.) and the following osteogenic supplements: 100 nM dexamethasone (Sigma), 50 µM L-ascorbic acid and 10 mM glycerol-2-phosphate disodium salt hydrate (Sigma). Chondrogenic differentiation of AFSCs in the agarose gels was assessed after 7, 14 and 21 days in the chondrogenic media, and then the gels were characterized for cellular viability with a Calcein AM assay, safranin-O staining, and immunofluorescence for aggrecan and collagen type II.

After both chondrogenic and osteogenic differentiation occurred in the two scaffolds, the constructs were combined by adding a drop of agarose (2 %) between the cell-encapsulated and the SPCL scaffolds to promote bonding of the two layers. Then, the bilayered constructs were cultured for 2 additional weeks in co-culture medium under static conditions to evaluate whether this medium could maintain differentiated AFSCs in both chondrogenic and osteogenic phenotypes simultaneously. The co-culture media was composed of DMEM-LG (HyClone Laboratories Inc.), 4 µg/mL sodium pyruvate, ITS (1x), 5 mM glycerol-2-phosphate, 50 µg/mL L-ascorbic acid, 10 mM dexamethasone, and 40 µg/mL L-proline. In some studies, the growth factor IGF-1 (100 ng/mL, Invitrogen) was added to the co-culture medium (IGF-1 (+)).

After 7 and 14 days in the co-culture media, constructs were removed and characterized for the osteo- or chondrogenic markers mentioned above. BAFC medium (i.e., the basal conditions) was used as a control for this experiment.

### **V.3.1. Viability assay with Calcein AM**

AFSCs encapsulated in the agarose gels were rinsed in PBS (HyClone Laboratories Inc.) and then were incubated in PBS containing 3 µM Calcein AM (Molecular Probes, Invitrogen) for 30 min at 37 °C in a 5 % CO<sub>2</sub> environment. This incubation was followed by a quick rinse in PBS and overnight fixation in 10 % buffered formalin (Surgipath Medical Ind., Inc, USA) at 4 °C.

AFSC viability was detected using a confocal microscope (Axiovert 100 M, Zeiss, Germany) equipped with argon/He-Ne laser sources.

### **V.3.2. SEM (scanning electronic microscopy)**

Bilayered constructs were rinsed in PBS, fixed in 10 % buffered formalin overnight, and dehydrated in a series of ethanol concentrations and critical point dried (EMS850X, Electron Microscopy Sciences, USA). The scaffolds were then sputtered with gold (Hummer 6.2 sputtering system, Anatech Ltd, USA). This procedure destroys the structure and morphology of AFSC-agarose systems and therefore, SEM observation was only used for the AFSC-SPCL constructs of the OC system (Hitachi S-2600N, Hitachi Science Systems, Ltd, Japan). Additionally, in order to detect specific ions that eventually became present at the surface of cell seeded SPCL constructs on the ECM, such as calcium (Ca) and phosphorus (P), an energy dispersive spectroscopy (EDS) analysis was performed with EDAX (Pegasus X4M, EDS/EBSD, EDAX B.V., Netherlands).

### **V.3.3. Histological characterization**

For histological evaluation, the samples were rinsed in PBS, fixed in 10 % buffered formalin overnight and processed using a tissue processor (Microm STP120, MICROM International GmbH, Germany). Next, each sample was embedded in paraffin blocks (Microm EC 350-2, ThermoScientific, Spain), and 10 µm thick sections were cut and stained with safranin-O (Fluka, Switzerland). Following deparaffinization of AFSC-agarose samples, slides were stained with Weigert's iron hematoxylin working solution (Sigma-Aldrich, Germany) for 7 minutes. Samples were rinsed in tap water for 10 minutes, and subsequently rinsed quickly in 1 % acetic acid (Fluka) solution for about 10 to 15 seconds and stained in 0.1 % safranin O solution for 5 minutes.

Immunofluorescence analysis for collagen type II and aggrecan was also carried out. Sections were cut from the paraffin blocks, deparaffinized and rehydrated with a graded series of ethanol concentrations. Prior to incubation with primary antibodies for either mouse anti-collagen II (MAB1330, Millipore, Spain) or mouse anti-human aggrecan (MCA1452, Serotec, Germany), slides were blocked with bovine serum albumin (BSA; 3 % in PBS) (Sigma-Aldrich, Germany) for 40 minutes. Samples were incubated with primary antibodies overnight in a 4 °C room. After washing, the samples were incubated with rabbit anti-mouse Alexa Fluor 488-

conjugated secondary antibody (A11059, Invitrogen, Spain) for 1 hour at room temperature. Samples were observed under a microscope (Zeiss Imager Z1m, Germany) and images were acquired using a digital camera (AxioCam MRm5).

## V.4. Results and Discussion

### V.4.1. AFSCs-agarose system

The AFSCs remained viable during the 21-day culture period regardless of the type of media used (basal or chondrogenic), as shown in Figure V.4.1.

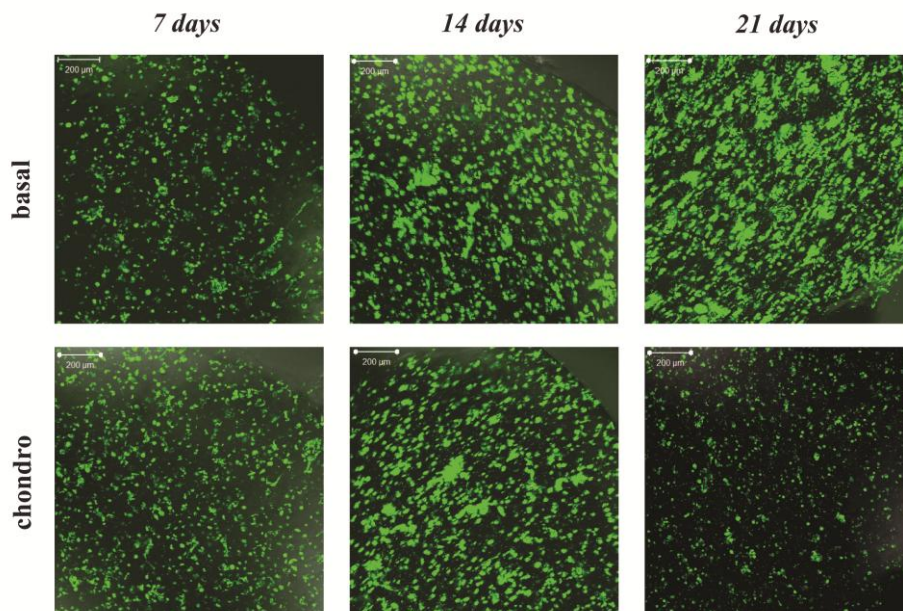


**Figure V.4.1** – Calcein AM stained samples of AFSCs encapsulated in agarose gels after 7, 14, and 21 days in chondrogenic and basal medium (control).

Nevertheless, the intensity of Calcein AM fluorescence found in samples cultured in basal culture media appeared to be higher than that observed in samples cultured in chondrogenic media.

Since basal medium is specifically formulated for cell maintenance and expansion, AFSCs may have been able to proliferate at a higher rate when cultured in basal medium. Conversely, chondrogenic medium directs AFSCs towards the chondrogenic differentiation process and thus, stimulates the cells to stop proliferating and begin expressing ECM proteins.

This result is expected, because during mammalian development, proliferation usually inhibits differentiation, while differentiation is accompanied by cell cycle withdrawal[29]. The inverted relationship between proliferation and differentiation has been previously reported in osteoprogenitor cells[30].

Besides water, the cartilage matrix consists of macromolecules in which collagen type II (around 80 % of the total tissue collagen) and proteoglycans (aggrecan) are the main structural representatives[31], and these molecules are responsible for tissue formation. Therefore, the differentiation of AFSCs into chondrocyte-like cells was assessed by examining the expression of collagen type II and aggrecan by immunofluorescent analysis.

Collagen type II expression was detected as early as 7 days into culture of AFSCs encapsulated in agarose gels, and by the end of week 3, the expression appeared to increase, especially when chondrogenic medium was used for culture. This is particularly evident if the amount of collagen type II in chondrogenic and basal medium cultured constructs is compared, as expression of collagen type II in the latter tends to decline with time in culture (Figure V.4.2).

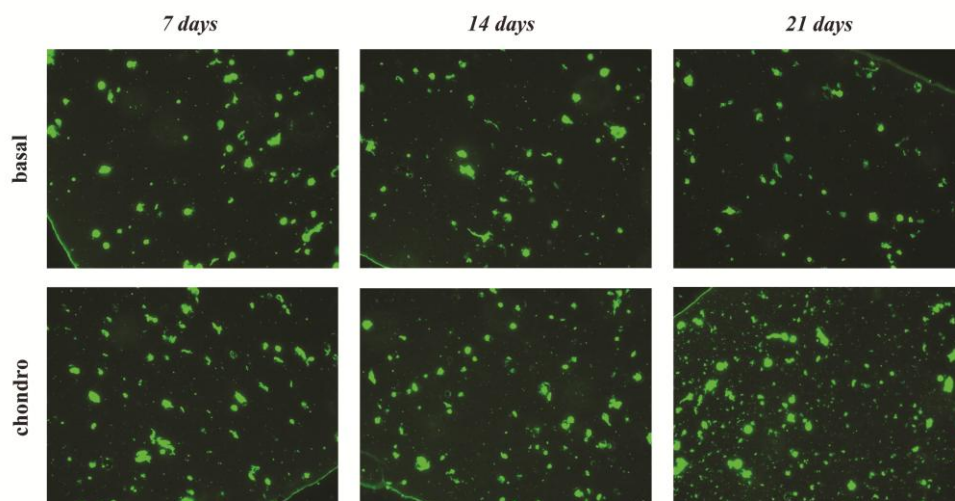


**Figure V.4.2** – Immunofluorescent analysis of collagen type II expression in AFSCs encapsulated in agarose gels after 7, 14, and 21 days in chondrogenic and basal media (control). Magnification, 200X.

Collagen type II expression is observed throughout the differentiation process of MSCs into chondrocytes[32]. Collagen is initially expressed at the final stage of undifferentiated MSCs, and then increases significantly as cells became chondroprogenitors, and again as fully differentiated chondrocytes[32]. This continuous expression of collagen II during chondrogenic



differentiation may explain why collagen type II is expressed at all time points in this study. Since AFSCs share several markers with MSCs[4, 33]; the chondrogenic differentiation of AFSCs may also follow a similar time course in terms of collagen type II expression, and be continuously expressed during our experiment.

However, it has been shown that the aggrecan is available in smaller amounts in cartilage ECM than collagen type II[31], and we have also observed this in our study (Figure V.4.3).

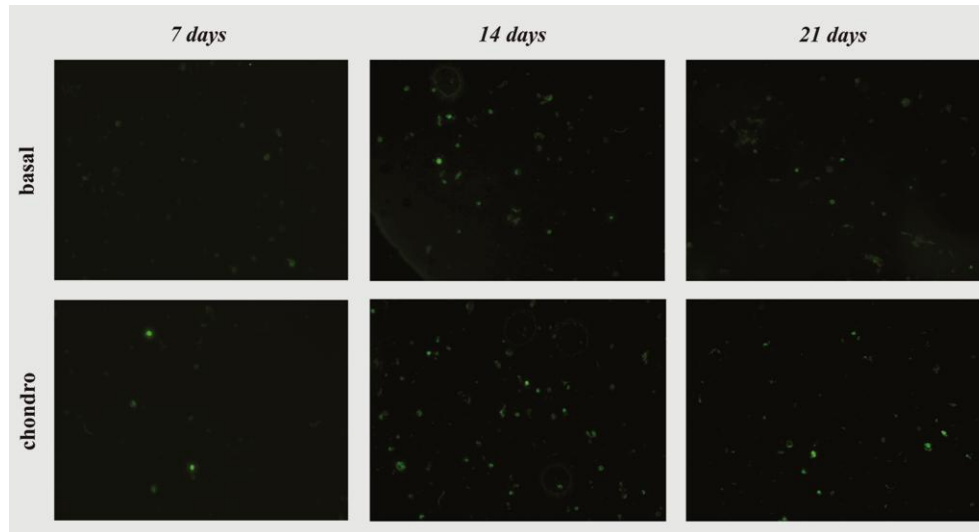


**Figure V.4.3** - Immunofluorescent analysis for aggrecan expression in AFSCs encapsulated in agarose gels after 7, 14 and 21 days in chondrogenic or basal media (control). Magnification, 200X.

In basal medium, AFSCs encapsulated in agarose gels expressed a low level of aggrecan for the 3 weeks of this experiment. Conversely, in chondrogenic culture medium, aggrecan expression is more evident, reaching a peak at 2 weeks that is followed by a slight decrease at 3 weeks. This pattern of expression is supported by data showing that during skeletogenesis, chondroprogenitor determination and chondrocyte differentiation are accompanied by dynamic ECM remodeling[32]. Aggrecan expression in the ECM increases as chondrocytes differentiate and become hypertrophic[32]. In addition, chondroprogenitor cells and chondrocytes express high levels of collagen type II and increasing levels of aggrecan in the ECM. Nevertheless, as chondrocytes move into a hypertrophic state, low expression levels of collagen type II and high aggrecan levels are observed[32]. Our results show that in the agarose gels, strong collagen type II expression and lower expression of aggrecan are present with some fluctuations from week 2 to week 3. This suggests that by week 3, AFSCs may still be in an early stage of chondrocyte differentiation.

## V.4.2. Agarose-SPCL bilayered system

### V.4.2.1. AFSCs-SPCL layer

The AFSCs seeded onto the SPCL scaffold proliferated well and were able to differentiate to osteogenic cell types in the different culture media. In the SEM micrographs of these constructs (Figure V.4.4), the cells were distributed throughout the scaffold, and some mineralization nodules could be seen at the surface of the SPCL fibers, suggesting the formation of a calcified ECM. Larger mineralized aggregates were found when IGF-1 was added to the OC culture medium after 1 week of culture in this medium. Although these nodules did not increase in size with time, the mineralization observed in the SPCL constructs was stable and was still evident after 2 weeks of culture in the OC medium.

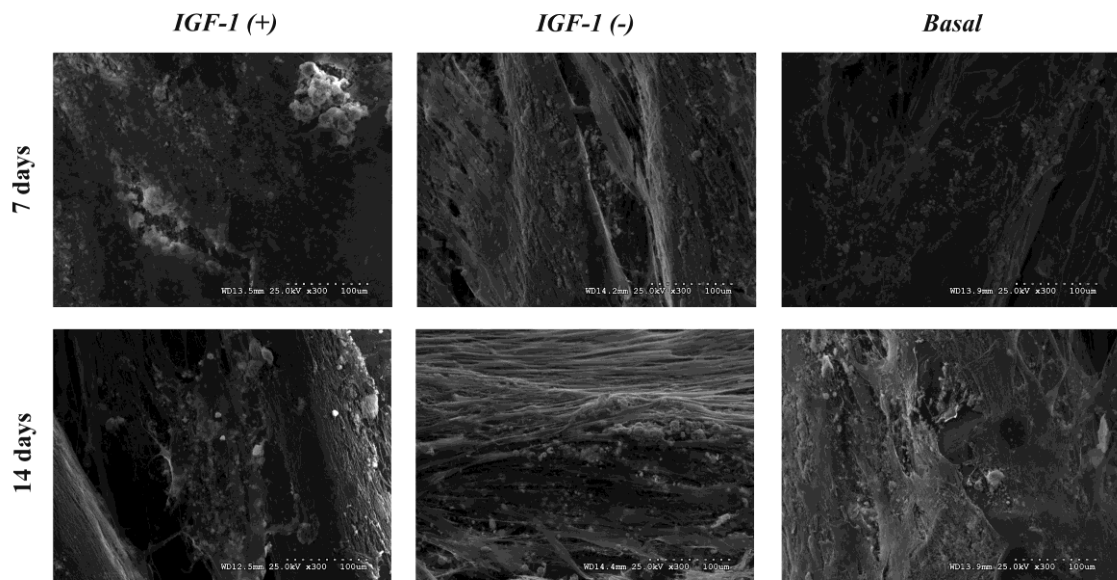


**Figure V.4.4** - SEM micrographs of the osteogenic layer (AFSCs seeded onto SPCL scaffold) of the bilayered scaffolds after 7 or 14 days in OC culture media. IGF-1(+) indicates culture medium supplemented with IGF-1 while IGF-1(-) refers to the same culture medium without IGF-1. The basal culture medium consisted of the basic medium currently used for AFSC expansion and maintenance, and was used as the control medium in these studies.

EDS analysis was also performed at the surface of the constructs after assembly of the OC constructs. Two EDS analyses were considered; the first was broader and included several areas of the construct that contained cells with and without mineralization nodules (Table

V.4.1), and the second analysis included only areas in which mineralization was present (Table V.4.2).

Table V.4.1 - Results obtained from EDS analysis of the atomic percentage (At %) of several ions present in AFSCs-SPCL layer after 7 and 14 days in the OC culture media.

<b>At (%)</b>	<b>Si</b>	<b>P</b>	<b>Ca</b>	<b>Ca/P</b>
<b>7 d IGF-1 (+)</b>	0.22	0.66	0.95	1.439
<b>7 d IGF-1 (-)</b>	0.09	0.56	0.55	0.982
<b>7 d Basal</b>	0.20	1.52	1.61	1.059
<b>14 d IGF-1 (+)</b>	0.13	0.58	0.47	0.810
<b>14 d IGF-1 (-)</b>	0.07	0.55	0.57	1.036
<b>14 d Basal</b>	0.08	0.46	0.46	1.000

Represented ions: Si-silicium, P-phosphorus, Ca-calcium. Ca/P stands for the ratio Calcium/Phosphorus.

Silicon (Si), a trace element that has an essential role in bone formation and is thought to be involved in the synthesis and/or stabilization of collagen[34] was found in all of the constructs at different end points. Si levels tended to decrease with culture time in OC media, although this decrease was larger in constructs cultured in basal medium.

The detection of calcium (Ca) and phosphorus ions (P) via EDS has been associated with the production of mineralized matrices by cells. In this study, although Ca and P levels decreased with culture time when the constructs were maintained in both basal and OC media without IGF-1, the Ca/P ratio was close to 1 at all time points. However, when IGF-1 was added to the media, the Ca/P ratio detected in the constructs cultured for 7 days was 1.439. This ratio is more similar to tricalcium phosphate (TCP) ratio[35].

In general, the decrease observed in the percentage of atomic concentrations with the culture end points may be related to the presence of a saturation point at which a balance of mineralized matrices might be established. When osteoblasts become entrapped in bone ECM, these cells eventually begin to die as part of the natural process of bone formation. Furthermore, if the cell proliferation rate is reduced because the cells have become entrapped in the mineralized matrices they produced, the synthesis of ECM will also decrease and stabilize. Nevertheless, when the analysis was performed specifically on mineralized nodules, some variations in the amounts of the studied ions were observed (Table V.4.2).

**Table V.4.2** - Results obtained from EDS analysis of the atomic percentage (At %) of several ions present in AFSCs-SPCL layer after 7 and 14 days in the OC culture media. EDS analysis was performed on areas of the constructs containing mineralized aggregates.

At (X)	Si	P	Ca	Ca/P
<b>7 d IGF-1 (+)</b>	0.41	4.44	4.94	1.113
<b>7 d IGF-1 (-)</b>	0.28	3.06	3.34	1.092
<b>7 d Basal</b>	0.33	5.78	6.85	1.185
<b>14 d IGF-1 (+)</b>	0.14	2.51	2.53	1.008
<b>14 d IGF-1 (-)</b>	0.10	2.88	3.07	1.066
<b>14 d Basal</b>	0.24	3.73	6.19	<u>1.660</u>

Represented ions: Si-silicium, P-phosphorus, Ca-calcium. Ca/P stands for the ratio Calcium/Phosphorus.

When only mineralized areas were studied, Si values decreased with time. Although calcium and phosphorus slightly decreased with culture time, the atomic concentrations of both of these minerals were higher than the ones observed in the broader analysis shown in Table V.4.1. This result is expected, since the EDS focused on areas of mineralization in the second analysis. When the Ca/P was calculated, all culture conditions but one resulted in a ratio around 1. The constructs cultured for 14 days in basal medium after the OC assembly were found to have a Ca/P ratio of 1.66, which is nearly the same as the Ca/P ratio found in naturally occurring bone hydroxyapatite, which is 1.67[35, 36]. During the process of bone hardening during aging, the Ca:P ratio gradually increases from 1 to 1.67, the hydroxyapatite ratio reported for healthy bone[37].

Although IGF-1 has been shown to be important for bone and cartilage tissue development, we did not find that the presence of this growth factor had any effect on the maintenance of the osteogenic phenotype of cells cultured in OC medium with IGF-1. Furthermore, the best results in terms of mineralization were observed in basal medium conditions after 2 weeks in culture, when the constructs demonstrated a Ca/P ratio similar to that seen in natural bone.

Runx-2 is an important transcription factor involved in osteogenic development and exogenous expression, which has been shown to enhance osteoblast-specific gene expression in rat bone marrow stromal cells as well as biological mineral deposition[38]. In our previous study, hAFSCs were shown to express RunX-2 during osteogenic differentiation over a period of up to 3 weeks in osteogenic medium. In the present study, we analyzed possible differences

in RunX-2 expression 2 weeks after the novel OC media was added to the constructs (Figure V.4.5).

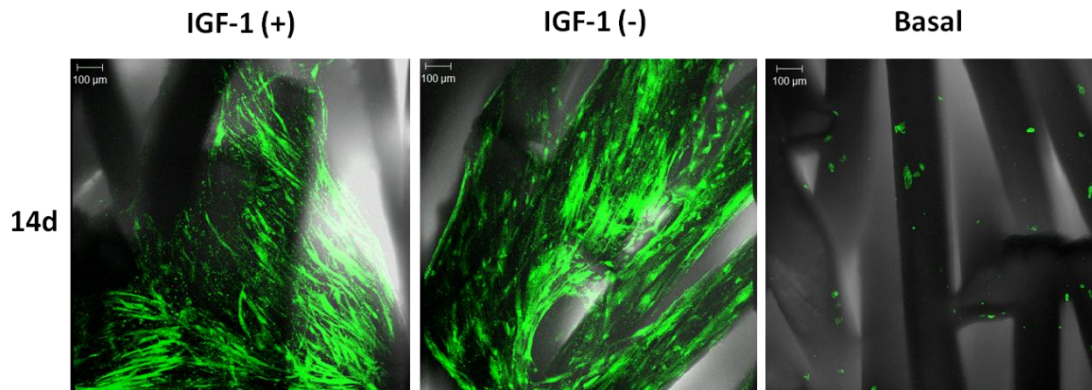


**Figure V.4.5** - Immunofluorescence for RunX-2 expression in the osteogenic layer (AFSCs seeded onto SPCL scaffolds) of the bilayered scaffolds after 14 days (14d) in the OC culture media. IGF-1(+) indicates culture medium supplemented with IGF-1 while IGF-1(-) refers to the same culture medium without IGF-1. “Basal” refers to the basic medium currently used for AFSC expansion and maintenance, and was used as a control in this assay.

Runx-2 expression was higher when the cells were cultured in OC media than when they were cultured in basal medium. In the basal medium, RunX-2 expression was almost nonexistent, which indicates that in OC media, with or without IGF, the osteogenic process is dynamic and evolving, and that mineralization may be taking place, since high levels of Runx2 expression have been shown to maintain the mineralization capacity of expanded marrow cells[38].

Cell viability in the hAFSC-containing agarose gels was qualitatively analyzed using a Calcein AM assay after the chondrogenic differentiation process.

Figure V.4.6 indicates that most cells remained viable during the culture period, and viability was independent of the medium used for culture. Furthermore, cellular viability was high both at the surface/border and in the center areas of the gels, indicating that the agarose gels were permeable enough to allow the exchange of nutrients and gases between the culture media and the encapsulated cells.

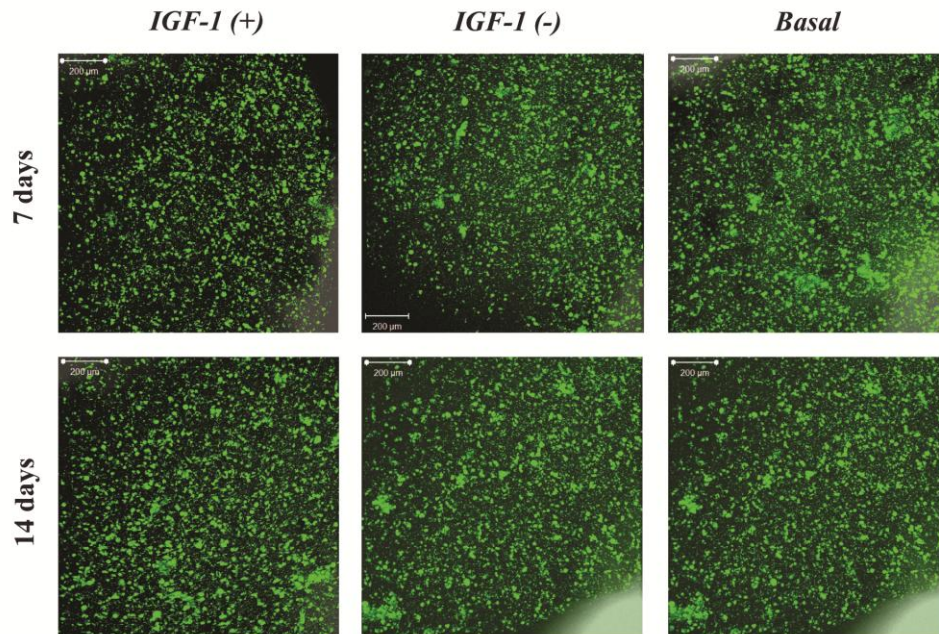


**Figure V.4.6** - Viability of the chondrogenic layer (AFSCs in agarose gels) of the bilayered scaffold after 7 (7d) or 14 days (14d) in the OC culture media. IGF-1(+) indicates culture medium supplemented with IGF-1 while IGF-1 (-) refers to the same culture medium without IGF-1. “Basal” represents the basic medium currently used for AFSC expansion and maintenance, and was used as a control.

Collagen type II expression within the gels was assessed by immunofluorescence. Figure V.4.7 indicates that collagen type II was present in the constructs for up to 14 days after the addition of OC media. However, expression of this chondrogenic marker was lower in the assembled bilayered construct than in AFSC-containing agarose gels alone, and this was true whether the constructs were cultured in basal or chondrogenic media.

A possible explanation is that the OC media is a rich cocktail that, together with the presence of the AFSC-SPCL constructs, might interfere with the chondrogenic process of encapsulated AFSCs.

Aggrecan levels were also measured in the bilayered constructs. They were found to be similar to the levels observed in the AFSC-agarose gels alone. This suggests that aggrecan expression is more stable than collagen type II expression in the presence of OC media (Figure V.4.8).

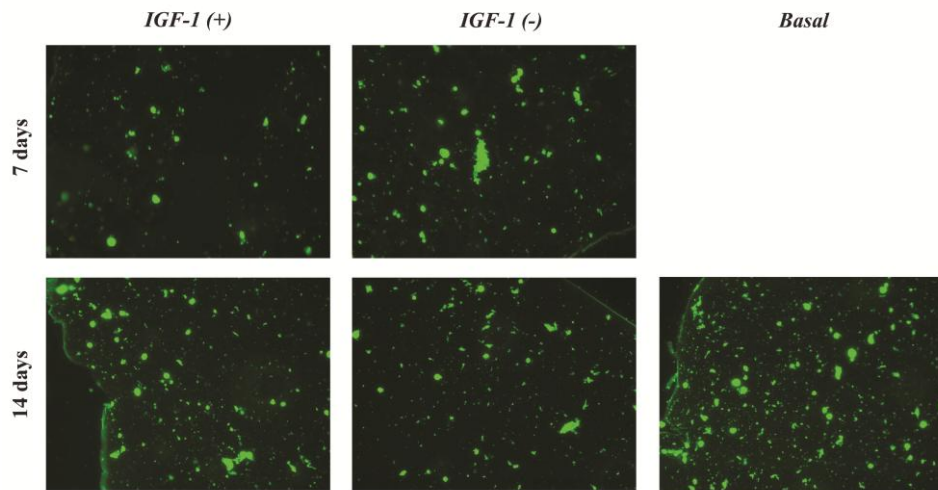


**Figure V.4.7** - Collagen type II expression (200x magnification) in the chondrogenic layer (AFSCs in agarose gels) of the bilayered scaffold after 7 or 14 days in OC culture medium. IGF-1(+) indicates culture medium supplemented with IGF-1 while IGF-1 (-) refers to the same culture medium without IGF-1. Cultures maintained in basal medium were used as controls.

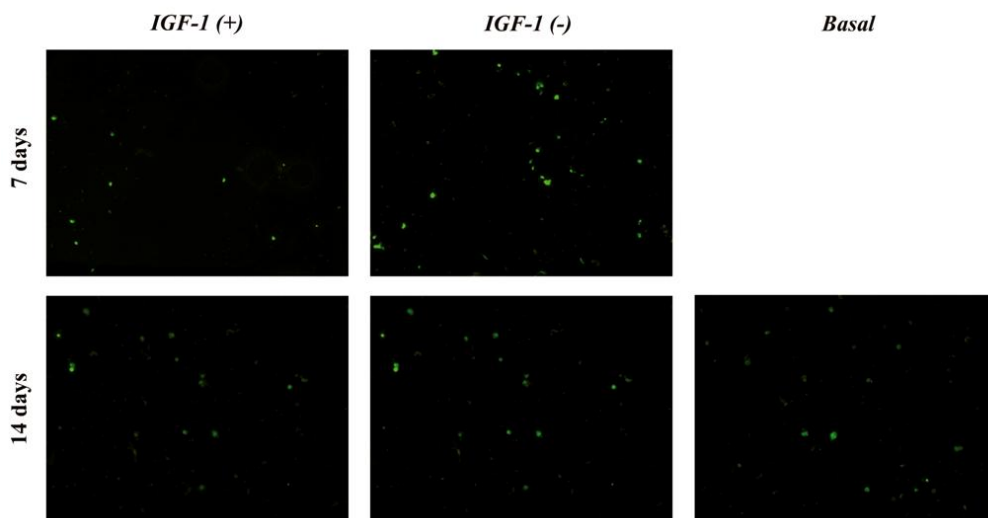


**Figure V.4.8** - Aggrecan immunofluorescence (200 x magnification) in the chondrogenic layer (AFSCs in agarose gels) of the bilayered scaffold after 7 or 14 days in OC culture medium. IGF-1(+) indicates culture medium supplemented with IGF-1 while IGF-1(-) refers to the same culture medium without IGF-1. Culture in basal medium was used as a control.

Safranin-O staining is used to identify areas of cartilage production in tissue sections. When we performed this stain on sections taken from the bilayered OC constructs, the chondrogenic



layer (AFSC-agarose gel) stained positively in sections from all samples cultured in OC medium without IGF-1 after 14 days of culture, as shown in Figure V.4.9.

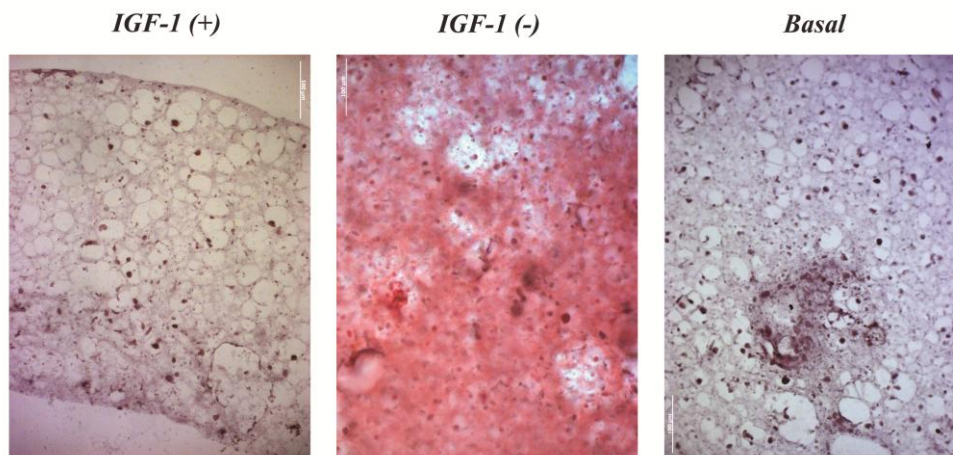


**Figure V.4.9** - Safranin-O (cartilage-specific) staining of the chondrogenic layer (AFSCs in agarose gels) of the bilayered scaffold after 14 days in OC culture medium. IGF-1(+) indicates culture medium supplemented with IGF-1 while IGF-1 (-) refers to the same culture medium without IGF-1. “Basal” represents the basic medium currently used for AFSC expansion and maintenance, and was used as a control. Magnification, 200X.

In basal medium as well as in medium containing IGF-1, the safranin-O staining intensity is very low. This suggests that the combination of other factors besides IGF-1 in the osteochondral medium maintains a higher level of chondrogenesis in the constructs, thus increasing the safranin-O staining in the constructs cultured in the OC medium.

Despite the fact that collagen type II and aggrecan expression were lower in the OC medium than in regular chondrogenic medium, these proteins were still present in the chondrogenic layer of the bilayered constructs cultured in OC medium, indicating that in this media, AFSCs continue to produce ECM.

However, because aggrecan levels remain low with time, and are independent of the culture media, it is unlikely that AFSC-derived chondrocyte-like cells became hypertrophic in these constructs. The decrease in protein production may have been a result of the reduced proliferation rate observed in these samples, which is typical of differentiated chondrocytes.



## V.5. Conclusions

The results obtained in this study demonstrated that AFSCs seeded onto SPCL scaffolds or encapsulated in agarose gel systems remained viable even after these constructs were cultured for additional time in the novel OC culture media described here. Furthermore, in the osteogenic layer (SPCL), osteogenically differentiated AFSCs did not require the OC media to maintain an osteogenic phenotype for up to 14 days, as they were able to continue producing mineralized ECM even when cultured in basal medium. In agarose gels, encapsulated AFSCs differentiated into chondrocyte-like cells that produced an ECM rich in collagen type II and aggrecan. When cultured in OC media, the expression of these markers decreased, but safranin-O staining clearly indicated that the cells continued to produce a cartilage-like ECM in OC medium without IGF supplement.

In this bilayered system, IGF was not essential for the maintenance of chondrogenic or osteogenic phenotypes in differentiated AFSCs as evidenced by marker expression studies. However the other supplements in the OC medium were shown to be very important for achieving long-term differentiation results.

This OC co-culture medium could be advantageous not only to simplify cell culture procedures but also to allow physical interaction between osteogenic and chondrogenic phenotypes while ensuring that the induced phenotype of chondrocytes and osteoblasts is maintained. In addition, this medium would reduce the time and production costs of a tissue engineered product and move it closer to a clinically applicable strategy for joint repair. Finally, the development of a bilayered OC system for tissue engineering of bone/cartilage interfaces could better mimic the integration of bone and cartilage in an OC defect by providing scaffolds that address tissue specific needs.

In this study, a bilayered scaffold of this type was successfully created in which both osteogenically and chondrogenically differentiated AFSCs maintained long term viability and phenotypic expression *in vitro*. Thus, the integrated agarose-SPCL scaffold proved to be functional *in vitro* and may lead to the development of new strategies for OC repair and regeneration.

## **V.6. References**

1. Naran KN, Zoga AC: Osteochondral lesions about the ankle. *Radiol Clin North Am* 2008, 46(6): 995-1002
2. Madry H, van Dijk CN, and Mueller-Gerbl M: The basic science of the subchondral bone. *Knee Surg Sports Traumatol Arthrosc* 2010, 18(4): 419-433.
3. Pape D, Filardo G, Kon E, van Dijk CN, and Madry H: Disease-specific clinical problems associated with the subchondral bone. *Knee Surg Sports Traumatol Arthrosc* 2010, 18(4): 448-462.
4. De Coppi P, Bartsch G, Jr., Siddiqui MM, Xu T, Santos CC, Perin L, Mostoslavsky G, Serre AC, Snyder EY, Yoo JJ, Furth ME, Soker S, and Atala A: Isolation of amniotic stem cell lines with potential for therapy. *Nat Biotechnol* 2007, 25(1): 100-6.
5. Kolambkar YM, Peister A, Soker S, Atala A, and Guldberg RE: Chondrogenic differentiation of amniotic fluid-derived stem cells. *J Mol Histol* 2007, 38(5): 405-413.
6. Prusa AR, Marton E, Rosner M, Bernaschek G, and Hengstschlager M: Oct-4-expressing cells in human amniotic fluid: a new source for stem cell research? *Hum Reprod* 2003, 18(7): 1489-1493.
7. Fauza D: Amniotic fluid and placental stem cells. *Best Pract Res Clin Obstet Gynaecol* 2004, 18(6): 877-891.
8. Diduch DR, Jordan LC, Mierisch CM, and Balian G: Marrow stromal cells embedded in alginate for repair of osteochondral defects. *Arthroscopy* 2000, 16(6): 571-577.
9. Gu WY, Yao H, Huang CY, and Cheung HS: New insight into deformation-dependent hydraulic permeability of gels and cartilage, and dynamic behavior of agarose gels in confined compression. *J Biomech* 2003, 36(4): 593-598.
10. Buschmann MD, Gluzband YA, Grodzinsky AJ, Kimura JH, and Hunziker EB: Chondrocytes in agarose culture synthesize a mechanically functional extracellular matrix. *J Orthop Res* 1992, 10(6): 745-758.
11. Mauck RL, Yuan X, and Tuan RS: Chondrogenic differentiation and functional maturation of bovine mesenchymal stem cells in long-term agarose culture. *Osteoarthritis Cartilage* 2006, 14(2): 179-189.
12. Santos MI, Fuchs S, Gomes ME, Unger RE, Reis RL, and Kirkpatrick CJ: Response of micro- and macrovascular endothelial cells to starch-based fiber meshes for bone tissue engineering. *Biomaterials* 2007, 28(2): 240-248.
13. Rodrigues MT, Gomes ME, Viegas CA, Azevedo JT, Dias IR, Guzón F, and Reis RL: Tissue Engineered Constructs based on SPCL Scaffolds Cultured with Goat Marrow Cells: Functionality in Femoral Defects. *J Tissue Eng Regen Med* 2011, 5(1): 41-49.

14. Gomes ME, Azevedo HS, Moreira AR, Ella V, Kellomaki M, and Reis RL: Starch-poly(epsilon-caprolactone) and starch-poly(lactic acid) fibre-mesh scaffolds for bone tissue engineering applications: structure, mechanical properties and degradation behaviour. *J Tissue Eng Regen Med* 2008, 2(5): 243-252.

15. Gomes ME, Holtorf HL, Reis RL, and Mikos AG: Influence of the porosity of starch-based fiber mesh scaffolds on the proliferation and osteogenic differentiation of bone marrow stromal cells cultured in a flow perfusion bioreactor. *Tissue Eng* 2006, 12(4): 801-809.

16. Gonçalves A, Costa P, Rodrigues MT, Dias IR, Reis RL, and Gomes ME: Effect of flow perfusion conditions in the chondrogenic differentiation of bone marrow stromal cells cultured onto starch based biodegradable scaffolds *Acta Biomaterialia* 2011, 7: 1644-1652.

17. Oliveira JT, Crawford A, Mundy JM, Moreira AR, Gomes ME, Hatton PV, and Reis RL: A cartilage tissue engineering approach combining starch-polycaprolactone fibre mesh scaffolds with bovine articular chondrocytes. *J Mater Sci Mater Med* 2007, 18(2): 295-302.

18. Leonard CM, Fuld HM, Frenz DA, Downie SA, Massague J, and Newman SA: Role of transforming growth factor-beta in chondrogenic pattern formation in the embryonic limb: stimulation of mesenchymal condensation and fibronectin gene expression by exogenous TGF-beta and evidence for endogenous TGF-beta-like activity. *Dev Biol* 1991, 145(1): 99-109.

19. Yoo JU, Barthel TS, Nishimura K, Solchaga L, Caplan AI, Goldberg VM, and Johnstone B: The chondrogenic potential of human bone-marrow-derived mesenchymal progenitor cells. *J Bone Joint Surg Am* 1998, 80(12): 1745-1757.

20. Grimaud E, Heymann D, and Redini F: Recent advances in TGF-beta effects on chondrocyte metabolism. Potential therapeutic roles of TGF-beta in cartilage disorders. *Cytokine Growth Factor Rev* 2002, 13(3): 241-257.

21. Aubin JE: Osteoprogenitor cell frequency in rat bone marrow stromal populations: role for heterotypic cell-cell interactions in osteoblast differentiation. *J Cell Biochem* 1999, 72(3): 396-410.

22. Maniopoulos C, Sodek J, and Melcher AH: Bone formation in vitro by stromal cells obtained from bone marrow of young adult rats. *Cell Tissue Res* 1988, 254(2): 317-330.

23. Franceschi RT, Iyer BS, and Cui Y: Effects of ascorbic acid on collagen matrix formation and osteoblast differentiation in murine MC3T3-E1 cells. *J Bone Miner Res* 1994, 9(6): 843-854.

24. Li J, Mareddy S, Tan DM, Crawford R, Long X, Miao X, and Xiao Y: A minimal common osteochondrocytic differentiation medium for the osteogenic and chondrogenic differentiation of bone marrow stromal cells in the construction of osteochondral graft. *Tissue Eng Part A* 2009, 15(9): 2481-2490.

25. Butler AA, Yakar S, Gewolb IH, Karas M, Okubo Y, and LeRoith D: Insulin-like growth factor-I receptor signal transduction: at the interface between physiology and cell biology. *Comp Biochem Physiol B Biochem Mol Biol* 1998, 121(1): 19-26.

26. Martel-Pelletier J, Boileau C, Pelletier JP, and Roughley PJ: Cartilage in normal and osteoarthritis conditions. *Best Pract Res Clin Rheumatol* 2008, 22(2): 351-384.
27. Vinatier C, Bouffi C, Merceron C, Gordeladze J, Brondello JM, Jorgensen C, Weiss P, Guicheux J, and Noel D: Cartilage tissue engineering: towards a biomaterial-assisted mesenchymal stem cell therapy. *Curr Stem Cell Res Ther* 2009, 4(4): 318-329.
28. Meinel L, Zoidis E, Zapf J, Hassa P, Hottiger MO, Auer JA, Schneider R, Gander B, Luginbuehl V, Bettschart-Wolfisberger R, Illi OE, Merkle HP, and von Rechenberg B: Localized insulin-like growth factor I delivery to enhance new bone formation. *Bone* 2003, 33(4): 660-672.
29. Beier F, Leask TA, Haque S, Chow C, Taylor AC, Lee RJ, Pestell RG, Ballock RT, and LuValle P: Cell cycle genes in chondrocyte proliferation and differentiation. *Matrix Biology* 1999, 18(2): 109-120.
30. Lian JB, Stein GS: Concepts of osteoblast growth and differentiation: basis for modulation of bone cell development and tissue formation. *Crit Rev Oral Biol Med* 1992, 3(3): 269-305.
31. Aigner T, Stove J: Collagens-major component of the physiological cartilage matrix, major target of cartilage degeneration, major tool in cartilage repair. *Adv Drug Deliv Rev* 2003, 55(12): 1569-1593.
32. Tuan RS: Biology of developmental and regenerative skeletogenesis. *Clin Orthop Relat Res* 2004, (427 Suppl): S105-17.
33. Hipp J, Atala A: Sources of stem cells for regenerative medicine. *Stem Cell Rev* 2008, 4(1): 3-11.
34. Jugdaohsingh R: Silicon and bone health. *J Nutr Health Aging* 2007, 11(2): 99-110.
35. Vallet-Regi M: Ceramics for medical applications. *Journal of the Chemical Society-Dalton Transactions* 2001, (2): 97-108.
36. Palmer LC, Newcomb CJ, Kaltz SR, Spoerke ED, and Stupp SI: Biomimetic systems for hydroxyapatite mineralization inspired by bone and enamel. *Chem Rev* 2008, 108(11): 4754-4783.
37. Dorozhkin SV: Calcium Orthophosphates as Bioceramics: State of the Art. *Journal of Functional Biomaterials* 2010, 1: 22-107.
38. Byers BA, Garcia AJ: Exogenous Runx2 expression enhances in vitro osteoblastic differentiation and mineralization in primary bone marrow stromal cells. *Tissue Eng* 2004, 10(11-12): 1623-1632.

## **SECTION IV**

**DOES STEM CELL ORIGIN INFLUENCE STEM CELL RESPONSE ?**



## Chapter VI

### **AMNIOTIC FLUID STEM CELLS VERSUS BONE MARROW MESENCHYMAL STEM CELLS AS A SOURCE FOR BONE TISSUE ENGINEERING**

*This chapter is based on the following publication:*

Rodrigues MT, Lee SJ, Gomes ME, Reis RL, Atala A, and Yoo J, Amniotic fluid stem cells versus bone marrow mesenchymal stem cells as a source for bone tissue engineering, *submitted*





### AMNIOTIC FLUID STEM CELLS VERSUS BONE MARROW MESENCHYMAL STEM CELLS AS A SOURCE FOR BONE TISSUE ENGINEERING

#### VI.1. Abstract

The ideal or universal cell source for tissue engineering (TE) is yet to be found. The widely studied bone marrow mesenchymal stem cells (BMSCs) have been evidencing important osteogenic characteristics, therefore becoming the gold standard for orthopaedic regeneration strategies. However, novel stem cell sources, for instance, amniotic fluid stem cells (AFSCs) are arising showing important and unique features that might lead to novel successful approach towards bone regeneration.

This study aims to originally compare the osteogenic potential of BMSCs and AFSCS towards bone TE strategies, under distinct culturing environments. The purpose is to analyse the origin-related response of stem cells to different external environments during the osteogenic differentiation process. Thus, the osteogenic differentiation was evaluated both on 2D and 3D, using a culture treated plate, and by means of seeding/culturing the cells onto fiber bonding SPCL scaffolds (a blend of starch and poly-caprolactone), respectively.

BMSCs and AFSCs were successfully differentiated into the osteogenic lineage, and developed mineralized ECM. Nevertheless, cells presented different expression patterns of bone-related markers as well as different timings of differentiation, indicating that both cell origins and the culturing environment have a significant impact in the progression of the osteogenic phenotype in AFSCs and BMSCs.

## VI.2. Introduction

The human body has an endogenous system of regeneration and repair through stem cells, which can be found in almost every living tissue[1-4]. Therefore, stem cells are an obvious choice for regenerative medicine applications, including bone tissue engineering therapies. Nevertheless, the selection of the most appropriate source of stem cells for efficient bone regeneration is still a major issue to be considered in the tissue engineering field[3, 5].

The ideal cell source should combine insignificant donor morbidity or tissue scarcity with no amount limitations, be easy to harvest, isolate and maintain *in vitro*, be available according to patients needs, have no issues of immunogenicity, no diseases transmission risks and be of low cost. So far, different cell sources match some of the parameters in this list, thus directing the applicability of cell sources into more specific strategies, yet always with some limitations.

Among adult stem cells, bone marrow mesenchymal stem cells (BMSCs) are possibly the ones most investigated. Their multipotential to differentiate into different lineages was confirmed by several research groups, including a high potential for bone regeneration strategies[5-8]. Nevertheless, BMSCs harvesting is an invasive and rather painful procedure to the donor. Furthermore, their numbers, proliferation, and differentiation potential decline with age[9, 10]. Some studies suggest that BMSCs are also sensitive to subculturing methodologies, and their stability in long-term *in vitro* culture is controversial[11, 12]. Nevertheless, BMSCs represent a promising cell source for cell-based therapeutics showing great promise in animal studies and some clinical trials[1, 13, 14].

Amniotic fluid derived stem cells (AFSCs) were recently introduced to bone TE [2, 15, 16] whose behavior and characteristics are not so deeply investigated so far. Nevertheless, these cells have demonstrated interesting characteristics, since they derive from embryonic and extra-embryonic tissues during the process of foetal development and growth. In fact, AFSCs have shown to be highly proliferative[12], with high self-renewal capability and have the potential to differentiate into several lineages, including the osteogenic phenotype[2, 17]. AFSCs are easy to obtain, representing an almost unlimited stem cell source with immunosuppressive properties[18] and, whose harvesting procedure does not raise ethical concerns, sometimes associated with human embryonic stem cell research[15, 16]. AFSCs have been also described to be in an intermediate stage between embryonic stem cells and adult stem cells due to their extensive ability for expansion and differentiation into functional cells of the three embryonic germ layers[1, 2], and thus exhibiting important potential in future regenerative strategies.

Few studies[12, 18, 19] established a comparison between human BMSCs and AFSCs to determine how the origin could influence the osteogenic differentiation potential of stem cells.

In mice, mesenchymal stem cells (MSCs) from different origins are known to vary in clonogenic capacity, surface markers and differentiation potential[19]. Studies with human cells indicate that MSCs isolated from fetal tissues are more plastic and grow faster than adult MSCs, while evidencing similar immunophenotypic characteristics and maintaining long and stable telomeres[12].

The culturing environment provided by the substrate/scaffold characteristics, such as the structure and mechanical properties may also deeply affect cell behavior[20, 21]. In this sense, we also propose to evaluate herein human AFSCs and BMSCs in 2D and 3D cultures by seeding and culturing these cells onto tissue culture well plates or onto a fiber bonding mesh scaffold made of a blend of starch and poly  $\epsilon$ -caprolactone (SPCL). SPCL scaffold, obtained by a fiber melt extrusion/fiber bonding process[22] were selected as 3D environment for osteogenic differentiation of both types of cells as these scaffolds have been extensively studied and characterized in the context of bone tissue engineering strategies [23-26].

The main objective of this study was to compare the osteogenic potential of marrow derived mesenchymal stem cells (BMSCs) and amniotic fluid stem cells (AFSCs) aiming at bone TE strategies. We proposed to evaluate osteogenic differentiation of these cells both on 2D and 3D cultures, and to compare the development of the osteogenic phenotype for up to 3 weeks in conditioned osteogenic medium. Furthermore, we selected a well characterized fiber bonding mesh scaffold made of a blend of starch and poly-caprolactone (SPCL) to analyse the osteogenic phenotype of both BMSCs and AFSCs when cultured in a 3D matrix.

Cells in both 2D and 3D conditions were cultured in the presence of osteogenic media for 0, 7, 14 and 21 days and then characterized for cellular viability using a MTS assay while osteogenic phenotypic expression and matrix formation were assessed by immunofluorescence for RunX-2, collagen I and ALP activity, and by EDS and calcium quantification, respectively.

This study may provide important cues of the cell behaviour of AFSCs and BMSCs when differentiating into the osteogenic phenotype and the variations induced by 2D and 3D seeding substrates.

### **VI.3. Materials and Methods**

#### **VI.3.1. Cell culture**

Human BMSCs, purchased from Lonza® (Walkersville, USA), were expanded in basal BMSCs medium composed of  $\alpha$ -MEM (HyClone Laboratories Inc.) supplemented with 10 % ES-FBS (HyClone Laboratories Inc.) and 1 % penicillin/streptavidin solution.

hAFSCs were isolated as previously described[2], and cultured in basic amniotic fluid cell (BAFC) medium composed of  $\alpha$ -MEM (HyClone) with 18 % Chang B (Irvine Scientific) and 1 % Chang C (Irvine Scientific) media as well as 2 % L-glutamine (HyClone Laboratories Inc.) and 15 % ES-FBS.

hBMSCs and hAFSCs were seeded onto tissue culture 6-well plates at passage 5 and passage 24, respectively, at a concentration of 30,000 cells/well. Cells were cultured in the well-plates for 3 days with basal medium, and then, exchanged to osteogenic medium, composed of DMEM (HyClone Laboratories Inc.) supplemented with 10 % FBS (HyClone) and 100 nM dexamethasone (Sigma), 50  $\mu$ M L-ascorbic acid (Sigma) and 10 mM glycerol 2-phosphate disodium salt hydrate (Sigma), for up to 3 weeks (0, 7, 14 and 21 days). Before osteogenic characterization, cells were briefly rinsed in PBS (HyClone Laboratories Inc.) and fixed in 10 % neutral buffered formalin (Surgipath Medical Industries, Inc.).

In order to study the behavior of hBMSCs and hAFSCs in a 3D environment, both type of cells were seeded onto SPCL scaffolds (7 mm x 4 mm cylinders) at a concentration of  $1.2 \times 10^6$  cells/scaffold and cultured in basal medium for 3 days and then in osteogenic media for up to 3 weeks. SPCL scaffold is a blend of starch and polycaprolactone, 30:70 (wt %) (Novamont) produced by fiber bonding technique as previously described[22].

Samples were retrieved after every 7 days in culture to be characterized for cellular viability with Calcein AM and for assessing the presence of osteogenic markers and matrix formation by alkaline phosphatase (ALP), Alizarin Red (AR) stainings as well as the presence of runx-2 and collagen I in the matrix by immunofluorescence. Cell morphology and matrix formation were also assessed by scanning electronic microscopy (SEM) in the 3D environment.

#### **VI.3.2. Calcein AM assay**

AFSCs- and hMSCs-SPCL constructs were rinsed in PBS and incubated in cell culture medium with 3  $\mu$ M Calcein AM (Molecular Probes, Invitrogen) for 30 minutes at 37 °C in a 5 % CO<sub>2</sub>

environment. Then, constructs were rinsed in PBS and fixed in 10 % buffered formalin (Surgipath Medical Industries, Inc.) overnight at 4 °C. AFSCs viability was observed under a confocal microscope (Axiovert 100 M, Zeiss) equipped with argon/He-Ne laser sources. DAPI (Molecular Probes, Invitrogen) was used as a nuclei marker in cells (live or dead).

### **VI.3.3. Alkaline Phosphatase (ALP) staining**

ALP staining was performed in 2D cultures to evaluate the osteogenic differentiation process of hAFSCs and hBMSCs in the tissue culture-well plates. Cells were fixed with 10 % buffered formalin solution overnight at 4 °C and then rinsed, and kept in PBS until incubating the cells in a staining solution of 0.25 % Naphthol AS-MX phosphate alkaline solution (Sigma-Aldrich) and Fast Violet B salt (Sigma) for 30 minutes. Afterwards, to remove excess of non-specific staining, samples were rinsed in PBS and observed under an inverted microscope (Leica, DMI4000B), and images acquired using a camera Q-Imaging (Retiga-2000RV).

### **VI.3.4. Alizarin Red Staining (AR)**

Alizarin Red staining was performed in both 2D and 3D osteogenic constructs after fixing the constructs as described above. For this purpose, a 2 % alizarin red solution (Sigma-Aldrich) was prepared (pH adjusted to 4.1-4.3) and samples stained by immersion for 2 minutes. After image acquisition of the stained cells and cells-scaffold constructs, AR staining was solubilized in cetylpyridinium chloride (Sigma) at pH 7.0 for 15 minutes under mild agitation and calcium-bounded to AR quantified at 562 nm, using a plate reader (SpectraMax MS, Molecular Devices).

### **VI.3.5. Immunofluorescence**

Immunofluorescence analysis was performed in samples retrieved from 2D and 3D conditions in order to assess the presence of bone related proteins, namely RunX-2 and Collagen type I. RunX-2 and Collagen type I (1:100 and 1:20 dilution, respectively), diluted in antibody diluent with background reducing components from Dako, were assessed by a regular immunofluorescence procedure using AlexaFluor 488 or 594 (Molecular Probes, Invitrogen, 1:200 dilution) as a secondary antibody. Protein-block serum free (Dako, Denmark) was used in the blocking step.

### VI.3.6. Scanning electronic microscopy (SEM)

Cell seeded scaffolds (3D condition) were observed by scanning electron microscopy (Hitacho S-2600N, Hitachi Science Systems, Ltd) to assess cell morphology, proliferation as well as the presence/absence of a mineralized ECM matrix produced by either AFSCs or BMSCs. SEM was performed in fixed constructs, after dehydrating the samples in a series of ethanol concentrations followed by drying in a critical point drying equipment (EMS850X, Electron Microscopy Sciences), and gold sputtered (Hummer 6.2 sputtering system, Anatech Ltd).

## VI.4. Results and Discussion

### VI.4.1. Osteogenic differentiation of AFSCs and BMSCs in a 2D culture environment

Immunofluorescence imaging (Calcein and DAPI staining) showed that both AFSCs and BMSCs attached and proliferated for up to 3 weeks in 2D cultures (Figure VI.4.1).

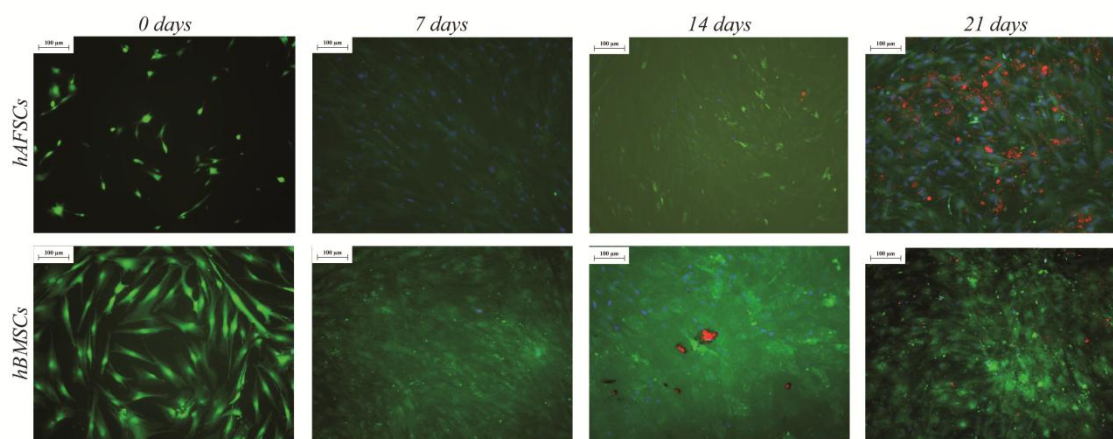


**Figure VI.4.1** – Viability assay (green) and Alizarin Red (red) staining of hAFSCs and hBMSCs cultured in 2D environment for 0, 7, 14 or 21 days in osteogenic medium.

The same pictures suggest an increase in AFSCs viability for 2 weeks in osteogenic medium while BMSCs maintained high viability levels during the 3 weeks of experiment (Figure VI.4.1).

Alizarin red staining was detected in both cell types after 14 days in culture (Figure VI.4.1), which tends to become more intense in hAFSCs by the end of week 3 in osteogenic medium. The increase in staining intensity is not so evident for hBMSCs for the same period of time.

Concerning the ALP staining that is associated to ECM maturation, hBMSCs cells express the highest ALP levels of the experiment after 2 weeks in osteogenic culture, indicating an active phase for the development of ECM. In contrast, AFSCs do not express significant amounts of ALP during the 2D experimental study (Figure VI.4.2).

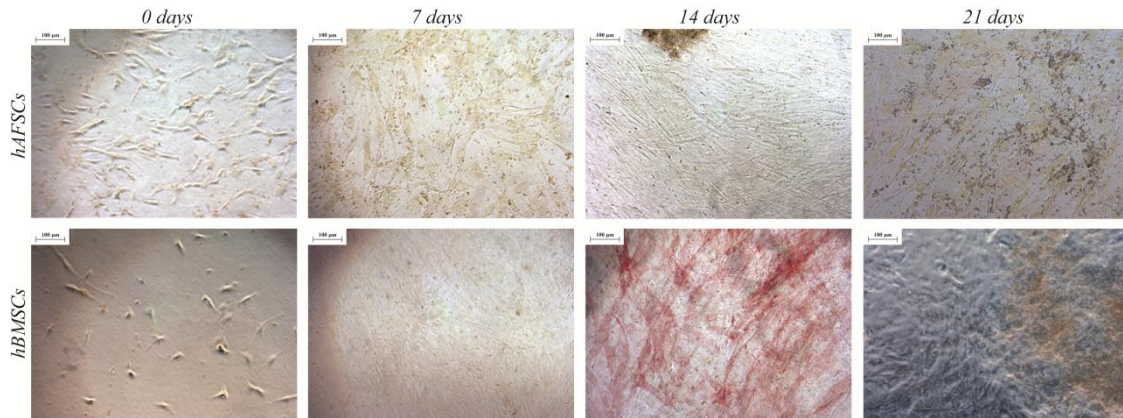


**Figure VI.4.2-** ALP staining of hAFSCs and hBMSCs cultured in 2D environment for 0, 7, 14 or 21 days in osteogenic medium.

RunX-2 is an important transcription factor (TF) involved in the osteogenic development which was also considered for the characterization of the osteogenic differentiation of AFSCs and BMSCs. In cell culture plates, RunX-2 is expressed by AFSCs and BMSCs at day 0. After 7 days, a weak signal is also detected in osteogenic culture, being more evident in BMSCs. After 14 days in culture, the presence of RunX-2 is hardly registered (data not showed).

Immunofluorescence for collagen I, an important protein in bone ECM, was not detected either in AFSCs or BMSCs (data not showed) for up to 3 weeks in 2D cultures.

Calcium levels were quantified using a microplate reader after solving alizarin red staining (Figure VI.4.3).

Up to week 2, calcium deposition by both cell types followed a similar pattern, exhibiting relatively low values during the first 14 days in osteogenic medium. After 21 days of culturing, the calcium amounts deposited by AFSCs increased dramatically (Figure VI.4.3), showing that AFSCs produce a higher amount of mineralized matrix in the 2D culturing environment when compared to hBMSCs.

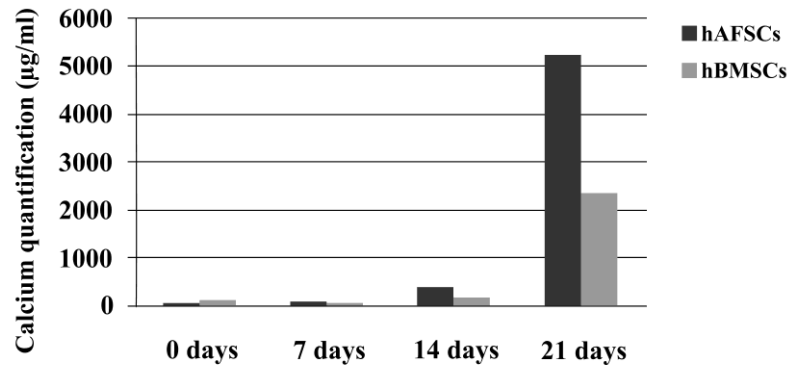


**Figure VI.4.3** – Calcium quantification ( $\mu\text{g/ml/well}$ ) of AFSCs and BMSCs in 2D cultures in osteogenic medium for 0, 7, 14 or 21 days.

#### VI.4.2. Osteogenic differentiation of hAFSCs and hBMSCs seeded on SPCL scaffolds (3D environment)

According to immunofluorescence observations, both stem cell types kept high viability when cultured on SPCL scaffolds (3D cultures) for up to 3 weeks (Figure VI.4.4).

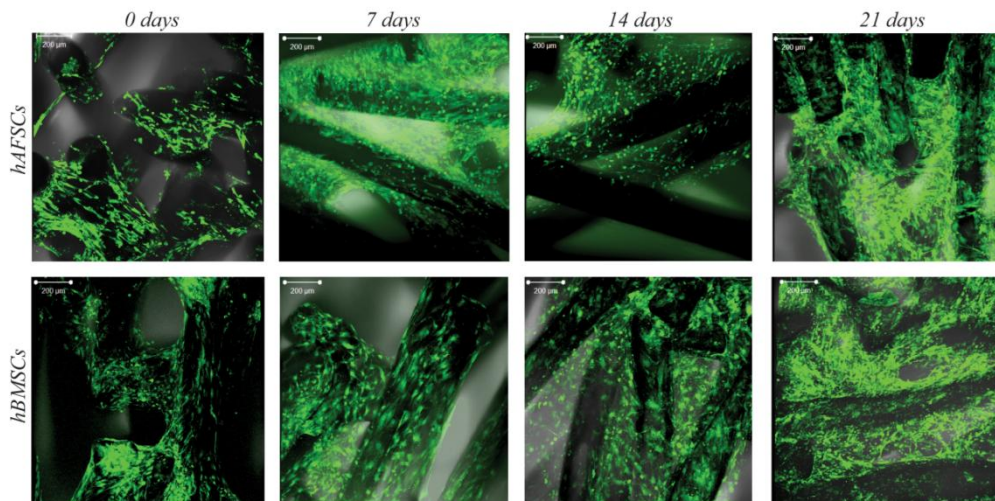


**Figure VI.4.4** – Viability assay of AFSCs and BMSCs seeded onto SPCL scaffolds and cultured in osteogenic medium for 0, 7, 14 or 21 days.

SEM micrographs revealed a good AFSCs and BMSCs proliferation and distribution on the SPCL scaffolds, clearly evidenced by the thick layer of cells throughout the entire scaffold (Figure VI.4.5). The same images suggest the presence of extracellular matrix in BMSCs-SPCL



constructs after 2 weeks in culture as well as some mineralization nodules (white dots in the SEM images), which increased in number after 3 weeks in osteogenic supplemented medium. In AFSCs constructs these nodules are only observed at week 3.

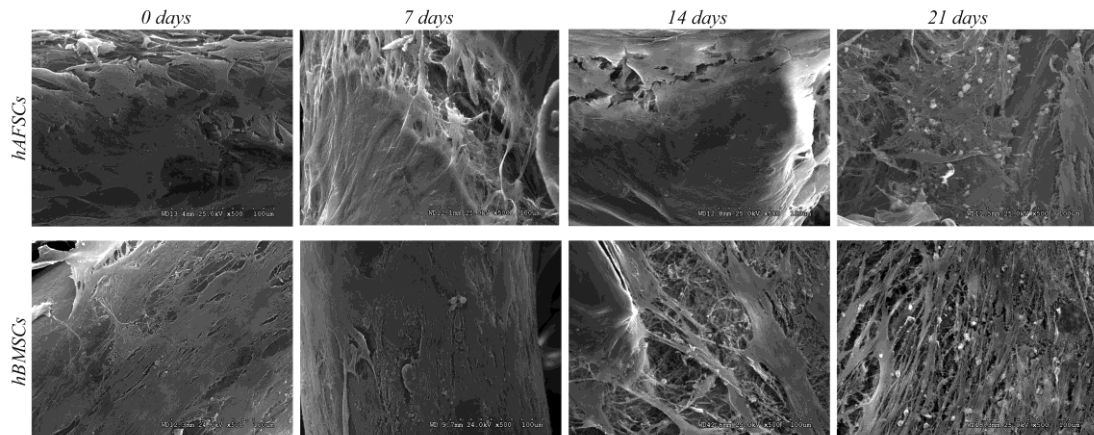


**Figure VI.4.5** - Scanning electron microscopy of AFSCs and BMSCs seeded onto SPCL scaffolds in osteogenic culture for 0, 7, 14 or 21 days.

The formation of mineralization nodules was also evaluated in BMSCs- and AFSCs-SPCL constructs by Alizarin Red staining (Figure VI.4.6) and in order to determine the presence of CaP in these aggregates.

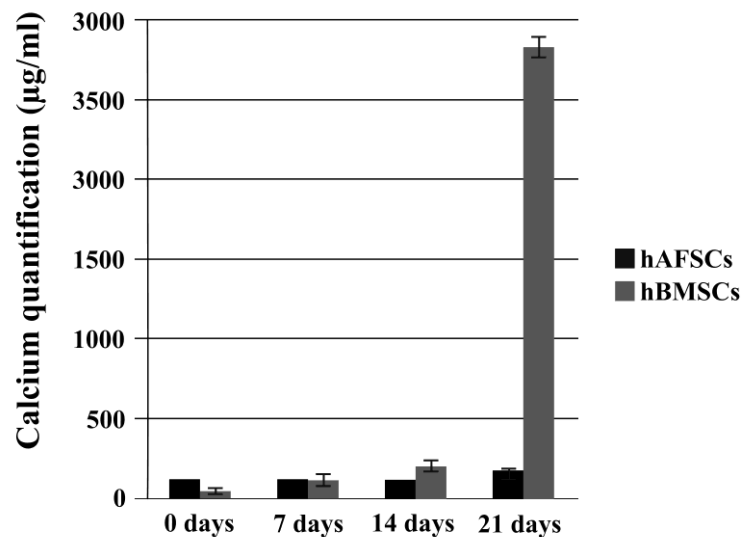


**Figure VI.4.6** - Calcium quantification ( $\mu\text{g/ml/construct}$ ) of AFSCs- and BMSCs-SPCL constructs in osteogenic medium for 0, 7, 14 or 21 days.

Concerning Alizarin Red staining, AFSCs required more calcium in the first days for metabolic processes, but this tendency changes after 2 weeks in osteogenic medium and by 3 weeks in culture, the calcium concentration produced by BMSCs in SPCL scaffolds is dramatically higher than in AFSCs-SPCL constructs (Figure VI.4.6).

SEM data are in agreement with results obtained from the calcium quantification assay in AFSCs- and BMSCs-SPCL constructs, showing that BMSCs are faster in achieving a calcified matrix in 3D fiber bonding SPCL scaffolds.

In SPCL scaffolds, BMSCs and AFSCs expressed similar RunX2 for the first week of osteogenic differentiation (Figure VI.4.7).

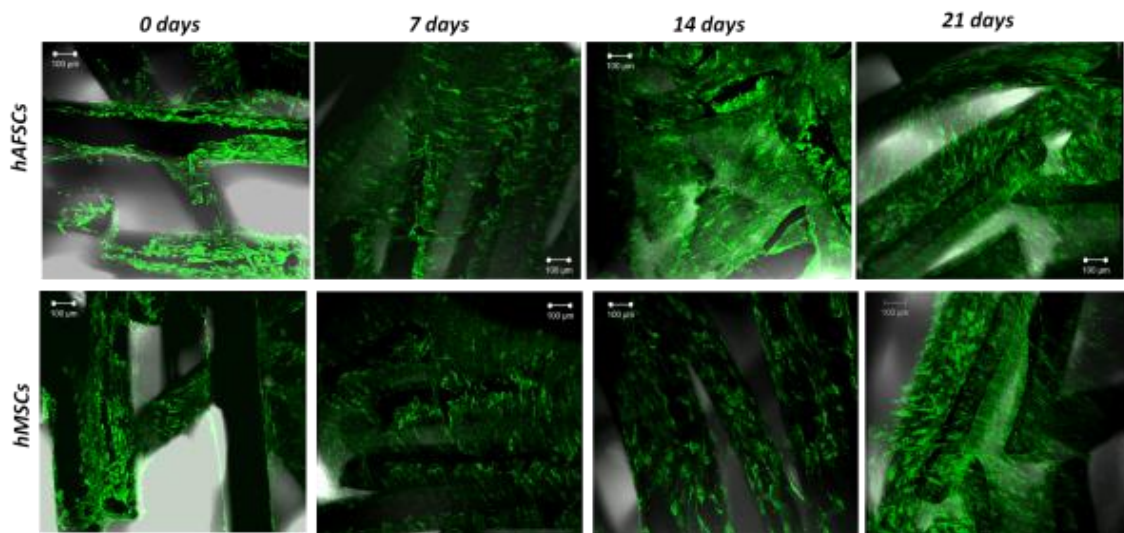


**Figure VI.4.7** – Immunofluorescence of RunX2 expression in AFSCs- and BMSCs-SPCL constructs in osteogenic medium for 0, 7, 14 or 21 days.

The intensity decreases from day 0 to day 7, increasing again after 2 weeks in osteogenic medium, especially for AFSCs. By the end of the third week, RunX2 expression is kept high with a bright green intensity, evidencing that the osteogenic process continues in the 3D constructs throughout a 3 week-time line and even in the presence of mineralized matrix.

Collagen I was strongly stained in cells seeded onto SPCL scaffolds during the experimental time (Figure VI.4.8). At day 0, an undifferentiated stage, similar detection levels were observed for AFSCs and BMSCs. After 7 and 14 days of culture in osteogenic media, a more intense fluorescence is observed in AFSCs constructs that tends to decrease on week 3, while in BMSCs-SPCL scaffolds, collagen I showed an increment in fluorescence intensity.

Furthermore, collagen fibers seem to be somehow oriented in some directions over the SPCL fibers, forming a dense ECM.

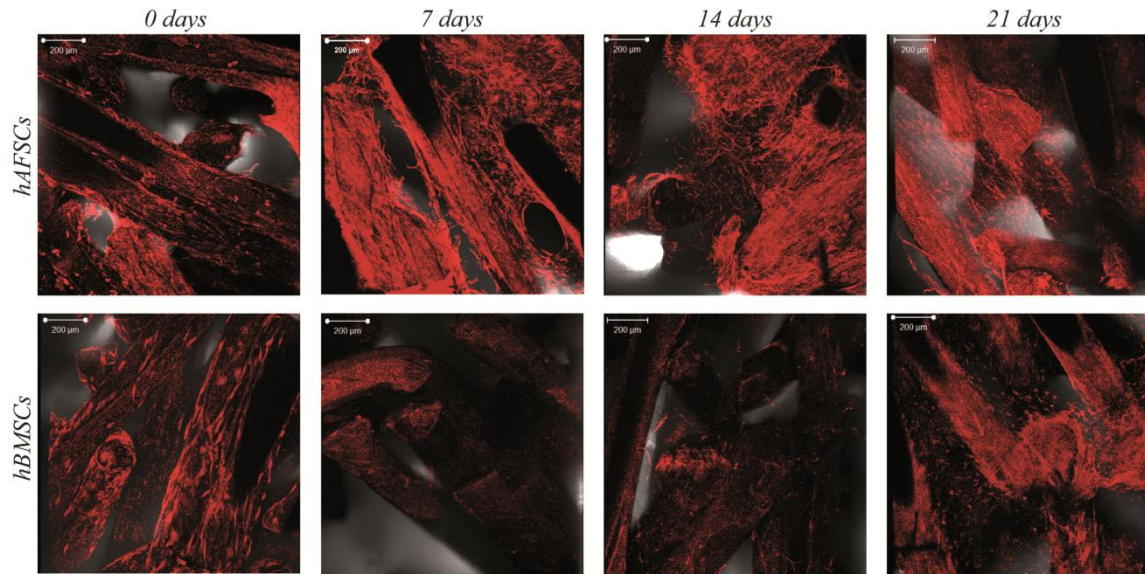


**Figure VI.4.8** – Immunofluorescence of Collagen I expression in AFSCs- and BMSCs-SPCL constructs in osteogenic medium for 0, 7, 14 or 21 days.

## VI.5. Discussion

In a 2D culturing environment (tissue culture plates), both AFSCs and BMSCs were able to differentiate into the osteogenic lineage and produce mineralized ECM, even in the absence of collagen I and RunX2 expression. Although collagen I accounts for the majority of the organic matrix of bone tissues, collagen I cannot initiate tissue mineralization since is not responsible for nucleation and post-nucleation growth of apatite crystallites[27]. Osteogenic cells can produce a layer of non-collagenous matrix *in vitro*, at the surface of nonbiological substrata, prior to a calcium and phosphorus rich ECM. This layer is described to be similar to the cement line *in vivo*[28]. In summary, despite some differences found between cells, AFSCs showed higher proliferation rates and enhanced mineralization of the ECM in 2D cultures when compared to BMSCs. However, the mineralization seems to compromise the viability of AFSCs in 2D cultures.

In a 3D environment, i.e., when cells are cultured onto the SPCL scaffolds, the mineralization observed at 14 days and 21 days for BMSCs and AFSCs, respectively, seems not to influence cell viability. AFSCs and BMSCs also showed changes in the expression of bone related markers from 2D to 3D cultures, indicating that culture environments play an important role in cellular response during the osteogenic differentiation process. Stem cells

have been described[20, 29, 30] to be quite sensitive to microenvironments and to respond to topographical patterns suggesting a physical contribution to the cellular expansion and differentiation process. Some osteoblast responses seem also to be rather substrate-dependent[31], evidencing the importance of culture surface in modulating cell proliferation, matrix and inflammatory factor expression.

Unlike the results registered for 2D cultures, in 3D scaffolds collagen I is present before the mineralization occurs in both AFSCs and BMSCs-SPCL scaffolds, providing the framework and spatial constraint for ordered crystal deposition and thus assisting formation of calcium phosphate nodules. The collagen fibers covering the scaffolds seem to be aligned, showing some degree of organization, which may be important in the process, since a natural regeneration typically involves an organized distribution of ECM rather than a random dispersed matrix, which, in the *in vivo* scenario, is associated to scar or fibrotic tissue formation.

Despite similar viability and RunX2 levels during the experimental study, as well as collagen I levels after 21 days in osteo culture, BMSCs and AFSCs showed a different behavior in terms of mineralization; not only mineralization occurs latter in AFSCs constructs but BMSCs also produced more mineralized matrix, when seeded onto SPCL scaffolds.

Besides culture substrate-ECM interactions, inductive factors also influence the programming of MSCs by matrix[20]. Multiple *in vitro* and *in vivo* studies confirmed that bone-specific growth factors exert autocrine and paracrine effects on the proliferation, differentiation, and maturation of osteoprogenitor cells. In this study, the participation of growth factors in the culture medium is quite evident, due to their pivotal role in achieving the osteogenic differentiation process. The continuous expression of RunX-2 in constructs also indicates that osteoblast differentiation process is likely to continue in time, reinforcing the ECM production and maturation.

In both environments, AFSCs and BMSCs were able to proliferate and differentiate into the osteogenic phenotype with the production of a mineralized matrix. The final goal was achieved although differences in osteo markers expression, such as ALP activity, RunX2 and collagen I were clearly observed. These differences may be related to different contribution from the external environment, as well as the influence of stem cell source in cellular responses towards the osteogenic differentiation process, which directly affects ECM production and composition.

AFSCs higher proliferative capacity and their ability to maintain their pluripotency at higher passages could be exploitable as a ready available source for large numbers of osteo

progenitor cells with applicability for allogeneous strategies, a broader spectrum than BMSCs, which may be limited to autologous interventions and to donor's age. Despite the limitations, BMSCs represent a promising cell source for cell-based therapeutics, especially in orthopaedics, since BMSCs are predisposed in a certain extent to follow the osteogenic phenotype due to their natural commitment to the mesenchymal lineage. The hBMSCs used in this study were at passage 5, as hBMSC gene expression profiles were demonstrated[32] to remain stable *in vitro* between passage 3 and passage 6, thus validating results obtained in this study from BMSCs. AFSCs share embryonic stem cells and adult stem cells characteristics, and described to be genetically and phenotypically stable pluripotent cells[11, 18]. Furthermore, these cells can be extensively expanded, while keeping long telomeres and a normal karyotype to over 250 population doublings, and differentiated into functional cells[2].

The origin of stem cells may also influence cellular response towards external signals, causing changes in ECM production and composition. Studies describe stem cells differences in proliferation[15] and differentiation[3, 15] potential, survival capacity[15], cytokines expression[16] and immunomodulatory properties[19], depending which tissues cells were obtained from. This is also observed for lineage specific markers such as ALP activity and RunX-2 expression[15]. Our data follows this trend, as cells from bone marrow and amniotic fluid derived stem cells act differently to different substrate matrices, affecting the timing of differentiation and bone related protein synthesis.

Animal studies are envisioned to understand the full potential and behaviour of both types of cells while observing the influence of cell source and 3D scaffold when implanted *in vivo* in a pre-clinical situation.

## VI.6. Conclusions

The application of stem cells might be an adequate alternative for translational practice, since these cells can be used to enhance the body's own regenerative potential or developing new therapies.

The present data showed cellular proliferation of AFSCs and BMSCs, and subsequent colonization of the substrate. In fact, in both 2D and 3D cultures, the surface was covered with adherent cells, forming a network that followed the osteogenic differentiation process for up to 3 weeks in inductive osteo medium. Osteogenic specific markers were detected and mineralized matrix was formed in 2D as well as 3D substrates seeded with AFSCs and BMSCs.

Interestingly, cells from different origins seem to express different bone-related markers at different end points, which may correlate to cell origin and to substrate properties. The interplay of ECM molecules, cells and culture surface results in a dynamic and balanced system with different possible outcomes.

In the adaptative process of osteogenic differentiation, the cell source origin seems to have an important role in selecting pathways involved in ECM synthesis, resulting in different cell responses to time frames, protein synthesis and culture substrate variations. Thus, AFSCs might be an interesting alternative to BMSCs for bone tissue engineering applications.

## **VI.7. References**

1. Bajada S, Mazakova I, Richardson JB, Ashammakhi N: Updates on stem cells and their applications in regenerative medicine. *J Tissue Eng Regen Med* 2008, 2: 169-183.
2. De Coppi P, Bartsch G, Jr., Siddiqui MM, Xu T, Santos CC, Perin L, Mostoslavsky G, Serre AC, Snyder EY, Yoo JJ, et al.: Isolation of amniotic stem cell lines with potential for therapy. *Nat Biotechnol* 2007, 25: 100-106.
3. Peng L, Jia Z, Yin X, Zhang X, Liu Y, Chen P, Ma K, Zhou C: Comparative analysis of mesenchymal stem cells from bone marrow, cartilage, and adipose tissue. *Stem Cells Dev* 2008, 17: 761-773.
4. Ringe J, Leinhase I, Stich S, Loch A, Neumann K, Haisch A, Haupl T, Manz R, Kaps C, Sittinger M: Human mastoid periosteum-derived stem cells: promising candidates for skeletal tissue engineering. *J Tissue Eng Regen Med* 2008, 2: 136-146.
5. Pittenger MF, Mackay AM, Beck SC, Jaiswal RK, Douglas R, Mosca JD, Moorman MA, Simonetti DW, Craig S, Marshak DR: Multilineage potential of adult human mesenchymal stem cells. *Science* 1999, 284: 143-147.
6. Krampera M, Pizzolo G, Aprili G, Franchini M: Mesenchymal stem cells for bone, cartilage, tendon and skeletal muscle repair. *Bone* 2006, 39: 678-683.
7. Mauney JR, Volloch V, Kaplan DL: Role of adult mesenchymal stem cells in bone tissue engineering applications: current status and future prospects. *Tissue Eng* 2005, 11: 787-802.
8. Tuan RS, Boland G, Tuli R: Adult mesenchymal stem cells and cell-based tissue engineering. *Arthritis Res Ther* 2003, 5: 32-45.
9. Stolzing A, Jones E, McGonagle D, Scutt A: Age-related changes in human bone marrow-derived mesenchymal stem cells: consequences for cell therapies. *Mech Ageing Dev* 2008, 129: 163-173.

10. Kretlow JD, Jin YQ, Liu W, Zhang WJ, Hong TH, Zhou G, Baggett LS, Mikos AG, Cao Y: Donor age and cell passage affects differentiation potential of murine bone marrow-derived stem cells. *BMC Cell Biol* 2008, 9: 60.
11. Rosland GV, Svendsen A, Torsvik A, Sobala E, McCormack E, Immervoll H, Mysliwicz J, Tonn JC, Goldbrunner R, Lonning PE, et al.: Long-term cultures of bone marrow-derived human mesenchymal stem cells frequently undergo spontaneous malignant transformation. *Cancer Res* 2009, 69: 5331-5339.
12. Poloni A, Maurizi G, Babini L, Serrani F, Berardinelli E, Mancini S, Costantini B, Discepoli G, Leoni P: Human Mesenchymal Stem Cells from chorionic villi and amniotic fluid are not susceptible to transformation after extensive in vitro expansion. *Cell Transplant* 2010.
13. Wakitani S, Mitsuoka T, Nakamura N, Toritsuka Y, Nakamura Y, Horibe S: Autologous bone marrow stromal cell transplantation for repair of full-thickness articular cartilage defects in human patellae: two case reports. *Cell Transplant* 2004, 13: 595-600.
14. Kuroda R, Ishida K, Matsumoto T, Akisue T, Fujioka H, Mizuno K, Ohgushi H, Wakitani S, Kurosaka M: Treatment of a full-thickness articular cartilage defect in the femoral condyle of an athlete with autologous bone-marrow stromal cells. *Osteoarthritis Cartilage* 2007, 15: 226-231.
15. Prusa AR, Marton E, Rosner M, Bernaschek G, Hengstschlager M: Oct-4-expressing cells in human amniotic fluid: a new source for stem cell research? *Hum Reprod* 2003, 18: 1489-1493.
16. Fauza D: Amniotic fluid and placental stem cells. *Best Pract Res Clin Obstet Gynaecol* 2004, 18: 877-891.
17. Kim J, Lee Y, Kim H, Hwang KJ, Kwon HC, Kim SK, Cho DJ, Kang SG, You J: Human amniotic fluid-derived stem cells have characteristics of multipotent stem cells. *Cell Prolif* 2007, 40: 75-90.
18. Sessarego N, Parodi A, Podesta M, Benvenuto F, Mogni M, Raviolo V, Lituania M, Kunkl A, Ferlazzo G, Bricarelli FD, et al.: Multipotent mesenchymal stromal cells from amniotic fluid: solid perspectives for clinical application. *Haematologica* 2008, 93: 339-346.
19. Nadri S, Soleimani M: Comparative analysis of mesenchymal stromal cells from murine bone marrow and amniotic fluid. *Cytotherapy* 2007, 9: 729-737.
20. Discher DE, Mooney DJ, Zandstra PW: Growth factors, matrices, and forces combine and control stem cells. *Science* 2009, 324: 1673-1677.
21. Khatiwala CB, Kim PD, Peyton SR, Putnam AJ: ECM compliance regulates osteogenesis by influencing MAPK signaling downstream of RhoA and ROCK. *J Bone Miner Res* 2009, 24: 886-898.
22. Gomes ME, Azevedo HS, Moreira AR, Ella V, Kellomaki M, Reis RL: Starch-poly(epsilon-caprolactone) and starch-poly(lactic acid) fibre-mesh scaffolds for bone tissue engineering applications: structure, mechanical properties and degradation behaviour. *J Tissue Eng Regen Med* 2008, 2: 243-252.

23. Gomes ME, Bossano CM, Johnston CM, Reis RL, Mikos AG: In vitro localization of bone growth factors in constructs of biodegradable scaffolds seeded with marrow stromal cells and cultured in a flow perfusion bioreactor. *Tissue Eng* 2006, 12: 177-188.
24. Gomes ME, Holtorf HL, Reis RL, Mikos AG: Influence of the porosity of starch-based fiber mesh scaffolds on the proliferation and osteogenic differentiation of bone marrow stromal cells cultured in a flow perfusion bioreactor. *Tissue Eng* 2006, 12: 801-809.
25. Rodrigues MT, Gomes ME, Viegas CA, Azevedo JT, Dias IR, Guzón F, Reis RL: Tissue Engineered Constructs based on SPCL Scaffolds Cultured with Goat Marrow Cells: Functionality in Femoral Defects. *J Tissue Eng Regen Med* 2011, 5: 41-49.
26. Santos MI, Fuchs S, Gomes ME, Unger RE, Reis RL, Kirkpatrick CJ: Response of micro- and macrovascular endothelial cells to starch-based fiber meshes for bone tissue engineering. *Biomaterials* 2007, 28: 240-248.
27. Gu LS, Kim J, Kim YK, Liu Y, Dickens SH, Pashley DH, Ling JQ, Tay FR: A chemical phosphorylation-inspired design for Type I collagen biomimetic remineralization. *Dent Mater* 2010, 26: 1077-1089.
28. Davies JE: In vitro modeling of the bone/implant interface. *Anat Rec* 1996, 245: 426-445.
29. Park JY, Takayama S, Lee SH: Regulating microenvironmental stimuli for stem cells and cancer cells using microsystems. *Integr Biol (Camb)* 2: 229-240.
30. Choi CK, Breckenridge MT, Chen CS: Engineered materials and the cellular microenvironment: a strengthening interface between cell biology and bioengineering. *Trends Cell Biol* 2010, 20: 705-714.
31. Tonnarelli B, Manferdini C, Piacentini A, Codeluppi K, Zini N, Ghisu S, Facchini A, Lisignoli G: Surface-dependent modulation of proliferation, bone matrix molecules, and inflammatory factors in human osteoblasts. *J Biomed Mater Res A* 2009, 89: 687-696.
32. Tsai MS, Hwang SM, Chen KD, Lee YS, Hsu LW, Chang YJ, Wang CN, Peng HH, Chang YL, Chao AS, et al.: Functional network analysis of the transcriptomes of mesenchymal stem cells derived from amniotic fluid, amniotic membrane, cord blood, and bone marrow. *Stem Cells* 2007, 25: 2511-2523.



**SECTION V**

***IN VIVO* STUDIES**



## Chapter VII

### **TISSUE ENGINEERED CONSTRUCTS BASED ON SPCL SCAFFOLDS CULTURED WITH GOAT MARROW CELLS: FUNCTIONALITY IN FEMORAL DEFECTS**

*This chapter is based on the following publication:*

Rodrigues MT, Gomes ME, Viegas CAA, Azevedo JT, Dias IR, Guzón F, and Reis RL, Tissue Engineered Constructs based on SPCL Scaffolds Cultured with Goat Marrow Cells: Functionality in Femoral Defects. *Journal of Tissue Engineering and Regenerative Medicine*, *Journal of Tissue Engineering and Regenerative Medicine*, 5: 41-49 (2011).



TISSUE ENGINEERED CONSTRUCTS BASED ON SPCL SCAFFOLDS  
CULTURED WITH GOAT MARROW CELLS: FUNCTIONALITY IN FEMORAL DEFECTS

**VII.1. Abstract**

This study aims to assess *in vivo* performance of cell-scaffold constructs of goat marrow mesenchymal stromal cells (gBMSCs) and SPCL (a blend of starch with polycaprolactone) fiber mesh scaffolds at different stages of development, using an autologous model. gBMSCs, from iliac crests, were seeded onto SPCL scaffolds and *in vitro* cultured for 1 or 7 days in osteogenic media. After 1 and 7 days, constructs were characterized for proliferation and initial osteoblastic expression by alkaline phosphatase (ALP) activity. Scanning electron microscopy analysis was performed to investigate cellular morphology and adhesion to SPCL scaffolds.

Non-critical defects (6 mm diameter, 3 mm depth) were drilled in posterior femurs of 4 adult goats, from which bone marrow and serum were previously collected. Drill defects alone and defects filled with scaffolds without cells were used as controls. After implantation, intravital fluorescence markers: xylene orange, calcein green and tetracycline were injected subcutaneously after 2, 4 and 6 weeks, respectively for bone formation and mineralization monitoring. Subsequently, samples were stained with Lévai Laczkó for bone formation and histomorphometric analysis.

gBMSCs adhered and proliferated on SPCL scaffolds and an initial differentiation into pre-osteoblasts was detected by an increasing level of ALP activity with the culturing time. *In vivo* experiments indicated that bone neof ormation occurred in all femoral defects.

Results obtained provided important information about the performance of gBMSC-SPCL constructs in an orthotopic goat model that enable to design future studies to investigate *in vivo* functionality of gBMSC-SPCL constructs in more complex models, namely critical sized defects and evaluate the influence of *in vitro* cultured autologous cells in the healing and bone regenerative process.

## VII.2. Introduction

Skeletal regeneration is initiated by a traumatic episode involving bone damage that often includes the periosteum, bone marrow spaces, and surrounding soft tissues. Trauma, such as fracture or surgical cutting and drilling, causes a physical disruption of the mineralized tissue matrix, death of many cell types, and interruption of the local blood supply. A key stage in bone regeneration is the differentiation of pluripotential mesenchymal cells from the initial granuloma containing several cellular types, towards cartilage, fibrous cartilage, fibrous tissue or bone[1].

Bone marrow mesenchymal cells (BMCs) have been widely used in studies involving TE strategies for bone and cartilage as they provide a potential autologous source of cells[2-5] that are able to differentiate into chondrogenic and osteogenic lineages in the presence of specific differentiation supplements such as transforming growth factor-beta and dexamethasone, respectively[6].

Though BMCs are abundant in skeletal tissues, damaged bone may fail to heal spontaneously and, in most cases, the use of marrow cells alone is not ideal to accomplish the necessary requirements for the repair and or replacement of injured tissues. In order to overcome the limitations of current treatments, the TE field proposes the use of bioactive or inductive factors as well as a scaffold structure to support and complement the role of reparative cells (differentiated or non-differentiated) when implanted on injured or dysfunctional areas.

The selection of a scaffold material for bone TE purposes is therefore of extreme significance[7]. Scaffolds must be biocompatible, biodegradable and, simultaneously, promote the easy diffusion of nutrients and cellular waste products as well as present suitable mechanical properties for cell support and new tissue ingrowth. Furthermore, the scaffold must possess adequate porosity, good interconnectivity and a degradation rate[8] adapted to the time required for tissue regeneration.

Several biodegradable polymers have been proposed to obtain three-dimensional scaffolds for bone TE, including a new range of natural origin polymers based on starch[8-10]. Starch-based polymers, such as starch-polycaprolactone blends (SPCL), are degradable and biocompatible polymers with distinct structural forms which had shown to be suitable for bone TE applications in several previous studies[11-15].

The seeding and extended *in vitro* culturing of cells within a biodegradable scaffold before implantation is a widespread TE approach. Some studies also report the importance of cell *in*

*in vitro* pre-culture period onto scaffolds as it may influence the osteogenic potential of bone marrow cells[16]. During the *in vitro* culturing, seeded cells are expected to proliferate and secrete growth factors and matrix proteins that possibly will stimulate other cells to accelerate or recover and, in more dramatic situations, to stimulate the natural regenerative functionality when transferred to the *in vivo* environment.

Ultimately and despite the relevance of achieved results from *in vitro* studies, the use of animal models is an essential step to evaluate TE constructs prior to their clinical application. Different animal models, such as rat, rabbit, dog, goat, sheep or monkey have been projected with the purpose of fairly accurate human model requests[17] and guide potential clinical applications.

In the last few years, goats are becoming increasingly popular as a valid animal subject in this research field. In fact, due to its nature of a higher level vertebrate and the non pet status when compared to dogs, goats play a significant role in the orthopaedics field as a feasible model for orthotopic applications. In addition, goats not only have metabolic and bone remodelling rates similar to that of humans but also comparable sequence of events in bone graft incorporation and healing capacities[18], which explains the fact that this model has been frequently used in studies of bone formation and regeneration[19-21], biocompatibility[10], and osteochondral[22, 23] regeneration.

Cell based strategies sustained by a support material have been applied to generate ectopic or orthotopic bone[24-27]. Although the latter presents a major potential for skeletal regeneration procedures, most of the *in vivo* studies are conducted using an ectopic approach and/or performed in small animal models, such as mice or rats[14, 26, 28-31]. Although non-critical sized defects are usually evaluated in ectopic models, orthotopic location provides a more accurate idea of the influence or local effects of implanted cells or cell-scaffold constructs where they were initially designed to be functional.

Autologous approaches have also been considered in recent studies[19, 21, 23] avoiding immune complex problems that interfere with the regenerative process as well as with the patient follow up.

The present work describes the assessment of the *in vivo* osteogenic ability of cell-scaffold constructs based on seeding marrow mesenchymal stromal cells onto SPCL fiber mesh scaffolds and *in vitro* cultured during different periods of time (using an autologous goat model). As mentioned before, these scaffolds have demonstrated a very good *in vitro* functionality in several studies performed by our group. Therefore, the aim of this work is to obtain the first data concerning the *in vivo* functionality of SPCL scaffolds and gBMSCs

constructs, in new bone formation of a orthotopic non critical defect in order to better understand the behaviour of cell-scaffold constructs implanted in femurs and to design future *in vivo* studies to be performed in the critical size defect model, which will be the ultimate applications for such TE strategies.

### **VII.3. Materials and Methods**

#### **VII.3.1. Production of SPCL scaffolds**

The polymer scaffolds used in this study are based on a blend of corn starch and  $\epsilon$ -polycaprolactone) (SPCL, 30/70 % wt) and were produced by a fiber bonding method into mesh structures with a porosity of around 75 % and cut into discs (6 mm diameter, 2 mm height) as described previously[12, 13]. All samples were sterilized using ethylene oxide and, prior to cell seeding, the scaffolds were immersed in 20 mL of serum free medium in 50 mL tubes for 30 minutes.

#### **VII.3.2. gBMSCs harvesting**

In order to harvest the gBMSCs, the animals were placed under general anaesthesia and iliac regions were shaved and disinfected. Animals were submitted to a preanesthetic medication with acepromazine maleate (5 mg EV, Calmivet®, Vetóquinol, France) and placed under general anaesthesia by induction with thiopenthal sodium (20-25 mg/Kg EV, Pentothal® sodium, Abbott Labs, USA), maintained by inhalation of a mixture of 1.5 % isoflurane (IsoFlo®, Abbott Labs, USA) and oxygen for a maximum of 30 minutes.

From each iliac crest of the goats, 10 mL samples of bone marrow aspirate were obtained, using a bone marrow aspiration needle (Inter.V, Medical Device Technologies, Inc.) and a 10 mL syringe, containing 1 mL heparin (5,000 U.I., Heparin sodium, B. Braun Medical, Inc.) to avoid marrow coagulation. The content of each syringe was then transferred into sterile 50 mL tubes and mixed with 30 mL of RPMI-1640 culture medium (Sigma-Aldrich), containing 1 % penicillin/streptomycin (Gibco) and an additional 1 mL of heparin (5,000 U.I.). Afterwards, gBMSCs were centrifuged for 10 minutes at 1200 rpm and a dense cellular pellet was collected and cultured in 75 cm<sup>2</sup> flasks (Corning) using basic culture medium – DMEM (Dulbecco's Modified Eagle's Medium) (Sigma-Aldrich) supplemented with 10 % of autologous serum



isolated from goat peripheral blood and 1 % antibiotic/antimicrobial solution (A/B, Invitrogen). Four days after the harvesting procedure, the medium containing non-adherent cells was removed and the adherent cells were rinsed with a sterile phosphate buffered saline (PBS, Sigma) solution and fresh medium was added. Cells were expanded in basic culture medium until about 80 % of confluence before being seeded onto SPCL scaffolds at 3 Pa.

During this study, every 3 weeks, goat peripheral blood samples were collected from jugular vein of each animal, in order to obtain autologous serum, and collected into serum tubes without anticoagulant (Sarstedt – Monovette® - Serum Gel S). Thirty minutes after collection, blood samples were centrifuged at 3,000 rpm for 10 minutes. Harvested sera was immediately stored in appropriate tubes and preserved at -20 °C until usage.

### **VII.3.3. *In vitro* cell seeding and culture**

In order to cell seed the scaffolds, gBMSCs cells were thawed and expanded until 90 % confluence. Afterwards, cells were enzymatically lifted with 0.05 % trypsin-EDTA (Invitrogen) and at 2 Pa, a cell suspension was prepared (2,500,000 cells/mL) and seeded onto the SPCL porous scaffolds in a drop-wise manner, at a cellular density of 500,000 cells per scaffold and using seeding chambers in order to improve cell seeding efficiency by avoiding cellular dispersion.

After *in vitro* seeding, cell-scaffold constructs were cultured in non-adherent 12-well plates (Costar, Becton Dickinson), to avoid cellular adhesion to the bottom of the plates, and using alpha-MEM (Minimal Essential Medium Eagle alpha modification, Sigma-Aldrich), autologous sera (10 %), A/B (1 %) and osteogenic supplements, namely, dexamethasone ( $10^{-8}$  M) (Sigma-Aldrich), ascorbic acid (50 µg/mL) (Sigma), and β-glycerophosphate (10 mM) (Sigma) for 1 and 7 days prior to implantation. An *in vitro* control of the experiment was kept, consisting of cell-scaffold constructs seeded and cultured under the same conditions and for the same periods of time. Autologous culture medium was changed twice a week in all cell cultures.

### **VII.3.4. *In vitro* characterization of cells-scaffold constructs**

Samples were collected on day 1 and day 7 after seeding for the assessment of proliferation by DNA quantification and initial osteogenic differentiation studies by ALP activity analysis. For these purposes, samples removed from culture were rinsed twice in a PBS solution and transferred into 1.5 mL microtubes containing 1 mL of ultra-pure water. Then, gBMSC-SPCL

constructs were incubated for 1 hour at 37 °C in a water-bath and stored in a -80 °C freezer, promoting a thermal shock variation and thus inducing cell lysis, until testing. Before assessing DNA and ALP levels, constructs were thawed and sonicated for 15 minutes.

A fluorimetric dsDNA quantification kit (PicoGreen, Molecular Probes) was used to determine the proliferation of cells in gBMSC-SPCL constructs. Samples and standards (ranging between 0 and 2  $\mu\text{g}\cdot\text{mL}^{-1}$ ) were prepared. Triplicates were made for samples and standards. Afterwards, the 96 well white plate (Costar, Becton Dickinson) was incubated for 10 minutes in the dark and the fluorescence was read using a microplate ELISA reader (BioTek, USA) at an excitation of 485/20 nm and an emission of 528/20 nm. A standard curve was developed in order to read DNA values of samples from the standard graph.

ALP activity was measured to detect initial osteogenic differentiation on day 1 and day 7. For this purpose, to each well of a 96-well plate (Costar, Becton Dickinson) were added 20  $\mu\text{l}$  of sample plus 60  $\mu\text{l}$  of substrate solution consisting of 0.2 % (wt/v) p-nitrophenyl phosphate (Sigma) in a substrate buffer with 1 M diethanolamine HCl (Merck), at pH 9.8. The plate was then incubated in the dark for 45 minutes at 37 °C. After the incubation period, 80  $\mu\text{l}$  of a stop solution (2 M NaOH (Panreac) plus 0.2 mM EDTA (Sigma), was added to each well. Standards were prepared with p-nitrophenol (10  $\mu\text{mol}\cdot\text{mL}^{-1}$ ) (Sigma) in order to achieve final concentrations ranging between 0 and 0.3  $\mu\text{mol}\cdot\text{mL}^{-1}$ . Samples and standards were prepared in triplicates. Absorbance was read at 405 nm and sample concentrations were read off from standard graph.

gBMSCs adhesion and morphology was also investigated using scanning electronic microscopy (SEM) by previously fixing cells-scaffold constructs in a 2.5 % glutaraldehyde solution (Sigma), rinsing and dehydrating through a series of ethanol concentrations, before coating them in a gold sputter.

### **VII.3.5. Animals Study**

Four skeletally adult female goats weighting 30-45 kg were used in this study. The housing care and experimental protocol were performed according to the national guidelines, after approval by the National Ethical Committee for Laboratory Animals (2007-07-27, document number 018939) and conducted in accordance with international standards on animal welfare as defined by the European Communities Council Directive of 2 November 1986 (86/609/EEC). During the entire study, adequate measures were taken to minimize any pain and discomfort.

Animals were kept in light and temperature controlled rooms and health parameters, such as appetite, weight maintenance or signs of infection were monitored at a daily basis.

### VII.3.5.1. Implantation procedures

Surgical procedures were performed under standard conditions and the drill-hole technique selected was based on the one described by *Hallfeldt et al.*[32].

After general anaesthesia each goat was positioned in lateral recumbency, prepared and draped in a sterile manner to perform a surgical access to the lateral diaphysis of femur. A skin incision was then performed from the greater trochanter and continued distally to the lateral femoral condyle. The subcutaneous tissue, tensor fascia lata and lateral fascia of the vastus muscle were incised. Biceps femoris muscles were retracted posteriorly, and the vastus muscle was retracted anteriorly, after being detached from the linea aspera and femora shaft, like the periosteum. Non-critical size defects (6 mm diameter and 3 mm depth) were drilled in the lateral diaphysis of both posterior femurs of the 4 adult goats with a bone drill (Synthes®, Switzerland). Eight drills were made in each posterior femur, with a separation distance between drills of 3 cm, in two non parallel sections in order to avoid fracture tension in the bone and also to avoid new bone formation among drills. Two of those were left empty and two were filled with scaffolds without cells, which were the controls for this experiment. The remaining drills were filled in with cells-scaffold constructs cultured for 1 day (2 defects) and 7 days (2 defects) (Figure VII.3.1).

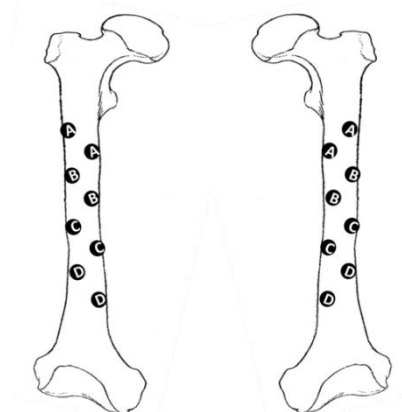


**Figure VII.3.1** - Diagram of the implantation site: A) empty drill defects, B) defects filled with SPCL (no cells), defects filled with cell-SPCL constructs after C) 1 day of culture and D) 7 days of culture in osteogenic medium. Implants were placed in the same anatomical site relative to both posterior femurs in each animal.

The implants were carefully pressed fit and placed into the bilateral defects. The muscle was replaced over the bone, and the fascia lata and skin were closed with resorbable and non-resorbable sutures, respectively.

After implantation, intravital fluorescence markers, namely, xylene orange (90 mg/kg, Aldrich), calcein green (10 mg/kg, Sigma) and tetracycline (25 mg/kg, Sigma) were injected subcutaneously (after 2, 4 and 6 weeks, respectively) for bone formation and mineralization monitoring, along with the implantation period.

In the ambulation, animals were observed at a daily basis and signs of infection or pain were monitored. During the first post-operative week, the animals were subject to an analgesic medication with flunixin meglumine (1 mg/kg IM, each 24 hours, Finadyne® P.A., Schering-Plough II) for two days and to an antibiotic therapy with amoxicillin (15 mg/kg IM, each 24 hours, Clamoxyl® L.A., Pfizer) for 7 days.

After implantation, animals were kept in a 25 m<sup>2</sup> room, with freedom of movement and full weight-bearing of the posterior limbs during the complete post-operative period.

#### **VII.3.5.2. Harvesting samples after implantation**

Six weeks after the implantation procedure, and 24 hours after tetracycline injection, animal euthanasia was performed using an overdose of pentobarbital sodium (Eutasil®, Sanofi, France). The femurs were then removed and cut into single defect-sections. Sections were fixed in a 4 % formaldehyde solution (pH 7.2) (Sigma) and embedded in glycol methacrylate (Technovit 7200® VLC–Heraus Kulzer GmbH, Germany) blocks. Thin sections with about 30 µm were prepared using a special microtome, according to the *Donath et al.* technique[33] using an Exakt-Cutting® System (Aparatbau GMBH, Germany) in order to slide calcified bone. Only the mid section of each block was used for observation at the fluorescence microscope (Olympus BX51, Germany) and for histomorphometric analysis.

Additional sections were also stained with *Lévai-Laczkó*[34] to observe the new bone formation using a stereo microscope (Olympus SZX9, Germany). Quantitative measurement for bone neof ormation was carried out after selecting relevant drill surrounding areas where neobone was marked and quantified using *Microimage 4.0 software*.

### VII.3.6. Statistical Analysis

Statistical analysis was carried out by mean  $\pm$  standard error of mean using T-Test and 2-way ANOVA for *in vitro* and for *in vivo* measurements, respectively. At least 4 samples were considered in the *in vitro* assays (DNA, ALP, SEM) while 16 samples were considered *in vivo* for each condition; A) empty drill, B) drill with SPCL scaffold, drills with SPCL seeded with gBMSCs for either C) 1 or D) 7 days in osteogenic medium).

In the present study, controls of the experiment were considered; indirectly by *in vitro* assessments of DNA and ALP activity studies and directly by the histometric analysis of induced drills performed in the posterior femurs of each animal.

## VII.4. Results and Discussion

### VII.4.1. *In vitro* characterization of autologous gBMSCs-SPCL constructs

SEM micrographs (Figure VII.4.1) indicated that gBMSCs attached to the SPCL fiber meshes, presented a typical elongated morphology and were homogeneously distributed throughout the surface of the SPCL scaffold.

These pictures also show an increase in gBMSCs proliferation with the culturing time, as observed by the cell layer formed on top of the fibers, when compared to cells cultured for 1 day in the same conditions.

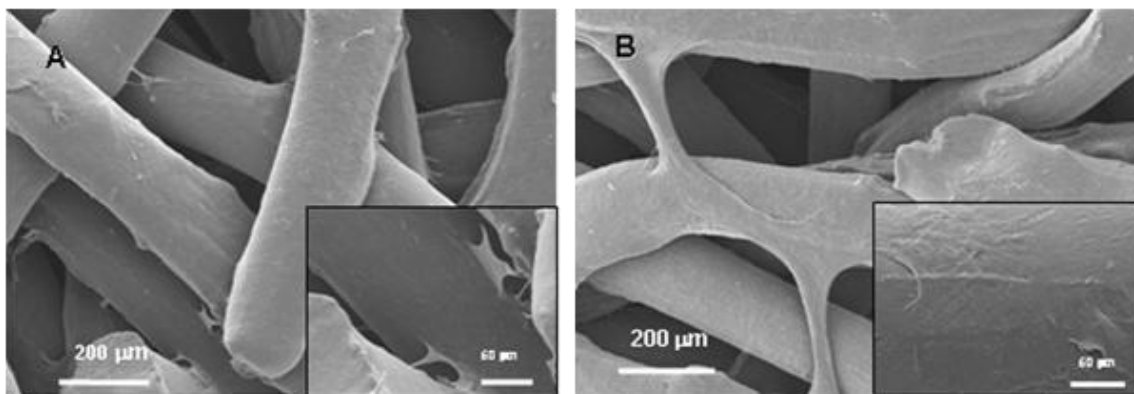


**Figure VII.4.1** - SEM micrographs of SPCL scaffolds seeded with gBMSCs and *in vitro* cultured in osteogenic culture for 1 day (A) or 7 days (B).

Regarding cell proliferation results, data obtained from the DNA content test (Figure VII.4.2) indicated that proliferation of gBMSCs seeded onto SPCL scaffolds seemed to slightly decrease after 7 days in culture although no statistically differences were found ( $p < 0.05$ , T-Test) to support these results. Nevertheless, the tendency to cell proliferation decrease could be directly associated to the increment of ALP activity of gBMSCs.

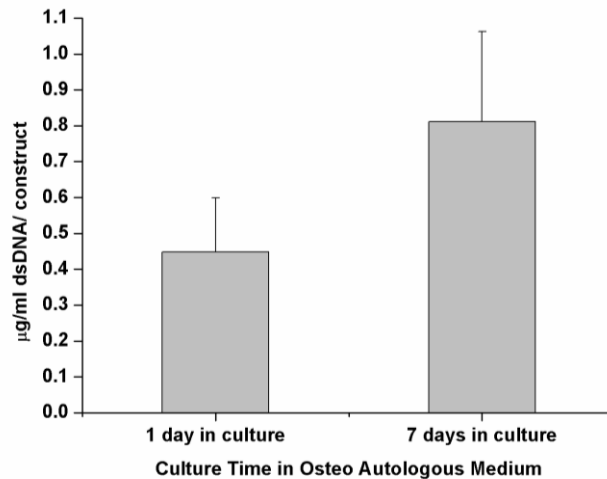


**Figure VII.4.2** - *In vitro* double strand DNA concentration in SPCL scaffolds seeded with gBMSCs cultured in osteogenic culture for 1 and 7 days.

Results obtained from the ALP assay revealed that, after 7 days in culture with osteogenic medium, there was a significant increment in ALP activity levels (Figure VII.4.3) ( $p < 0.05$ , T-Test) when compared to levels obtained for 1 day of culture as expected, since these cells were biochemically stimulated towards the osteogenic pathway[6, 35, 36].

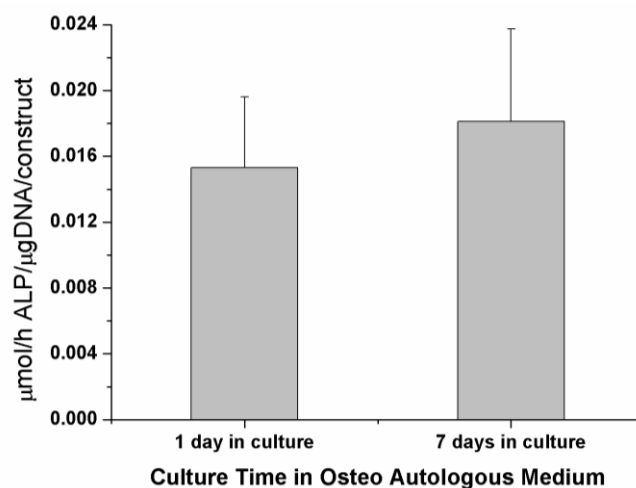


**Figure VII.4.3** - *In vitro* ALP activity in SPCL scaffolds seeded with gBMSCs cultured in osteogenic culture for 1 or 7 days.

#### **VII.4.2. In vivo studies**

All animals completed the study. No weight differences were observed and no signs of infection or inflammation were found nearby the implantation areas after 6 weeks.

In this pilot study, orthotopic defects were drilled to determine the influence of SPCL scaffolds alone and osteogenic differentiation stage of gBMSCs seeded onto SPCL scaffolds in bone neoformation. In this way, cells were cultured on SPCL scaffolds, after 1 day in osteogenic culture, practically undifferentiated, or after 7 days in culture when cells have already initiated the osteogenic process as indicated by *in vitro* ALP activity levels and by previous studies performed at our group.

Prior to constructs characterization, femurs were cleaned from muscle as the induced drills were not easily detected 6 weeks after implantation (both controls and drills containing the cell-SPCL constructs) due to an excellent regeneration process, which occurred in all cases. In order to expose the drills and access the inner region, bone was longitudinally cut.

Under macroscopic observation of femoral defects, defects filled with cell-SPCL constructs seemed to have higher bone growth than empty drill defects or defects filled with SPCL materials alone.

##### **VII.4.2.1. Histologic and Fluorescence analysis**

The observation of sections stained with *Lévai-Laczkó*, a specific neobone marker (Figure VII.4.4), shows that there was bone formation in all drill-defects as expected in non-critical defects. Nevertheless, there was an enhanced neobone formation in defects containing SPCL scaffolds seeded with gBMSCs, which suggest the importance of the presence of these cells in the constructs to stimulate bone formation. Giant cells were present in one of the studied samples, which indicated that after 6 weeks, scaffold materials are being absorbed by the body, according to some research works[37].

The sequentially administration of fluorescent dyes allowed to monitor bone ingrowth during the overall period of implantation.

Again, the presence of gBMSCs seems to positively influence bone ingrowth with the time, especially two weeks after implantation when calcein green was subcutaneously injected (Figure VII.4.5).

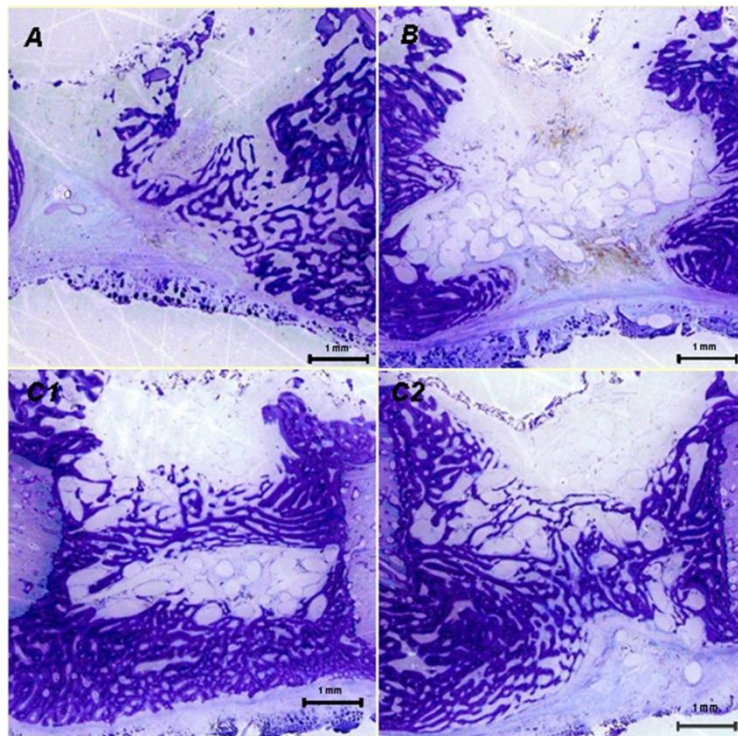


**Figure VII.4.4** - Drill sections marked with Lévai-Laczkó staining. In A) Control 1 – empty drill defects, B) Control 2 – defects filled with SPCL (no cells), C) defects filled with cells-SPCL constructs after C1) 1 day of culture and C2) 7 days of culture in osteogenic medium.

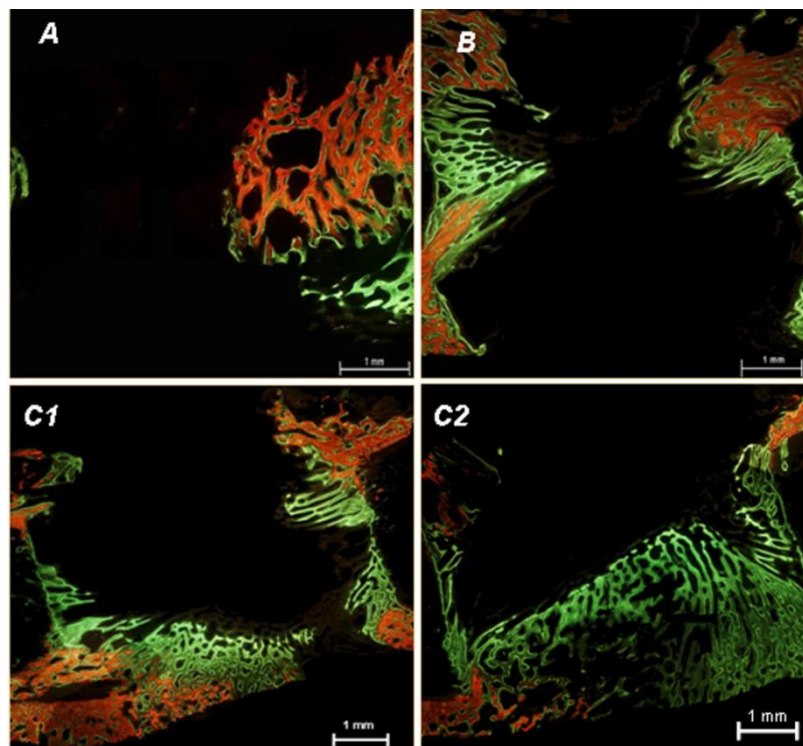


**Figure VII.4.5** - Drill sections marked with Xylenol Orange (red), Calcein Green (green) and Tetracycline (not observed) fluorescence stainings. In A) Control 1 – empty drill defects, B) Control 2 – defects filled with SPCL (no cells), C) defects filled with cell-SPCL.



However, the degradation rate of each staining was faster than expected, likely because of the fast metabolism of these animals. Due to this, in some section regions, bone formation was dark just before the subsequent fluorescent stain was injected. In some pictures is still possible to observe dark neobone areas, as the new bone was formed. As tetracycline dye was injected just 24 hours before samples retrieval, the fluorescence mark was too light to be easily observed in the drill defect images. Even though the stain has reached the bone drills, 24 hours was probably an insufficient period of time for the fluorescence to be imprinted in the fresh bone.

Besides a qualitative analysis, histomorphological parameters of bone neof ormation were measured, to obtain quantitative data regarding the percentage of new bone formation and new bone roundness. The percentage of neobone present in each drill was compared with the remaining drills and statistically analyzed (Figure VII.4.6).

The amount of new bone formation tended to increase in the presence of cell seeded scaffolds although the quantitative analysis performed did not reveal significant differences between the values measured for new bone formation (%) between defects with and without gBMSCs.

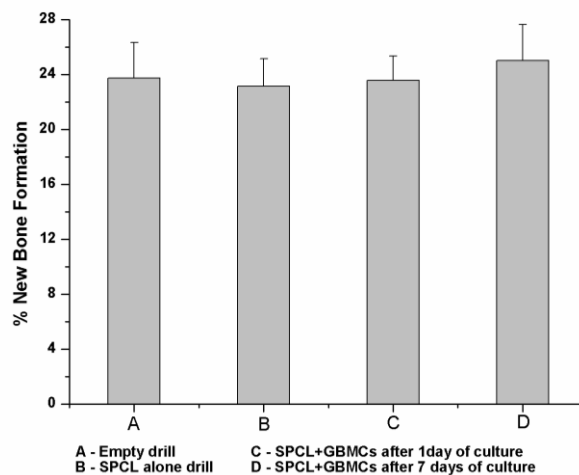


**Figure VII.4.6** – New bone formation percentage in the different induced drills: A) empty drill defects, B) defects filled with SPCL (no cells), defects filled with cell-SPCL constructs after C) 1 day of culture and D) 7 days of culture in osteogenic medium.

Other parameters namely, roundness of new bone formation, were also considered in order to evaluate the spreading of neobone tissue into the induced defects.

As it can be observed in Figure VII.4.7, there was a tendency to an increment in new bone roundness obtained in defects filled with cell seeded scaffolds (with increasing culturing times)

when compared to empty defects. This fact may be associated to a cellular stimulation provided by autologous cells implanted in the animals.

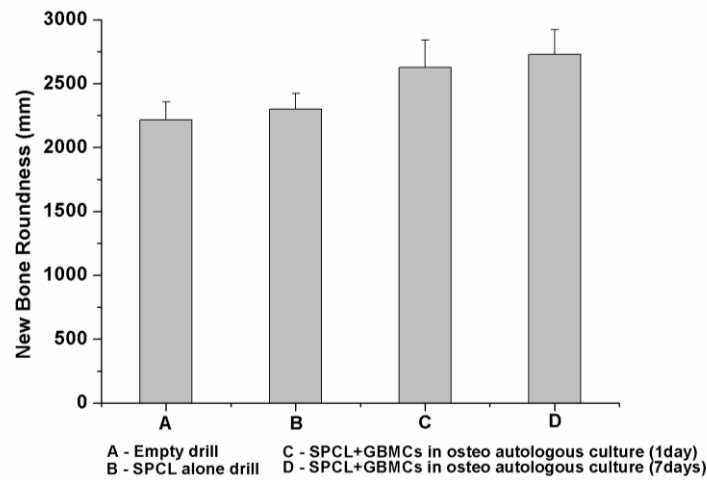


**Figure VII.4.7** - New bone roundness measured for the different induced drills: A) empty drill defects, B) defects filled with SPCL (no cells), defects filled with cell-SPCL constructs after C) 1 day of culture and D) 7 days of culture in osteogenic medium.

Neither inflammatory response after 6 weeks of implantation nor animal behaviour modifications in terms of food intake, movement or general health was detected. The presence of fiber mesh SPCL scaffolds allowed for neobone ingrowth in the induced defects. Furthermore, traces of cell-mediated absorption were observed in one of the retrieved samples by the presence of fibrous tissue containing an occasional multinucleated giant cell on the implant surface. This may indicate that locally, material absorption can initiate at an early stage of bone regeneration.

## VII.5. Conclusions

In the present study it was possible to observe the neoformation of bone in all orthotopic induced drills in the goat femurs, as expected for non-critical defects. Nevertheless, it was found an increased neobone formation as well as cellular distribution into the defect where the gBMSC-SPCL constructs were implanted. This increment is enhanced with the *in vitro* culturing time which indicates that *in vitro* culturing time of gBMSCs onto the SPCL constructs may also play an important role in new bone growth. The data obtained concerning *in vitro*

proliferation and differentiation of these constructs suggest that, the *in vitro* culturing time of gBMSCs in osteogenic medium, though still in a very early stage, is likely to play an important role in bone growth onto these defects.

However, further studies should provide better understanding of the importance of the number of cells and their differentiation stage as well as the time needed for osteogenic supplementation to induce significant changes in bone formation *in vivo*. Nevertheless, SPCL fiber mesh scaffolds showed a great potential for the development of adequate tissue 3D support for the regeneration of bone in non-critical defects.

Thus, results obtained provided important information about the performance of gBMSCs-SPCL constructs in an orthotopic goat that enable to design future studies to investigate the *in vivo* functionality of gBMSC-SPCL constructs in more complex models, namely in induced critical sized defects and evaluate the influence of *in vitro* cultured autologous cells in the healing and bone regenerative process.

## VII.6. References

1. Dennis R, Carter GSB: Chapter 7 - Skeletal Tissue Regeneration. *In Skeletal Function and Form - Mechanobiology of Skeletal Development, Aging and Regeneration*. Edited by: Cambridge University Press; 2001:161-200.
2. Mauney JR, Volloch V, Kaplan DL: Role of adult mesenchymal stem cells in bone tissue engineering applications: current status and future prospects. *Tissue Eng* 2005, 11: 787-802.
3. Muraglia A, Cancedda R, Quarto R: Clonal mesenchymal progenitors from human bone marrow differentiate *in vitro* according to a hierarchical model. *J Cell Sci* 2000, 113 (Pt 7): 1161-1166.
4. Pittenger MF, Mackay AM, Beck SC, Jaiswal RK, Douglas R, Mosca JD, Moorman MA, Simonetti DW, Craig S, Marshak DR: Multilineage potential of adult human mesenchymal stem cells. *Science* 1999, 284: 143-147.
5. Tuan RS, Boland G, Tuli R: Adult mesenchymal stem cells and cell-based tissue engineering. *Arthritis Res Ther* 2003, 5: 32-45.
6. Oliveira JM, Rodrigues MT, Silva SS, Malafaya PB, Gomes ME, Viegas CA, Dias IR, Azevedo JT, Mano JF, Reis RL: Novel hydroxyapatite/chitosan bilayered scaffold for osteochondral tissue-engineering applications: Scaffold design and its performance when seeded with goat bone marrow stromal cells. *Biomaterials* 2006, 27: 6123-6137.

7. Hutmacher DW, Schantz JT, Lam CX, Tan KC, Lim TC: State of the art and future directions of scaffold-based bone engineering from a biomaterials perspective. *J Tissue Eng Regen Med* 2007, 1: 245-260.
8. Gomes ME, Reis RL: Biodegradable polymers and composites in biomedical applications: from catgut to tissue engineering - Part 1 - Available systems and their properties. *International Materials Reviews* 2004, 49: 261-273.
9. Gomes ME, Azevedo HS, Moreira AR, Ella V, Kellomaki M, Reis RL: Starch-poly(epsilon-caprolactone) and starch-poly(lactic acid) fibre-mesh scaffolds for bone tissue engineering applications: structure, mechanical properties and degradation behaviour. *J Tissue Eng Regen Med* 2008, 2: 243-252.
10. Mendes SC, Reis RL, Bovell YP, Cunha AM, van Blitterswijk CA, de Bruijn JD: Biocompatibility testing of novel starch-based materials with potential application in orthopaedic surgery: a preliminary study. *Biomaterials* 2001, 22: 2057-2064.
11. Gomes ME, Sikavitsas VI, Behravesh E, Reis RL, Mikos AG: Effect of flow perfusion on the osteogenic differentiation of bone marrow stromal cells cultured on starch-based three-dimensional scaffolds. *J Biomed Mater Res A* 2003, 67: 87-95.
12. Gomes ME, Holtorf HL, Reis RL, Mikos AG: Influence of the porosity of starch-based fiber mesh scaffolds on the proliferation and osteogenic differentiation of bone marrow stromal cells cultured in a flow perfusion bioreactor. *Tissue Eng* 2006, 12: 801-809.
13. Gomes ME, Bossano CM, Johnston CM, Reis RL, Mikos AG: In vitro localization of bone growth factors in constructs of biodegradable scaffolds seeded with marrow stromal cells and cultured in a flow perfusion bioreactor. *Tissue Eng* 2006, 12: 177-188.
14. Mendes SC, Bezemer J, Claase MB, Grijpma DW, Bellia G, Degli-Innocenti F, Reis RL, de Groot K, van Blitterswijk CA, de Bruijn JD: Evaluation of two biodegradable polymeric systems as substrates for bone tissue engineering. *Tissue Eng* 2003, 9 Suppl 1: S91-101.
15. Santos MI, Fuchs S, Gomes ME, Unger RE, Reis RL, Kirkpatrick CJ: Response of micro- and macrovascular endothelial cells to starch-based fiber meshes for bone tissue engineering. *Biomaterials* 2007, 28: 240-248.
16. Sikavitsas VI, van den Dolder J, Bancroft GN, Jansen JA, Mikos AG: Influence of the in vitro culture period on the in vivo performance of cell/titanium bone tissue-engineered constructs using a rat cranial critical size defect model. *J Biomed Mater Res A* 2003, 67: 944-951.
17. Buma P, Schreurs W, Verdonschot N: Skeletal tissue engineering-from in vitro studies to large animal models. *Biomaterials* 2004, 25: 1487-1495.
18. Pearce AI, Richards RG, Milz S, Schneider E, Pearce SG: Animal models for implant biomaterial research in bone: a review. *Eur Cell Mater* 2007, 13: 1-10.
19. Kruyt MC, Dhert WJ, Yuan H, Wilson CE, van Blitterswijk CA, Verbout AJ, de Bruijn JD: Bone tissue engineering in a critical size defect compared to ectopic implantations in the goat. *J Orthop Res* 2004, 22: 544-551.

20. Li X, Feng Q, Liu X, Dong W, Cui F: Collagen-based implants reinforced by chitin fibres in a goat shank bone defect model. *Biomaterials* 2006, 27: 1917-1923.
21. Zhu L, Liu W, Cui L, Cao Y: Tissue-engineered bone repair of goat-femur defects with osteogenically induced bone marrow stromal cells. *Tissue Eng* 2006, 12: 423-433.
22. Lane JG, Massie JB, Ball ST, Amiel ME, Chen AC, Bae WC, Sah RL, Amiel D: Follow-up of osteochondral plug transfers in a goat model: a 6-month study. *Am J Sports Med* 2004, 32: 1440-1450.
23. Niederauer GG, Slivka MA, Leatherbury NC, Korvick DL, Harroff HH, Ehler WC, Dunn CJ, Kieswetter K: Evaluation of multiphase implants for repair of focal osteochondral defects in goats. *Biomaterials* 2000, 21: 2561-2574.
24. Giannoni P, Mastrogiacomo M, Alini M, Pearce SG, Corsi A, Santolini F, Muraglia A, Bianco P, Cancedda R: Regeneration of large bone defects in sheep using bone marrow stromal cells. *J Tissue Eng Regen Med* 2008, 2: 253-262.
25. Kirker-Head C, Karageorgiou V, Hofmann S, Fajardo R, Betz O, Merkle HP, Hilbe M, von Rechenberg B, McCool J, Abrahamsen L, et al.: BMP-silk composite matrices heal critically sized femoral defects. *Bone* 2007, 41: 247-255.
26. Kruyt MC, Dhert WJ, Oner FC, van Blitterswijk CA, Verbout AJ, de Bruijn JD: Analysis of ectopic and orthotopic bone formation in cell-based tissue-engineered constructs in goats. *Biomaterials* 2007, 28: 1798-1805.
27. Meinel L, Betz O, Fajardo R, Hofmann S, Nazarian A, Cory E, Hilbe M, McCool J, Langer R, Vunjak-Novakovic G, et al.: Silk based biomaterials to heal critical sized femur defects. *Bone* 2006, 39: 922-931.
28. Livingston T, Ducheyne P, Garino J: In vivo evaluation of a bioactive scaffold for bone tissue engineering. *Journal of Biomedical Materials Research* 2002, 62: 1-13.
29. Mauney JR, Jaquiere C, Volloch V, Herberer M, Martin I, Kaplan DL: In vitro and in vivo evaluation of differentially demineralized cancellous bone scaffolds combined with human bone marrow stromal cells for tissue engineering. *Biomaterials* 2005, 26: 3173-3185.
30. Mastrogiacomo M, Papadimitropoulos A, Cedola A, Peyrin F, Giannoni P, Pearce SG, Alini M, Giannini C, Guagliardi A, Cancedda R: Engineering of bone using bone marrow stromal cells and a silicon-stabilized tricalcium phosphate bioceramic: evidence for a coupling between bone formation and scaffold resorption. *Biomaterials* 2007, 28: 1376-1384.
31. Trojani C, Boukhechba F, Scimeca JC, Vandenbos F, Michiels JF, Daculsi G, Boileau P, Weiss P, Carle GF, Rochet N: Ectopic bone formation using an injectable biphasic calcium phosphate/Si-HPMC hydrogel composite loaded with undifferentiated bone marrow stromal cells. *Biomaterials* 2006, 27: 3256-3264.
32. Hallfeldt KK, Stutzle H, Puhlmann M, Kessler S, Schweiberer L: Sterilization of partially demineralized bone matrix: the effects of different sterilization techniques on osteogenetic properties. *J Surg Res* 1995, 59: 614-620.

33. Donath K: Preparation of histologic sections by the cutting-grinding technique for hard tissue and other material not suitable to be sectioned by routine methods. In *Equipment and methodical performance*. Edited by: Exakt-Kulzer-Publication; 1995.
34. Jenő L, Geza L: A simple differential staining method for semi-thin sections of ossifying cartilage and bone tissues embedded in epoxy resin. *Mikroskopia* 1975, 31: 1-4.
35. Rodrigues MT, Oliveira JM, Gomes ME, Viegas CA, Dias IR, Mano JF, Reis RL: Novel hydroxyapatite/chitosan bilayer scaffolds for the regeneration of osteochondral defects using a tissue engineering approach based on culturing and differentiation of goat marrow cells into osteoblasts or chondrocytes. In *World Congress on Tissue Engineering and Regenerative Medicine April Pittsburgh, Pennsylvania, USA: 2006*.
36. Rodrigues MT, Leonor I, Tuzlakoglu K, Gomes ME, Viegas CA, Dias IR, Reis RL: Novel In Situ Approach for the Design of Osteoconductive and Osteoinductive 3D Wet-Spun Fibre Mesh Scaffolds for Bone Tissue Engineering. In *Tissue Engineering International and Regenerative Medicine Society - Asia Pacific Chapter Meeting 2007; Tokyo, Japan: 2007*.
37. Pego AP, Van Luyn MJ, Brouwer LA, van Wachem PB, Poot AA, Grijpma DW, Feijen J: In vivo behavior of poly(1,3-trimethylene carbonate) and copolymers of 1,3-trimethylene carbonate with D,L-lactide or epsilon-caprolactone: Degradation and tissue response. *J Biomed Mater Res A* 2003, 67: 1044-1054.

## Chapter VIII

### THE EFFECT OF THE DIFFERENTIATION STAGE OF AMNIOTIC FLUID STEM CELLS SEEDED ONTO BIODEGRADABLE SCAFFOLDS IN THE REGENERATION OF NON-UNION DEFECTS

*This chapter is based on the following publication:*

Rodrigues MT, Lee BK, Shiner T, Lee SJ, Gomes ME, Reis RL, Atala A, and Yoo J, The effect of the differentiation stage of amniotic fluid stem cells seeded onto biodegradable scaffolds in the regeneration of non-union defects, *submitted*





THE STAGE OF DIFFERENTIATION OF AMNIOTIC FLUID STEM CELLS  
SEEDED ONTO BIODEGRADABLE SCAFFOLDS IN THE REGENERATION OF NON-UNION DEFECTS

**VIII.1. Abstract**

Bone tissue engineering (TE) strategies mainly require cells with high proliferative and osteogenic potential and a suitable scaffold to support cellular development towards new bone tissue formation. This study aimed at evaluating the effect of the differentiation stage of human amniotic fluid stem cells (hAFSCs) in the regeneration of femoral critical sized defects in a nude rat model. For this purpose, hAFSCs were seeded onto a starch-polycaprolactone (SPCL) scaffold and *in vitro* cultured for different periods of time in osteogenic medium in order to obtain: i) undifferentiated cells, ii) cells committed to the osteogenic phenotype and iii) “osteoblastic-like” cells. *In vitro* results indicated that hAFSCs kept a high viability for up to 3 weeks seeded onto SPCL scaffolds. Furthermore, hAFSCs were considered to be osteogenically committed by the end of week 2 and osteoblastic-like after 3 weeks in culture.

The constructs, obtained by *in vitro* culturing hAFSCs onto SPCL scaffolds until reaching these three differentiation stages, were then implanted in femoral critical sized defects induced in nude rats for 4 or 16 weeks. Empty defects and defects filled with scaffold alone were used as controls. The quality of new tissue formed in the defects was evaluated based on micro-CT and histological analysis of samples retrieved at 4 and 16 weeks of implantation. *In vivo* neoformation of bone was observed in all conditions. Nevertheless, the best bridging between the two sections of the defect was observed in the presence of SPCL scaffolds seeded with osteogenically committed AFSCs after 16 weeks. Furthermore, the presence of blood vessels in the inner sections of the SPCL scaffold seeded with hAFSCs provides further evidence of the great potential of SPCL scaffolds combined with hAFSCs for bone regeneration and angiogenesis in non-union defects.

## VIII.2. Introduction

Fracture healing is a complex physiological phenomenon involving the spatial and temporal coordinated action of different cell types, proteins and the expression of several genes working towards the restoration of tissue structure and function in a proper mechanical environment. Age, gender, mechanism of injury and type of fracture (e.g. force impact, stress or negligible injuries combined with particular medical conditions, such as osteoporosis, bone cancer or *osteogenesis imperfecta*), associated injuries, comorbidities, lifestyle and pharmacological agents are all factors that could interfere with the fracture healing response and contribute to the development of non-union of fractures[1]. Of all the fracture injuries, up to 10 % will progress into complicated fractures, which may result in non-union defects[2]. This represents a contemporary problem associated with an increasing clinical burden. Despite the bone innate fracture repair mechanisms, non-unions or critical size segmental defects are still a major challenge in reconstructive orthopedic surgery[3].

The current clinical strategy to treat fracture non-union is autologous bone grafting, where bone chips are removed from a secondary site into the fracture to participate in the healing process. Although bone graft remains the gold standard treatment of non-unions[4], some problems may be associated to, such as bone graft tissue site morbidity and limited quantity or quality of autologous bone graft material. In order to find an alternative solution, synthetic materials have been developed with suitable degradation kinetics and interesting properties to match the requirements in bone applications. Nevertheless, a highly osteogenic cell source is required, together with a 3D scaffold, to improve the bone regenerative potential. This need is even more important in larger injuries to establish cellular and molecular communications *in situ*, promoting a bond between the implant and the native systems. Several studies emphasized the importance of implanting cells into the defect to ensure the bone regenerative process[5-7]. Undifferentiated stem cells are multipotent and, once at the injury site, they can differentiate into the type of cell necessary according to the regenerative natural timing, while recruiting important growth factors[8] that stimulate *in situ* repair.

Among the sources of stem cells, amniotic fluid arises as an attractive source of pluripotent stem cells without raising the ethical concerns associated with the use of human embryonic stem cells[9]. Additionally, AFSCs have a highly self-renewal capability and have the potential to differentiate along several lineages[10, 11], including bone[10, 12], due to their origin from embryonic and extra-embryonic tissues. AFSCs also present advantages compared to other primary cells; unlike osteoblasts or bone marrow cells, AFSCs are not limited by tissue

insufficient supply and morbidity, host immune responses and disease transmission risks. Furthermore, due to AFSCs high proliferative capacity and their ability to maintain their pluripotency at higher passages, these cells may be a readily available source for large numbers of osteo progenitor cells aimed at bone TE strategies.

Despite the potential of cell application in a scaffold to promote the regenerative process *in locus*, few studies addressed the effect of the cell differentiation stage in the regenerative process of bone[13, 14]. Since the bony milieu is a rich cocktail of growth factors, and molecular signals, where diverse cell types are present in several stages of differentiation, it is likely that the number or concentration of a particular molecule or cell type might result in a different role in promoting bone healing. Furthermore, undifferentiated or partially differentiated cells, due to their plasticity potential may participate in an immediate response towards an injury or trauma event, and activate signaling pathways that may not be naturally triggered by differentiated cells, such as osteoblasts.

In this work, we hypothesize that the stage of differentiation of human AFSCs into the osteogenic lineage may affect differently the evolution of the regenerative process in non-union defects of bone. The pre-culture period of hAFSCs in osteogenic supplemented medium may be a critical factor, affecting the osteoinductive potential and consequently, the new bone formation when orthotopically implanted.

Therefore, the main purpose of this study was to evaluate the influence of the differentiation stage of human amniotic fluid stem cells (hAFSCs) cultured onto starch and polycaprolactone (SPCL) scaffolds, and in the regeneration of bone critical sized defects.

In order to achieve our goals, stem cells from amniotic fluid were expanded in basic amniotic fluid cell medium, seeded onto SPCL scaffolds and cultured in osteogenic medium for different periods of time in order to have i) stem cells, ii) cells committed to the osteogenic phenotype and iii) “osteoblastic” cells. After reaching each stage of differentiation, samples were implanted in critical sized defects in the right femur of nude rats and kept for 4 or 16 weeks. *In vivo* bone regeneration was monitored through micro-CT and histological analysis was performed after each end point.

### **VIII.3. Materials and Methods**

#### **VIII.3.1. In vitro Study**

SPCL scaffolds were produced by a fiber bonding technique described previously[15, 16, 17], cut into cylinders with 3.8 mm diameter and 6.0 mm length and sterilized by ethylene oxide.

Human AFSCs were isolated and characterized as previously described[10] and cultured in basic amniotic fluid cell (BAFC) medium containing  $\alpha$ -MEM (HyClone Laboratories IncUSA), 2 % Chang B (Irvine Scientific, USA) and 18 % Chang C (Irvine Scientific, USA) media as well as 1 % L-glutamine (HyClone Laboratories Inc., USA) and 15 % embryonic stem screened fetal bovine serum (ES-FBS, HyClone Laboratories Inc., Logan, Utah, USA). Then, hAFSCs were seeded onto SPCL scaffolds at a density of  $1.2 \times 10^6$  cells/scaffold and cultured in BAFC medium for 3 days.

hAFSCs were characterized in terms of the osteogenic differentiation process. Osteogenic commitment was related to hAFSCs ability to express markers associated to the osteo lineage while osteoblastic stage was to be accomplished with the production of a mineralized ECM.

Following 3 days in BAFC medium, hAFSCs seeded onto the SPCL scaffolds were cultured in osteogenic medium, composed of DMEM (HyClone Laboratories Inc., Logan, Utah, USA) supplemented with 10 % FBS (HyClone Laboratories Inc., USA) and osteogenic supplements; 100 nM dexamethasone (Sigma, USA), 50  $\mu$ M L-ascorbic acid (Sigma, USA) and 10 mM glycerol 2-phosphate disodium salt hydrate (Sigma, USA) for different periods of time (0, 1, 2 and 3 weeks), determined in a preliminary study, so as to obtain i) undifferentiated cells or stem cells, ii) cells committed to the osteogenic phenotype and iii) “osteoblastic-like” cells. After each culturing period, hAFSCs-SPCL samples were characterized for osteogenic phenotypic expression and matrix formation by alkaline phosphatase (ALP) and Alizarin Red (AR) stainings as well as the presence of collagen I in the matrix. The detection of a mineralized matrix was further analyzed by Fourier transformed infra red attenuated spectroscopy (FTIR-ATR). Cell morphology and matrix formation were also assessed by scanning electronic microscopy (SEM).

##### **VIII.3.1.1. Alizarin Red (AR) and Alkaline phosphatase (ALP) staining**

Alizarin Red and ALP staining were performed in hAFSCs-SPCL constructs cultured in either BAFC (0 days) or osteogenic medium after each culturing period namely, 1, 2 and 3 weeks.

Macroscopic sections of hAFSCs-SPCL construct, approximately 2 mm x 5 mm each, were considered for ALP and AR stainings, where constructs were fixed with 10 % buffered formalin solution overnight at 4 °C and then rinsed and kept in PBS until usage.

**AR:** Samples were stained with a photosensitive solution of AR (0.2 %, Sigma-Aldrich, USA), previously prepared (pH adjusted to 4.1-4.3), for about 2 minutes at room temperature using a bench shaker. Then, samples were rinsed in PBS and AR staining was solubilized in a cetylpyridinium chloride (Sigma, USA) solution at pH 7.0 for 15 minutes using a bench shaker. Calcium-bound AR was quantified by spectrophotometric measurements in a plate reader (SpectraMax MS, Molecular Devices, Sunnyvale, CA, USA) at 562 nm.

**ALP:** constructs were incubated in a staining solution of 0.25 % Naphthol AS-MX phosphate alkaline solution (Sigma-Aldrich, USA) and Fast Violet B salt (Sigma, USA) for 30 minutes. Samples were rinsed in PBS to remove excess of non-specific staining.

#### **VIII.3.1.2. SEM (scanning electronic microscopy)**

Human AFSC-SPCL constructs were rinsed in PBS and fixed in 10 % buffered formalin overnight, dehydrated in a series of ethanol concentrations and kept in absolute ethanol until critical point drying (EMS850X, Electron Microscopy Sciences, USA). Afterwards, constructs were gold sputtered (Hummer 6.2 sputtering system, Anatech Ltd, USA), before SEM (Hitachi S-2600N, Hitachi Science Systems, Ltd, Japan) observation of the morphology of hAFSCs seeded SPCL scaffolds after 0, 7, 14 and 21 days in osteogenic culture.

Also, in order to detect calcium (Ca) and phosphorus (P) ions present in the ECM matrix, an energy dispersive spectroscopy (EDS) equipment (Leica Cambridge S360, UK) was used.

#### **VIII.3.1.3. FTIR-ATR (Fourier transform attenuated total reflectance infrared spectroscopy)**

hAFSCs-SPCL samples, obtained from each end point, were dehydrated and air dried, before proceeding to a FT-IR analysis. FT-IR was performed with an attenuated total reflectance[18] in the spectral range of 1800-600  $\text{cm}^{-1}$  using the Spectrum 400 FT-IR/FT-NIR spectrometer (Perkin Elmer, USA).

#### **VIII.3.1.4. Immunofluorescence**

hAFSC-SPCL constructs were rinsed in PBS and fixed in formalin prior to the detection of mouse monoclonal to collagen type I (Abcam, 1:100 dilution in antibody diluent with background reducing components from Dako, Denmark) by a regular immunofluorescence procedure using anti-mouse AlexaFluor 594 (Molecular Probes, Invitrogen; 1:200 dilution) as a secondary antibody. Instead of animal serum, blocking step was performed using protein block serum free (Dako, Denmark). Constructs were then observed under a confocal microscope (Axiovert 100 M, Zeiss, Germany) equipped with argon/He-Ne laser sources.

#### **VIII.3.2. *In vivo* Study**

All surgical procedures were performed in accordance with Wake Forest University Animal Care and Use Committee (ACUC) approved protocols (protocol number; A07-063/A10-032). In this study, male athymic nude rats (36-40 week old) weighing 420-560 g (n=60) were purchased from Charles River. Animals were randomly assigned into 5 groups (n=6 / group) as follows: 1) no-repair group (empty defects, no implant), 2) scaffold-only group, and 3) scaffold with undifferentiated hAFSCs cell group, 4) scaffold with hAFSC osteogenically committed group, and 5) scaffold with hAFSCs differentiated into osteoblast like cells group.

Anesthesia was induced with 3 % isoflurane (USP, Novaplus) prior to surgical procedures. The dorsolateral side of the right leg was shaved and sterilized with routine aseptic agent. Under aseptic conditions, a 20 mm long incision was made on the skin over the femur of the right hind limb. The skin and the gluteus muscle were dissected to approach the femur. A periosteal incision was made on the periosteum of the femur, and the periosteum and the attached muscles were elevated to expose the femur. Retracting adjacent tissues, a 3.0 mm thick and 2.2 cm long custom-made bone plate was placed along the intact femur and was fixed with 4 stainless steel screws using a micro drill system (BS72-4950, Harvard apparatus, USA) to stabilize the femur after scaffold implantation. A 5 mm bone segment in between screwed areas at both ends was removed from the femur using a bone cutting bur. The created defects were thoroughly irrigated with sterile saline to avoid residual bone particles at the site. Subsequently, the scaffolds and cell-scaffold constructs from the different study groups, according to our experimental design, were implanted to the bony defects and fixed with a press-fit manner. After inserting the scaffolds/constructs, the muscle and the skin were

closed layer by layer using 5-0 *Vicryl* sutures (Ethicon, USA). The animals were maintained postoperatively according to the guideline of the ACUC.

Radiographic 2D images of the femoral defects were obtained from each animal every 4 weeks, using C-arm equipment (Siremobil Compact L, Siemens) to monitor plate stability and select animals for micro-CT analysis. Animals were kept under general anaesthesia during both (x-rays and micro-CT) procedures.

Rats were euthanized 4 or 16 weeks after implantation accordingly to ACUC guidelines. Right femurs were retrieved, rinsed in PBS, placed in 10 % buffered formalin for 96 h and then kept in 60 % ethanol until histological processing.

#### **VIII.3.2.1. $\mu$ -CT scanning**

Real time live imaging of the rat femoral defects was obtained using an  $\mu$ -CT equipment, Siemens MicroCAT II (Siemens Preclinical Solutions, USA) and MicroCAT II version 1.9d software was used to acquire raw data.

Scans were performed with an x-ray voltage of 70 kVp, anode current of 500  $\mu$ A, and an exposure time of 1600 ms (BIN Factor of 2, 360 ° rotation, 360 steps, 36 micron isotropic voxel dimension).

RVA version 4.2.9 and COBRA EXXIM version 4.9.52 were used to reconstruct the raw data into raw slice images, and then Amira version 3.1 was used for conversion to DICOM images. Analysis was done after transfer of images to TeraRecon AquariusNET Server (TeraRecon, Inc., USA) using TeraRecon software AquariusNET version 1.8.1.6. Another software packages used for image analysis and volumetric measurements included Mimics version 13 (Materialise, Belgium).

#### **VIII.3.2.2. Tissue processing**

Explants were decalcified using an acid solution of Immunocal® (Decal Chemical Corp, USA), and tissue processed in a graded series of ethanol, xylene and embedded in paraffin blocks. Sections of 10  $\mu$ m were obtained for histological characterization by Hematoxylin/Eosin (H&E) staining and for immunocytochemistry (ICC) for goat anti-Collagen I (1310-01, Southern Biotech; 1:20 dilution), goat polyclonal anti- Osteocalcin (OC) (V-19, Santa Cruz Biotechnology, 1:100) and rabbit polyclonal anti-VEGF (147, Santa Cruz Biotechnology, 1:100) antibodies. All primary antibodies were diluted in antibody diluent with background reducing components

from Dako (Denmark). Biotinylated secondary antibodies were purchased to Vector Lab (Burlingame, CA, USA) as well as R.T.U. HRP/Straptavidin (SA-5704). Immunohistochemistry visualization was assessed by NovaRED substrate kit (SK-4800), followed by a brief counterstain with Gill's hematoxylin. Specimen slides were observed under a microscope (Imager Z1m, Zeiss, Germany) equipped with a digital camera (AxioCam MRc5).

### **VIII.3.2.3. Histomorphometrical Analysis**

Quantitative measurement for bone related markers, namely osteocalcin and collagen I as well as VEGF vascular marker were carried out for the *in vivo* study. After selecting an interest area within the defect, the protein expression was detected and quantified by *Cell D* software (analysis image processing) and *MicroImage* software from Olympus Optical Co.

### **VIII.3.3. Statistical Analysis**

Statistical analysis was carried out by mean  $\pm$  standard deviation for *in vitro* assays, while histomorphometric analysis was carried out by mean  $\pm$  standard error of mean. Two Way ANOVA test was also applied to check the existence of statistical differences between sample groups followed by Bonferroni's Multiple Comparison test (\* =  $p < 0.05$ ).

## **VIII.4. Results and Discussion**

### **VIII.4.1. *In vitro* study**

hAFSCs adhered and maintained viability when seeded onto the SPCL scaffolds during the experimental time up to 3 weeks (data not showed). According to SEM pictures (Figure VIII.4.1), cells, independently of their differentiation stage, bridged between scaffold microfibers covering the scaffold surface, without obstructing most pores, randomly distributed throughout the scaffold.



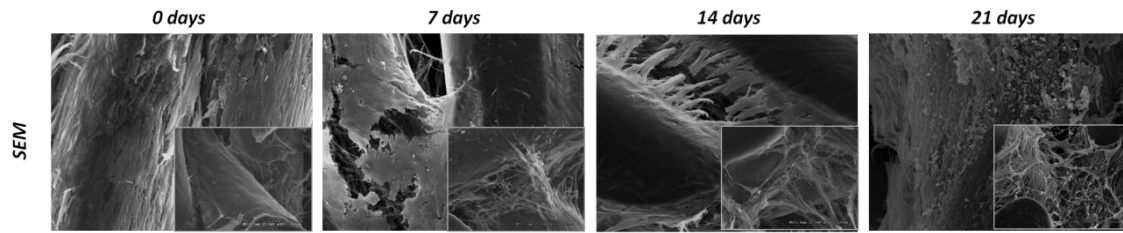


**Figure VIII.4.1** - SEM micrographs of hAFSC-SPCL constructs after 0, 7, 14 or 21 days in osteogenic medium.

When constructs were sectioned, the presence of cells was also observed inside the scaffold (Figure VIII.4.1; SEM insets), showing that the seeding was efficient and the scaffold is suitable for nourish human AFSCs.

Furthermore, after 2 weeks in osteogenic culture medium, cells were positively stained for ALP (Figure VIII.4.2) and for immunofluorescence of collagen type I (Figure VIII.4.3).



**Figure VIII.4.2** – Characterization of AFSC-SPCL constructs for ALP staining after 0, 7, 14 or 21 days in osteogenic culture.

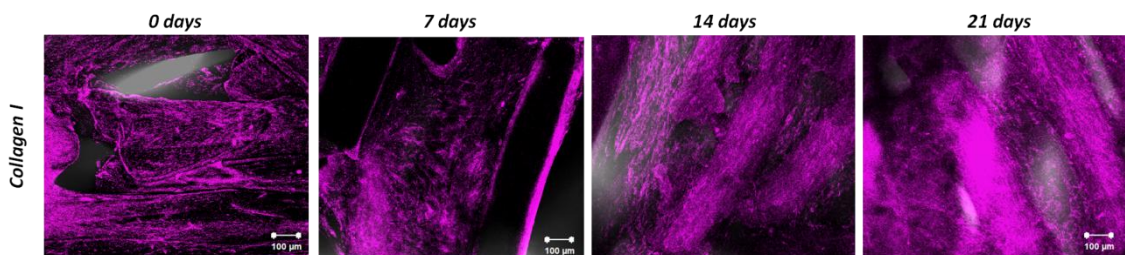


**Figure VIII.4.3** - Characterization of AFSC-SPCL constructs for collagen I by immunofluorescence, after 0, 7, 14 or 21 days in osteogenic culture.

Osteoblastic differentiation is usually accompanied by an initial decrease in the cellular proliferation rate, changes in gene and protein expression of several osteogenic markers, such as ALP and type I collagen, and later on by the deposition of minerals on the ECM matrix.

The production of organic ECM by AFSCs after 2 weeks in osteogenic medium shows a cellular commitment towards the osteogenic lineage, characterized by an ALP and collagen I

strong expression. ALP is a glycoprotein associated with the formation and maturation of the ECM[19], while collagen type I is the major constituent of bone inorganic matrix. The presence of both markers in AFSCs-SPCL constructs point out a rich collagen-based ECM (Figure VIII.4.2 and VIII.4.3). Besides the structural support, ECM plays a critical role in cellular interactions and sustains mineral nucleation, critical for bone functional properties.

Furthermore, after 14 days in osteo culture, thin, nano sized fibers surrounding the cells that may represent matrix, were found at the surface and in inner sections of the construct in SEM micrographs. Although cells are producing an ECM by 2 weeks in osteogenic culture, the ECM mineralization only occurs after 3 weeks in osteogenic supplemented culture, with the deposition of calcium and phosphate ions. In SEM images from 3 weeks in osteo medium, calcium phosphate (CaPs) aggregates are found throughout the construct (Figure VIII.4.1 and Figure VIII.4.4), confirmed by EDS analysis, calcium quantification, and FTIR (Figure VIII.4.4, Figure VIII.4.5 and Figure VIII.4.6, respectively).

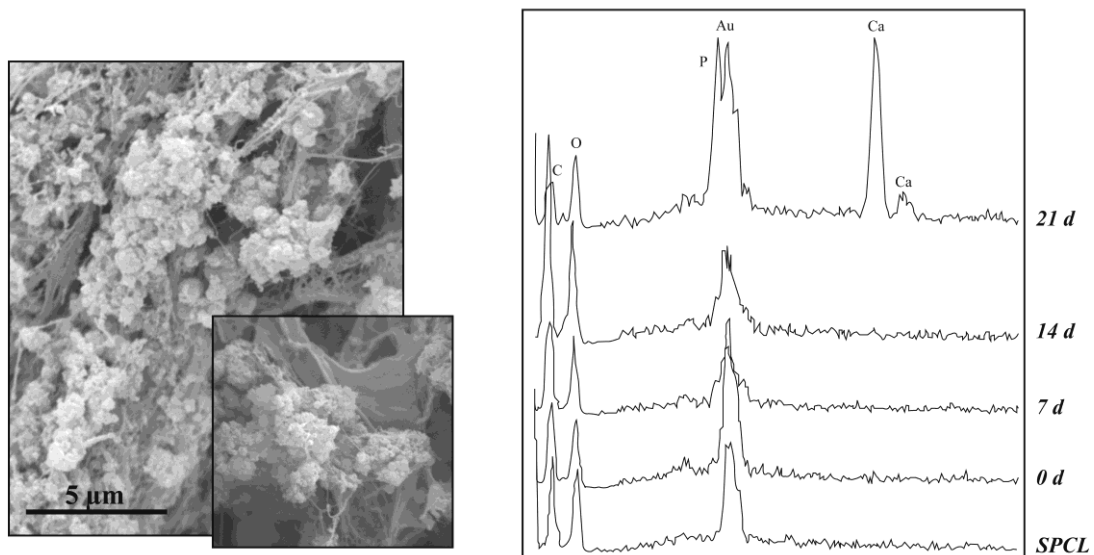


**Figure VIII.4.4** – Characterization of AFSC-SPCL constructs by SEM and EDS analysis. SEM magnified images of calcium phosphate nodules at the surface and inside (inset) of these constructs after 21 days in osteogenic medium. The presence of calcium and phosphorus atoms was detected by EDS analysis after 0, 7, 14 and 21 days in osteogenic culture. SPCL spectrum represents a SPCL scaffolds without seeded cells.

Calcium quantification in the constructs indicated that the presence of calcium is kept at a basal level from 0 to 14 days in culture and, at the third week in culture, this value increases

about 50 %, which indicates that calcium is being added to the matrix, inducing the formation of a calcified matrix produced by AFSCs.

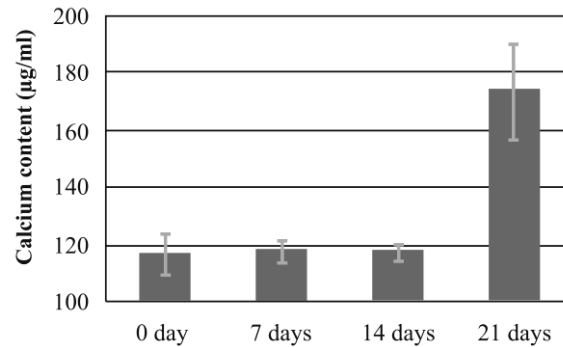


**Figure VIII.4.5** - Calcium content measurement in AFSC-SPCL constructs after 0, 7, 14 or 21 days in osteogenic culture.

Vibrational spectroscopy in the mid-infrared region can provide molecular structure information about mineralized tissue[18]. The infrared spectrum in Figure VIII.4.6 showed the presence of specific types of chemical bonds, associated to the major molecular species found in bone; phosphate (bands  $\sim 900-1100\text{ cm}^{-1}$ ), carbonate (from carbonate substitution for hydroxyl and phosphate groups, bands  $\sim 850\text{ cm}^{-1}$ ), and amide I, II, and III (bands  $\sim 1650\text{ cm}^{-1}$ ,  $1550\text{ cm}^{-1}$  and  $1250\text{ cm}^{-1}$ , respectively) from the protein constituents (mainly type I collagen). The spectrum of unseeded SPCL scaffold does not exhibit any of these bands, and the intensity of these bands increases with the time in osteogenic culture. An increase in the intensity values may be associated to the number of chemical bonds, and thus, molecular species, present at the surface of the scaffold.

The presence of calcium phosphate (CaPs) aggregates in SEM micrographs correspond to ECM mineralization, either at the surface and inner section of AFSC-SPCL constructs (Figure VIII.4.1 and Figure VIII.4.4 – SEM after 21 days in culture), pointing toward the osteoblastic-like status of AFSCs after 3 weeks under osteogenic supplements.

The time frame of the osteogenic process confirms these results as mineral deposition is accomplished largely by the precipitation of hydroxyapatite, which requires the presence of collagen fibrils.

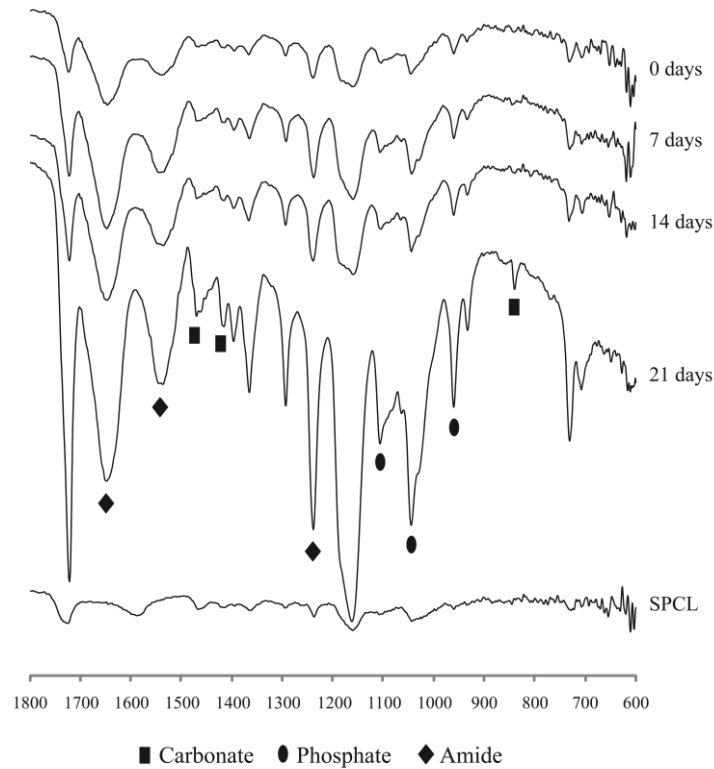


**Figure VIII.4.6** - Characterization of AFSC-SPCL constructs by FT-IR analysis. The presence of calcium and phosphorus groups was detected after 0, 7, 14 or 21 days in osteogenic culture. SPCL spectrum represents a SPCL scaffolds without seeded cells.

#### VIII.4.2. *In vivo* study

No animal subjected in this study showed any infection (Figure VIII.4.7), however some rats (n= 14) showed bone plate loosening or small cracks during the surgery and were excluded from this study.



**Figure VIII.4.7** - Picture of dissected femurs after an end point. Femur on the left represents a femur post-implantation and on the right, the left rear femur, control.

**VIII.4.2.1. Neobone formation assessment**

Neobone formation to some extent was observed in all experimental groups, as expected, both at 4 and 16 weeks by micro-CT analysis (Figure VIII.4.8).

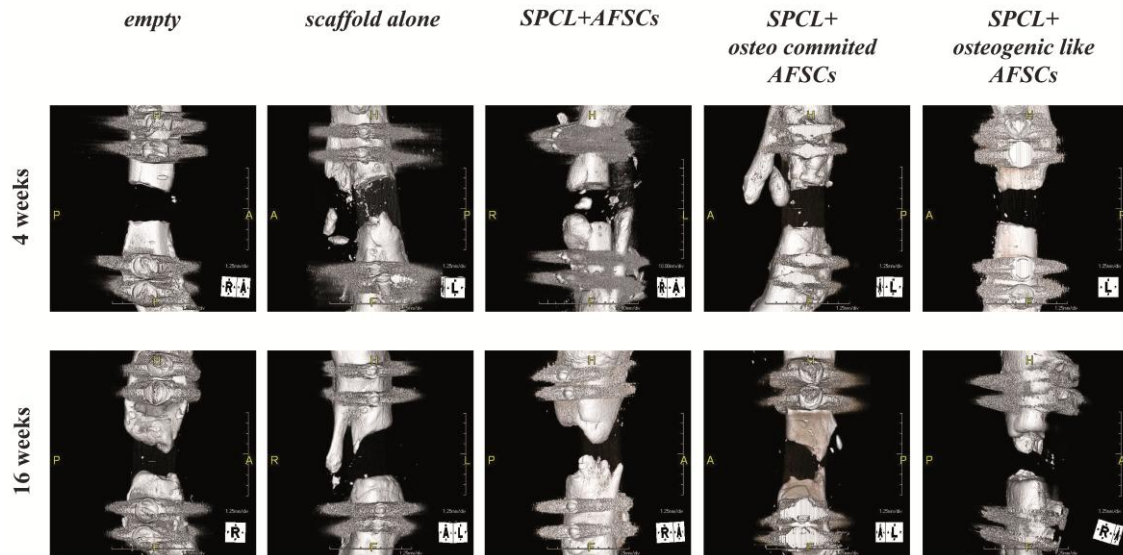


**Figure VIII.4.8** - m-CT images obtained from all defect conditions after 4 and 16 weeks of implantation.

The formation of bone is observed 4 weeks after implantation at the segment ends of the defect. In empty defects, new bone formation resulted in an increased appositional growth of the bone in the border areas of bony segments, which could have resulted as a response of the organism to the trauma in the femur during surgery (Figure VIII.4.8 and Figure VIII.4.9).

In all other conditions, interstitial bone growth was observed, and bridging bone was evident in the presence of SPCL and SPCL seeded with cells (Figure VIII.4.9). The micro-CT images also suggest that the presence of osteogenically committed hAFSCs seeded in the SPCL scaffolds induced the best bridging with bone formation between the two sections of the defect after 16 weeks of implantation. In the case of undifferentiated cells, bridging structures were only observed in half of the specimens after 16 weeks.

Small particles of bone were also detected within the defect gap in SPCL and SPCL seeded with cells conditions, suggesting that an initial new bone forming process starts as early as 4 weeks after implantation (Figure VIII.4.9). Although this bone ingrowth is reduced, when compared to the 16 week group, these results also support the relevance of the SPCL scaffold in new bone development with the time of implantation.

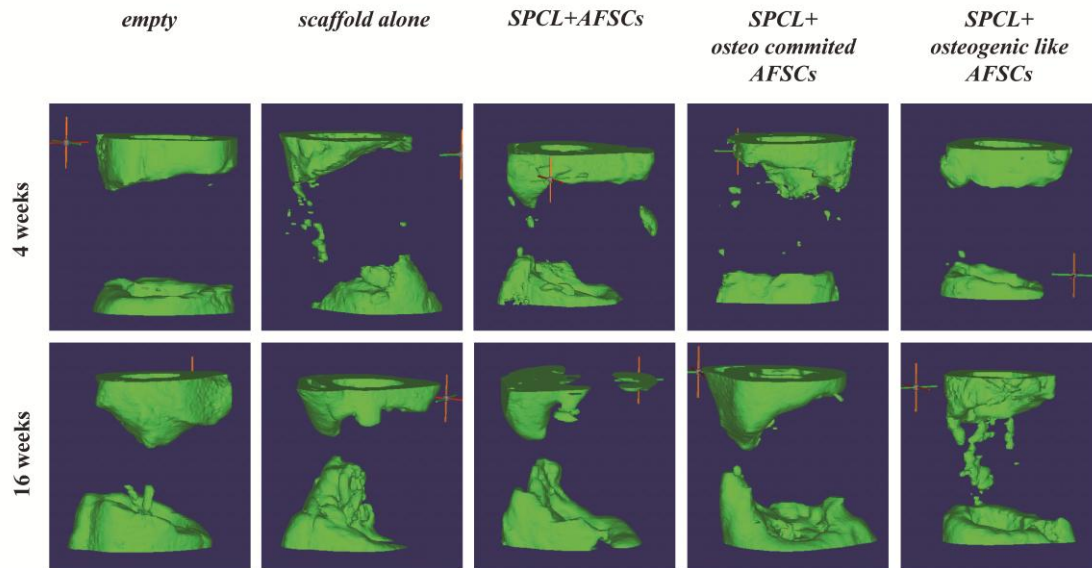


**Figure VIII.4.9** – Volumetric measurements of the defect section obtained from mCT analysis using Mimics software, representing the bone neoformation area.

At 16 weeks, the volumetric measurements of bone increase in all conditions, but the attempt of new bone to penetrate into the defect gap, and establish a link between the native bone segments is only detected in the presence of SPCL and SPCL seeded with cells.

Furthermore, in most specimens analysed a lateral mineralized structure was formed and observed in all conditions after 16 weeks but not detected in animals with empty defects by the end of the first end point (4 weeks) (Figure VIII.4.8). This formation tends to increase in length with the implantation time and is not typically described in non-union defects studies.

We believe that this new bone formation is associated to a secondary healing process frequently observed in human fractures of skeletally mature or elder individuals. Not only marrow bone formation is more limited in adult organisms, but bone marrow cells tends to decrease in number and functionality with aging, and so does their stemness potential, compromising the bone regeneration capacity[20-22].

In young individuals, bone growth through medulary influence is frequent and results in a complete restoration of the affected tissue. In senior organisms, this route tends to be replaced by alternative regeneration processes in order to create stability in motion and sustain load bearing forces under a partial or absent medulary influence. Since the animals of our study are geriatric rats, the secondary healing is the most likely process of bone regeneration. Nevertheless, in the presence of SPCL scaffolds, the medulary effect seems to be stimulated by the bridging formation in the femur defect. SPCL scaffolds are likely to indirectly

participate in the hemostasis process that initiates the healing cascade by entrapping small blood clots, resultant from the initial injury (defect surgery), that together with cells, are important mediators for new bone formation. Thus, we believe that SPCL scaffolds assist the molecular communication between the segmental areas leading to a bridging effect, not observed in empty defects, the negative control of our experience.

#### **VIII.4.2.2. Histology characterization**

In general, H&E staining showed that cells were able to migrate into all induced defects, colonizing between fibers of the SPCL scaffolds with matrix production at any time points. The matrix formed by cells also increased with the implantation time. Empty defects, in particular, showed a more irregular, dispersed and disorganized distribution of the cells and matrix.

At 4 weeks of implantation, cartilage tissue was also observed in sections of the implanted area of several conditions, namely, empty defects, SPCL alone, SPCL-undifferentiated hAFSCs and SPCL seeded with osteogenic differentiated hAFSCs. After 16 weeks of implantation, only SPCL seeded with undifferentiated hAFSCs showed cartilaginous areas. The cartilage seems to be associated to the endochondral ossification process, one of the two bone formation processes, in which cartilage is formed and ultimately develops into new bone tissue. Furthermore, bone remodeling at the end of bone segments is also observed (Figure VIII.4.10), especially in empty, SPCL alone and SPCL seeded with undifferentiated hAFSCs by 4 weeks of implantation.

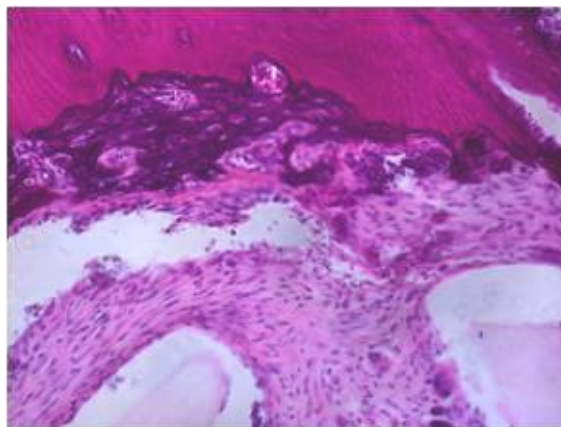


**Figure VIII.4.10** – Detailed image of native bone and SPCL scaffold interface *in vivo* after 4 weeks showing the native bone remodeling process aiming at defect regeneration (200x magnified).



In the scaffold implanted groups, general inflammatory response appeared to be moderate at 4 weeks group and to be little at 16 week group which imply that our scaffold is biocompatible. Additionally, in analyzed sections, some giant cells were also detected in the defects implanted with SPCL scaffolds. The foreign body reaction, composed of macrophages and foreign body giant cells, is the end-stage response of the inflammatory and wound healing responses following implantation of a medical device, prosthesis or biomaterial[23]. The presence of giant cells may also be a good indicator for SPCL *in vivo* degradation. As previously showed[15, 16, 17], SPCL is a biodegradable scaffold and the adhesion of these cells to some surface areas of the scaffold may stimulate the releasing of degradation mediators, such as reactive oxygen intermediates, and expose SPCL to a higher concentration of these factors, increasing scaffold susceptibility to degradation[23, 24].

#### VIII.4.2.2.1. Histomorphometric Analysis

Histomorphometric analysis was performed for collagen I, osteocalcin, and VEGF antibodies so as to quantify the expression of these proteins in the regenerative process of our strategy for bone non-unions regeneration.

Considering collagen I expression (Figure VIII.4.11), higher values were found in empty defects although no statistical significance was found when compared to all other conditions.

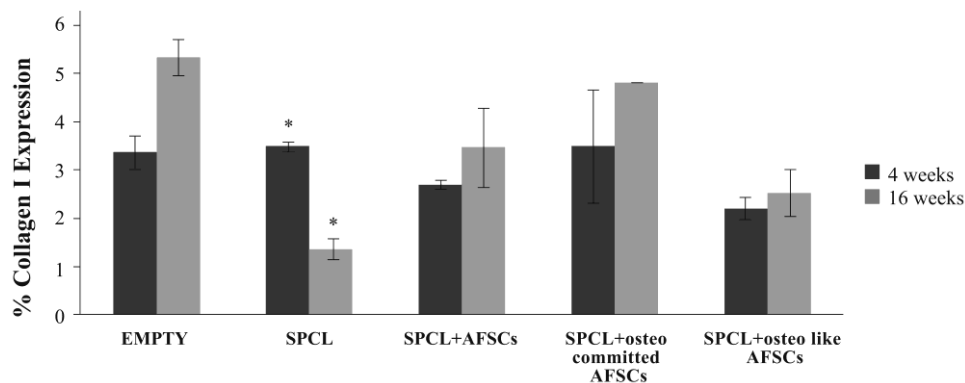


**Figure VIII.4.11** – Histometric analysis for collagen I expression (%) in the studied conditions. Values are represented by mean  $\pm$  standard error of mean. Symbol \* denote study groups with statistically significant differences ( $p < 0.05$ ), as using Two Way ANOVA method.

Although collagen I is the major component of bone, it is also present in scar tissue, when tissue heals by repair, and at the proliferation and extracellular matrix maturation during the



osteoblast differentiation process. In defects filled with SPCL scaffolds, the expression of collagen I decreases over time ( $p < 0.05$ ), while in SPCL with hAFSCs conditions, the expression seems to be stable during the experiment.

Osteocalcin is a non-collagenous protein only secreted by osteoblasts, described to be involved in the pro-osteoblastic process of bone, and often associated to bone mineralization[25]. As observed in Figure VIII.4.12, osteocalcin expression tends to increase from 4 to 16 weeks of implantation in all induced defects except the empty condition.

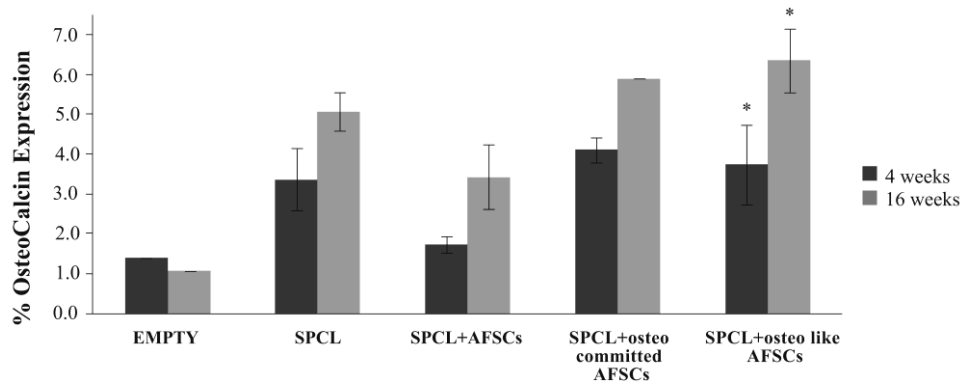


**Figure VIII.4.12** – Histometric analysis for osteocalcin expression (%) in the studied conditions. Values are represented by mean  $\pm$  standard error of mean. Symbol \* denote study groups with statistically significant differences ( $p < 0.05$ ), as using Two Way ANOVA method.

Moreover, the percentage of osteocalcin is higher in defects implanted with SPCL alone and SPCL seeded with cells than in empty defect condition, which seems to indicate that tissue engineered implants may participate in the osteogenic mechanism for bone mineralization. Increasing values found in SPCL seeded with osteogenic like hAFSCs were found to be statistically relevant ( $p < 0.05$ ) with the implantation time.

In the literature[26], higher levels of collagen I are found in osteoprogenitor to pre-osteoblast (osteogenic committed) cells while in mature osteoblasts, collagen I levels decreases and osteocalcin protein increases significantly to promote mineralization. Our results follow this tendency showing a higher percentage of collagen I in constructs of SPCL seeded with hAFSCs or osteogenic committed hAFSCs, while SPCL with hAFSCs (undifferentiated) express lower levels of osteocalcin, conversely to SPCL seeded with osteo committed or osteoblast like hAFSCs. In this sense, implanted hAFSCs seem to get involved, and somehow participate in the regenerative process.

However, as observed by micro-CT analysis, bone formation (calcified matrix) is formed in all conditions where SPCL is present, mainly around or at the scaffold periphery, but it does not seem to occur inside the scaffold likewise. This demonstrates that SPCL seem to promote the communication between the 2 bone segments of the femur as bone is formed at the boundaries of the defects but degradation time of the scaffold should be optimized to facilitate new bone formation inside of the scaffold.

As new bone was less formed inside the implanted scaffold, and cells were expressing collagen I and osteocalcin, a possible explanation could reside on the influence of environmental growth factors to the bone that are more widely accessible in peripheral regions of the scaffold.

Since the process of a successful bone healing requires a good vascular network, as bone is a highly vascularised tissue, angiogenesis plays a pivotal role in skeletal development and bone fracture repair[27, 28]. VEGF is a signal protein associated to vasculogenesis and angiogenesis. During bone repair, VEGF is required not only for blood vessel formation, but also for normal callus volume and mineralization[29]. Furthermore, VEGF was described to inhibit osteoblast apoptosis and stimulate osteogenic differentiation, indicating that VEGF may be the major signal to couple angiogenesis and osteogenesis during bone repair[29, 30].

In our study, VEGF expression showed some variation among different animals from the same condition, especially after 16 weeks of implantation (Figure VIII.4.13).

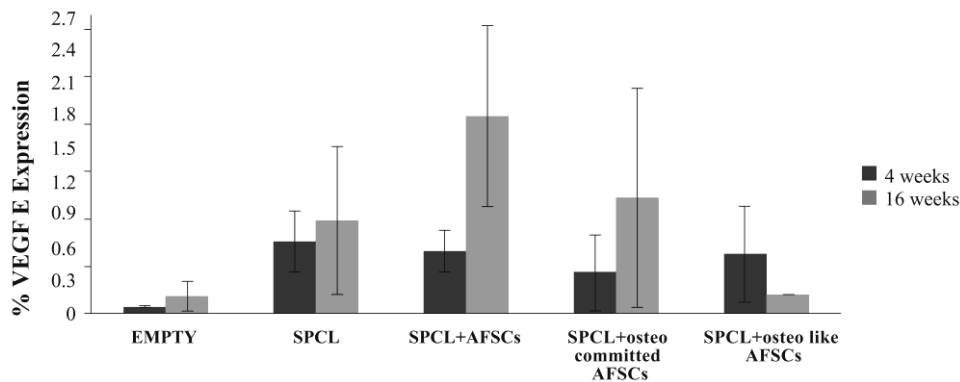


**Figure VIII.4.13** – Histometric analysis for VEGF expression (%) in the studied conditions. Values are represented by mean  $\pm$  standard error of mean.

Again, a basal expression of around 0.15 % was detected in empty controls, in which no vascularization was significantly observed. VEGF expression tends to increase from 4 to 16 weeks in all conditions except SPCL with osteoblastic like cells.

In this study, blood vessels were also microscopically visualized in all retrieved samples, corresponding to all the different conditions analyzed, at both implantation periods (Figure VIII.4.14).

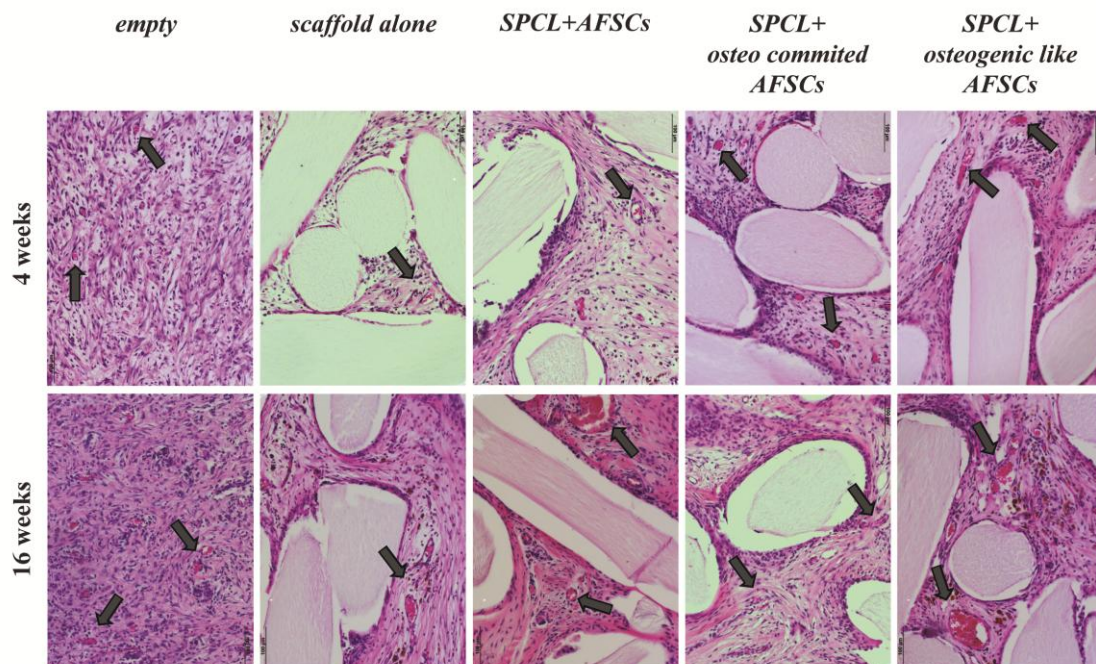


**Figure VIII.4.14** – Detection of blood vessel formation in H&E stained sections for all conditions studied after 4 or 16 weeks of implantation. Pictures were 200x magnified.

In accordance to VEGF histometric data, after 4 weeks of implantation, the smallest vessels were found in the empty defects while the largest sized vessels were found in defects filled with SPCL scaffolds cultured with undifferentiated hAFSCs. After 16 weeks of implantation, blood vessels in empty defects are only observed close to the bone segment top. The largest vessels were found in seeded SPCL scaffolds with undifferentiated cells, followed by SPCL seeded with osteogenic-like cells. These observations are in accordance to VEGF histomorphometrical data as the highest levels of VEGF are expressed in SPCL-hAFSCs condition.

These findings suggest that hAFSCs may have a role in the angiogenic/inflammatory processes, particularly the undifferentiated hAFSCs seeded on the SPCL scaffolds.

The innate stem cell nature of hAFSCs, as compared to the hAFSCs osteogenically committed, can induce the production or migration of secreting factors, or responding to the presence of local environmental contributions, towards angiogenesis[27] and consequently bone formation. The fact that SPCL-osteoblast-like hAFSCs present larger vessels in Figure VIII.4.14 but low percentage of VEGF in Figure VII.4.13 can be explained together with the data

obtained for collagen I and osteocalcin. In SPCL-osteoblast-like hAFSC constructs, mineralization is being achieved and the blood vessels have been already formed, as observed in Figure 12 so VEGF expression decreases, and a bigger input is given to the mineralization stage of regeneration. Nonetheless, the presence and distribution of blood vessels in all SPCL conditions indicated that SPCL scaffolds assist a good angiogenesis of the defect area, since an active blood vessel network is an essential pre-requisite for constructs maintenance and integration with existing host tissue.

### VIII.5. Conclusions

*In vitro* results indicated that hAFSCs proliferated and differentiated into the osteogenic lineage, when seeded onto SPCL scaffolds. hAFSCs were considered to be osteogenically committed after 2 weeks in osteogenic medium with the expression of some bone related markers and a protein rich extracellular matrix. By the end of week 3, cells became osteoblast-like with the production of a mineralized matrix.

After assessing *in vitro* functionally, *in vivo* studies were performed and, accordingly to micro-CT analysis, all defect conditions showed new bone formation to some extent from 4 to 16 weeks of implantation. The amount of new bone was increased over time. No bridging formation was observed in empty defects, and despite the fact that the bridging process was not complete in any of the other conditions by 16 weeks; the presence of osteogenically committed hAFSCs in the SPCL scaffolds showed the shortest gap (bridging) between the femoral bone segments, after 16 weeks of implantation.

The presence of vascular vessels in the middle of the SPCL or hAFSCs-SPCL constructs also indicates that SPCL scaffolds and hAFSCs participate in the angiogenesis in the defect, showing that SPCL scaffolds are an interesting support for bone regeneration and angiogenesis in non-union defects, especially when seeded with human amniotic fluid stem cells committed to the osteogenic phenotype.

We conclude that our SPCL scaffold system can be a useful candidate for reconstructing a long bone defect in the near future. Furthermore, the presence of hAFSCs can induce a synergistic effect in this system, but additional studies will be needed to optimize degradation time of the scaffold and use of hAFSCs condition.

## **VIII.6. References**

1. Calori GM, Albisetti W, Agus A, Iori S, Tagliabue L: Risk factors contributing to fracture non-unions. *Injury* 2007, 38 Suppl 2: S11-18.
2. Giannoudis PV, Atkins R: Management of long-bone non-unions. *Injury* 2007, 38 Suppl 2: S1-2.
3. Tseng SS, Lee MA, Reddi AH: Nonunions and the potential of stem cells in fracture-healing. *J Bone Joint Surg Am* 2008, 90 Suppl 1: 92-98.
4. Mahendra A, Maclean AD: Available biological treatments for complex non-unions. *Injury* 2007, 38 Suppl 4: S7-12.
5. Petite H, Viateau V, Bensaid W, Meunier A, de Pollak C, Bourguignon M, Oudina K, Sedel L, Guillemain G: Tissue-engineered bone regeneration. *Nat Biotechnol* 2000, 18: 959-963.
6. Liu X, Li X, Fan Y, Zhang G, Li D, Dong W, Sha Z, Yu X, Feng Q, Cui F, et al.: Repairing goat tibia segmental bone defect using scaffold cultured with mesenchymal stem cells. *J Biomed Mater Res B Appl Biomater*. 2010, 94(1): 44-52.
7. Dupont KM, Sharma K, Stevens HY, Boerckel JD, Garcia AJ, Guldberg RE: Human stem cell delivery for treatment of large segmental bone defects. *Proc Natl Acad Sci U S A* 107: 3305-3310.
8. Jager M, Degistirici O, Knipper A, Fischer J, Sager M, Krauspe R: Bone healing and migration of cord blood-derived stem cells into a critical size femoral defect after xenotransplantation. *J Bone Miner Res* 2007, 22: 1224-1233.
9. Prusa AR, Marton E, Rosner M, Bernaschek G, Hengstschlager M: Oct-4-expressing cells in human amniotic fluid: a new source for stem cell research? *Hum Reprod* 2003, 18: 1489-1493.
10. De Coppi P, Bartsch G, Jr., Siddiqui MM, Xu T, Santos CC, Perin L, Mostoslavsky G, Serre AC, Snyder EY, Yoo JJ, et al.: Isolation of amniotic stem cell lines with potential for therapy. *Nat Biotechnol* 2007, 25: 100-106.
11. Kim J, Lee Y, Kim H, Hwang KJ, Kwon HC, Kim SK, Cho DJ, Kang SG, You J: Human amniotic fluid-derived stem cells have characteristics of multipotent stem cells. *Cell Prolif* 2007, 40: 75-90.
12. Sun H, Feng K, Hu J, Soker S, Atala A, Ma PX: Osteogenic differentiation of human amniotic fluid-derived stem cells induced by bone morphogenetic protein-7 and enhanced by nanofibrous scaffolds. *Biomaterials* 31: 1133-1139.
13. Rodrigues MT, Gomes ME, Viegas CA, Azevedo JT, Dias IR, Guzón F, Reis RL: Tissue Engineered Constructs based on SPCL Scaffolds Cultured with Goat Marrow Cells: Functionality in Femoral Defects. *J Tissue Eng Regen Med* 2011, 5: 41-49.
14. Peters A, Toben D, Lienau J, Schell H, Bail HJ, Matziolis G, Duda GN, Kaspar K: Locally applied osteogenic predifferentiated progenitor cells are more effective than undifferentiated

mesenchymal stem cells in the treatment of delayed bone healing. *Tissue Eng Part A* 2009, 15: 2947-2954.

15. Gomes ME, Bossano CM, Johnston CM, Reis RL, Mikos AG: In vitro localization of bone growth factors in constructs of biodegradable scaffolds seeded with marrow stromal cells and cultured in a flow perfusion bioreactor. *Tissue Eng* 2006, 12: 177-188.

16. Gomes ME, Azevedo HS, Moreira AR, Ella V, Kellomaki M, Reis RL: Starch-poly(epsilon-caprolactone) and starch-poly(lactic acid) fibre-mesh scaffolds for bone tissue engineering applications: structure, mechanical properties and degradation behaviour. *J Tissue Eng Regen Med* 2008, 2: 243-252.

17. Santos MI, Fuchs S, Gomes ME, Unger RE, Reis RL, Kirkpatrick CJ: Response of micro- and macrovascular endothelial cells to starch-based fiber meshes for bone tissue engineering. *Biomaterials* 2007, 28: 240-248.

18. Boskey A, Pleshko Camacho N: FT-IR imaging of native and tissue-engineered bone and cartilage. *Biomaterials* 2007, 28: 2465-2478.

19. Lian JB, Stein GS: Concepts of osteoblast growth and differentiation: basis for modulation of bone cell development and tissue formation. *Crit Rev Oral Biol Med* 1992, 3: 269-305.

20. Stolzing A, Jones E, McGonagle D, Scutt A: Age-related changes in human bone marrow-derived mesenchymal stem cells: consequences for cell therapies. *Mech Ageing Dev* 2008, 129:163-73.

21. Kretlow JD, Jin YQ, Liu W, Zhang WJ, Hong TH, Zhou G, Baggett LS, Mikos AG, Cao Y: Donor age and cell passage affects differentiation potential of murine bone marrow-derived stem cells. *BMC Cell Biol* 2008, 9: 60.

22. Yu JM, Wu X, Gimble JM, Guan X, Freitas MA, Bunnell BA: Age-related changes in mesenchymal stem cells derived from rhesus macaque bone marrow. *Aging Cell*. 2011, 10: 66-79.

23. Anderson JM, Rodriguez A, Chang DT: Foreign body reaction to biomaterials. *Semin Immunol* 2008, 20: 86-100.

24. Pego AP, Van Luyn MJ, Brouwer LA, van Wachem PB, Poot AA, Grijpma DW, Feijen J: In vivo behavior of poly(1,3-trimethylene carbonate) and copolymers of 1,3-trimethylene carbonate with D,L-lactide or epsilon-caprolactone: Degradation and tissue response. *J Biomed Mater Res A* 2003, 67: 1044-1054.

25. Neve A, Corrado A, Cantatore FP: Osteoblast physiology in normal and pathological conditions. *Cell Tissue Res* 343: 289-302.

26. Lian JB, Stein GS: Development of the osteoblast phenotype: molecular mechanisms mediating osteoblast growth and differentiation. *Iowa Orthop J*. 1995, 15: 118-40.

27. Kanczler JM, Oreffo RO: Osteogenesis and angiogenesis: the potential for engineering bone. *Eur Cell Mater* 2008, 15: 100-114.

28. Carano RA, Filvaroff EH: Angiogenesis and bone repair. *Drug Discov Today* 2003, 8: 980-989.

29. Filvaroff EH: VEGF and bone. *J Musculoskelet Neuronal Interact* 2003, 3: 304-307; discussion 320-301.

30. Wernike E, Montjovent MO, Liu Y, Wismeijer D, Hunziker EB, Siebenrock KA, Hofstetter W, Klenke FM: VEGF incorporated into calcium phosphate ceramics promotes vascularisation and bone formation in vivo. *Eur Cell Mater* 19: 30-40.





## **SECTION VI**

### **GENERAL CONCLUSIONS**



## **Chapter IX**

### **FINAL REMARKS AND FUTURE STUDIES**



*Theory guides. Experiment decides.  
(an old saying in science)*

### **IX.1. General Conclusions**

The broad subject of this Thesis permitted to reach further insights in some key issues of tissue engineering strategies for the regeneration of bone and osteochondral tissues, namely on scaffold development, stem cells sources and synergies between scaffold design, stem cells, and culturing conditions. Additionally, *in vivo* studies allowed obtaining important data regarding the relevance of using scaffolds alone or scaffolds with stem cells at different stages of osteogenic differentiation in the treatment of bone defects. The results obtained are described below:

#### *i) Scaffold design and composition for bone and osteochondral defects regeneration*

The development of multi-layered PCL-TCP scaffolds was successfully achieved, as well as the *in vitro* assessment of their application aiming at bone tissue engineering (TE) strategies. In the study described in chapter III, a PCL polymer was used as a nanofiber mesh substrate. Despite the fact that PCL is a well described polymer for TE strategies, the relevance of this study is not so much the polymer by itself but the nano structure obtained by means of using electrospinning. Considering that bone extracellular matrix (ECM) is essentially an organic-inorganic composite and nano-scaled organized, the integration of nano-structures in 3D scaffolds could be an interesting structural approach. The main issue in this approach is the fact that nano-structures do not support the mechanical needs of bone as for weight loading or other mechanical stresses. To fulfill this gap, the study describes the idea of developing multi-layered structures to adjust to the dimension of bone defects, and sustain body weight whenever necessary during the regenerative process. Furthermore, to induce some osteogenic activity, and eventually stimulate a bond between construct and native bone in an *in vivo* situation, TCP granules were added, due to their osteoconductive properties. Thus, the

combination of PCL with calcium phosphates was shown to be more efficient to generate scaffolds with higher osteoconductive ability, but this was an expected result since TCP is an osteoconductive material. However, particularly interesting was to conclude also that PCL-TCP scaffolds did not required osteogenic supplements in the culture medium to induce the osteogenic phenotype of gBMSCs, as long as constructs were cultured in dynamic conditions. Furthermore, the detection of a calcified ECM in the absence of osteogenic medium indicated an excellent cellular response to the scaffold and to mechanical stimuli. This study demonstrated for the first time a composite multi-layered structure inspired in the natural organic-inorganic nanostructure of bone with interesting results for bone applications.

SPCL is a blend of PCL with starch, a natural polymer, which has been widely studied at the 3Bs Research Group. SPCL scaffolds can be obtained by several processing methodologies as described in this Thesis. The processability of SPCL using different techniques allows achieving constructs with different designs and porous structures. For instance, with a fiber bonding procedure, using melt spun fibers, it is easier to obtain 3D scaffolds with higher mechanical properties, while wet-spinning technology produces a fiber mesh scaffold, where functional groups can be incorporated in a single step procedure, and thus tailor the SPCL surface composition. In chapter IV, the bioactivity behavior of wet-spun SPCL scaffold with silanol groups (SPCL-Si) was demonstrated in the presence of a SBF solution. The presence of the silanol groups showed to stimulate the osteogenic differentiation of bone marrow stromal cells *in vitro*, but the ability to form an apatite layer together with the osteoconductive and osteogenic properties might also have a significant impact *in vivo*, as the ideal implanted construct should stimulate damaged tissue regeneration and restore its functionality. However, presently, this process does not allow obtaining scaffolds with larger dimensions very easily, and their mechanical properties are slightly lower than those for SPCL meshes obtained from melt spun fibers. Nevertheless, SPCL-Si scaffolds might offer an alternative in flat bone regeneration strategies, fitting the anatomically leveled areas such as calvarian bone. SPCL scaffolds obtained by bonding of melt spun fibers are well characterized, and were described in previous studies, particularly for bone engineered strategies. Thus, in chapter VI, VIII and V, fiber bonding SPCL scaffolds were used in osteogenic and osteochondral studies, respectively.

The application of a bilayered scaffold is quite attractive for osteochondral interfaces due to the natural differences in cellular and tissue needs between cartilage and bone tissues. Osteochondral studies from chapter V revealed that the assembly of a bilayered scaffold is possible, and after AFSCs differentiation is achieved, cell viability is kept high, and both osteo-

or chondro-genic differentiation are maintained in the osteochondral bilayered system. Although not essential, after assembling the bilayer system, the presence of osteochondral medium seems to maintain the osteogenic and chondrogenic phenotypes of human AFSCs. The advantages of this system rely on the individual culture layers for selective differentiation, which can be quickly and easily assembled, and maintained in basal culture medium. Besides the simplification for the maintenance of differentiated cells in culture, a co-culture medium would assist the communication between osteoblast- or chondrocyte-like cells to be maintained in a bilayered system until construct implantation. With this strategy, time and cost of a tissue engineered product could be eventually reduced, and become closer to a clinical application. Again, SPCL suitability for bone applications is confirmed with great potential to spread out into osteochondral strategies.

*ii) Stem cells sources and relevance of the differentiation stage – in vitro studies*

Although stem cells can be found in almost every tissue, cell origin can influence their response either mechanically, physically or chemically. Bone marrow stem cells (BMSCs) are the most studied, and frequently associated to autologous approaches regardless of the donor age-affected and self-renewal limitations. Other stem cells sources, such as amniotic fluid could overcome these limitations. Despite the potential of human amniotic stem cells (AFSCs), few studies assessed AFSCs behavior both *in vitro* and implanted in an animal model. Since no comparative analysis has been done to assess possible differences between BMSCs and AFSCs due to origin outcomes, in chapter VI, a comparative study was performed to find out the cell response to substrate and media supplementation. Results indicated that both cell types were able to proliferate and differentiate into the osteogenic phenotype in 2D and 3D substrates. Nevertheless, cells from different origins expressed different bone-related markers at different end points, which may be related to cellular origin and substrate properties. In fact, besides the influence of cell origin, stem cells response can be further tailored by scaffold materials, namely by the design and chemical composition. Features, such as stiffness/softness or elasticity, can be tailored to induce a determined cell response, as these characteristics are known to be detected and understood differently by the ECM of the cells. The physical contact between cells-scaffold will result in a series of cellular signals, through which cells attempt to adapt to the surrounding environment. Additional stimulus, such as dynamic culturing conditions can also act synergistically with the scaffold material, as showed in chapter III, thus enhancing a specific cell response. Despite the fact that some stem cell sources might be more

sensitive to certain stimuli than others, it is likely that the combination of different physical and chemical signals, similarly to those present in their native environment, will lead cells more easily to a specific target response. Thus, the selection of a particular stem cell type may not be a simple and direct process and relies on the TE strategy to be assessed, firstly *in vitro* and later in an *in vivo* environment.

*iii) Functionality assessment of scaffold-stem cells based strategies in bone tissue engineering: in vivo studies*

Cell-scaffold constructs were evaluated *in vitro* in terms of proliferative and selective differentiation potential, following the evolution of the sequential stages of the differentiation process from stem cells into osteoblast-like cells. After *in vitro* assessment of the promising systems of SPCL-AFSCs or SPCL-BMSCs, the functionality of these constructs was evaluated *in vivo* under two different studies considered in chapter VII and VIII.

Non-critical sized defects were induced in the rear femurs of skeletally mature goats using an autologous cellular approach. One of the greatest advantages of autologous approaches is the fact that xenogenic animal cells and medium supplements are avoided, thought to be critical for successful future clinical procedures with human patients. Thus, several conditions were acknowledged so as to comprehend the influence of scaffold, and scaffold seeded with bone marrow cells (BMSCs) or with osteogenic committed BMSCs in the regeneration of bone. This is particularly important since the stage of osteogenic differentiation can be critical for achieving tissue-like functional substitutes. As expected, the neof ormation of bone occurred in all orthotopic induced defects. Nevertheless, results obtained indicated that neobone formation and cellular distribution increased in the presence of cell seeded SPCL scaffolds, which strongly shows the influence of implanted cells in the bone regeneration process. In addition, the pre-differentiation of goat BMSCs into the osteogenic phenotype seems to increase the neobone ingrowth into the defects, revealing not only the importance of implanted cells but also of their differentiation stage in the communication process between implant and native bone environment. This study also evaluated the orthotopic behaviour of SPCL biomaterial revealing a biocompatible scaffold that does not contribute to an overreaction from the immune response against the implant. Additionally, SPCL scaffolds showed a great potential for the development of adequate tissue 3D support for the regeneration of bone.



Although autologous approaches are the perfect tailored TE solution for individual needs, they are quite time demanding, and some patients may not have a healthy and available stem cell pool to harvest from, due to age or disease limitations. Thus, researchers have been looking for a novel cell source that could be used for a wide range of therapies suiting patients worldwide. Amniotic fluid has been studied aiming at a non-immunogenic and universal stem cell source. These are advantageous features that brought AFSCs into highly complex bone defects - non-unions or critical sized defects- to validate our strategy. Again, results indicated that a greater amount of neobone in the presence of SPCL scaffolds and a bridging effect is more prominent in the defects filled with scaffolds seeded with cells committed to the osteogenic phenotype. The presence of large blood vessels in the defect areas, especially in SPCL scaffolds seeded with undifferentiated cells, followed by SPCL seeded with osteogenic-like cells, also indicates the suitability of these constructs for the regeneration of non-union defects as vascularization is important to assure local transport of nutrients, oxygen and growth factors to the cells.

In summary, biomaterials described in this Thesis showed an interesting potential in different strategies aiming at bone and osteochondral TE applications. Composite scaffolds showed prospective interest under dynamic conditions for strategies involving flat bones and cell culturing media without osteogenic supplements. Bioactive wet-spun fiber meshes of SPCL-Si scaffolds also showed intrinsic properties able to sustain *in vitro* osteogenic features of goat BMSCs. Nevertheless, SPCL meshes obtained from melt spun fiber are one step ahead as scaffold structures, showing to provide the necessary support to novel and under development bone and osteochondral TE strategies using different sources of stem cells and animal models.

The combination of cells and SPCL scaffolds showed the best results in pre-clinical models, either in autologous (goat BMSCs) or heterologous (human AFSCs) cell sources. Moreover, the stage of osteogenic differentiation seems to be an important factor to consider in the complex process of bone regeneration.

*Research is to see what everybody else has seen,  
and to think what nobody else has thought.*

*Albert Szent-Györgi (1893-1986)*

## **IX.2. Final Remarks and Future Studies**

It would be exciting and very promising to develop a scaffold to stimulate osteogenic differentiation and new bone formation in the absence of specific osteogenic supplements. The cost of the tissue engineered products would decrease significantly, the culture conditions simplified and short-termed, and some risks concerning the use of animal origin supplements avoided. Herein we reported the development of multi-layered nanofiber scaffolds that may fulfill these requirements, yet their mechanical properties may limit their application to flat bone strategies.

We also reported here the advantageous features of wet spun SPCL fiber meshes that can be *in situ* functionalized in one-step processing methodology, thus enabling a cost-effective technology to produce scaffolds with an osteogenic stimulating surface, onto which BMSCs differentiate into osteoblast-like cells, while producing a mineralized extracellular matrix. Thus, future studies should address the influence of SPCL-Si scaffold in osteogenic differentiation in basal culture medium. Since these scaffolds are bioactive, as TCP granules from composite scaffolds of chapter III, perhaps silanol groups could provide a similar motivation as TCPs towards the osteogenic differentiation of BMSCs, with or without the synergistic effect of a dynamic environment. Additionally, the combination of starch with PCL could accelerate the *in vivo* degradation rate, while bone tissue was naturally being regenerated.

Furthermore, *in vivo* studies are envisioned to understand SPCL-Si scaffolds functionality *in vivo*, which is likely to be favorable for bone regeneration due to its intrinsic bioactivity.

A new approach for the treatment of osteochondral interfaces was also assessed, demonstrating promising results. In these studies, described in chapter V, the selected osteochondral medium showed to maintain the phenotypic expression of pre-differentiated cells; future studies should investigate the influence of this medium in promoting simultaneous osteo- or chondro-genic differentiation of stem cells seeded onto SPCL scaffolds or encapsulated in agarose gels, without employing differentiation media. Also, more chondrogenic related markers should be assessed, especially after cell maintenance in

osteocondral media, to determine how medium supplements are affecting the chondrogenic process.

Concerning cell culturing, stem cells from different sources were differentiated into the osteogenic phenotype, although cell response variations were found in commonly associated bone markers. It is important to understand the mechanisms associated to cellular communication between cells and substrate or culture medium. It is very likely that different molecular pathways may be involved and stimuli triggered accordingly to cell origin and scaffold structural and chemical properties. In addition, could osteogenic supplements be radically eliminated from the medium? That seems to be possible for composite scaffolds, and can be enlarged to other scaffolds playing with the unique properties of each type of scaffold as well as all the other factors (such as lineage specific supplements, dynamic environment, scaffold tri-dimensionality) known to participate in the progression into the osteogenic lineage and, consequently in bone regeneration.

The experimental study comparing bone marrow and amniotic fluid stem cells showed some interesting results and rose novel questions that need to be addressed in future studies. Since the ideal cell source is yet to be found, currently available sources should be evaluated considering the aimed application. Also, animals are known to be more resilient to diseases, to immune reactions and to healing abilities than humans. It should be interesting to evaluate if different animal sources of stem cells behave similarly to human correspondent ones.

As mentioned before, both critical and non-critical defects were studied for SPCL scaffolds as well as the influence of cell seeded scaffolds in the regeneration of bone. Results demonstrated that SPCL might fasten the repair of non-critical defects as well as to promote the healing of non-union defects. The presence of cells and their differentiation stage also impacts the new bone tissue formation. Yet, further studies are required to understand the importance of the number of implanted cells versus their differentiation stage and to determine the mechanisms that illicit such different responses in bone metabolism. It is likely that cells undergoing different stages of differentiation may communicate differently with the *in vivo* environment through the release of distinct cytokines and growth factors inducing variations in the organism healing response. Understanding how these processes occur may provide important cues to match the advantageous and promising features of the experimental setups to a fully successful route towards human clinical therapies.